DEVELOPMENT OF DEEP EUTECTIC SOLVENTS FOR AROMATIC SEPARATION FROM ALIPHATIC HYDROCARBONS

By

Aminu Abdullahi MUHAMMAD, B.Eng. (ABU, 2000) MSc. (ABU, 2011)

(P14EGCE9003)

A THESIS SUBMITTED TO THE

SCHOOL OF POSTGRADUATE STUDIES.

AHMADU BELLO UNIVERSITY, ZARIA

IN PARTIAL FULFILMENT OF THE REQUIREMENT FOR THE AWARD OF

DOCTOR OF PHILOSOPHY DEGREE IN CHEMICAL ENGINEERING

DEPARTMEMT OF CHEMICAL ENGINEERING

FACULTY OF ENGINEERING

AHMADU BELLO UNIVERSITY, ZARIA

NIGERIA

APRIL, 2021

DECLARATION

I hereby declare that the work in this thesis titled “Development of Deep Eutectic Solvents for Aromatic Separation from Aliphatic Hydrocarbons” was performed by me in the Department of Chemical Engineering Under the supervision of Prof. B. Y. Jibril, Prof. A. S. Olawale and Dr S. M. Waziri.

The information derived from the literature has been duly acknowledged in the text and a list of references provided. No part of this work has been submitted for another degree or diploma at any institution.

Aminu Abdullahi Muhammad	----------	----------
Name	Signature	Date

CERTIFICATION

This thesis titled "DEVELOPMENT OF DEEP EUTECTIC SOLVENTS FOR AROMATIC SEPARATION FROM ALIPHATIC HYDROCARBONS" BY Aminu Abdullahi MUHAMMAD meets the regulation governing the award of the degree of Doctor of Philosophy (Ph.D.) of the Ahmadu Bello University, and is approved for its contribution of knowledge and literary presentation.

Prof. B. Y. Jibril	----------	----------
Chairman, Supervisory Committee	Signature	Date
Prof. A. S. Olawale.	----------	----------
Member, Supervisory Committee	Signature	Date
Dr S. M. Waziri.	----------	----------
Member, Supervisory Committee	Signature	Date
Dr. J. A. Muhammad	----------	----------
Head of Department	Signature	Date
Prof. S. A. Abdullahi	----------	----------
Dean, School of Postgraduate Studies	Signature	Date

DEDICATION

To my elder brother and mentor Samaila Abdullahi Mohammed

ACKNOWLEDGEMENT

All praises and utmost gratitude are to Almighty Allah, for in His infinite mercy that has made this work a reality. May His unending blessings be with His beloved prophet Muhammad (S AW), his households, companions and those that followed them in righteousness up to the day of resurrection.

To my parents for their immeasurable sacrifices, unending support and love, to my sisters and brothers for their constant support, to my in law and his family, and to my wife (Fatima) and children (Fatima, Khidir, Zulaikha, Saliha, Abdullahi and Muhammad) for their patience, understanding and support, I thank and love you all. May our ties be stronger!

I would like to express my sincere appreciation and gratitude to my supervisors, Prof. B. Y. Jibrin, Prof. A.S. Olawale, Dr. S. M. Waziri and Dr. Farouq S. Mjalli,(while in Oman) for their constant guidance, support and encouragement throughout this journey. My appreciations also go to The Research Council (TRC) of Oman and Sultan Qaboos University Oman for providing the laboratory and financial support to the work carried out in this thesis. To the faculty and non-faculty members of the Department of Petroleum and Chemical Engineering, Sultan Qaboos University and Chemical Engineering Department Ahmadu Bello University Zaria, thank you for your assistance especially during the experimental phase of this work. These include but not limited to Prof. Fatope Majek of Chemistry Department SQU, Dr J. Naseer

My sincere appreciation goes to Prof M. S. Haruna (EVC/CEO NASENI) and staff of PEEMADI for their support.

Finally, I would like to acknowledge the assistance of Dr Omar Umar for his patience and assistance during my experiments while in Oman. My special acknowledgements to my class mates, friends and colleagues; Abdulsalam Badamasi, Bashir Inuwa, Yusuf Mustapha, Dr. Suleman Shuwa, Dr. Abdulkarim Abubakar, Dr.Z. S. Gano, Waqar Ahmed, Mal Usman Baba Suleman, Abdullahi Bukar and Dr. Auwal Aliyu. A special and sincere thanks goes to my brother and friend Adam Ibrahim and his wife for making my life even easier while in Oman. Thank you all.

ABSTRACT

The separation of aromatic from the aliphatic hydrocarbons poses a challenge to the petrochemical industry due to the formation of azeotropes and close boiling point components. The potential application of deep eutectic solvents (DESs) as a low cost and environmentally friendly alternative to the conventional organic solvent in the separation of aromatic/aliphatic hydrocarbon mixtures has been investigated in this thesis.

Deep Eutectic Solvents (DESs) synthesis were carried out with eight 14 ammonium and phosphonium salts and 13 hydrogen bond donors (HBDs) at varied combinations of molar ratios (1-2 ratio for salts and 1-6 ratios for HBDs). A total of two hundred and twenty-eight different types of salt: HBD combinations were tested as DESs

Ten DESs were selected and re- synthesised in large quantities for the experiments on this thesis at a salt: HBD molar ratio of 1:2. The DESs were formed from tetrabutyl ammonium bromide (TBAB), tetrabutyl phosphonium bromide (TBPB) and Tetrabutyl phosphonium methane sulphonate (TBPMS) as salts, with Polyethylene Glycol 200 (PEG200), Polyethylene Glycol 600 (PEG600), Dimethyl Sulphuroxide (DMSO); and Dimethyl formamide (DMF) as HBDs.

Physical properties of the selected DESs which includes density, viscosity, conductivity and refractive index were measured as function of temperature ranging from 303 K to 363 K with the exception of viscosity which was measured between 303K and 353 K at atmospheric pressure. The dependency of density and refractive index with temperature was found to be linear and the correlation coefficient for density and refractive index giving a satisfactory fitting with R^2 ranging between 0.99 and 1.00 for all the studied DESs. Viscosity and conductivity were modeled using the Arrhenius-like and the Vogel-Fucher Tamman (VFT) equations for all the DESs. Model parameter fittings were done for viscosity and conductivity. The percent average absolute deviation (%AAD) VFT equation range for viscosity and conductivity are between 0.17 – 1.00 and 0.76 – 2.12 respectively. The percent average absolute deviation (%AAD) Arrhenius-like equations range for viscosity and conductivity are between 2.62 – 15.22 and 1.36 – 7.58 respectively.

The potential applications of the synthesised DESs for the separation of aromatic from aliphatic hydrocarbons were carried out. Ternary diagrams for the DESs systems and the solute distribution coefficients and selectivity for the studied DESs were determined. The TBAB: PEG600 based DESs showed higher distribution coefficients and selectivity values ranging between 1.23 – 1.40 and 5.0 – 10.0 respectively, at low toluene composition, which indicates the extraction potentials of the DESs.

Thermodynamic modelling using Non-Random Two Liquid (NRTL) model and Universal Quasi Chemical (UNIQUAC) model were carried out from the experimental liquid-liquid equilibrium compositions. The NRTL model gave a better fit when compared to UNIQUAC model with Root Mean Square Deviation (RMSD) ranging between 0.0064 – 0.0008 and 0.2472 – 0.2250 respectively.

Multistage extraction processes were also carried out from model fuel of toluene and octane mixture. The toluene removal efficiency for all the DESs is greater than 90% at the eight equilibrium extraction stage. This shows the ability of the DESs to separate toluene from octane to a lower concentration. Also the removal efficiency of benzene and toluene is greater than 90% and less than 80% for xylene at the 10^{th} equilibrium extraction stage for the three DESs (TBAB: PEG600; TBPB: PEG600 and TBPMS: PEG600) during multistage extraction with synthetic naphtha feed.

DESs regeneration were also carried out. The regenerated DESs shows a performance similar to the original DESs. After the three regeneration cycles the toluene removal efficiency of the studied DESs ranged between 20 – 30 percent.

Table of Content

List of Figures

List of Tables

List of Abbreviation

Abbreviation	Chemicals
ACN	Acetonitrile
AcOH	Acetone
BZTPCl	Benzyltrimetylphosphonium chloride
ChCl	Choline Chloride
DMF	Dimethyl formamide
DMSO	Dimethyl sulfoxide
DEA	Diethylamine
DMAC	Dodecylmethylammonium chloride
EG	Ethylene glycol
ETPPI	Ethyltriphynyl phosphonium iodide
FF	Furfural
GLY	Glycerol
HPLC:	High performance liquid chromatography
LevA	Levulinic acid
MTPPB	Methyltriphenyl phosphonium bromide
MeOH	Methanol
[mmim] [BF4]	1,3-dimethylimidazolium tetraflouroborate
[bupy] [BF4]	N-butylpyridinium tetraflouroborate
4MMP	4 Methy morpholine
[mmimMeSO4]	1,3-dimethylimidazolium methylsulfate

NRTL	Non-random two-liquid
PYRD	Pyrrolidine
PEG	Poly ethylene glycol
PTMAC	Phenyltrimethylammonium chloride
PRD	Pyridine
TBPMS	Tetrabutylphosphoniummethanesulphonate
TEApTS	Tetraethylammonium p-toluenesulfonate
TBPB	Tetrabutyl phosphonium bromide
TMPAB	Trimethylphenylammonium bromide
TBAB	Tetrabutylammonium bromide
TBAC	Tetrabutylammonium chloride
TEAB	Tetraethylammonium bromide
THAB	Tetrahexyl ammonium bromide
TMAB	Tetramethylammonium bromide
TPAB	Tetrapropylammonium bromide
2,2,2 TFAB	2,2,2 Triflouracetamide
UNIQUAC	Universal quasi-chemical
VLE	Vapour liquid equilibrium

CHAPTER ONE

INTRODUCTION

1.1 Background

Aromatic hydrocarbons are raw materials for producing plastics and polymers. Aromatics are mostly obtained by separating aromatic-rich fractions produced from gasoline reforming and naphtha cracking processes for olefin manufacture. The separation of high purity aromatic hydrocarbons (benzene, toluene, ethylbenzene and xylenes) from naphtha feeds is challenging since these hydrocarbons have boiling points in a close range and several combinations form azeotropes. The feed stock to the naphtha cracker contains 10 – 25 % aromatics range, depending on the source of the feed (naphtha or gas condensate). During cracking processes, the aromatic hydrocarbons present in the naphtha feed tend to foul the radiation sections by coking of the coils, thereby reducing the thermal efficiency of the cracker. They also occupy a large part of the capacity of the furnace, which results to putting of extra load on the separation section of C5+ aliphatic compounds (Meindersma, 2005).

The industrial processes used for recovering aromatics from hydrocarbon mixtures, includes; azeotropic distillation, for higher aromatic content (>90 wt. %), extractive distillation, for the concentration between 65 and 90 wt. %, liquid-liquid extraction, the most widely used process and suitable for the range of (20 to 65) wt. % aromatic (Weissermel and Arpe, 2003). The current process for the separation of aromatic compounds is after the furnace section. This shows that there are no separation processes available for processing feed stock with an aromatic content below 20 wt.% (Weissermel and Arpe, 2003). Removing the aromatic

hydrocarbons from the feed to the cracker section would bring much benefits: higher furnace capacity, higher thermal efficiency and less fouling in the furnace.

The solvents used for these processes includes sulfolane (Tetrahydrothio- phene 1,1-dioxide), N-methyl pyrrolidone (NMP), -formyl morpholine (NFM), ethylene glycol, propylene glycol, N,N-dimethylformamide (Sarwono *et al.*, 2013). However, these solvents are generally volatile, toxic, flammable and difficult to recover. Hence, solvents, that are environmentally friendly, are needed for effective separation in order to replace the volatile organic solvents. These solvents should have high distribution ratio and high selectivity.

In the last few years, several solvents have been studied as an alternative to the conventional solvents, amongst them are Ionic liquids (ILs). ILs are organic molten salts that are liquid at low temperatures (<100 °C) consisting of cations and anions. Most cations are methylimidazolium [Rmim], N-butylpyridinium [R-N-bupy], quaternary ammonium or phosphonium ions, and anions such as hexafluorophosphate, tetrafluoroborate, alkylsulfates, alkylsulfonates, chloride, bromide, nitrate sulfate, aluminium chloride, triflate etc. The variability of the R group of the cation (e.g. methyl, ethyl,butyl, etc.). and of the anion is mostly used to adjust the chemical and physical properties of the ionic liquids (Brennecke and Maginn, 2001).

ILs are composed of large, asymmetric and loosely coordinating organic cations and small inorganic or organic anions. The loose coordination of the cations and anions prevents it from packing and therefore inhibits crystallization of the salt. IL possess some of the properties that are desired for good solvents, such as non-flammability, have a high thermal stability, high ionic conductivity and low vapor pressure. These properties permit their use

in many fields, such as in homogeneous catalysis, synthesis media and extractive media as in liquid/liquid extraction processes (Smith *et al*., 2012).

Ionic liquids (IL) represents a potential alternative, however, there is still a challenge for the large scale application of IL due to complicated synthesis processes and expensive raw materials.

Eutectic mixtures called Deep Eutectic Solvents (DESs) have emerged as a low cost alternative of ILs. Deep eutectic solvents (DESs) share many characteristics and properties with ILs, that is why they are now widely acknowledged as a new class of ionic liquid (IL) analogues (Smith *et al*., 2012).

DESs provide other interesting advantages in comparison with pure ILs, such as the fact that DES preparation may be carried out with 100% atom economy without purification being required, which would favour large scale applications of DESs. Likewise, advantages of DESs such as wide liquid range, water compatibility, low vapor pressure, non flammability, biocompatibility and biodegradability favour their use in many possible technologies (Garcia *et al*., 2015). DESs are mixtures of one or more hydrogen bond acceptors (HBA) and one or more hydrogen bond donors (HBD) that when mixed together in the proper molar ratio, show a big decrease in the melting point compared to the initial compounds (Kareem *et al*., 2013, Hayyan *et al*., 2013). They are usually obtained by the complexation of a quaternary ammonium salt with a metal salt or hydrogen bond donor (HBD).

DESs are recognized by a substantial reduction of lattice energy and hence lowering the freezing point of mixture at eutectic temperature. The decrease in melting point of a mixture in comparison with the melting point of both pure constituents comes from the reduction of

lattice energy through the charge density reduction due to the delocalization of charge from the formation of hydrogen bonding between halide ion and the moiety of hydrogen bond donor (Abbott *et al*., 2003).

DESs are chemically tailorable solvents since they can be designed by properly combining various quaternary ammonium or phosphonium salts (e.g. Choline Chloride) with di erent hydrogen bond donors (HBD). Hence, task-specific DESs with di erent physicochemical properties such as freezing point, viscosity, conductivity, and pH, among others, can be prepared (Zhang *et al.*,2012). Owing to their favourable properties, DESs have found numerous applications in the areas of synthesis media, homogeneous catalysis, metal processing application, extractive media and gas separations.

There is an increasing number of articles dedicated to DESs (Sander *et al*., 2015). The application of DESs in the separation of aromatic/aliphatic hydrocarbons was first reported by Kareem et al 2012. They were the first group to report the use DESs for the extraction of aromatic from aliphatic hydrocarbons. They synthesised DESs from methyl triphenylphosphonium bromide as salt with ethylene glycol as hydrogen bond donor. The DESs was used to separate benzene from benzene/hexane mixtures. The synthesised DESs exhibits superior performance compared to that of N-formlymorpholine and sulfolane as commercially used solvents (Kareem et al., 2012). Toluene was also separated from toluene/heptane mixtures using DESs synthesised from tetrabutylphosphonium bromide as salt with sulfolane and ethylene glycol as hydrogen bond donors to form two different types of DESs (Kareem et al., 2012a). Two DESs were also synthesised from benzyltrimethyl ammonium chloride as salt with ethylene as hydrogen bond donor. Also tetraethylammonium p-toluenesulphonate as salt with sulfolane. These DESs were used to

separate octane from octane/ ethylbenzene mixture at 25^{o} C., with aromatic composition ranges from 10 – 90 wt% aromatics. Low distribution coefficient values were gotten after the liquid -- liquid equilibrium experiments especially when compared with other solvents for similar systems (Hadj-Kali, 2015).

The use of DESs for the separation of aromatic/aliphatic mixtures were reported by many, Sarwono, *et al.*, (2013), Mulyono *et al*., (2014), Hizaddin *et al*., (2015), Sander *et al*., (2015) and Kiki, *et al*., (2016). Most of the works reported in literature show the potential applications of DESs for aromatic extractions. However, the liquid distribution coefficients and selectivity reported were lower than what was reported for conventional solvents like sulfolane.

Liquid-liquid extraction using DESs as extractive solvents for the removal of aromatic compounds is seen as an attractive alternative process that can be operated under mild conditions (room temperature and atmospheric pressure). The efficiency of this process greatly depends on solvent performance.

In this work, a group of ammonium and phosphonium based deep eutectic solvents were synthesized. The solvents were screened and the physical properties of the successful ones were also determined. The extraction capabilities of the solvents were tested for the separation of aromatic and aliphatic compounds via the liquid-liquid extraction (LLE).

1.2 Problem Statement

The conventional methods for the separation of aromatic hydrocarbons from naphtha is energy intensive. Separation using conventional organic solvent for liquid-liquid extraction is expensive and has environmental challenges. There is a need to develop alternative approach such as using Deep Eutectic Solvents (DESs) which are considered

green solvents due to their low volatility for aromatic separation before the furnace section. This is viewed as an alternative process that can be operated under mild temperature and atmospheric pressure conditions.

1.3 Aim and Objectives

1.3.1 Aim

The aim of this work is to investigate the use of novel deep eutectic solvents as non-conventional solvents for the liquid-liquid extraction to separate the aliphatic and aromatic hydrocarbons. This is achieved by utilizing the favourable properties of deep eutectic solvents as alternative solvents

1.3.2 Objectives

The objectives of this research work are to:

i. Synthesised a group of ammonium and phosphonium based deep eutectic solvents

ii. Select suitable DESs for the extraction of aromatic from aromatic / aliphatic mixtures.

iii. Characterisation of the synthesised DESs

iv. Testing the new DESs in liquid-liquid equilibrium experiments of the ternary systems (Toluene + Octane + DESs) at 30, 40 and 50 ^{O}C and atmospheric pressures for the selected ammonium and phosphonium based DESs.

v. Thermodynamic modelling of the liquid-liquid equilibrium data using NRTL and UNIQUAC models.

vi. Testing of the DESs in multi stage extraction and solvent regenerability.

1.4 Justifications

i. This research would contribute in the establishment of a new field of research that would be a seed for green chemical engineering applications. In addition, the following deliverables will be targeted:

ii. Introduction of novel green solvents for potential industrial applications

iii. contribution to the generation of physical properties data for the DESs and LLE data base

1.5 Scope

This research is to cover the synthesis of DESs from ammonium and phosphonium based salts, the determination of the physical properties of the synthesized DESs, the development of LLE data for the synthesized DESs and to benchmark the newly synthesized solvent. The toluene/octane mixture will be used as a model fuel.

CHAPTER TWO

LITERATURE REWIEW

2.1 Deep Eutectic Solvents

Deep eutectic solvents (DESs) are mixtures of one or more hydrogen bond acceptors (HBA) and one or more hydrogen bond donors (HBD) that when mixed together in the proper molar ratio, results in a big decrease in the melting point when compared to the initial compounds (Rodriguez, *et al*., 2015 and Hayyan *et al*., 2013). DESs are new generation solvents that have gained increasing attention as a low cost alternative to ILs. They are usually formed by the complexation of quaternary ammonium or phosphonium salts with a metal salt or hydrogen bond donor (Zhang, *et al.*, 2012 and Smith *et al*., 2012). DESs contains large, non-symmetric ions that have low lattice energy and hence low melting points (Smith *et al*., 2012). The reduction of lattice energy results from the charge density reduction due to the delocalization of charge through the formation of hydrogen bonding. This is responsible for a decrease in melting point of a mixture in comparison with the melting point of the pure components (Abbott *et al.*, 2003 and Zhang *et al*., 2012). Most DESs are liquid at room temperature and up to 150 ^{o}C. They are classified into four categories with their general formulae as shown in Table 2.1 (Smith *et al.*, 2012).

Table 2.1 General formulae for the classification of DESs

Types	**General formula**	**Terms**
Type I	$Cat^{+}X^{-} + zMCl_x$	M=Zn,In,Sn,Al,Fe,Ga
Type II	$Cat^{+}X^{-} + zMCl_x.yH_2O$	M=Cr,Ni,Cu,Fe,Co
Type III	$Cat^{+}X^{-} + zRZ$	Z= $COONH_2$, COOH, OH
Type IV	$MCl^{x}+zRZ$	M = Al, Zn and Z = $COONH_2$, OH

DESs like ionic liquids (ILs), are tailorable by simply changing one or both of the components, gives the possibility of forming a huge number of eutectic mixtures with different properties. They have comparable properties to ILs, especially the low vapour pressure which indicates its non-volatility.

DESs exhibits a broad range of properties, such as wide liquid range, water compatibility, low vapor pressure, non flammability, bio compatibility, and biodegradability favor their use in many possible technologies (Garcia *et al.*, 2015), which makes them suitable solvents for different applications. Recently, they find applications in many fields, including production and purifications of biodiesel, gas adsorption, metal processing, extraction and synthesis media. Figure 2.1. shows the typical structures of the salts and hydrogen bond donors used in the formation of deep eutectic solvents.

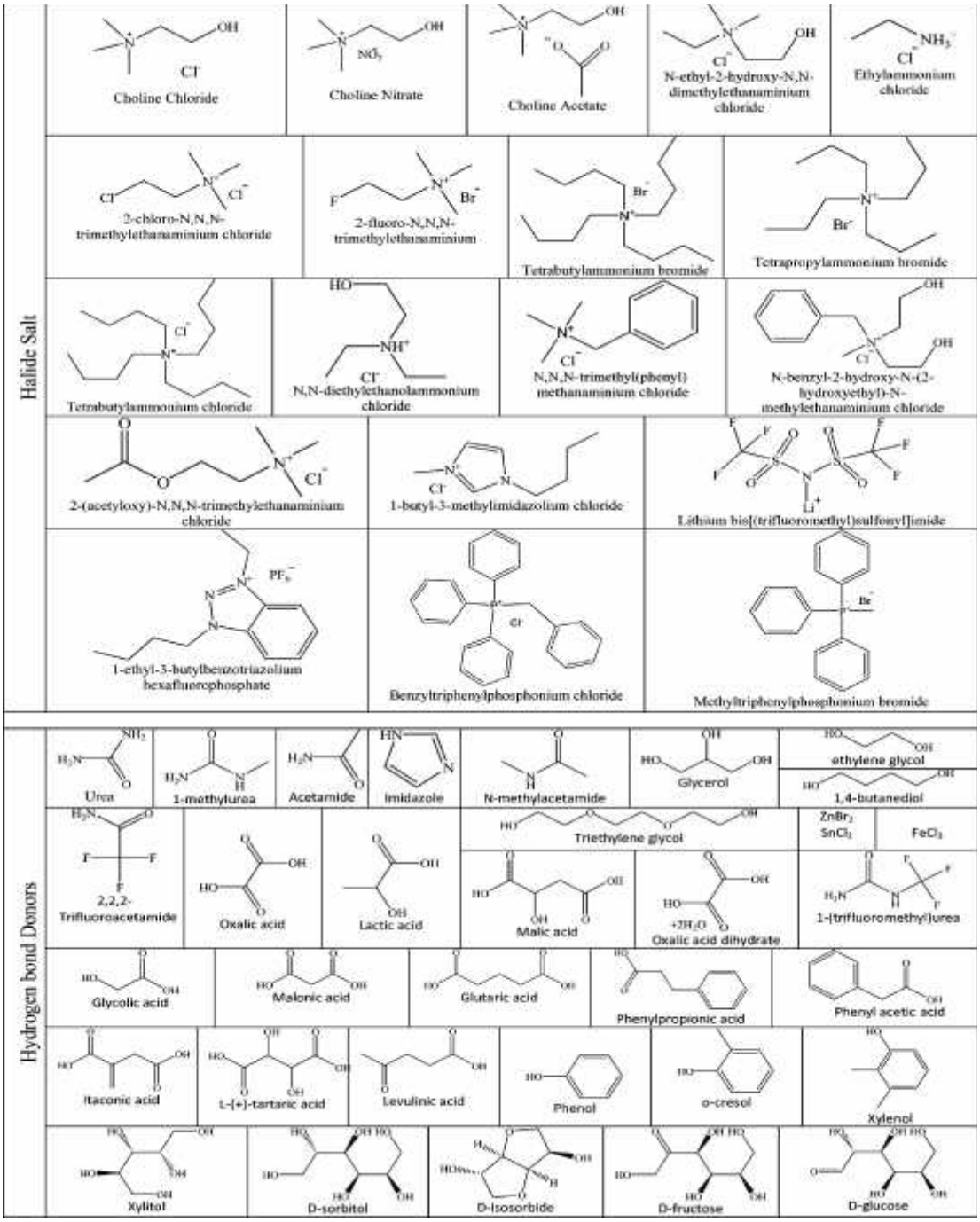

Figure 2.1: Typical structures of the salts and hydrogen bond donors used in the formation of deep eutectic solvents.

2.2 Application of DESs as extracting agents or as separation media

The applications of DESs as extracting agents or as separation media that have been reported so far are in the separation of azeotropic mixtures, desulphurization of fuels and separation of aromatic/aliphatic hyrocarbons. Glycerin was extracted from palm oil-based biodiesel using ChCl/glycerin DESs, (Hayyan *et al.*, 2010). The efficiency of the extraction process was examined based on the composition of the DES: biodiesel ratio. The standard specifications for the biodiesel as a fuel in terms of glycerin content were met after the final analysis.

Azeotropic mixture of ethanol and *n*-heptane were separated using three DESs that are made from ChCl/glycerol, ChCl/levulinic acid and ChCl/EG all at a salt: HBD ratio of 1:2. The DESs synthesised from ChCl/glycerol and ChCl/EG have lower distribution coefficient and high selectivity, especially when compared with ChCl/ levulinic acid having high distribution ratio and low selectivity (Oliveira, *et al.*, 2013). The separation of azeotropic mixtures of ethanol / n-heptane and ethanol / hexane with DESs were also reported by (Rodriguez, *et al.*, 2015). They synthesised DESs from ChCl with lactic acid and glycolic acid with salt: HBD ratio of 2:1 and 1:1 respectively. They reported that the solute distribution coefficient and the selectivity values of the DESs were higher when compared to previously studied ILs. DESs were also reported in the deep extractive desulphurization of liquid fuel. DESs was synthesised from tetrabutylphosphonium bromide and stannous chloride at a molar ration of 1:1. It was then used in the extractive desulphurization of dibenzothiophene (DBT) and thiophene as Sulphur compounds from simulated fuel. The results showed the potential of the DESs to extract the DBT and thiophene at 69.57% and

47.28% efficiency respectively. (Gano, 2015). Table 2.2: is the reviewed works on separation of aromatic/aliphatic hydrocarbons using ILs

Table 2.2: Reviewed works on separation of aromatic/aliphatic hydrocarbons using ILs.

Aromatics/Aliphatics Mixtures	Solvent (ILs)	T (^{o}C)	S	D	%R	References.
Heptane/Ebenzene	[Bpy][NO_3]	25.15	42.93	0.49		Enyati (2017)
Octane/Ebenzene		25.15	53.85	0.60		
Decane/Ebenzene		25.15	70.85	0.68		
Toluene/Heptane	[emmim]Tf_2N	40	22.7	0.61		Larriba (2013)
Toluene/Heptane	[emmim][SCN]	40	97.7	0.12		
Toluene/Heptane	[bupy]BF_4	40	74.4	0.43		Garcia (2010)
Toluene/Heptane	[hpy]BF_4	40	25.6	0.67		
Toluene/Heptane	[mmim][Tf2N]	40	37.6	0.72		Garcia (2011)
Toluene/Heptane	[emim]Tf2N	40	30.3	0.93		
Benzene/Cyclohexane	[BMim][MSO_4]	25	18.23	0.71		Dominguez (2012)
Benzene/Methylcyclohexan			35.04	0.78		
EthylBenzene/Cyclohexane			4.89	0.18		
EthylBenzene/Methylcyclohexane			8.63	0.19		
EthylBenzene/Cyclooctane			8.81	0.16		
Benzene/Cyclohexane	[bmpy][BF_4]*	30			43.05	Abu-Eisha (2008)
Toluene/Cyclohexane					32.61	
Ethylbenzene/Cyclohexane					20.61	
Toluene/Heptane	[MMim][$MeSO_4$]	45	66.01	0.085		Reina (2013)

S = selectivity, D = Distribution coefficients, %R, = percentage aromatic removal

2.3 Application of DESs in separation of aromatic/aliphatic hydrocarbons

The application of ILs for liquid-liquid separation of aromatic/aliphatic has been reported by many researchers. One of the favourable characteristics of ILs that makes them suitable solvents is their non-volatile nature (Canales and Brennecke, 2016, Meindersma, 2005). Table 2.2 gives a review works dealing with the separation of aromatic/aliphatic using ILs. Similarly, DESs provide other interesting advantages in comparison with pure ILs. This includes the fact that DES preparation may be carried out with 100% atom economy without purification being required, which would favour largescale production and applications of DESs.

The use of DESs in the separation of aromatic/aliphatic hydrocarbons was first reported by (Kareem *et al*., 2012). Ternary liquid-liquid equilibrium experiments for systems comprising of phosphonium based DESs with benzene and hexane at different temperatures was carried out. The DESs was formed from methyltriphenylphosphonium bromide (MTPPBr) with ethelyne glycol (EG) at salt:HBD molar ratios of 1:4, 1:6 and 1:8 and used to separate benzene from *n*-hexane (Kareem *et al*., 2012). They reported that all prepared DESs showed superior results compared to that of sulfolane and N-formylmorpholine in terms of distribution coefficients, selectivity and cross solubility. The same group later reported the separation of toluene from n-heptane using tetrabutylphosphonium bromide (TBPB) with ethylene glycol or sulfolane at various ratios to form the DESs (Kareem *et al.,* 2012a). Two DESs were synthesised from choline chloride: urea (ChCl: Ur) and choline chloride: glycerol (ChCl: Gly) at 1:2 molar ratios. The DESs were used to separate pyridine from its mixture with hexane. The DESs synthesised from (ChCl: Gly) give a better performance as an extracting solvent. (Sander, *et al.,* 2015). The potential of two DESs synthesised from tetrahexyl ammonium bromide

(THAB) as salt and ethylene glycol and glycerol as hydrogen bond donor at a molar ratio of 1:2 were tested for the removal of benzene with its mixture with hexane. The liquid liquid equilibrium composition data were used to plot the ternary diagram. It was observed that the solvent was not present in the extract phase, indicating the non-cross mixing of solvents, a property that is desired of a good solvent. (Rodriguez, *et at*., 2015). The mixtures of benzene, toluene, ethylbenzene and xylene (BTEX) were formed each octane. Each of the aromatic was separated from its mixture from octane using DES synthesised from tetrabutyl ammonium bromide and sulfolane at 1:4 molar ratios and at 25 ^{O}C. Equilibrium data for the ternary systems of (BTEX), octane and DES were plotted. It was reported that the distribution coefficient and selectivity values of the systems have comparable values with those of commercial solvents. (Mulyono, *et al.,* 2014).

Table 2.3 presents a review of the available works on the separation of aromatic from aliphatic hydrocarbons using different combination of DESs and also the feed mixtures. Most of the works reported showed the potential applications of DESs for aromatic extractions. However, the liquid distribution coefficients and selectivity reported were lower than what was reported for conventional solvents like sulfolane with liquid distribution coefficient of 0.48 in weight percent basis, and selectivity of 30. (Meindersma, 2005).

Table 2.3: Reviewed works on separation of aromatic/aliphatic hydrocarbons using DESs.

Aromatics/Aliphatics mixtures	Solvent (DES)	T (^oC)	S	D	Reference
Benzene +n-haxene	MTPPB:EG(1:4)	45	93.672	2.21	Kareem, (2012)
	MTPPB:EG(1:6)	35	70.813	2.33	
	MTPPB:EG(1:8)	45	26.038	1.30	
Toluene + n-heptane	TBPB:EG(1:2)	40	15.38	0.95	Kareem (2012a)
	TBPB:EG(1:4)	40	12.44	0.51	
	TBPB:EG(1:6)	30	22.27	0.44	
	TBPB:EG(1:8)	30	25.89	0.38	
	TBPB:SOLF(1:2)	50	9.87	0.82	
	TBPB:SOLF(1:6)	40	13.28	0.25	
	TBPB:SOLF(1:8)	60	17.60	0.66	
Toluene + n-heptane	ETPPI:EG(1:6)	40	37.02	0.16	Kareem (2013)
	ETPPI:EG(1:8)	60	20.75	0.13	
	ETPPI:EG(1:10)	50	65.83	0.22	
	ETPPI:SOLF(1:4)	30	44.21	0.57	
	ETPPI:SOLF(1:6)	30	44.75	0.39	
	ETPPI:SOLF(1:8)	50	34.40	0.57	
Ethylbenzene + n-octane	BZTACl:EG	25	10.12	0.05	Hadji-Kali (2015)
	TEApTS:SOLF	25	32.20	0.21	
Benzene + n-hexane	ChCl:Glucose (1:1)	25	36.05	0.12	Kiki (2016)
Toluene + n-toluene		25	14.27	0.05	
Pyridine + n-hexane		25	17.16	0.66	
Ethylbenzene + n-octane	TBAB:EG(1:8)	25	7.4	0.99	Hizaddin (2015)
	TBAB:PRD(1:4)	25	8.7	0.18	
	TBAB:PRD:EG(1:4:4)	25	8.7	0.18	
	TBAB:PRD:EG(1:4:6)	25	15.8	0.24	
	TBAB:PRD:EG(1:6:4)		14.2	0.88	
Toluene + n-Octane	TBAB:SOLF(1:4)	25	25.7	0.50	Mulyono (2014)
Xylene + n-Octane			27.2	0.42	
Benzene + n-Octane			46.4	0.40	
Ethylbenzene+n-Octane			18.7	0.45	
Hexane + Benzene	THABr:Gyl(1:2)	25	8.58	1.41	Rodriquez (2015)
	THABr:EG(1:2)		4.94	1.07	
Ethylbenzene+Octane	TEApTS:EG(1:4)	25	11.11	0.07	Sarwono (2013)
	BZTBACl:LA(1:4)		12.53	0.03	
	TBAB:SOLF(1:4)		18.69	0.51	
	TEApTS:SOLF(1:4)		16.20	0.62	

S = selectivity, D = Distribution coefficients

2.3 Properties of Deep Eutectic Solvents

DESs have similar physico-chemical properties to ILs, such as freezing points, viscosity, density, conductivity and refractive index among others.

2.3.1 Density

Density is one of the important property of solvents as its measurements is used in mass transfer calculations and in the design of many chemical processes. Most DESs exhibit higher densities than water. Temperature effect of density is required for the development of industrial processes (Garcia *et al.*, 2015). Density is a thermo physical property, and it has been studied for many DESs, and most of these densities values falls within 1.0 – 1.35 g/cm^3 range at 298.15 K (Garcia *et al.*, 2015). The densities of some DESs also falls within the range of 1.10 – 1.34 g/cm^3 at 298.15 K (Zhang *et.al.*, 2012).

2.3.2 Viscosity

Viscosity data are very important for equipment design and fluid flow calculations. Temperature effects on viscosity also helps in knowing the energy requirements for processing of solvents (Hayyan *et al*., 2013, Zhang *et.al*., 2012.and Naser *et al*., 2013). Most DESs exhibits relatively high viscosity (> 100 cp) especially when compared to water with 0.89 cp at room temperature (Zhang *et.al.*, 2012).The high viscosity of DESs is often attributed to the presence of an extensive hydrogen bond network between each component, which results in a lower mobility of free species within the DESs. This high viscosity values of most DESs is also as a result of large ion size, small void volume and presence of other forces such as electrostatic or van der Waals interactions (Zhang *et.al*., 2012). Table 2.4 shows the viscosities of some selected DESs at different temperatures.

Table 2.4: Viscosities of some selected DESs at different temperatures

Organic salts	Hydrogen bond donors (HBD)	Salt:HBD molar ratio	Viscosity (cP)
ChCl	Urea	1:2	750 (25 ^{o}C)
ChCl	Urea	1:2	169 (40 ^{o}C)
ChCl	EG	1:2	36(20 ^{o}C)
ChCl	EG	1:2	37 (25 ^{o}C)
ChCl	EG	1:3	19 (20 ^{o}C)
ChCl	EG	1:4	19 (20 ^{o}C)
ChCl	Glucose	1:1	34400 (50 ^{o}C)
ChCl	Glycerol	1:2	376 (20 ^{o}C)
ChCl	Glycerol	1:2	259 (25 ^{o}C)
ChCl	Glycerol	1:3	450 (20 ^{o}C)
ChCl	Glycerol	1:4	503 (20 ^{o}C)
$ZnCl_2$	Urea	1:3.5	11340 (25 ^{o}C)
Bu_2NBr	Imidazole	3:7	810 (20 ^{o}C)
$EtNH_3Cl$	Accetamide	1:1.5	64 (40 ^{o}C)

Source: Zhang *et., al*. 2012.

2.3.3 Freezing point

DESs are usually characterized by significant depression of freezing point. The freezing point of any DES mixture is dependent on these major factors; the individual lattice energy of the salts (quaternary ammonium or phosphonium), the degree of the interaction between the hydrogen bond donating group of the HBD and the entropy change for the formation of liquid phase (Abbott *et al*., 2004). For example, when ChCl and Urea are mixed together in a molar ratio of 1:2, the freezing point of the eutectic is 12 ^{o}C, which is lower for ChCl and Urea with 303 and 133 ^{o}C respectively (Zhang *et.al.*, 2012). The freezing points of some DESs were reported as low as 150 ^{o}C, some appear to be more attractive solvents with freezing point lower than 50 ^{o}C, since they can be used as cheap and safe solvents.

2.3.4 Refractive index

Refractive index provides useful information when studying the force between molecules or their behaviour in solutions. It is a measure of the electronic polarizability of a

molecule (Florindo, *et al*., 2014). Refractive index is the ratio of speed of light in vacuum relative to that in a given sample. It is used to measure the purity of a sample or concentration of solute in a solution (Kareem *et al*., 2010). Typical values of refractive indices decrease with increasing temperature as a result of decreasing density of the substance.

2.3.5 Conductivity

Conductivity is a function of the mobility of ions in solutions. Most DESs exhibits poor ionic conductivities (lower than 2 mS/cm at room temperature). Generally, conductivities increase significantly as the temperature increases due to a decrease in the viscosity, hence the ions move faster. The electrical conductivities of some studied DESs were reported to exhibits exponential behaviour with temperature (Bahadori *et al*., 2013).

2.4 Liquid-Liquid Extraction

Liquid-liquid extraction (LLE) is a process for separating components dissolved in a liquid feed by contact with a second liquid phase. The extraction process produces a solvent-rich stream called the extract that contains a portion of the feed and an extracted feed stream called the raffinate. LLE is used primarily when direct distillation is not economical, where distillation would require excessive amounts of heat, when the relative volatility is near unity, when the formation of azeotropes limits the degree of separation obtainable in distillation, when heating must be avoided, when the components to be separated are quite different in nature (Richardson and Harker 2002). Important applications of liquid liquid extraction include the separation or extraction of penicillin from fermentation broth by contact with amyl or butyl acetate, separation of aromatic (rings) from aliphatic (straight chains) by contact with tri ethylene glycol.

Liquid-liquid extraction process is widely applied in petroleum, hydrometallurgical, pharmaceutical, and nuclear industries (Rodriguez *et al*., 2015, and Hayyan *et al.*, 2013). Two extraction parameter values, solute distribution coefficient and selectivity are used in evaluating the performance of the solvent the extraction processes. (Letcher and Reddy 2004). The solubility difference of a solute between two phases as a result of the difference in the strength of interactions between molecules of the solute and those of the two solvents is the basis of separation, rather than differences in relative volatilities as in distillations. The suitability of a solvent to perform liquid-liquid extraction, is assessed using these parameters. They are usually calculated from the experimental LLE data as follows:

Solute distribution coefficient, β, as :

$$\beta = \frac{x_S^{e\ \ \ pha}}{x_S^{r_i\ \ \ pha}} \qquad 2.1$$

selectivity, S, as:

$$S = \left[\frac{x_S^{e\ \ \ pha}}{x_S^{r_i\ \ \ pha}}\right] / \left[\frac{x_d^{e\ \ \ pha/c}}{x_d^{r\ \ \ pha/c}}\right] \qquad 2.2$$

where x is the mole fraction.(Hansmier, *et al.*, 2010).

The solute distribution coefficient is related to the amount of solvent required for the extraction process and to the capacity of the solvent to extract the solute of interest. A high distribution coefficient means high solubility of the solute in the solvent. The selectivity evaluates the efficiency of the solvent used and indicates the ease of extraction of a solute from the diluent. High values of selectivity means low solubility of the carrier in the solvent. Large values of these parameters indicate a good degree of separation of the solute with a small amount of solvent. Theoretically, a higher solute distribution coefficient means a smaller equipment dimensions and lower operating costs while a

higher selectivity corresponds to fewer stages for a given separation and less residual diluent in the extract (Kareem *et al*., 2012).

2.4.1 Thermodynamic Considerations.

Models for the description of real mixture behaviour are of fundamental importance for the synthesis, simulation, design, and operation of many separation processes used in industry (e.g. distillation and extraction). Since often 60-80% of the total costs arise in the separation step, knowledge of the phase equilibrium behaviour of the system to be separated is of special importance to industrial practitioners (Gmehling, 2009).

Thermodynamic models were developed in order to quantify deviation of liquid mixtures from ideal solution. These models are mainly based on developing excess-Gibbs-energy equations and cover both aqueous electrolyte and organic non-electrolyte systems. These deviations are usually characterized by activity coefficients. In the last years' different thermodynamic models, theoretical or semi empirical, have been developed in order to calculate the activity coefficients of liquid mixtures as a function of composition and temperature (Li, 2015).

2.4.2 Wilson Model

The Wilson model (Equation 2.3) uses the concept of "local composition" it has two binary interaction parameters, , G_{ij} and G_{ji} for each pair of components and these parameters are related to the pure component molar volumes and is given by equation 2.4, and is able to predict multi-component properties from binary data (Wilson, 1964).

$$ln\,\gamma_K = 1 - ln\,\sum_{j=1}^{m} x_j G_K \; - \sum_{i=1}^{m} \frac{x_i G_{ij}}{\sum_{j-1}^{m} x_j G_{ij}} \qquad 2.3$$

$$G_{ij} = \frac{V_j^L}{V_i^L} \exp\left[-\left(\lambda_{ij} - \lambda_{ii}\right)/R\right] \qquad 2.4$$

G_{ij} parameters that can be obtained from experimental data and we have $G_{ii} = G_{jj} = 1$, V_i^L is molar volume of pure liquid component i. λ_{ij} are interaction energy between components i and j, where we have $\lambda_{ij} = \lambda_{ji}$. T is absolute temperature in Kelvin and R is universal gas constant. The Wilson model is unable to predict limited miscibility; this drawback significantly limits its usage in solvent extraction. The Wilson's equation should be used for liquid systems that are completely miscible or else for those limited regions of partially miscible systems where only single liquid phase is present (Prausnitz *et al*.,1999).

2.4.3 The Non-Random Two Liquid Model (NRTL)

The NRTL model (Equation 2.5) is the most extensively used model for liquid-liquid equilibrium to date. The equation was developed by Renon, H. and Prausnitz, J.M., (Renon and Prausnitz, 1968). They postulated that the NRTL model accepts the non-randomness of the distribution of molecules in a solution, that is the molecules are 'semi ordered'. The NRTL model introduces the non-randomness parameter, α_{ij}, which is intended to account for the non-random distribution of type i molecules in solution relative to type j molecules. In case, αij is equal to zero, the mixture is said to be completely random (ideal solution). This parameter gives an additional degree of freedom to the NRTL model. It makes its application over a large variety of binary and ternary mixtures and allows a very good prediction of LLE., (Kareem *et al.*, 2013). This parameter is considered to be independent of temperature. When this model is applied, the authors suggested values of, αij from 0.2 to 0.47, depending on the type of compounds present in the mixture.

$$ln\ \gamma_i = \left(\frac{\sum_{j-1}^{N} x_j \tau_j G_j}{\sum_{k=1}^{N} x_k G_k}\right) + \sum_{j-1}^{N}\left(\frac{x_j G_i}{\sum_{j=1}^{N} x_k G_k}\right) * \left(\tau_i - \frac{\sum_{k-1}^{N} x_k \tau_k G_k}{\sum_{k=1}^{N} x_k G_k}\right) \quad 2.5$$

where

$$G_j = e^{(-\alpha_j * \tau_j)} \qquad \alpha_j = \alpha_i$$

$$\tau_i = \frac{g_i - g_j}{R} = \frac{\Delta g_i}{R}, \qquad \tau_j = \frac{g_j - g_i}{R} = \frac{\Delta g_j}{R},$$

In this model, each pair of molecules have two adjustable energy parameters (τ_{ji} and τ_{ji}) and one non-randomness parameter (α_{ij}) that can be either adjustable or fixed to characterise the non-ideality of solutions. The model is able to correlate VLE and LLE systems with satisfactory accuracy and has the capability to predict equilibria of ternary systems from binary data, including strongly non-ideal mixtures, especially partially immiscible systems.

2.4.4 UNIQUAC Model

The Universal Quasi-Chemical (UNIQUAC) equation was derived by extending the quasi-chemical theory of Guggenhein for non-random mixtures to solutions containing molecules of different size (Abrams, and Prausnitz, 1975). The model is applicable to a wide range of non-electrolyte systems including polymer solutions. The (UNIQUAC) model (Equation 2.7) has two parts, a combinatorial (Equation 2.8) and residual (Equation 2.9). The former attempts to describe the dominant entropic combination and it is determined by the composition, size and shape of the molecules from pure components data. The residual part is intermolecular force dependent and it accounts for the enthalpy of mixing. It has two binary adjustable parameters for each molecular pair.

The activity coefficient equation can be written as

$$ln\ \gamma_i = ln\ \gamma_i^c + ln\ \gamma_i^r \quad 2.7$$

$$ln\ \gamma_i^c = ln\ \frac{\Phi_i^*}{x_i} + \frac{z}{2} q_i ln\ \frac{\theta_i}{\Phi_i^*} + l_i - \frac{\Phi_i^*}{x_i} \sum_{j=1}^{N} x_i l_i \quad 2.8$$

$$ln\ \gamma_i^r = q_i' - q_i' ln\left(\sum_{j=1}^{N} \theta_j' \tau_j\right) - q_i' \sum_{K=1}^{N} \frac{\theta_j' \tau_i}{\sum_{k=1}^{N} \theta_k' \tau_k} \quad 2.9$$

$$l_j = \frac{z}{2}.(r_j - q_j) - (r_j - 1)$$

The segment fraction Φ_i^* and area fraction $\theta\ a \quad \theta^i$ are given by

$$\Phi_i^* = \frac{r_i x_i}{\sum_{j=1}^{N} r_j x_j}$$

$$\theta_i = \frac{q_i x_i}{\sum_{j=1}^{N} q_j x_j}$$

$$\theta_i' = \frac{q_i' x_i}{\sum_{j=1}^{N} q_j' x_j}$$

$$\tau_i = e. \left(-\frac{U_i - U_j}{R.T}\right)$$

where z is the lattice coordination number arbitrary given the value 10., r, q and q' are pure component molecular structural parameter, dependent on molecular size and external surface area. The τ_i is binary parameter for a j-i pair of molecules and U_i is the energy of interaction. $q_i = q_i'$ for components other than water and lower alcohols.

The UNIQUAC model uses only two adjustable binary parameters for each pair of molecules, which requires pure-component constants and it is applicable to a vast variety of non-polar, or polar liquid mixtures such as hydrocarbons for VLE and LLE with high accuracy as that of NRTL (Li, 2015).

CHAPTER THREE

MATERIALS AND METHODS

3.1. Materials

This section covers the list of equipment and material / chemical used in this thesis.

3.1.1 High performance liquid chromatography (HPLC Agilent 1260) equipment

A high performance liquid chromatography equipment (HPLC Agilent 1260) infinity series equipped with variable wave length detector and a reversed column was used. The column specifications are 150 x 4.6 mm, 5µm, 100A (Ecosil C18-extend). Figure 3.1 show the HPLC.

Figure 3.1: Agilent(R) high performance liquid chromatography (HPLC) equipment

3.1.2 Spectrophotometer equipment

A PerkinElmer Lambda 25 UV-visible spectrophotometer A quartz cuvette was employed; measurements were carried out in the UV region (200-400 nm). Other parameters utilized include slit width of 1 nm, scan speed of 480 nm/min, lamp change at 326 nm and data interval of 1 nm.

3.1.3 Thermomixer equipment

The thermomixer, ThermoMixer® MKR 13 and MHR 23 has the specification presented in Table 3.1; Figure 3.2 shows the picture of the thermomixer used in this work.

Table.3.1: Thermomixers Specifications

	Specifications	
Parameter	**MKR 13**	**MHR 23**
Temperature work range	Amb-16°C – 373.15°C	Amb+3°C – 373.15°C
Temperature adjustable range	-10°C – +105°C	272.15°C – 410.15°C
Accuracy / Resolution	+/- 0.1°C / 0.1°C	+/- 0.1°C / 0.1°C
Maximum heating rate	6.0°C / min	9.5°C / min
Maximum cooling rate	12°C / min	No cooling
Shaking frequency	200 – 1,500 rpm	200 – 1,500 rpm
Orbit	3 mm orbital	3 mm orbital
Dimensions (W x D x H)	220 x 330 x 144 mm	220 x 330 x 109 mm
Capacity	1 thermoblock	2 exchangeable thermoblock
Weight (without block / blocks)	9 kg	7 kg
Electrical heating- / cooling-power	130 W	350 W
Electrical supply	115 V / 230 V, 50-60 Hz	115 V / 230 V, 50-60 Hz

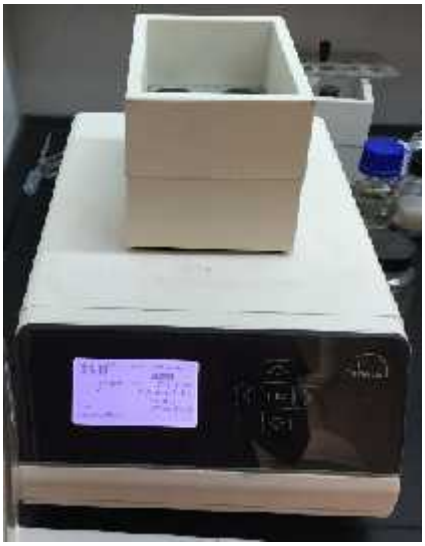

Figure 3.2: Cooling thermomixer equipment used in this work

3.1.4 Mass balance

SHIMADZU(R) (model: AUW220D) mass balance equipped with an internal auto calibration procedure. The balance has an accuracy of ±0.0001g for measurements less than 220g and ±0.00001g for measurements less than 82g.

3.1.5 Density meter

Anton Paar (R)DMA4500M density meter equipped with internal temperature controller as shown in Figure 3.3.

Figure 3.3. Anton Paar (R)DMA4500M density meter

3.1.6 Viscometer

The viscosity measurement was done with Brookfield DV-II Pro(R) viscometer equipped with Tchne-Tempette TE-E8 external water circulator for controlling temperature.

3.1.7 The conductivity measurement was done with Jenway conductivity meter (Model 4520)

3.1.8 Refractometer

The refractive index measurement was done with Mettler Toledo Portable Excellence RM 40 Digital Bench top refractometer the refractometer as shown in Figure 3.4.

Figure 3.4. Mettler Toledo refractometer

3.1.9 PerkinElmer Fourier transform infrared spectroscopy (FTIR) The model of the FTIR used was the Frontier with a serial number of LR 64912C equipped with class 1 Laser product, BS EN & IEC 60825 - 1: 2007. Scans were made at a resolution of 32 cm^{-1} and accumulation set at 64. Prior to the FTIR analysis, a drop of the DES is added to an appropriate amount of KBr (palatalizing matrix) and grounded to powder before the analysis.

3.1.10 Rotary evaporator (IKA RV 10) (R) using tap water at room temperature as the cooling fluid.

Figure 3.5 Rotary evaporator (IKA RV 10) (R)

Table 3.2 Names of chemical used

	CAS No.	**Purity (wt%)**	**Molecular weight(g/mol)**	**Manufacturer**
Tetrabutylammonium bromide		>99.9		Aldrich
Tetrabutylphosphonium bromide		99.00		Alfa
2,3,4,5-tetrahydrothiophene-1,1-dioxide (sulfolane)	126-33-0	>99.00	120.17	Acros organics
Poly(ethylene glycol) 200 (PEG 200)	25322-68-3	-	190-200	Merck
Poly(ethylene glycol) 400 (PEG 400)	25322-68-3	-	390-400	Merck
Poly(ethylene glycol) 600 (PEG 600)	25322-68-3	-	590-600	Merck
Ethylene glycol		99.00		Merck
TetrabutylphosphoniumMethanesulfonate $[P_{4444}][MeSO_3]^+$	98342-59-7	≥ 98	354.50	Aldrich
Hexane		99.99		Aldrich
Toluene	108-88-3	99.00	92.14	Honeywell
Octane		99.99		Merck
Heptane		99.99		Aldrich
Xylene		>99.00		Aldrich
Dimethyl formamide (DMF)		99.00		Merck
Acetonitrile (ACN)	75-05-8	>99.90	41.05	VWR chemicals
Dimethyl sulfoxide (DMSO)	67-68-5	99.99	78.13	Fischer chemicals
Methanol (MeOH)	67-56-1	99.99	32.04	VWR chemicals (Fischer chemical)
Acetone	67-64-1	≥99.50	58.08	Sigma aldrich
Benzene				
Benzyltriphenylphosphonium chloride		NA		Merck
Methyltriphenylphosphonium bromide		98		Merck

3.2 Methods

This section describes the methodology used in carrying out this thesis. The section is divided into five subsections; DESs synthesis and selections, characterization of the selected DESs, liquid-liquid equilibrium experiments, multistage extraction with model and synthetic (real) naphtha feed and solvent regeneration experiments.

3.2.1 DESs Synthesis

DESs were prepared by measuring and mixing the ammonium or phosphonium salts with the hydrogen bond donor HBD to form the solvent. The salts to HBD are usually in fixed molar ratio. The mixture was heated up to 80 ^{o}C and 600rpm inside screw capped bottles for an hour until a clear homogeneous liquid is formed (Kareem *et al.*, 2013).

The DESs synthesis were performed in small vials of about 20 cm^3, by measuring the salts with the hydrogen bond donor HBD or complexing agents, in a fixed molar ratio. 14 ammonium and phosphonium salts with 13 HBDs at varied combinations molar ratio (1-2 ratio for salts and 1-6 ratios for HBDs) were tested during the synthesis experiments. The molar combinations that forms the homogeneous solution were termed successful DESs, while those that could not were termed unsuccessful DESs.

3.2.2 DESs Screening

The successful DESs were further re-synthesized in a larger quantity as samples for screening experiments. The following factors were considered during the screening and selection of the DESs used in this thesis: Aromatic removal efficiency, High distribution ratio, high selectivity, cost and states at room temperature for facilitating easier handling and usage (Hadji-Kali *et al*., 2016, Kareem, *et al*., 2013).

The extraction potential of the successful DESs were carried out via liquid-liquid equilibrium extraction. Mixtures of toluene and octane using 10 wt.% of toluene in octane as the model fuel (feed). DESs as solvent were added to the model fuel at a feed to solvent mass ratio of 1: 1. Liquid liquid equilibrium experiments were carried on the solvent fuel mixture at 40 ^{o}C inside a screw caped bottles. (Meimdersma, 2005). Detailed LLE experiment is in section 3.2.4.

The aromatic removal efficiency was calculated from Equation 3.0

$$A\ o \qquad r\epsilon \qquad e \qquad = \frac{C_o - C_a}{C_o} . 100 \qquad 3.0$$

where Co is the initial toluene concentration, Ca is the toluene concentration in the raffinate phase after extraction with the DESs, (Hadj-Kali, *et al*., 2016; Kareem *et al*., 2013).

3.2.3. Deep Eutectic Solvents Characterization

All the DESs samples were stored in well-sealed vials after the preparation. The following physical properties of the selected DESs, which include density, viscosity, conductivity and refractive index with temperature were determined.

The physical property measurement was carried out in the temperature range of 303.15 K to 363.15 K. The density measurement was done using Anton Paar DMA4500M density meter equipped with internal temperature controller. The densities of the studied DESs were measured at different temperatures ranging from 30 to 80 . The viscosity measurement was done with Brookfield DV-II Pro viscometer equipped with Tchne-Tempette TE-E8 external water circulator for controlling temperature. The viscosity measurement was done at 30 to 80 . The refractive index measurement was done with metler Toledo refractometer at 30 to 80 . The conductivity measurement was done with Jenway conductivity meter (model 4520)

3.2.4 Liquid-liquid equilibrium experiments

Mixtures of toluene and octane were prepared in five different concentrations of (2.5, 5.0, 10.0, 15.0, and 20.0 wt. % toluene), to form the feed. DESs as solvent were added to the feed samples at a feed: solvent mass ratio of 1: 1. Each set of experiment was conducted at 30, 40 and 50 ^{o}C. The mixtures of the solvent and the feed were put in a screw capped vials. The vials were put inside a ThermoMixer MKR 13 and MHR 23 with specification presented in Table 3.1 capable of controlling the temperature and the speed. The mixture was agitated for 6 hours at 600 rpm and allowed to settle for 12 hours to attain equilibrium (Kareem *et al.*, 2013). Micropipette was used to separate the top raffinate layer and the bottom layers which were analyzed using high performance liquid chromatography (Agilent 1260) infinity series equipped with variable wave length detector and a reversed column.

Table 3.3: HPLC Methods

	Sample	Wave length (nm)	Mobile phase	Injection volume	Elution time	Temperature ^{o}C	Flow rate	Methods R^2
1	Toluene	230	100% MeOH	3 µL	4 min	25	1	0.9999
2	BTX	230	80%ACN 20%H_2O	3 µL	5 min	25	1	0.9978

3.2.5 Thermodynamic modelling

The non-random two liquid (NRTL) and the universal quasi-chemical (UNIQUAC) models are excess energy models that are used in correlating non-ideal liquid phase activity coefficient of components in liquid mixtures.

The condition for thermodynamic equilibrium for multicomponent liquid-liquid systems can be expressed as in Equation 3.1 and 3.2 (Hizadin, 2015).

$$x_i^I \gamma_i^I - x_i^{I\prime} \gamma_i^{I\prime} = 0 \quad 3.1$$

$$K_i = \frac{x_i^{II}}{x_i^I} = \frac{\gamma_i^I}{\gamma_i^{II}} \quad 3.2$$

The calculated liquid-liquid equilibrium phase compositions for the extract and raffinate phases are obtained by solving the modified Richford-Rice isothermal flash calculations, Equation 3.3 – 3.7 (Bharti *et al*., 2017).

$$f(\varphi) = \sum_{i=1}^{c} \frac{Z_i(1-K_i)}{1+\varphi(K_i-1)} = 0 \quad 3.3$$

$$Z_i = \frac{x_i^I - x_i^I}{2} \quad 3.4$$

$$\varphi = \frac{L_i}{F} \quad 3.5$$

$$x_i^I = \frac{Z_i}{1+\varphi(K_i-1)} \quad 3.6$$

$$x_i^{I\prime} = K_i \; x_i^I \quad 3.7$$

where γ_i is the activity coefficient of component i in phase I or phase II, predicted using the NRTL and UNIQUAC model. x_i^I and $x_i^{I\prime}$ are mole fractions of component i in phase I and II respectively and Z_i is the feed concentration and K_i is the distribution coefficient.

The binary interaction parameters are obtained from the experimental LLE data using the objective function $F_{ob,}$ (Equation 3.8) which minimizes the sum of square of the difference between the experimental and the calculated compositions as described by the modified

Richford-Rice flash algorithm in Figure 3.6, using genetic algorithm (GA) toolbox in Math lab software.

$$F_o = \sum_{k=1}^{m}\sum_{i=1}^{c}\sum_{l=I}^{l_i}(x_{ki}^{l} - \hat{x}_{ki}^{l})^2 \qquad 3.8$$

The root-mean-square deviation (RMSD) values, provides a measure of comparison between the experimental and calculated compositions of each components in the two liquid phases and is given by Equation 3.10

$$R = \left[\frac{F_o}{2m}\right]^{1/2} \qquad 3.9$$

$$R = \left[\sum_{k=1}^{m}\sum_{i=1}^{c}\sum_{l=I}^{l_i}\frac{(x_{ki}^{l} - \hat{x}_{ki}^{l})^2}{2m}\right]^{1/2} \qquad 3.10$$

where x_{ki}^{l} and $\hat{x}_{ki}^{l}$ are the respective experimental and predicted values of mole fraction for component i for the kth tie line in phase l, m is the number of tie lines and c is the number of components. (Bharti *et al*., 2017).

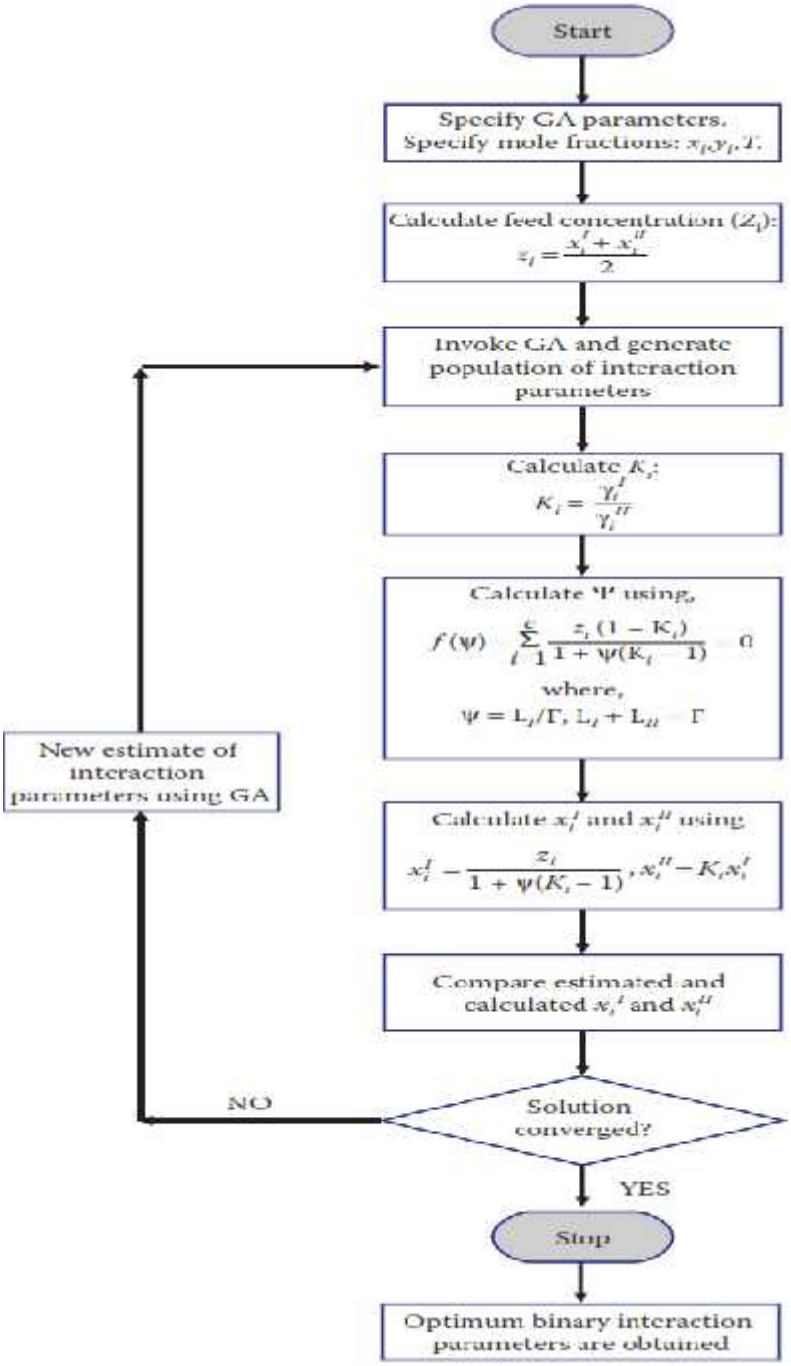

Figure 3.6 Modified Richford-Rice flash algorithm (Bharti *et al*., 2017).

3.2.6 Multi stage extraction

Multiple successive aromatics removal with the studied DESs were carried out each time with fresh DESs. LLE experiments was carried out with the DESs and model fuel having 10 wt.% toluene, at 40 ^{o}C. These represents the first extraction stage. After the first extraction, the model fuel, now as the raffinate of the first stage was collected for the next LLE experiments with fresh DESs (second extraction stage). The process was repeated to the last extraction stage as shown in Figure 3.7. After each stage the raffinate was analysed with HPLC to get the extent of the aromatic removal.

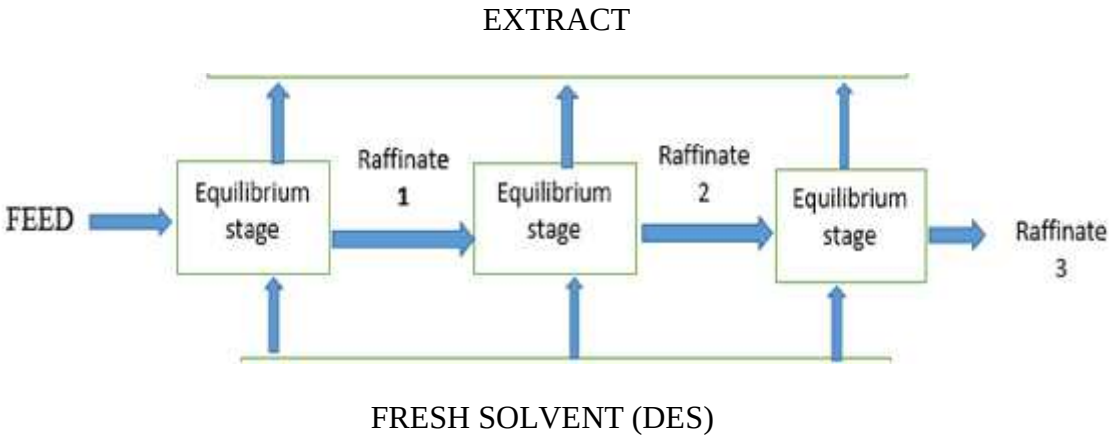

Figure 3.7 Multistage extraction with fresh solvent at every equilibrium extraction stage

3.2.7 Multi stage extraction with synthetic naphtha feed

Multi stage extraction was carried out with synthetic naphtha feed. Table 3.4 shows the composition of the synthetic naphtha feed based on 10 wt.% aromatics. The same procedure was followed as in multi stage extraction with model oil consisting of toluene and octane.

Table 3.4. Composition of synthetic naphtha feed.

S/N	Aliphatics	Composition (wt%)	Aromatics	Composition (wt%)
1	Hexane	43.20	Toluene	3.60
2	Heptane	15.80	Benzene	3.30
3	Octane	31.00	p-Xylene	3.10
	Total	90		10

3.2.8 Solvent regeneration

The deep eutectic solvents regeneration was carried out using rotary evaporator at 75 ^{o}C, 200 mbar for 5 hours. The extract from LLE experiments at 40 ^{o}C with the DESs and 10 wt.% toluene / octane as model fuel was used as solvent for the first regeneration experiments. The regenerated DESs were used to perform another LLE experiments with another 10 wt.% toluene / octane as model fuel at 40 ^{o}C. The extract was regenerated (to be used for another LLE experiments) representing the second regeneration experiments, following the same procedures for the subsequent regeneration experiments.

CHAPTER FOUR

RESULTS AND DISCUSSION

4.1 Synthesis and screening

4.1.1 Synthesis

The molar combinations that forms DESs are presented as homogeneous liquid and are termed successful DESs, while those that did not form DESs are termed unsuccessful DESs. The results of the synthesis experiments are presented in Table 4.1 and 4.2. the successful DESs are mostly formed by tetrabutyl ammonium and phosphonium based salts irrespective of the hydrogen bond donors used. All the successful DESs were further re-synthesized in a larger quantity as samples for further screening applications experiments these DESs are shown in plate 1. The successful DESs from Table 4.1 and 4.2 are mostly formed from tetrabutyl ammonium bromide or chloride and tetrabutyl phosphonium bromide salts with different hydrogen bond donors. This show that these salts formed complexes with the hydrogen bond donors with the formation of a homogeneous liquid or eutectics having low melting points (Abbott *et al*., 2003).

Table 4.1: Synthesized Ammonium based DESs

S/No	Salt/HBD	Successful DESs	Unsuccessful DESs
1	TBAB:PEG200	1:1, 1:2; 1:3	--
2	TBAB:PEG400	1:1, 1:2; 1:3	--
3	TBAB:PEG600	1:1, 1:2; 1:3	--
4	TBAB:DEA	1:1;1:2;1:3	--
5	TBAB:DMF	1:1;1:2;1:3	--
6	TBAB:DMSO	1:1;1:2;1:3	--
7	TBAB:MP	1:2,1:4	--
8	TBAB:4MMP	1:2,1:4	--
9	TBAB:PRD	1:2,1:4.1:6	--
10	TBAB:FF	1:2,1:4	--
11	TBAB:SF:PRD	1:2:2 , 1:6:4	--
12	TBAB:SF:FF	1:2:2 , 1:4:4	--
13	TBAB:SR:PYRD	1:2:2 , 1:6:4	--
14	TPAB:SF	--	1:2,1:4,1:6
15	TPAB:EG	1:2,1:4, 1:6	--
16	TPAB:MP	--	1:2,1:4, 1:6
17	TPAB:4MMP	--	1:2,1:4, 1:6
18	TPAB:PRD	--	1:2,1:4, 1:6
20	TMAB:SF	--	1:2, 1:3,1:4
21	TMAB:EG	1:2,1:4,1:6	--

Table 4.1: Synthesized Ammonium based DESs. Continued

S/No	Salt:HBD	Successful DESs	Unsuccessful DESs
22	PTMAC:DMSO	--	1:1,1:2,1:3,1:4,1:5,1:6
23	PTMAC:EG	--	1:1,1:2,1:3,1:4,1:5,1:6
24	PTMAC:Solfolane	--	1:1,1:2,1:3,1:4,1:5
25	PTMAC:PEG200	--	1:1,1:2,1:3,1:4,1:5
26	PTMAC: PEG600	--	1:1,1:2,1:3,1:4,1:5
27	TMPAB:EG	--	1:1,1:2,1:3
28	TMPAB:Solfolane	--	1:1,1:2,1:3,1:4,1:5
29	TMPAB:DMSO	--	1:1,1:2,1:3,1:4,1:5
30	TBAC:EG	1:1, 1:2; 1:3	--
31	TBAC:DMSO	1:1, 1:2; 1:3	--
32	TBAC:PEG200	1:1, 1:2; 1:3	--
33	TBAC:PEG600	1:1, 1:2; 1:3	--
34	DMAC:Solfolane	--	1:2,1:3,1:4
35	DMAC:EG	1:2,1:3,1:4	--
36	DMAC:Morpholine	--	1:2,1:3,1:4
37	DMAC:Pyridine	--	1:2,1:3,1:4

Table 4.1: Status of Synthesized Ammonium based DESs. Continued

S/No	Salt/HBD	Successful DESs	Unsuccessful DESs
38	TEAB:Solfolane	--	1:2
39	TEAB:EG	1:4	1:2
40	TEAB:EG:Pyridine	1:2:2	--
41	TEAB:EG:Pyridine	1:4:4	--
42	TEAB:EG:Pyridine	1:4:2	--
43	TEAB:Morpholine	1:2	1:4, 1:8
44	TEAB:Pyridine	1:2	1:4, 1:8

Table 4. 2: Synthesized Phosphonium based DESs .

S/No	Salt:HBD	Successful DESs	Unsuccessful DESs
1	BPPC:EG	--	1:1,1:2,1:3,1:4,1:5,1:6
2	BPPC:DMSO	--	1:1,1:2,1:3,1:4,1:5,1:6
3	BPPC:DMF	--	1:1,1:2,1:3,1:4,1:5,1:6
4	BPPC:PEG200	--	1:1,1:2,1:3,1:4,1:5
5	BPPC:PEG600		1:1,1:2,1:3,1:4,1:5
6	TBPB:EG	1:1,1:2,1:3,1:4,1:5	--
7	TBPB:DMSO	1:1,1:2,1:3,1:4,1:5	--
8	TBPB:DMF	1:1,1:2,1:3,1:4,1:5	--
9	TBPB:PEG200	1:1,1:2,1:3,1:4,1:5	--
10	TBPB:PEG600	1:1,1:2,1:3,1:4,1:5	--
11	TBPMS:DMSO	1:1,1:2,1:3,1:4,1:5	--
12	TBPMS:DMF	1:1,1:2,1:3,1:4,1:5	--
13	TBPMS:PEG200	1:1,1:2,1:3,1:4,1:5	--
14	TBPMS:PEG600	1:1,1:2,1:3,1:4,1:5	--

Table 4. 2: Synthesized Phosphonium based DESs . Continued

S/No	Salt:HBD	Successful DESs	Unsuccessful DESs
15	MPPB:Solfolane	1:8	1:1, 1:2; 1:3
16	MPPB:MP	--	1:1,1:2,1:3,1:4,1:5
17	MPPB:MMP	--	1:1,1:2,1:3,1:4,1:5
18	MPPB:PRD	--	1:1,1:2,1:3,1:4,1:5
19	MPPB:PYR	--	1:1,1:2,1:3,1:4,1:5
20	MPPB:SF : FF	1:6:4	1:2:2
21	MPPB:SF : PRD	1:6:4	1:2:2

4.1.2 Screening of ammonium based DESs

The DESs that were synthesized from TBAB: MP (1:2), TBAB: MMP (1:2), TBAB: PYRD (1:2), TEAB: PYRD (1:2) AND TEAB: MP (1:2) were recrystallized during the LLE experiments and no further test was carried on them. This was possibly due to the disruption of hydrogen bond that exist between the salt and the HBD as a result of adding the hydrocarbons as model fuel.

The result for TBAB: FF (1:2) showed no extraction of toluene when the resulting raffinate was analysed and also, the resulting mixtures forms three phases; DES, model fuel, and a thin yellow layer at the top that is possibly Furfural from the DES component. The DESs that were formed from TBAC were screened out for further test because of the high price of TBAC.

LLE extractions were carried out successfully on the DESs that were synthesized from TBAB: PEG 200 (1:2), TBAB: PEG 400 (1:2), TBAB: PEG600 (1:2), TBAB: DEA (1:2), TBAB: DMF (1:2), TBAB: DMSO (1:2) and TPAB:EG (1:2). The aromatic removal efficiency, liquid distribution coefficient and selectivity for these DESs were calculated as shown in Table A.1. (Appendix I). The analysis of the raffinate showed no traces of DESs for TBAB: PEG 400 (1:2), TBAB: PEG600 (1:2), TBAB: DEA (1:2), TPAB:EG (1:2) solvents, an indication that the DESs does not dissolves into the fuel phase, a property that is desired for a good solvent. For TBAB: DMF (1:2), TBAB: DMSO (1:2), the results showed some traces of DESs in the raffinate phases when analysed using HPLC. These DESs were also found to be liquid at room temperature, which is also a property that is desired for the DESs as solvents.

The extraction efficiencies for TBAB: DMF and TBAB: DMSO were the highest with 32.21 and 31.33% respectively when compared with the other ammonium based DESs. There was an increase in the extraction efficiencies of the ethylene glycol based DESs with TBAB: PEG600 (1:2) > TBAB: PEG 400 (1:2) > TBAB: PEG 200 (1:2) > TBAB:EG (1:2) as shown in Figure 4.1., The observed trend is possibly due to the increasing polymer chain for the EG based DESs. TBAB:EG being the least with 10.16% and TBAB: PEG600 the highest with 24.48. Figure 4.2. shows the trend in distribution coeficients. The highest distribution coefficient of 1.3763 comes from TBAB: PEG600 possibly due to its extended polymer chain. TPAB:EG have the least with 0.246.

The DESs that are formed from TBAB: DMF and TBAB: DMSO had distribution coefficients of 0.7962 and 0.9099 respectively, these values are more than the distribution coefficients for the other EG based DESs with the exception of TBAB: PEG600. Figure 4.3. show the selectivity of the successful ammonium based DESs., all the selectivity values are greater than unity which shows that separations with these DESs are possible (Rodriguez, *et al*., 2015).

Three components DESs were formed from TBAB: SF: PRD (1:2:2), TBAB: SF: PRD (1:6:4), TBAB: SF: FF (1:2:2) and TBAB: SF: FF (1:4:4), these DESs recrystallized during the LLE experiments and no further test was carried on them. TBAB: SF: PYRD (1:2:2) and TBAB: SF: PYRD (1:4:4) separated and recrystallized on the addition of the fuel phase prior to LLE experiments. The three components DESs that were formed from TEAB:EG: PRD in the ratio of (1:2:2), (1:4:4) and (1:4:2) also recrystallized during the LLE experiments and no further test was carried on them.

The following TBAB based DESs; TBAB: PEG200, TBAB: PEG600, TBAB: DMF and TBAB: DMSO were selected due to their favourable properties. TBAB: PEG400 was discontinued for further investigations due to its small quantity as at the time of the research. TBAB: DEA and TPAB:EG were also dropped due to their relatively low distribution coefficient.

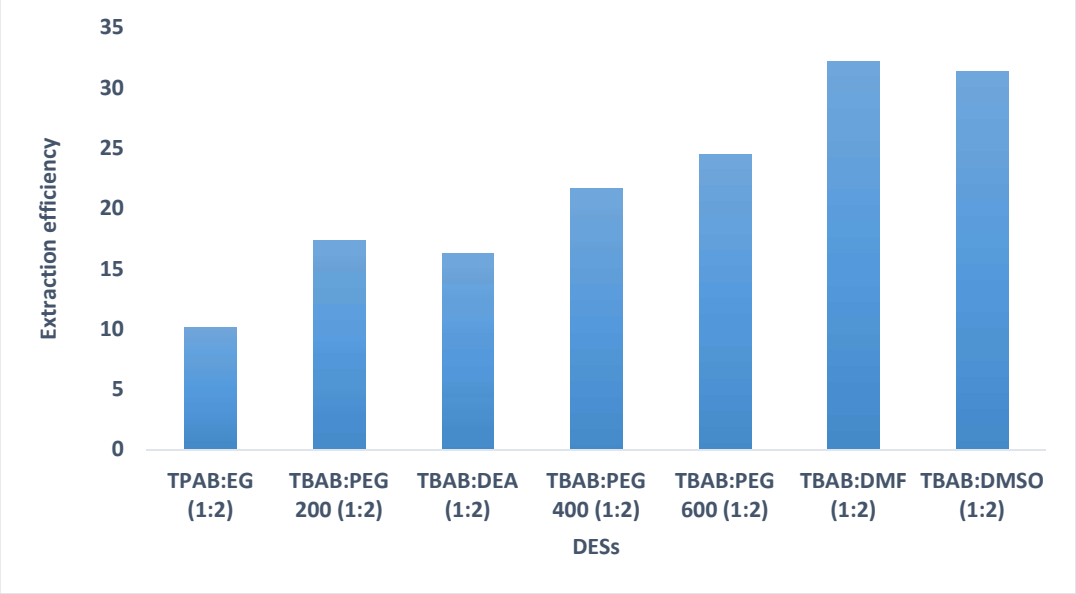

Figure 4.1 Extraction efficiencies of the successful ammonium based DESs

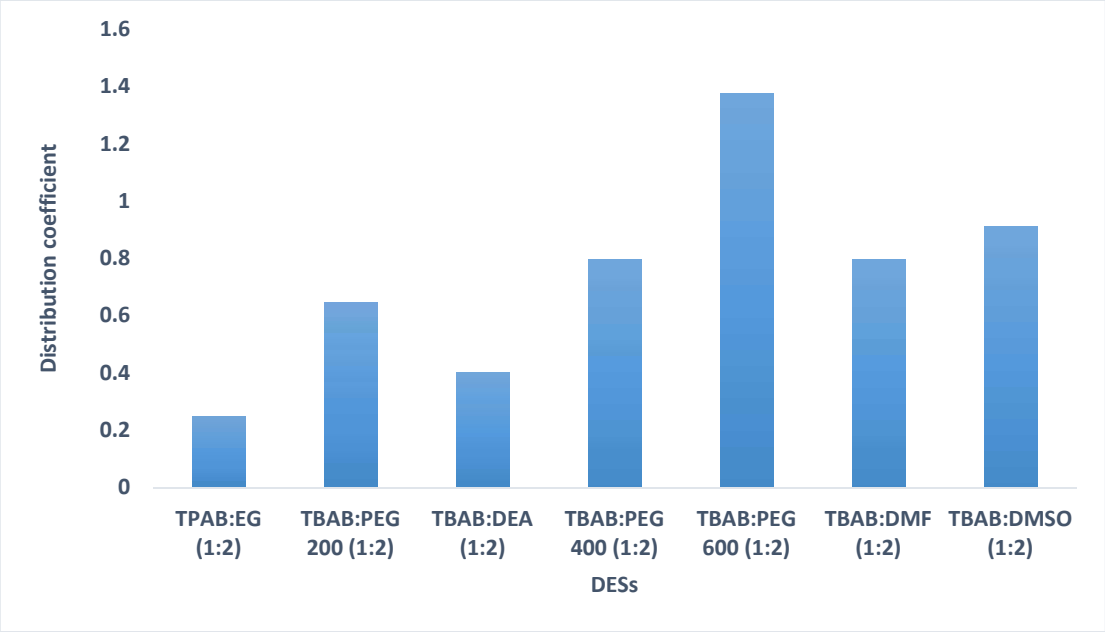

Figure 4.2. Distribution coeficients of the successful ammonium based DESs

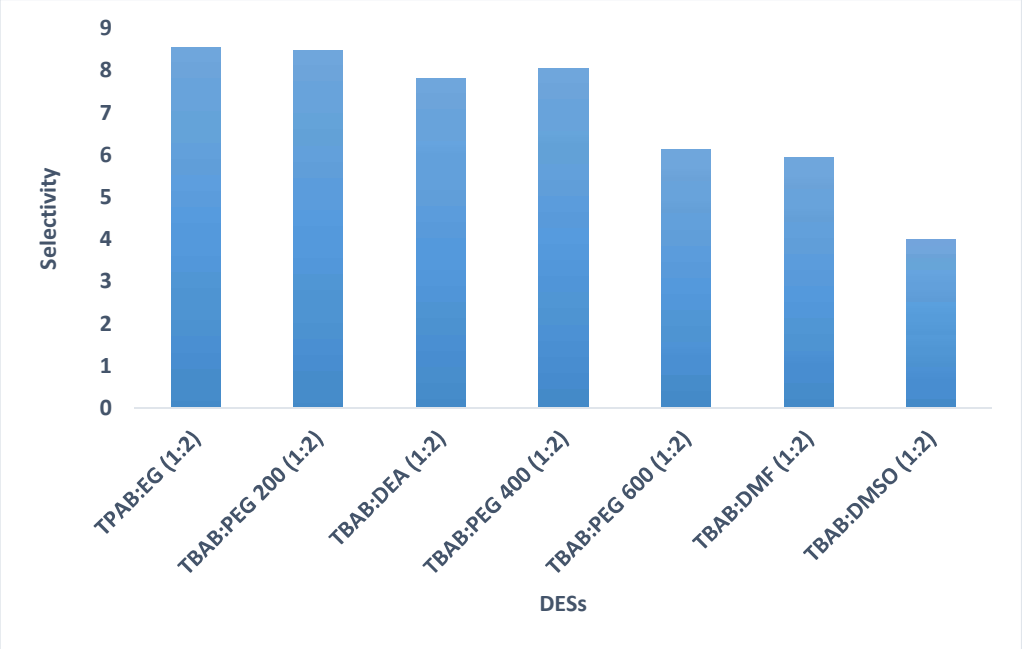

Figure 4.3. Selectivity of the successful ammonium based DESs

4.1.3 Screening for Phosphonium based

The two phosphonium based salts, TBPB and TBPMS (ionic liquid) formed DESs with the following hydrogen bond donors and the complexing agents EG, PEG 200 PEG 600, DMF and DMSO. Liquid-liquid equilibrium extraction experiments were carried out successfully on these DESs, the aromatic removal efficiency, liquid distribution coefficient and selectivity for these DESs were calculated as shown in Table A.2. (Appendix I). The analysis of the raffinate showed no traces of DESs for TBPB:EG (1:2), TBPB: PEG200 (1:2), TBPB: PEG600 (1:2), TBPMS: PEG200 (1:2) and TBPMS: PEG600 (1:2). The DESs that are formed from TBPB: DMF (1:2), TBPB: DMSO (1:2), TBPMS: DMSO (1:2) and TBPMS: DMF (1:2) show some traces of DESs in the raffinate phases when analysed using HPLC. All these phosphonium based DESs were also found to be liquid at room temperature.

TBPB:DMSO and TBPB:DMF have the highest extraction efficiencies of 40.10 and 31.83% respectively when compared with the other phosphonium based DESs. There was an increase in the extraction efficiencies with increasing polymer chain for the EG based DESs. TBPB:EG being the least with 15.27% and TBPB: PEG 600 the highest with 21.30% as can be seen in Figure 4.4. Figure 4.5. shows the distribution coefficients for the phosphonium based salts. TBPB: PEG 600 (1:2) have the highest distribution coefficients of 1.345 then followed by TBPMS: PEG 600 (1:2) with distribution coefficients of 1.3168. These phosphonium based DESs all have distribution coefficients greater than 0.6 with the exception of TBPB:EG (1:2) having distribution coefficients of 0.247. This is an indication of the separation capabilities of these screened DESs. The distribution coefficients surpass some of the previously reported values in the literature as seen in Table 3.2. Figure 4.6. showed the selectivity values of the successful phosphonium based DESs. All the selectivity

values of these phosphonium based DESs are greater than unity which shows that separations with these DESs are possible (Rodriguez *et al.*, 2015).

Three components DESs that were formed from MTPPBr:SF:FF(1:6:2) and MTPPBr:SF:PRD(1:6:2) recrystallized during the LLE experiments and no further test were carried on them. The following phosphonium based DESs, TBPB:PEG600 (1:2) , TBPB: PEG200 (1:2) , TBPB:DMF(1:2) , TBPB:DMSO (1:2), TBPMS:PEG200 (1:2) and TBPMS:PEG600 were selected due to their favourable properties. TBPMS:DMSO (1:2) and TBPMS:DMF (1:2) were dropped for further investigations due to their presence of the former in the raffinate phase, relatively small quantity of TBPMS and also its cost. TBPB:EG (1:2) was discontinued for further investigations due to its relatively low distribution coefficient.

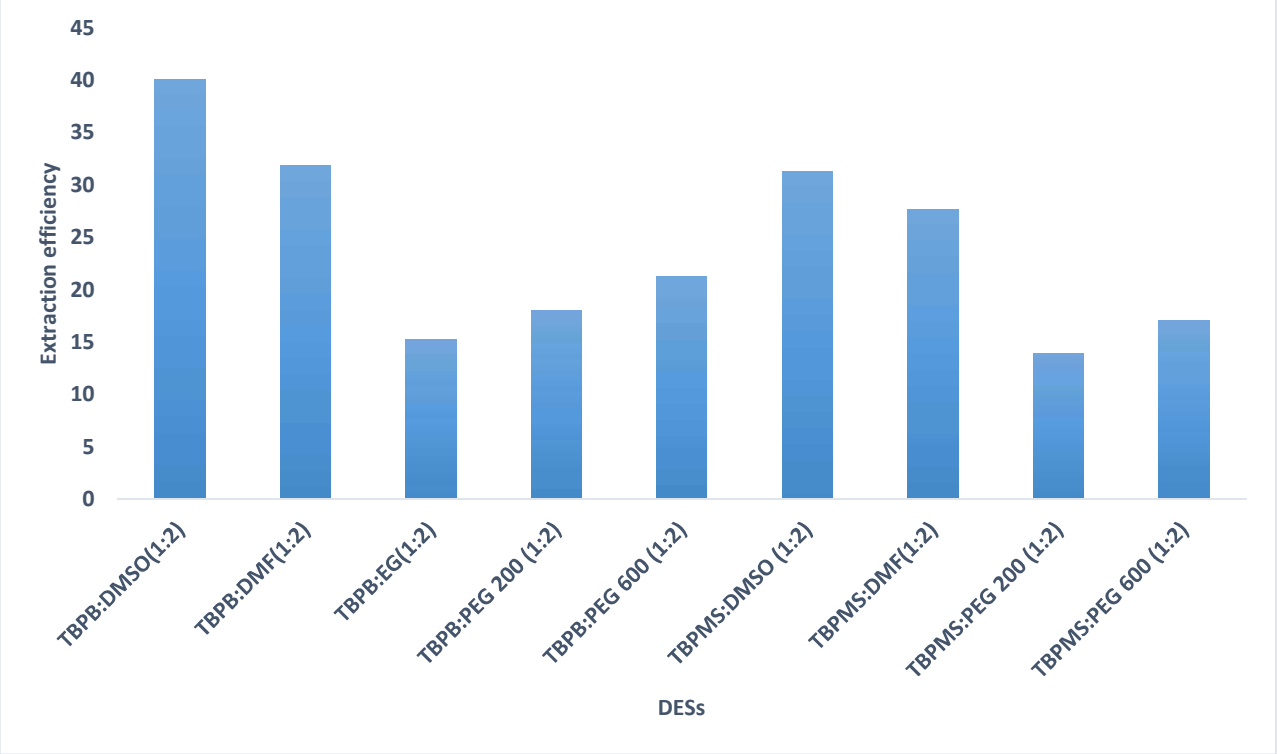

Figure 4.4 Extraxtion efficiencies of the successful phosphonium based DESs

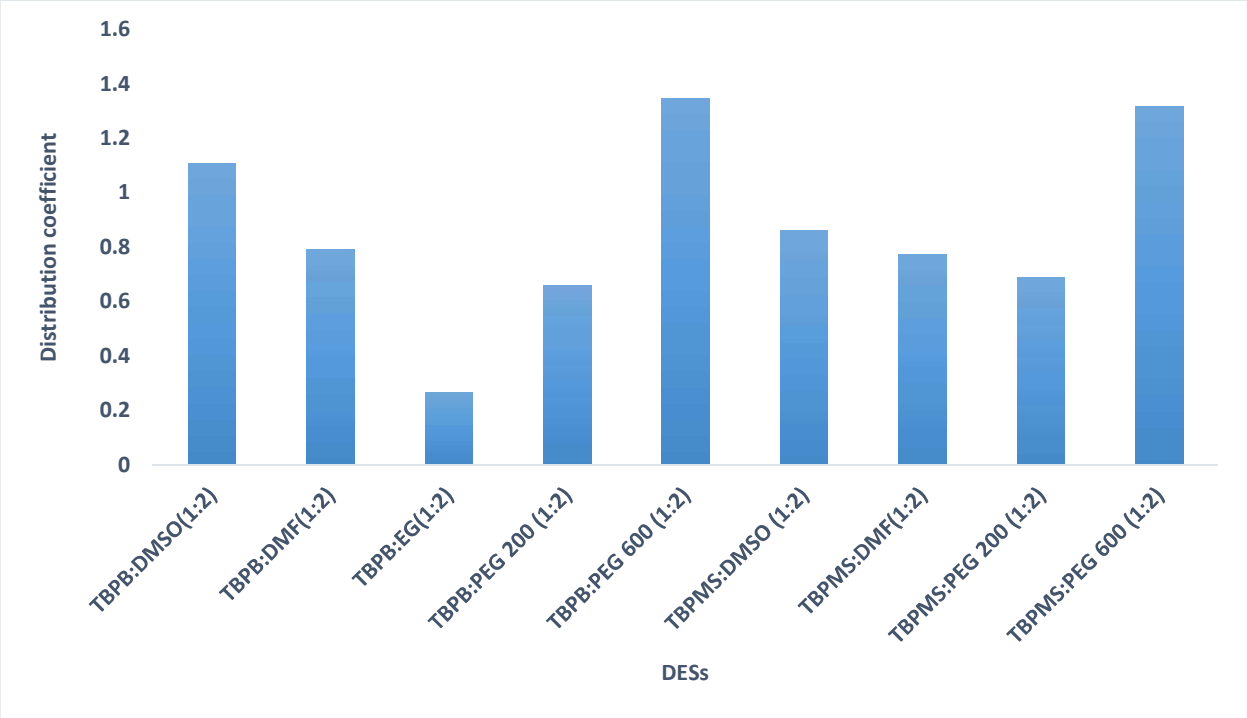

Figure 4.5. Distribution coeficients of the successful phosphonium based DESs

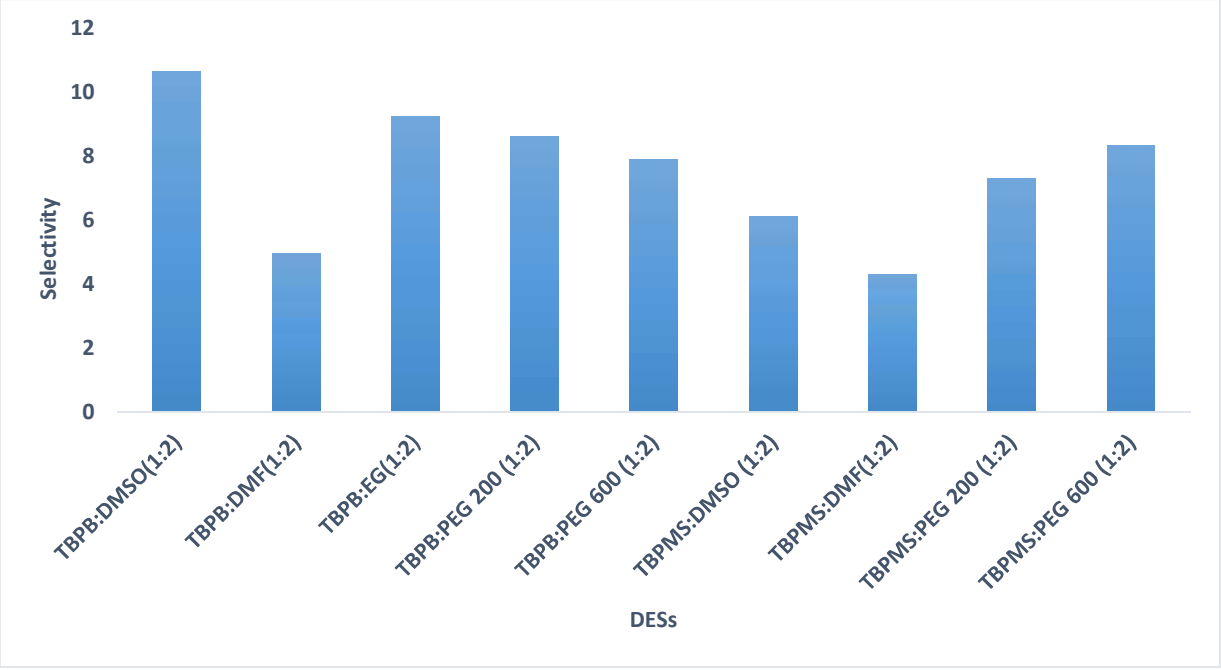

Figure 4.6. Selectivity of the successful phosphonium based DESs

As at 2016, there are 8 publications dealing with aromatic/aliphatic hydrocarbons separations with the first publication reported by Kareem *et al.*, (2012). Considering the low number of relevant publications, information in literature on some properties of DESs such as selectivity, distribution coefficients among others, are scarce, and the screened DESs are novel. Therefore, the screening of suitable DESs cannot be entirely based on literature data.

The following DESs were selected from the successful ratios and since they met some of the criteria

Ammonium based DESs

1. Tetrabutyl ammonium bromide: Polyethylene glycol 200 TBAB:PEG200 [1:2]
2. Tetrabutyl ammonium bromide: Polyethylene glycol 600 TBAB:PEG600 (1:2)
3. Tetrabutyl ammonium bromide: Dimethylesulfoxide TBAB:DMSO (1:2)
4. Tetrabutyl ammonium bromide:Dimethyleformamide TBAB:DMF (1:2)

Phosphonium based DESs

1. Tetrabutyl phosphonium bromide:Polyethylene glycol 200 TBPB:PEG200 (1:2)
2. Tetrabutyl phosphonium bromide:Polyethylene glycol 600 TBPB:PEG600 (1:2)
3. Tetrabutyl phosphonium bromide:Dimethylesulfoxide TBPB:DMSO (1:2)
4. Tetrabutyl phosphonium bromide:Dimethyleformamide TBPB:DMF (1:2)
5. Tetrabutyl phosphonium methane sulfonate: Polyethylene glycol 200 TBPMS:PEG 200 (1:2)
6. Tetrabutyl phosphonium methanesulfonate: Polyethylene glycol 600 TBPMS:PEG 600 (1:2)

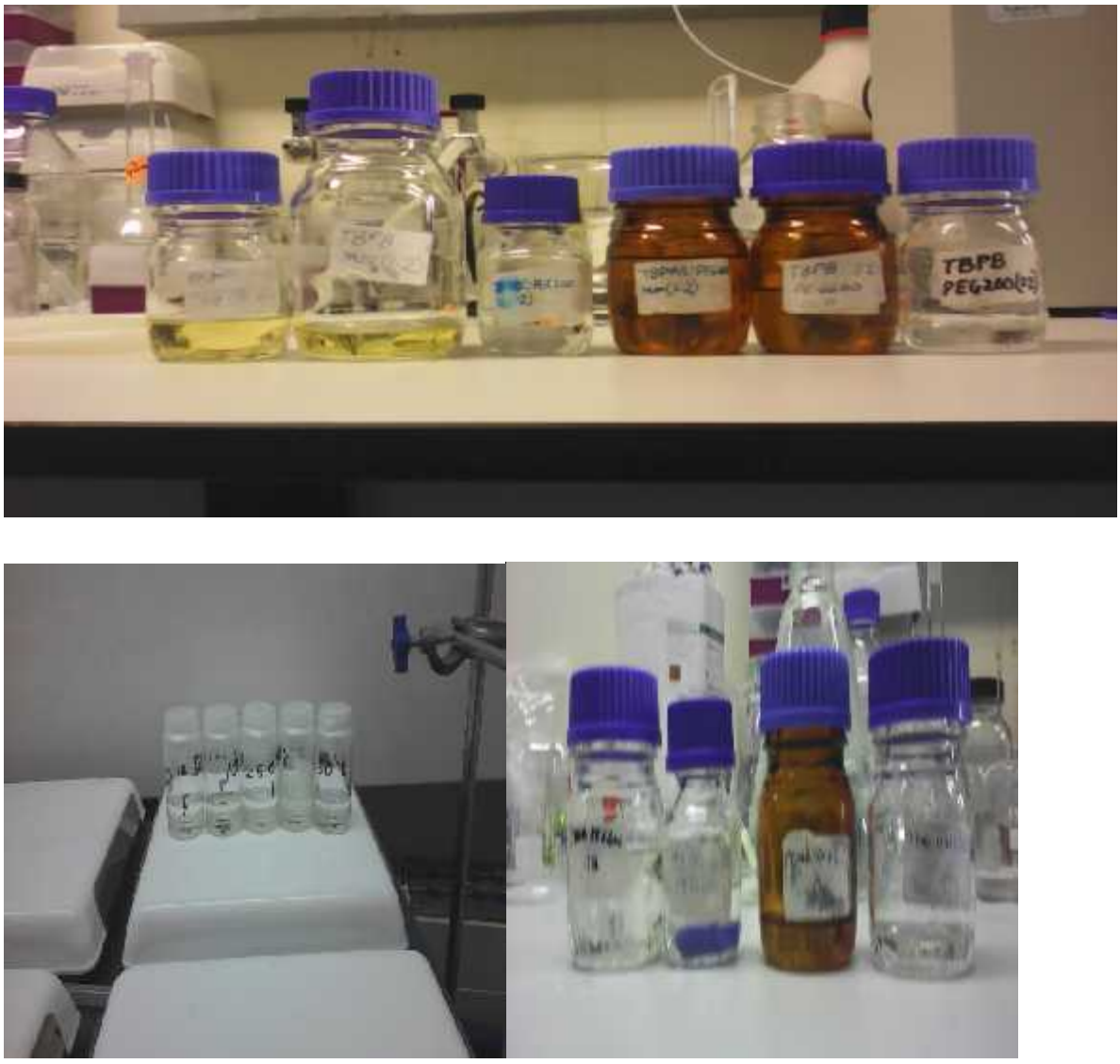

Plate 1.0: Synthesised DESs

4.2 Deep Eutectic Solvents Characterization

The physical properties of the selected DESs were determined, the properties included density, viscosity, conductivity and refractive index.

4.2.1 Density

Density is one of the important property of solvents as its measurements is used in mass transfer calculations and in the design of many chemical processes. The densities of the studied DESs were measured at different temperatures ranging from 303 K to 363 K. Table B.1 and Table B.2 in Appendix II showed the experimental density values with temperature for the ammonium and phosphonium based DESs respectively

4.2.1.1 Effects of temperature on density

The variations of density with temperature for the ammonium and phosphonium based DESs are shown in Figure 4.7 and Figure 4.8 respectively. Mostly, the density decreases with increasing temperature. (Garcia *et al*., 2015, Troter *et al*., 2016, Yusuf *et al*., 2014). This decrease in density may be as a result of increase in temperature which makes the molecules to move faster and the thermal expansion of the DESs volumes which create more space. As a result, the density values reduce. The dependence of the temperature with density can be expressed through a linear relationship: (Hayyan *et al*., 2013, Bahadori *et al*., 2013, Garc *et al*., 2015, Troter *et al*., 2016, Kareem *et al.,* 2010)

$$\rho\left(\frac{g}{c^{3}}\right) = a + b\ (K) \qquad 4.1$$

Where ρ is the density in $g.cm^{-3}$, T is the temperature in Kelvin and a and b are adjustable parameters. Where a is the density at 0 K in g/cm^3, b is the coefficient of volume expansion in kg/m^3k. These parameters and the correlation factor R^2 for the ammonium and the

phosphonium based DESs are given in Table 4.3 and Table 4.4., respectively. A very good correlation with an R^2 values between 0.97 and 1.0 was observed for the studied systems. This indicates that linear model approximate the experimental data satisfactorily.

Table 4.3. Parameters values and the correlation factor R^2 for the ammonium based DESs

	Coefficients of equation 4.1		
Ammonium Based DESs	α	b	R^2
TBAB:PEG600	1.3298	-0.0007	0.999
TBAB:PEG200	1.2956	-0.0007	1
TBAB:DMF	1.2539	-0.0008	0.9895
TBAB:DMSO	1.3908	-0.001	0.9712

Table 4.4. Parameters values and the correlation factor (R^2) for Phosphonium Based DESs

Coefficients of equation 4.1			
Phosphonium Based DESs	α	b	R^2
TBPB:PEG600	1.3298	-0.0007	0.9998
TBPB:PEG200	1.2975	-0.0007	1
TBPMS:PEG200	1.2666	-0.0007	1
TBPMS:PEG600	1.3143	-0.0007	1
TBPB:DMSO	1.2844	-0.0007	1
TBPB:DMF	1.2475	-0.0007	1

The highest density exhibited by the ammonium based DESs was by TBAB: PEG 600 (1.10465 g/m^3), followed by TBAB: PEG600 (1.08867 g/m^3), TBAB: DMSO (1.08335 g/m^3) and TBAB: DMF (1.02599 g/m^3) at 303.15 K. As expected, there is decrease in the density values with increasing temperatures through a linear relationship, with correlation factor between 0.97 – 1.00 for the ammonium based DESs as shown in Figure 4.7.

For the phosphonium based DESs, TBPB: PEG600 gave the highest density of (1.10342g/m^3) followed by TBPB: PEG200 with (1.08806 g/m^3) and TBPMS: PEG600 with (1.08947 g/m^3), with identical density values, followed by TBPB: DMSO having (1.06528

g/m^3), TBPMS: PEG200 with (1.05961 g/m^3), and TBPB: DMF (1.02517 g/m^3), which shows the least density value at 303 K. There were decrease in the density values with increasing temperatures for these systems and also showed a good correlation factor of 1, indicating a very good degree of correlation.

Most of the studied DESs were reported to have densities in the range of 1.0 – 1.35 g/m^3 at 298.15 K, the metallic salts based DESs like $ZnCl_2$ have densities in the range of 1.30 – 1.35 g/cm^3 (Zhang, *et al*., 2012, Yusuf *et al*., 2014), reported the densities TBAB based DESs with EG, 1,3-propanediol, (1,3-PD), 1,5-pentanediol (1,5-PD) and glycerol (GLY) as HBDs. The highest density observed was by TBAB: GLY at 1.1867 g/m^3 for 90% glycerol at 30 ^{o}C, which is greater than the highest density value obtained in this work. The lowest reported value was 0.9770 g/m^3 for TBAB: 1,5-PD at 85.7% of 1,5-PD at 60 ^{o}C., which are lower than the density values reported in this work at the same temperature. The densities of some phosphonium based DESs synthesized from MTPPB: GLY (1:1.75), MTPPB:EG (1:4) and MTPPB:2,2,2TFAB (1:8) at 30 ^{o}C were 1.25, 1.42 and 1.1.31 g/cm^3 respectively. Also, at 80 ^{o}C, the density values of 1.194, 1.332 and 1.254 g/cm^3 respectively were reported for the DESs, these values are higher than the density values obtained in this work at the two temperatures (Kareem *et al*., 2010).

So far, there is only one work by Rodriguez *et al*., (2015), which reports the density values of DESs that were employed for aliphatic and aromatic separations. Two DESs were synthesized from THAB:EG (1:2) and THAB: GLY (1:2) with density values of 1.0013 and 1.0393 g/cm^3 respectively. These values are less than the values obtained in this work at 303.15 K.

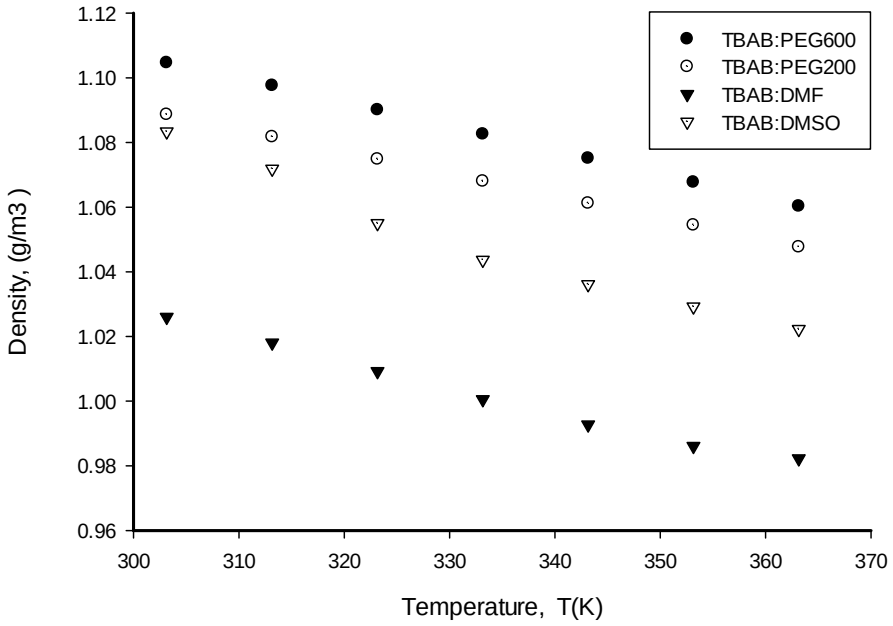

Figure 4.7: Variation of density with temperature for the ammonium based DES

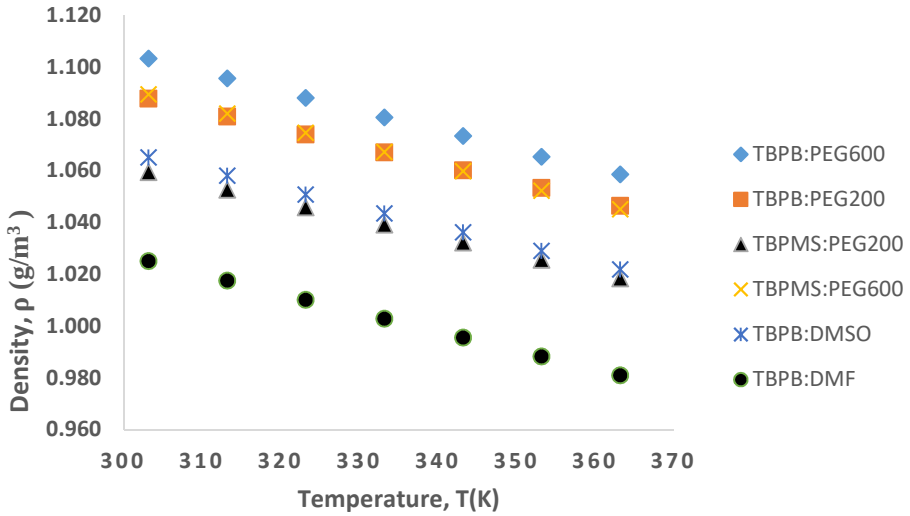

Figure 4.8: Variation of density with temperature for the phosphonium based DESs

4.2.1.2. Effects of hydrogen bond donor (HBD) on the density.

Figure 4.9 shows the density relationship between the DESs synthesized from TBAB and TBPB as salts with PEG600 and PEG 200 as HBD with temperature. There is a slight change

in the densities of the DESs pair, TBAB: PEG600 and TBPB: PEG600, and also with TBAB: PEG200 and TBPB: PEG200 with temperature. Their density profiles are almost similar, the density of the DESs made from PEG600 appears to be higher than that of PEG 200 irrespective of the salts used.

Similarly, Figure 4.10 also show the density relationships between the DESs synthesized from TBAB and TBPB with DMSO and DMF with temperature. The density of TBAB: DMSO and TBPB: DMSO and also with TBAB: DMF and TBPB: DMF are almost similar irrespective of the salt used. This observed behaviour could be that the DESs density is strongly affected by the type of HBDs or the complexing agent used (Abbott *et al.*, 2007).

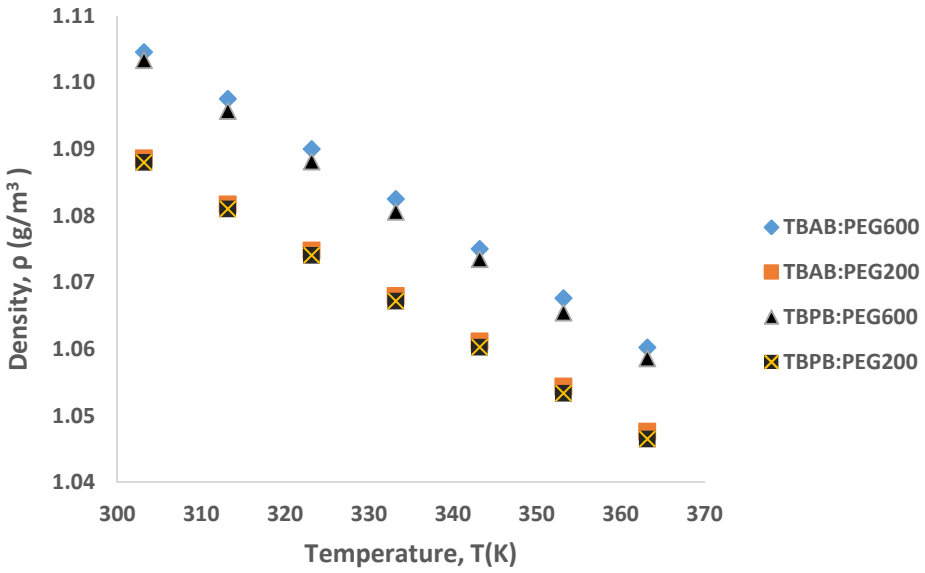

Figure 4.9 Density relationship between TBAB and TBPB with PEG600 and PEG 200 with temperature.

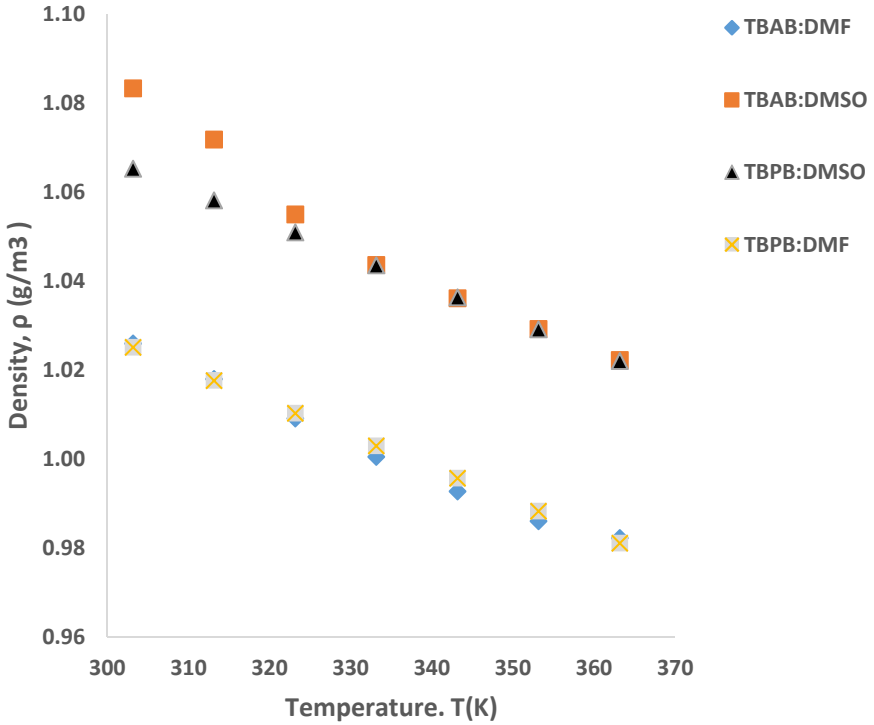

Figure 4.10 Density relationships between TBAB and TBPB with DMSO and DMF with temperature

4.2.2 Viscosity

Viscosity is a very important property especially, in the area of equipment design and fluid flow calculations. The effect of temperature on viscosities of the selected DESs at different temperatures ranging from 303.15 K to 353.15 K were determined. Experimental values of viscosities are tabulated in Table B.3 and B.4. in Appendix II. Figure 4.11 and Figure 4.12. show the variation of viscosity with temperature for the ammonium and phosphonium based DESs respectively. The knowledge of temperature effect on viscosity is very important most especially for energy requirements in processing these fluids, equipment design and fluid flow calculations.

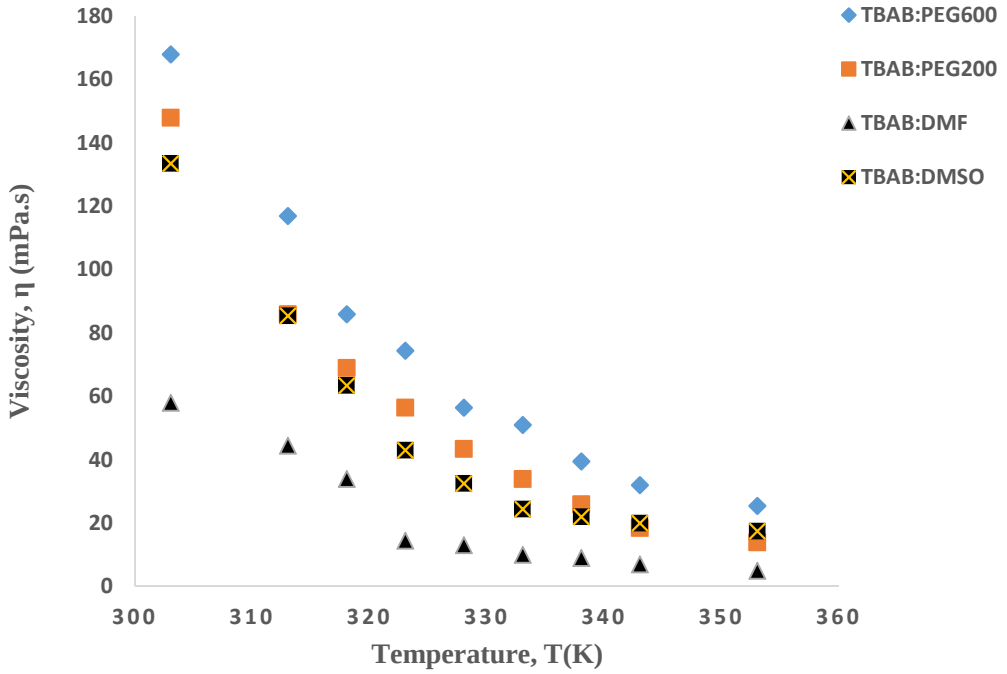

Figure 4.11 Variation of viscosity with temperature for the ammonium based DESs

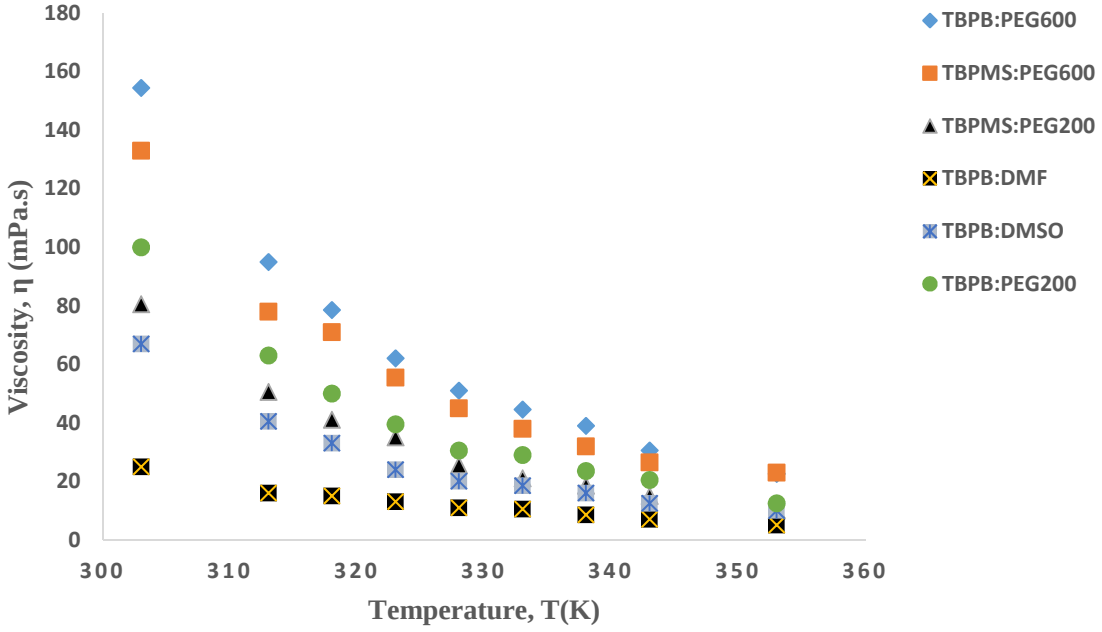

Figure 4.12 Variation of viscosity with temperature for the phosphonium based DESs

Exponential decay profile has been reported for many ionic liquids (ILs) as well as some DESs.. As expected the viscosity of the studied DESs decrease with increasing temperature. The viscosities of the studied DESs were fitted using the Arrhenius-like equation 4.2.

$$\mu = \mu_0 \exp[-\frac{E_a}{R}] \qquad 4.2$$

where μ (mPa.s) is the viscosity, μ_0 is a fitting parameter (constant), E_a is the activation energy (J/mol/K), R is the gas constant and T is the temperature in Kelvin. (Abbott *et. al*., 2004, Hayyan *et. al*., 2012, and Troter *et al.*, 2017). The Vogel-Fucher Tamman (VFT) equation is the most popular three-parameter equation used in correlating the changes in viscosity with temperature. The VFT equation suitably correlates, as a function of temperature, not only the viscosities of pure ILs but also the viscosities of the mixtures for the binary systems throughout the composition range (Rodriguez, and Brennecke, 2006). The VFT equation which has three parameters is expected to give a better fitting than the Arrhenius equation with only two parameters. The VFT equation is shown in equation 4.3.

$$\mu = A\, e^{\left(\frac{B}{T - T_0}\right)} \qquad 4.3$$

Where A (mPa.s), B (K) and T_0 (K) are the fitting parameters. The parameter T_0 is also related to Tg the glass transition temperature. (Yadav & Pandey, 2014, Sun *et al.*, 2015, Rodriguez, *et al*., 2015, Mirza *et al*., 2016, and Troter *et al.*, 2017).

The fitting parameters for the Arrhenius equation and VFT are shown in Table 4.5. and Table 4.6 together with their average absolute deviation (AAD). for the ammonium and phosphonium based DESs., respectively. The AAD is calculated from the following equation

$$\%A = \frac{1}{N} \sum_1^N \frac{\mu_c - \mu_e}{\mu_c} \qquad 4.4$$

Where μ_c a μ_e represents the calculated and experimental viscosity and N the number of data points. (Siongco, *et al.*, 2013). It can be observed from Table 4.5 and Table 4.6 that the VFT equation describes the temperature – viscosity relationships with higher accuracy than the Arrhenius like equation and this is due the higher number of parameters in the VFT equation.

Table 4.5. Parameters of Arrhenius and VFT equations for ammonium based DESs.

Arrhenius constants				VFT equation constants			
Ammonium based DESs	μ_o	Ea	%AAD	A	B	T_0	%AAD
TBAB:PEG600	0.00017	-34857	4.227081	0.00031	3833.3	12.81	0.944671
TBAB:PEG200	5.85E-06	-43023	4.035639	8.05E-05	3791.11	40.1983	0.742146
TBAB:DMF	3.77E-07	-47715	15.21983	0.00204	1749.3	133.429	1.006814
TBAB:DMSO	1.86E-05	-39592	12.21131	0.02608	1191.98	163.697	0.825939

Table 4.6. Parameters of Arrhenius and VFT equations for phosphonium based DESs.

Arrhenius constants				VFT equation constants			
Phosphonium based DESs	μ_o	E	%AAD	A	B	T_0	%AAD
TBPB:PEG600	0.00022	-33783	2.625244	0.00088	3347.42	24.7064	0.339223
TBPMS:PEG600	0.00037	-32068	5.321165	1.38045	370.579	221.86	0.397891
TBPMS:PEG200	3.53E-05	-36913	2.702119	0.00606	1788.39	114.799	0.401935
TBPB:DMF	0.00054	-27041	4.16499	0.00217	2766.59	4.46222	0.165276
TBPB:DMSO	9.10E-05	-33820	5.297432	0.00348	1877.93	112.569	0.379734
TBPB:PEG200	7.19E-05	-35590	4.32522	0.00049	3078.17	51.0427	0.43236

4.2.2.1. Effects of temperature on viscosity

The viscosities of the DESs changes significantly with temperature for both the ammonium and phosphonium based DESs. The highest viscosity obtains for the ammonium based DESs is from TBAB: PEG 600 with (168.0 mPa.s), then followed by TBAB: PEG 200 with (148.0 mPa.s) then TBAB: DMSO (133.5 mPa.s) and finally TBAB: DMF having (58.0 mPa.s) at 303 K. As expected the viscosity values decreased with increasing temperatures for all the DESs as observed in Figure 4.11. These DESs attain their lowest viscosities at 353.15 K, with 25.5, 17.5, 14.0, and 5.0 mPa.s for TBAB: PEG 600, TBAB: PEG 200, TBAB: DMSO and TBAB: DMF respectively.

Similarly, the same trend was observed for the phosphonium based DESs with TBPB: PEG 600 having the highest viscosity of 154.5 mPa.s then followed by TBPMS: PEG 600 with 133.0 mPa.s, TBPB: PEG200 (100.0 mPa.s), TBPMS: PEG 200 (80.5 mPa.s), TBPB: DMSO (67.0 mPa.s) and finally TBPB: DMF (25.0 mPa.s). The decrease in the viscosity values with increasing temperature as observed in Figure 4.12, could be associated with heating which weakens the attractive forces of the molecules and hence increase in the kinetic energy. Also, the observed non-smoothing or scattering of the viscosity profile at the upper temperature range could be as a result of the existence of complex bonding between the salt and the HBDs (Hayyan *et al*, 2012).

The viscosities of some DESs formed choline chloride (ChCl) with sugar derivatives were reported by Zhang *et al*., (2012). These DESs are exhibiting very high viscosity, for example; ChCl: sorbitol DESs at 20 ^{o}C has 12730 mPa.s., ChCl: GLY (1:2) has 376 mPa.s. these reported viscosity values are more than the values obtained in this thesis. It should be noted

that the minimum viscosity value in this thesis is 30 ^{o}C, the VFT equation fitting were therefore used to estimate the viscosities of the studied DESs at 20 ^{o}C., also ChCl: Glucose (1:1) with 34400 mPa.s. at 50 ^{o}C this viscosity values is also more than the values reported in this thesis. The viscosity values of two DESs synthesized from THAB:EG (1:2) and THAB: GLY (1:2) at 30 ^{o}C were 131.9 mPa.s and 567 mPa.s respectively (Rodriquez *et al*., 2015).

4.2.2.2. Effects of hydrogen bond donor (HBD) on viscosity

The HBDs have strong effects with regards to the viscosity of DESs, as observed in Figure 4.13 and Figure 4.14 for the ammonium and phosphonium based DESs. There is observed difference in viscosity of the DESs formed from PEG 600 as HBD with TBAB, having the highest, then followed by TBPB and finally, TBPMS. Similarly, for PEG 200 as HBD, the viscosity of the DESs formed increased in the order TBAB > TBPB > TBPMS. This observed difference in viscosity could be as a results of the differences in the degrees of the hydrogen bond functionalities of the HBD (Abbott *et al.*, 2007). Although PEG 600 and PEG 200 might present the same OH functionalities for the HBD, the observed difference in the viscosity could be as a result of the differences in the alkyl chain length. Similar results were observed when $ZnCl_2$ formed eutectic mixture with 1,6 – hexanediol, ethyleneglycol, acetamide and urea as HBD (Abbott *et al.*, 2007).

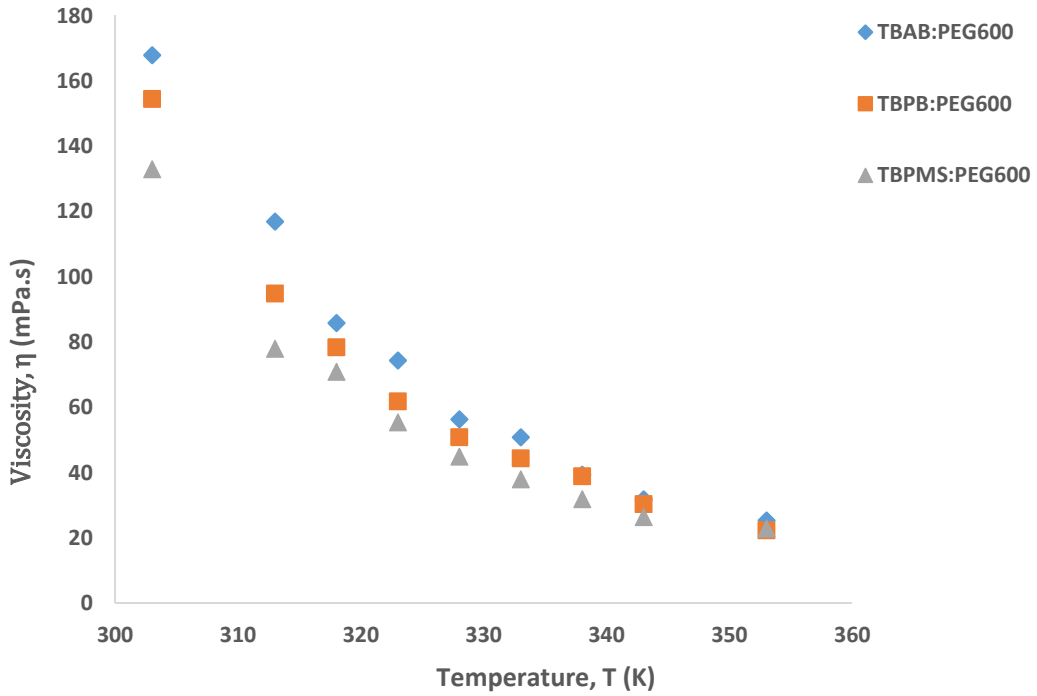

Figure 4.13: Effects of PEG600 (HBD) on viscosity for DESs.

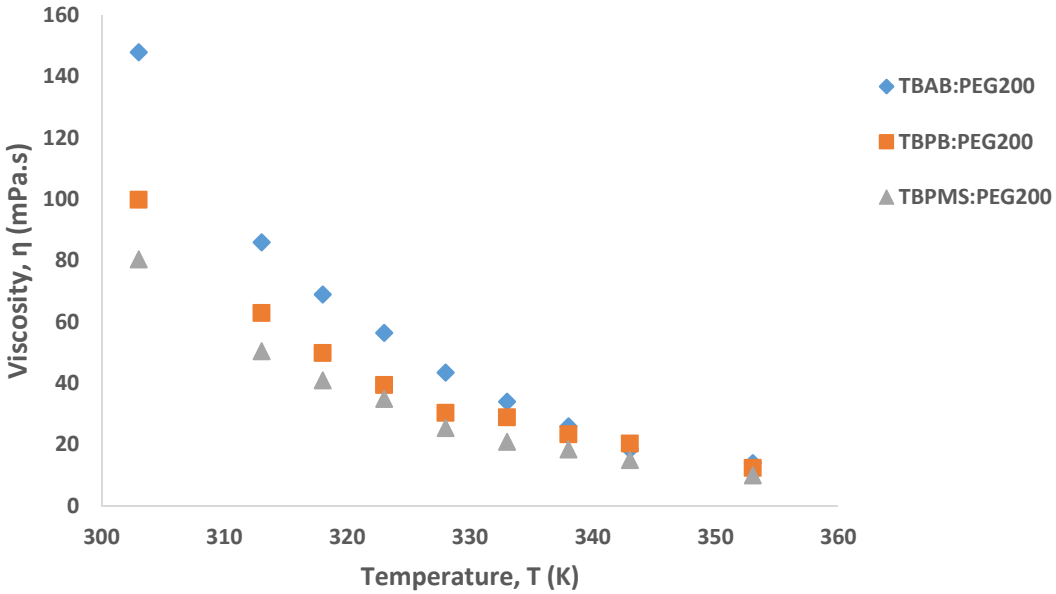

Figure 4.14: Effects of PEG200 (HBD) on viscosity for DESs.

4.2.2.3 Percentage decrease in viscosity values.

Percentage decrease in viscosity values for the ammonium and phosphonium based DESs was calculated as follows. (Hadji Kali *et al*., 2016).

$$P \quad d \quad = \frac{u \quad vi \quad v \quad -lc \quad v \quad v}{u \quad v \quad v} x\ 100 \qquad 4.5$$

The calculated values are tabulated in Appendix II. Table B 4 and Table B 5.for the ammonium and phosphonium based DESs. Figure 4.14 and Figure 4.15 show the plot of the percentage decrease against the temperature ranges for the ammonium and phosphonium based DESs., respectively.

The percentage decrease in the viscosity values for the ammonium based DESs., at the temperature range of 303 – 313 k. For TBAB: PEG600 is 30.357%, TBAB: PEG200 is 41.892%, TBAB: DMF is 23.276% and 35.955% for TBAB: DMSO. Similarly, the percentage decrease in the viscosity values for the phosphonium based DESs., at the temperature range of 303 – 313 K are TBPB: PEG600 (38.511%), TBPMS: PEG600 (41.353%), TBPMS: PEG200 (37.267%), TBPB: DMF (36.00%), TBPB: DMSO (39.552%) and 37.00% for TBPB: PEG200. These values for all the studied DESs are greater than 30% except for TBAB: DMF with 23.276%. these percent decrease of 30 % in viscosity from 303 – 313 K of their initial values could strongly reduce the negative effect of viscosity at low temperatures which can lead to high pumping cost and low mass transfer rates. Therefore, for low temperature operations involving the studied DESs as process fluids, 313.15 K could be a suitable temperature.

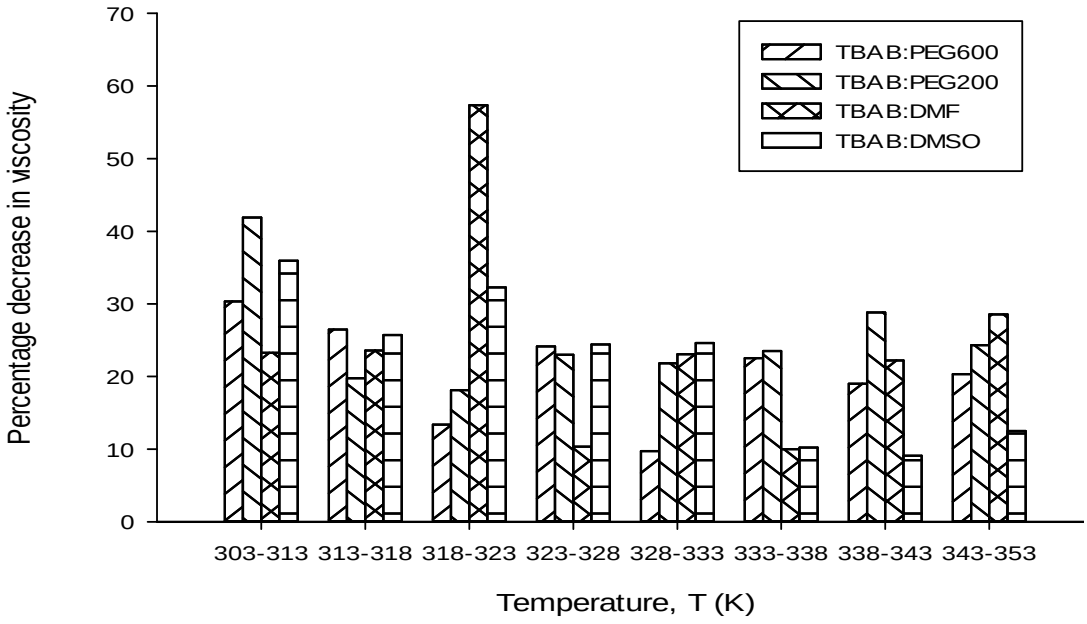

Figure: 4.15 Percentage decrease in viscosity values with temperature for the ammonium based DESs.

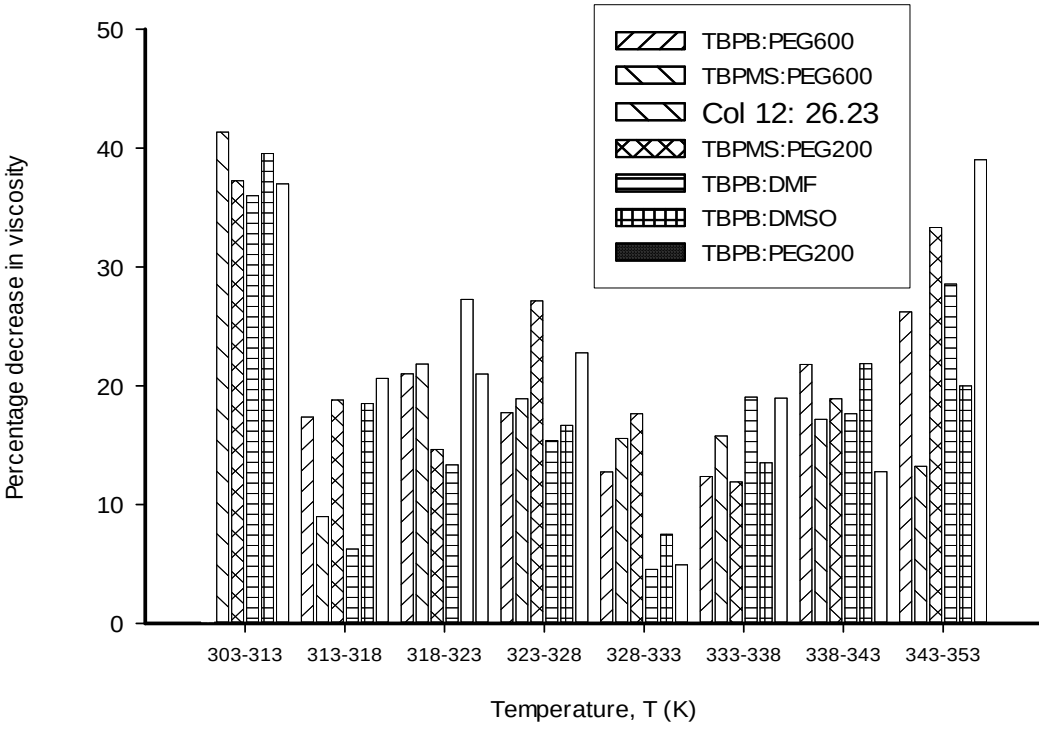

Figure: 4.16 Percentage decrease in viscosity values with temperature for the phosphonium based DESs.

4.2.3 Refractive index

The refractive index of the studied DESs were measured at different temperatures ranging from 303.15 K to 363.15 K. These values obtained are tabulated in Appendix II by Table B.6 and Table B.7, for the ammonium and phosphonium based DESs respectively. Figure 4.16 and Figure 4.17 show the variation of refractive index with temperature for the ammonium and phosphonium based DESs respectively. Refractive index is the ratio of speed of light in vacuum relative to that in a given sample. It is used to measure the purity of a given sample or estimate the concentration of solute in a given solution (Hayyan *et al*., 2012).

Table 4.7 Parameters values and the correlation factor R^2 of refractive index for ammonium based DESs

	Coefficients of equation 4.6		
Phosphonium Based DESs	α	b	R^2
TBPB:PEG600	1.5794	-0.0003	1
TBAB:PEG200	1.57	-0.0003	1
TBAB:DMF	1.595	-0.0003	0.9992
TBAB:DMSO	1.5972	-0.0003	0.9986

Table 4.8 Parameters values and the correlation factor R^2 of refractive index for phosphonium based DESs

	Coefficients of equation 4.6		
Phosphonium Based DESs	α	b	R^2
TBPB:PEG600	1.5782	-0.0003	0.9999
TBPB:PEG200	1.5767	-0.0003	0.9999
TBPMS:PEG600	1.5736	-0.0003	0.9987
TBPMS:PEG200	1.5624	-0.0003	1
TBPB:DMF	1.5879	-0.0003	0.9999
TBPB:DMSO	1.6253	-0.0004	0.9961

4.2.3.1 Effects of temperature on refractive index

The refractive index of the studied DESs decreases with increasing temperature. The observed behaviour were fitted linearly according to the following equation

$$R = a + b \ (K) \qquad 4.6$$

Where R is the refractive index, a and b are adjustable parameters, T is the temperature is Kelvin. These parameters and the correlation factor R^2 for the ammonium and the phosphonium based DESs are presented in Table 4.6 and Table 4.7 respectively. A very good correlation with an R^2 value of 0.999 for the ammonium and phosphonium based DESs were observed for the studied DESs.

The experimental refractive index values for all the ammonium and phosphonium based DESs decreases with increasing temperature. The refractive index values for the ammonium based DESs ranges from 1.4739 for TBAB: PEG600 which is the lowest, to l.4944 for TBAB: DMSO as the highest value. For the phosphonium based DESs the refractive index values fell between 1.4675 and 1.4992 for TBPMS: PEG200 and TBPB: DMSO respectively at 303 K. The refractive index values for the studied DESs are lower than those reported by Hayyan *et. al*., (2012) and (Kareem *et al*., (2010). The refractive index of TBPMS: PEG200 and TBPMS: PEG600 were similar. This observed behaviour could be as a result of the increase in the mobility of the DESs molecules with subsequent decrease in molecular interaction and increase in the refractive index values (Siongco *et al.*, 2013). Similar trend was observed for density, in which the density values increased with increasing temperature. A comparison shows that all the DESs with high density values also recorded high refractive

index values. The salt/HBD molar ration, temperature and molecular weight also have effect on the refractive index of the DESs (Ghaedi *et al.*, 2017).

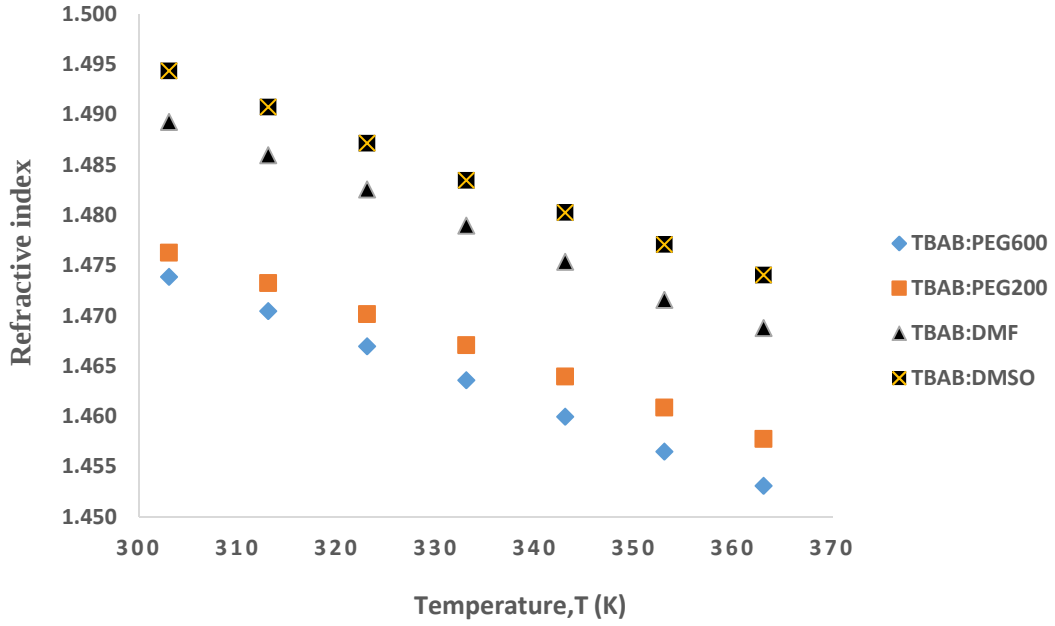

Figure 4.17 Variation of Refractive index with temperature for the ammonium based DESs

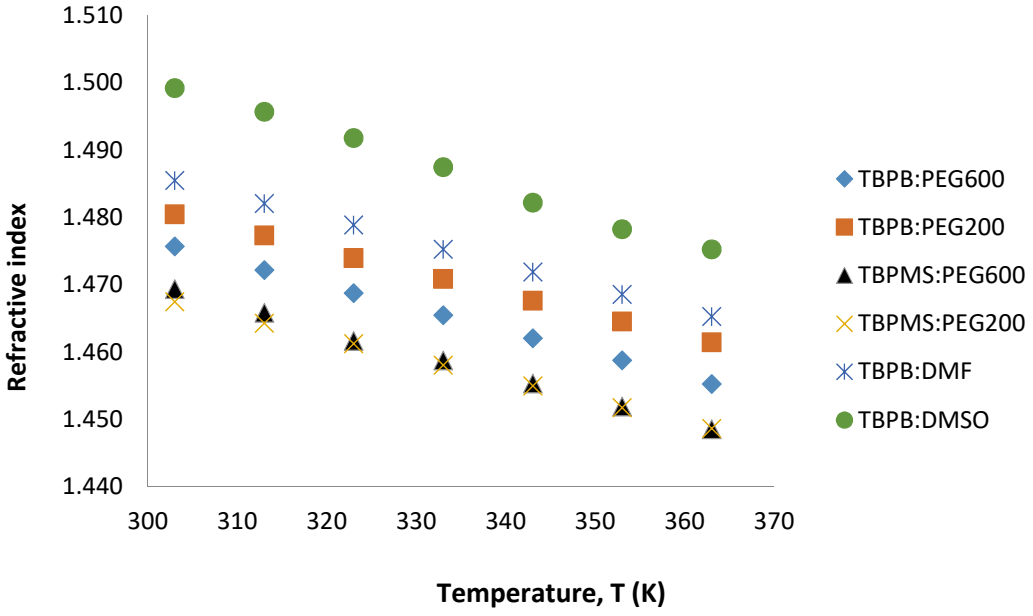

Figure 4.18 Variation of Refractive index with temperature for the phosphonium based DESs

4.2.4. Conductivity

The conductivity of the studied DESs were measured at different temperatures ranging from 303 K to 363 K. These values are tabulated in Appendix II, Table B.8. and Table B.9. Figure 4.18 and Figure 4.19 show the variation of conductivity with temperature for the ammonium and phosphonium based DESs respectively.

4.2.4.1 Effect of temperature on conductivity

The effect of temperature on conductivity of the studied DESs is very profound as the temperature increases the conductivity also increases. The Arrheniuns-like equation which has been used by many to correlate the behaviour for the studied DESs (Kareem *et al*., 2010 . Sun *et. al*., 2015 and Troter *et al*., 2017).

$$K = K_U e^{\left[-\frac{E}{R}\right]} \qquad 4.7$$

where K is the conductivity ($\mu S.cm^{-1}$), K_o is a constant, E is the activation energy of conductivity and R is the gas constant. The Vogel-Fucher Tamman (VFT) equation was also used to correlate dependency of temperature on conductivity (Sun *et. al*., 2015 , Troter *et al*., 2016 and Troter *et al.*, 2017).

The VFT equation for conductivity (σ) is shown in equation 4.8.

$$\sigma = \sigma_U e^{\left(\frac{B}{T-T_U}\right)} \qquad 4.8$$

Where σ_U ($\mu S.cm^{-1}$), B (K) and T_0 (K) are the fitting parameters. The parameter T_0 is also related to Tg the glass transition temperature.The fitting parameters for the Arrhenius equation and VFT are shown in Table 4.8. and Table 4.9. together with their average absolute deviation (AAD) for the ammonium and phosphonium based DESs., respectively.

The percentage average absolute deviation is calculated as follows

$$\%A = \frac{1}{N} \sum_{1}^{N} \frac{\sigma_c - \sigma_e}{\sigma_c} \quad 4.9$$

where σ_c a σ_e represents the calculated and experimental conductivity and N the number of data points. (Siongco, *et al.,* 2013). It can be observed from Table 4.8 and Table 4.9, the VFT equations describe the temperature – conductivity relationships with higher accuracy than the Arrhenius like equation and this is due the higher number of parameters in the VFT equation.

Table 4.9. Parameters for Arrhenius and VFT equations of conductivity for ammonium based DESs.

	Arrhenius constants			VFT equation constants			
Ammonium based DESs	Ko	Ea	%AAD	σ_o	B	T0	%AAD
TBAB:PEG600	6.69E+07	-1.25E+04	3.292229	3309.187	-1664.68	-388.297	1.798344
TBAB:PEG200	4.76E+08	-1.31E+04	7.576752	11975.43	-5954.38	-1371.43	2.115731
TBAB:DMF	8.34E+07	-1.03E+04	2.613392	31368.24	-16128.3	-3835.29	1.123139
TBAB:DMSO	8.01E+07	-1.11E+04	4.428043	24049.62	-12044	-2797.69	1.985108

Table 4.10. Parameters for Arrhenius and VFT equations of conductivity for phosphonium based DESs.

	Arrhenius constants			VFT equation constants			
Phosphonium based DESs	Ko	Ea	%AAD	σ_o	B	T0	%AAD
TBPB:PEG600	6.89E+07	-1.22E+04	4.761781	5020.829	-2508.79	-581.561	2.041695
TBPMS:PEG600	3.33E+07	-1.16E+04	3.77414	4033.583	-2050.33	-482.78	1.40314
TBPMS:PEG200	4.84E+07	-1.05E+04	2.904171	14342.98	-7305.91	-1722.94	1.408676
TBPB:DMF	2.16E+07	-8.65E+03	2.511436	39106.18	-20351	-4894.15	0.758025
TBPB:DMSO	1.46E+08	-1.10E+04	4.64181	28385.22	-14384.2	-3374.41	1.514974
TBPB:PEG200	8.47E+07	-1.11E+04	1.633602	15298.14	-7837.14	-1858.53	1.208819

The studied DESs shows increasing conductivity with increasing temperature range from 303 K to 363 K. At 303 K the conductivity for the ammonium based ranges between 134 – 4650 $uScm^{-1}$ in the order TBAB: DMF > TBAB: DMSO > TBAB: PEG200 > TBAB: PEG600. Similarly, the conductivity for the phosphonium based DESs ranges between 186.9 and 10710 $\mu Scm^{1}$and are in the increasing order TBPB: DMF> TBPB: DMSO> TBPB: PEG200≥ TBPMS: PEG200> TBPB: PEG600≥ TBPMS: PEG600.

This observed behavior could be that the studied DESs contain ionic species that are able to dissociate in the DESs and move independently as a result being conductive. The ions conductivity is determined by the availability of a suitable hole and the type and strength of the ion – HBD interactions (Garcia *et al*., 2015). Also the ions usually move while complexed with the corresponding HBD (Abbott *et al*, 2004). The ionic conductivity of TBAB:EG falls between 118.3 $\mu S \cdot cm^{-1}$ to 528.5 $\mu S \cdot cm^{-1}$, TBAB:1,3-propanediol is 63.7 to311.5 $\mu S \cdot cm^{-1}$ TBABr:1,5-pentanediol is from 38.7 to 168 $\mu S \cdot cm^{-1}$ when HBD was added from 66.7% to 85.7%. and TBAB: glycerol is from 29.6 to 77.7 $\mu S \cdot cm^{-1}$ when HBD reduced from 90% to 75%. at a temperature range of 303 to 333 K (Yusuf *et al.*, 2014).

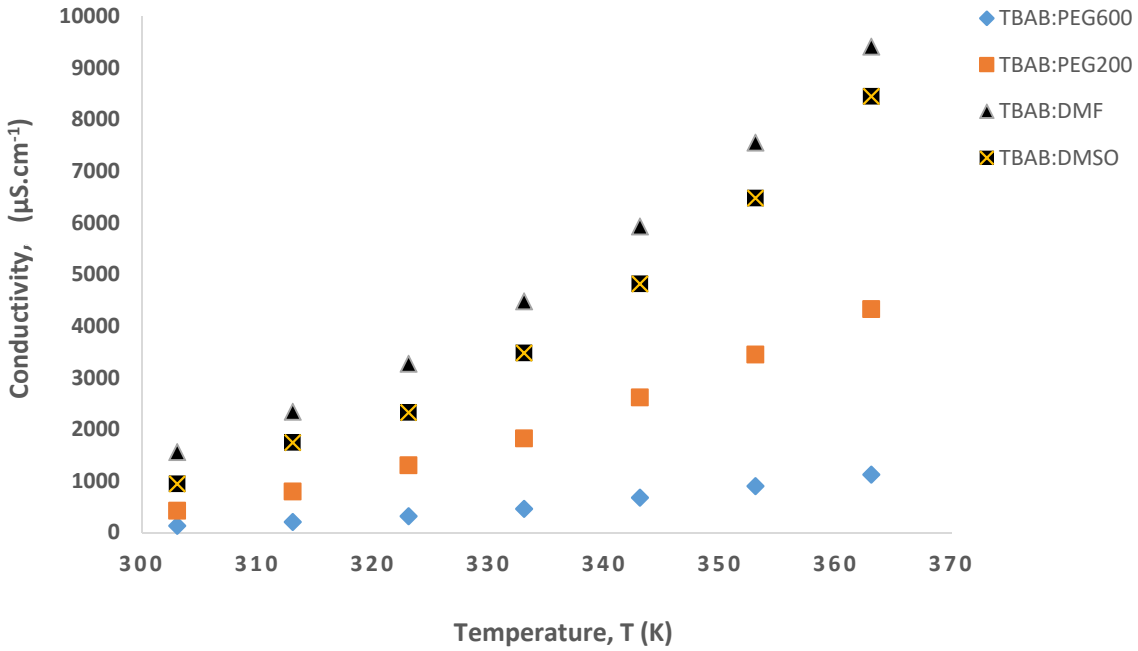

Figure 4.19 Variation of conductivity with temperature for the ammonium based DESs.

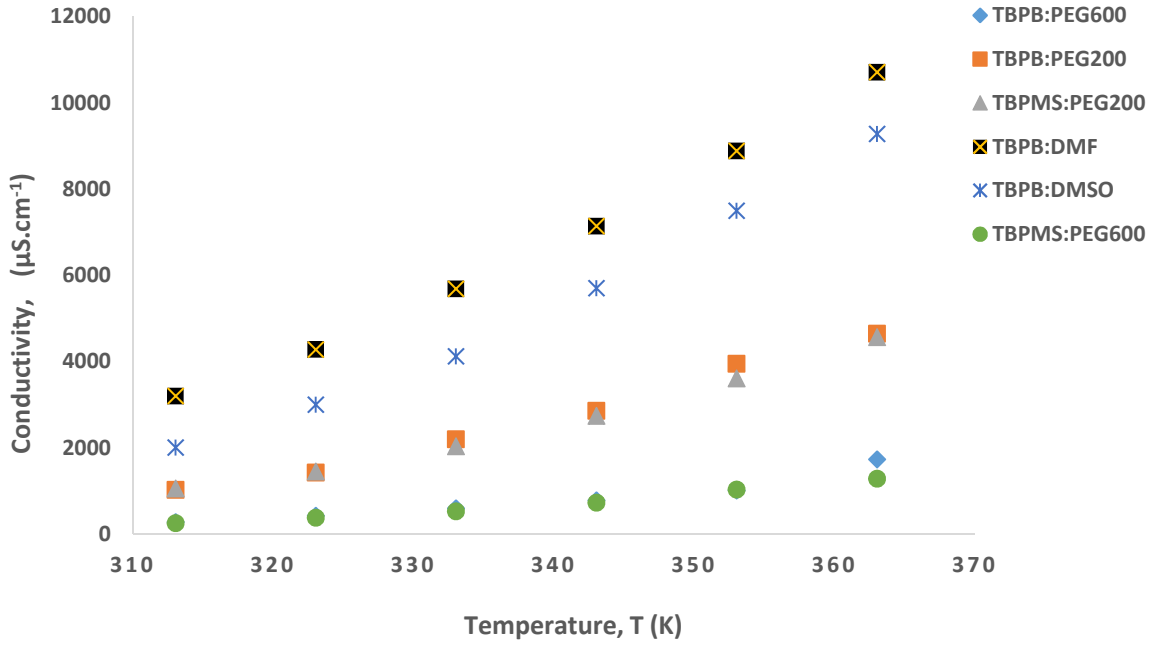

Figure 4.20 Variation of Conductivity with temperature for the phosphonium based DESs.

4.2.4.2 Effects of HBD on conductivity

The effects of HBD can be observed from Figure 4.19 and 4.20. The DESs with the lowest conductivity are the ones having the highest viscosity values which is as a result of type of the HBDs. As observed in Figure 4.20., the conductivity values of TBPB: PEG600 with TBPMS: PEG600 and, TBPB:PEG200 with TBPMS:PEG200 are similar. Although, the salts are different but the HBD are the same for each pair. This observed behaviour could be due to of the effect of the HBDs.

The dependency of conductivity is both on the salt and the HBDs, in some cases, the conductivity decreases with increasing salt concentration as in TBAC:EG system or conductivity increases with increasing salt concentration and through a maximum as in ChCl: EG systems (Garcia *et al*., 2015). Hence, it will be difficult to come up with a clear relationship pattern in this work, and therefore the need for systematic study on the effect of the salt and the HBD type on conductivity.

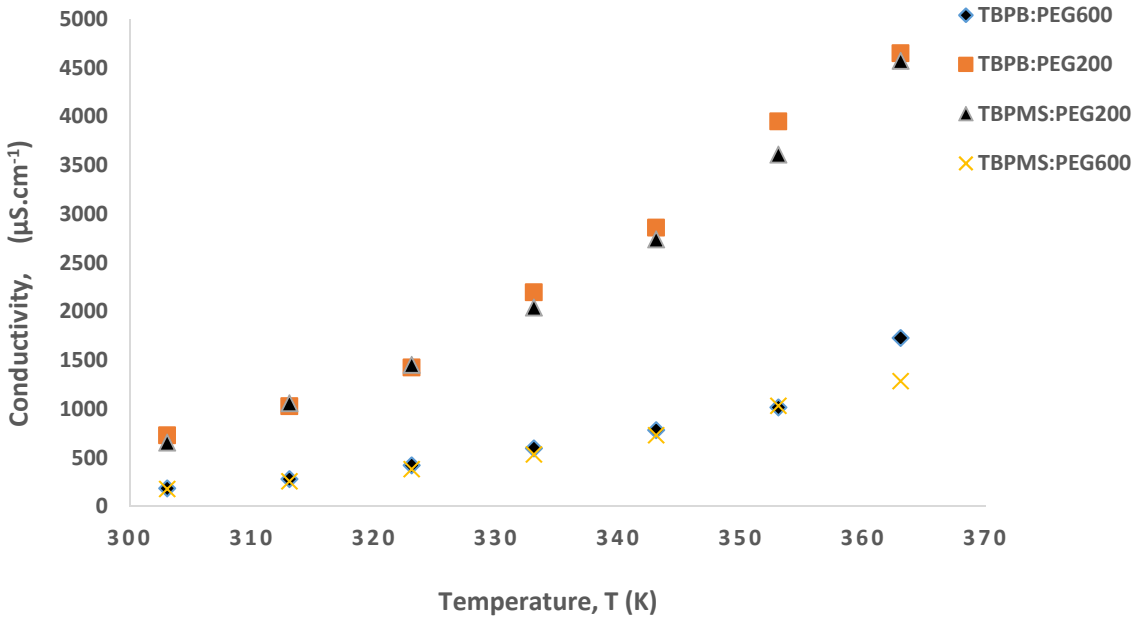

Figure 4.21: Effects of HBD on Conductivity

4.3 Liquid – Liquid Equilibrium Experiments

The experimental liquid-liquid equilibrium of the systems containing (octane + toluene + DESs) were measured at 30, 40 and 50 ^{o}C, and atmospheric pressure. The toluene/octane concentration used were 2.5, 5.0, 10.0, 15.0 and 20.0 wt.% toluene. The obtained experimental data for the DESs are tabulated in Appendix III. Table C2 – C31. The tie lines for the ternary systems DESs + OCTANE + TOLUENE at 30, 40 and 50 ^{o}C and their corresponding distribution coefficient (B) and selectivity (S) as a function of mole fraction of toluene in the raffinate phase are represented in Figure 4.25 through 4.43.

4.3.1 Consistency of the liquid–liquid equilibrium data

In this study Othmer–Tobias (Othmer and Tobias, 1942), and Hand (Hand, 1961) correlations were used to ascertain the consistency of the experimental results based on the linearity of the plots (values of R^2) and is given by Equations 4.10 and 4.11 respectively:

$$ln\left[\frac{1-w_D^R}{w_D^R}\right] = a + b\,ln\left[\frac{1-w_D^E}{w_D^E}\right] \qquad 4.10$$

$$ln\left[\frac{w_T^R}{w_D^R}\right] = c + d\,ln\left[\frac{w_T^E}{w_D^E}\right] \qquad 4.11$$

where w_T^E and w_D^E are mass fractions of toluene and the DES in the extract phase (solvent rich layer), w_T^R and w_C^R are the mass fraction of toluene and n-octane in the raffinate phase (hydrocarbon rich layer), a and b are the fitting parameters of the Othmer-Tobias correlation and c and d are the fitting parameters of the Hand correlation for all the ternary systems and are given in Table 4.11. and the plots for the studied DESs are in APPENDIX III. Figure C1 – C10 The degree of the consistency of the data depends on the linearity of the plot and how close the correlation factor R^2 is close to unity. As can be seen from Table 4.11 the values

of correlation factor for all the studied DESs is between 0.9562 to 0.9999 which indicates a satisfactory fitting for the studied systems and high degree of consistency of the experimental data. Similar results for Othmer-Tobias and Hand correlation factor which lies between 0.6412 – 0.999 (Kareem *et al*., 2013), 0.973 – 0.996 ,Sarwono, *et al*., 2013 and 0.985 – 0.997 Mulyono *et al.*, 2014).

Table 4.11. Othmer-Tobias and Hand correlation parameters and regression coefficients for ternary systems of each of the studied DESs.

	Othmer-Tobias			Hand		
	a	b	R^2	c	d	R^2
1.TBAB:PEG200						
@ 30 ºC	7.4259	3.7636	0.8915	1.4286	1.0515	0.9979
@ 40 ºC	7.4572	3.9706	0.9727	1.1437	0.9912	0.9855
@ 50 ºC	8.2385	4.3902	0.9710	1.3272	1.0268	0.9984
2.TBAB:PEG600						
@ 30 ºC	0.1579	3.4322	0.9682	-0.5637	0.9854	0.9942
@ 40 ºC	-0.3427	2.9851	0.9737	-0.6674	0.9763	0.9942
@ 50 ºC	-0.6826	1.8752	0.9986	-0.5569	0.9919	0.9993
3.TBAB:DMF						
@ 30 ºC	2.5762	2.5055	0.90805	0.7986	1.0917	0.9982
@ 40 ºC	3.282	3.0648	0.9848	0.6198	1.0443	0.9993
@ 50 ºC	1.0935	1.8223	0.9895	0.4637	1.0076	0.9995
4.TBAB:DMSO						
@ 30 ºC	2.9683	3.0814	0.9715	0.1931	0.8756	0.9883
@ 40 ºC	3.6353	3.4524	0.9627	0.5442	0.9987	0.9989
@ 50 ºC	3.8077	3.6963	0.9205	0.0221	0.7994	0.8392
5.TBPB:PEG200						
@ 30 ºC	0.3797	3.3457	0.9273	1.5013	1.0776	0.985
@ 40 ºC	2.5162	2.4087	0.9899	0.5248	1.0211	0.999
@ 50 ºC	2.1372	2.0084	0.8024	0.9853	0.9667	0.9986
6.TBPB:PEG600						
@ 30 ºC	6.3032	3.4479	0.9884	1.1717	1.0475	0.9997
@ 40 ºC	4.4553	2.8323	0.9923	1.1500	1.0639	0.9987
@ 50 ºC	5.5163	3.5972	0.9759	1.0622	1.0376	0.9983
7.TBPB:DMF						
@ 30 ºC	1.1941	2.4944	0.9866	0.0775	0.9872	0.9991
@ 40 ºC	0.8362	2.2085	0.9875	-0.0019	0.9892	0.9995
@ 50 ºC	2.3419	3.1173	0.9983	0.2054	1.0255	0.9990
8.TBPB:DMSO						
@ 30 ºC	3,3151	3.0258	0.9776	0.4009	1.0496	0.9940

@ 40 ºC	1.8183	2.051	0,6412	0.7319	1.0337	0.9944
@ 50 ºC	3.0164	2.8859	0.8847	0.6775	1.0346	0.9940
9.TBPMS:PEG2000						
@ 30 ºC	1.7110	2.3196	0.9915	0.3474	1.0155	0.999
@ 40 ºC	3.0629	3.7162	0.9855	0.3322	1.0363	0.9995
@ 50 ºC	2.8701	3.5287	0.8969	0.3983	1.0491	0.9995
10.TBPMS:PEG600						
@ 30 ºC	-0,0157	2.4951	0.9754	-0.4599	1.0495	0.9998
@ 40 ºC	-0.5918	1.9615	0.9789	-0.584	0.9865	0.9995
@ 50 ºC	-0.5024	2.808	0.9520	-0.6387	1.0087	0.9954

4.3.2 Solute distribution coefficient and selectivity

Solute distribution coefficient and selectivity are two important parameters that are used to assess the potential application of a solvent as an extracting agent in liquid-liquid equilibrium studies. These parameters can be calculated from the experimental data for the extraction aromatic and n-octane hydrocarbon mixture with DES using Equations 4.13 and 4.14:

$$\beta_a = \frac{x_T^E}{x_T^R} \qquad 4.13$$

$$S = \frac{x_T^E \cdot x_O^R}{x_T^R \cdot x_O^E} \qquad 4.14$$

where x is the mole fraction of aromatic and aliphatic in the raffinate (R) and extract (E) phase respectively. (Hansmier, *et al.,* 2010).

The experimental LLE data are shown in Table C2 – C31 in Appendix III, while the ternary diagrams are presented in Figures 4.25 through 4.43. for the studied systems. The ternary diagrams show the shape and size of the immiscibility region and also the slope of the tie lines. The ternary phase diagram of the studied systems corresponds to the type I based on the classifications proposed by Sørensen, and Arlt. (1980), the systems contain only one immiscibility pair (Octane – DESs); the Octane – DESs pair are partially miscible, while the

toluene dissolves completely in octane or DESs. The tie lines TBAB: PEG600, TBPB: PEG600 and TBPMSP: PEG600 show positive slope, indicating that the toluene affinity is more towards these DESs. Hence, toluene extraction is possible over the initial feed composition and also small amount of solvent (DESs) is sufficient for separation.

The ternary diagrams for TBABPEG200 ,TBABPEG600 , TBPBPEG200, TBPBPEG600 and TBPMSPEG600, Show the absence of DESs in the raffinate phase, these implies that the DESs are completely immiscible with octane in the ternary systems. Similar behaviour was observed between heptane – TBAB: EG systems (Kareem *et al*., 2012) and octane – TBAB: Solfolane (Mulyono *et al*., 2014). The ternary diagrams for TBAB: DMF TBAB: DMSO, TBPB: DMF, TBPB: DMSO., show the presence of DESs in the raffinate; that is cross mixing of solvents, a situation that is not desired for a solvent. These makes the DESs less attractive when compared to the other PEG 600 based DESs.

The variation of distribution coefficients and selectivity with the composition of toluene in the hydrocarbon rich (raffinate) phase are plotted in Figures 4.26 through 4.44. From these plots, the distribution coefficients of TBABPEG600 and TBPBPEG600 and TBPMSPEG600 lies within the range of 1.23 – 1.40 at 30,40 and 50 ^{o}C and the selectivity values lie within range at 5.0 to 10.0 at the three different temperatures. The distribution coefficient of TBPB: PEG200 TBPMS:PEG200, TBAB: DMF, TBAB: DMSO, TBPB: DMF, TBPB:DMSO also lies within 0.65 – 0.96 while the selectivity values were 5.0 to 10.0

Distribution coefficient usually decreases with increasing mole fraction of the aromatics in the raffinate (Kiki *et al*., 2016; Rodriguez, *et al*., 2016; Kareem *et al*., 2012). From Figures

4.26 – 4.44 it can be observed that the distribution coefficient as well as selectivity of the studied DESs didn't show monotonic trends in their values. This is possibility due to interaction between the aromatics and the DESs being polar and temperature dependent (Domanska, *et al*., 2007;Kareem *et al*., 2012). This trend is also observed in the region of low mole fraction of aromatics in the raffinate (Mulyono *et al*., 2014; Kareem *et a*l., 2013;Kareem *et a*l., 2012). This observed trend may be attributed to the unusual complexation between the DESs constituents which is not the case with the on conventional solvents which are based on single molecule based (Kareem, *et al*., 2013).

The decrease in distribution coefficient with increasing aromatic composition may also be attributed to the aromatic – DESs interaction that is pi – pi type. By increasing aromatic composition, the distance between the aromatics and the anion of ionic liquids (in this case DESs) becomes larger. This results to decrease in the interaction strength and consequently, the distribution coefficients (Hansmier, 2010; Kareem, *et al*., 2013). Also the pi electrons around the aromatic molecule is responsible for stronger electrostatic field leading to electron cloud around the aromatic compounds. These pi electron cloud leads to a higher electrostatic attraction between the aromatic – DESs pairs more than in aliphatic – DESs pairs, which results in weaker interactions (Hossain, *et al*., 2012; Arce, *et al*., 2007).

The distribution coefficients at low mole fraction of aromatics in the raffinate are relatively higher; this indicates that the separation of aromatics is feasible with DES. The values of selectivity of the studied systems were also found to be greater than one, which is also a good indication that separation of aromatics is feasible with DES. Kiki *et al*., (2016)., reported that aromatic compounds structures have influence on the distribution coefficients

as well as selectivity values based on the work he carried out with benzene, toluene and pyridine and the nitrogen attached to pyridine is responsible for higher distribution coefficients and selectivity values. The methyl group attached to benzene ring reduces the polarity of toluene, which results to toluene having the lowest distribution coefficient and selectivity values. He concluded that the aromatic removal is in the order of pyridine > benzene > toluene this order is possibly due to their relative polarities.

4.3.3 Influence of temperature on the liquid - liquid experiments

The influence of temperature on liquid-liquid extraction was investigated for the selected DESs at low temperature. Three different temperatures 30, 40, and 50 ^{o}C were used. The mole fraction of toluene in the extract phase was plotted against the mole fraction of toluene in the raffinate phase at the three different temperatures for all the selected DESs. The intercept was set at zero and the slope gives the average distribution coefficient for each temperatures, given by Equation 4.17.

$$x_T^E = D \,.\, x_T^R \qquad 4.17$$

where x_T^E is the mole fraction of toluene in the extract phase, x_T^R mole fraction of toluene in the raffinate phase. (Hansmier, 2010). The average distribution coefficients and the regression coefficients at 30, 40, and 50 ^{o}C, for all the selected DESs are shown in Appendix III, Table C1.

Figure 4.22 show the average distribution coefficients for all the DESs at 30, 40, and 50 ^{o}C. The average distribution coefficients for TBAB: PEG 600, TBPB: PEG600 AND TBPMS: PEG 600 have distribution coefficients in the range of 1.256 – 1.368, while the remaining DESs falls within the range of 0.650 – 0.955. TBPB: DMF shows an exception with

distribution coefficients of 0.815,0.891 and 0.930 at 30, 40 and 50 ^{o}C respectively. It can be seen that the distribution coefficients have very similar values at all the temperatures for a particular DESs. This shows that temperature have little effect on the distribution coefficient within the three experimental temperature range

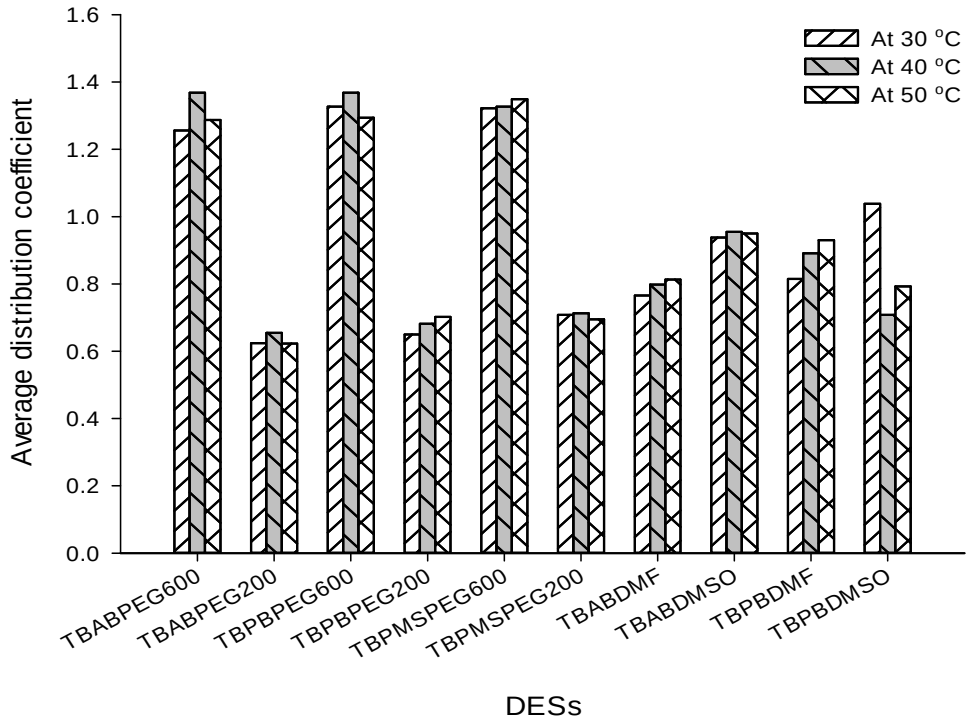

Figure 4.22. Average distribution coefficients at three different temperatures for the studied DESs.

4.3.4 Effects of HBDs

The DESs that were formed from PEG 600 as HBD have a very strong influence on both the distribution coefficients and selectivity. As can be seen in Figure 4.22. TBAB: PEG600, TBPB: PEG600 and TBPMSPEG600 their distribution coefficients values are greater than one at 30,40 and 50 ^{o}C. But for corresponding salts with different HBDs such as, TBAB: PEG200, TBPB: PEG200 and TBPMS: PEG200 their distribution coefficients are less than

one. This is likely due to the differences in the polymer chain in the PEGs. The DESs that are made from TBAB: DMF, TBAB: DMSO, TBPB: DMF and TBPB: DMSO have distribution coefficients in the range of 0.5 – 1.0, also these DESs were also found in the raffinate phase during the LLE experiments. These makes them to be less attractive when compared to those of PEGs.

4.3.5 Literature comparison of distribution coefficients and Selectivity values

Table 4.23. show the literature comparison in terms of distribution coefficient and selectivity for toluene + octane systems with the studied DESs and sulfolane as solvents (organic and DES). The work of Mohsen-nia *et al.*, 2008., Lin & Kao, 2002 and Doulabi, 2006., have reported their distribution coefficient values in mass fraction basis, therefore, our mass fraction values will be used for comparison Figure 4.23. The toluene distribution coefficient in mass fraction D(w) for the studied systems is in the range of 0.31 – 0.81. The Dw values for the PEG based DESs is less than those values reported in literature (Figure 4.23) for similar systems with sulfolane as solvent. The comparison with sulfolane is used as a bench mark because it is one of the solvent used in industries. The Dw for PEG based DESs falls within the range of what was obtained by Mohsen-nia et al., 2008., for EG. The Dw values for the studied systems is within the lower range of what was obtained by Lin & Kao, 2002 and Doulabi, 2006., for sulfolane, with higher values at the upper range. The selectivity values for the studied DESs are very low when compared with the reported systems especially at their upper range values.

Figure 4.24 is the Literature comparison for the studied DESs with distribution coefficient in mole fraction basis D(x). The distribution coefficient values for the studied systems are higher than 0.25 – 0.59 as obtained by Mulyono et al., 2014, for TBAB:SOLF (1:4).

The studied DESs showed low distribution coefficient values when compared to sulfolane. However, in terms of economic efficiency, using the studied DES especially the PEG based DESs, means less energy requires during solvent regeneration due to the negligible vapour pressures of DESs as compared to volatile organic solvents like sulfolane.

Table 4.12. Literature comparison in terms of distribution coefficient and selectivity

systems	solvents	D (x)	D(w)	S	T (K)	Reference
Toluene + Octane	TBABPEG600	1.44	0.39	8.49	303.15,313.15 323.15	This work
	TBABPEG200	0.75	0.31	10.39		
	TBPBPEG600	1.61	0.42	10.01		
	TBPBPEG200	0.74	0.36	8.62		
	TBPMSPEG600	1.51	0.37	9.51		
	TBPMSPEG200	0.74	0.33	9.18		
	TBABDMF	0.81	0.63	6.10		
	TBABDMSO	1.00	0.58	5.08		
	TBPBDMF	0.97	0.67	5.61		
	TBPBDMSO	1.14	0.81	10.25		
	TBAB:SOLF	0.57	nil	25.70	298.15	Mulyono et al., 2014
	EG	nil	0.33	33.93	295.15, 307.15	Mohsen-nia et al., 2008
	SOLF1	nil	0.68	34.00	323.15,373.15, 348.15	Lin & Kao, 2002
	SOLF	nil	0.88	15.69	303.15,313.15	Doulabi, 2006

D(x) = distribution coefficient in mole fraction basis, D(w) = distribution coefficient in mass fraction basis, S = selectivity

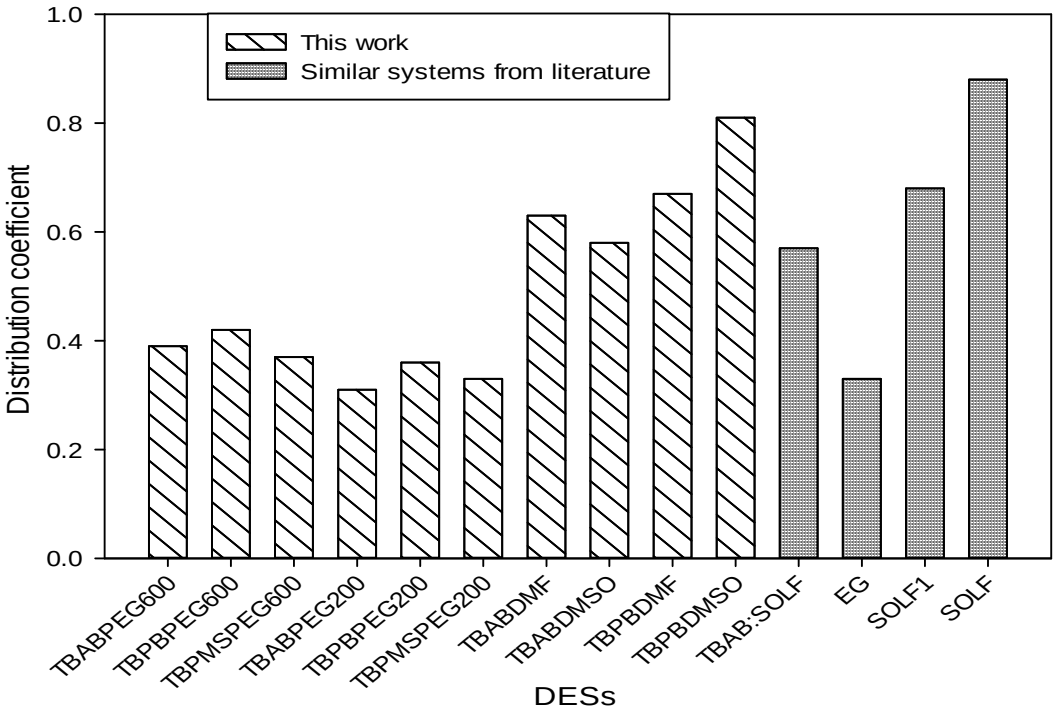

Figure 4.23. Literature comparison for the studied DESs with distribution coefficient in mass fraction basis.

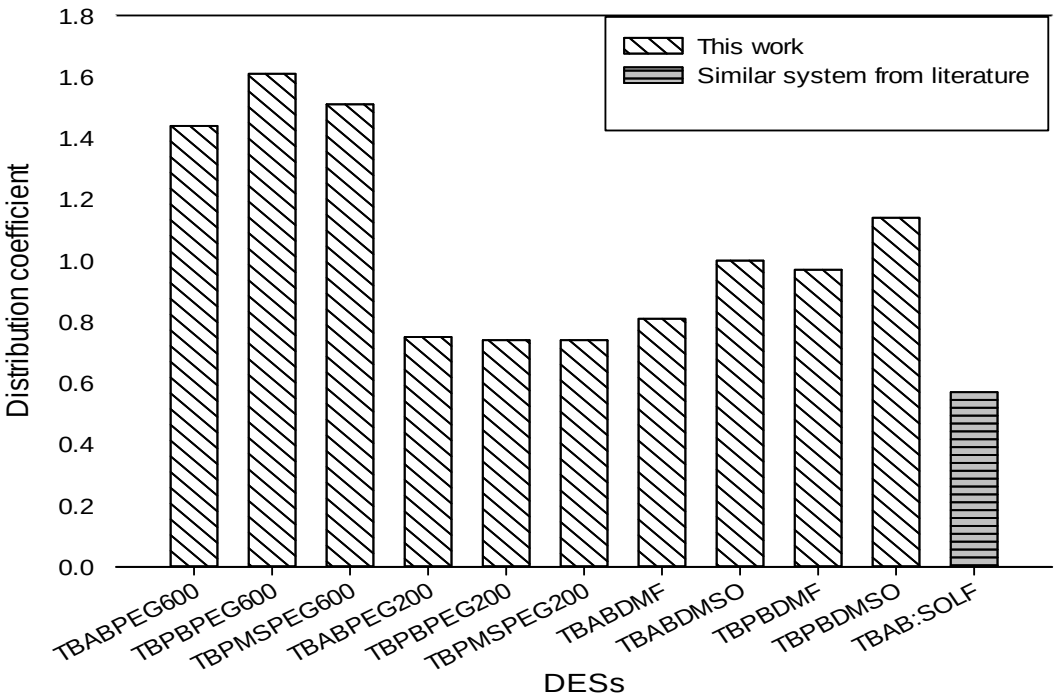

Figure 4.24 Literature comparison for the studied DESs with distribution coefficient in mole fraction basis

4.4 Thermodynamic modelling

4.4.1 UNIQUAC volume and structural parameters for the DESs

The binary interaction parameters and the RMSD of the studied ternary systems are presented in Table 4.13 – 4.22. The non-randomness parameter αij for the NRTL model was set at 0.2. the experimental and the calculated compositions are presented in Appendix III Table C2 – C31. The volume (r) and surface area (q) structural parameters for the UNIQUAC model were predicted using the following equation (Bharti *et al*., 2017).

$$r = \frac{(V^{Pl} \quad A^{3})(1\,X\,1\ ^{-\Box}c\ )^{3}}{V_w} N_a \qquad 4.15$$

$$q = \frac{(A^{Pl} \quad A^{2})(1\,X\,1\ ^{-\Box}c\ )^{2}}{A_w} N_a \qquad 4.16$$

The estimate of the overall surface area A^{Pl} and the overall volume V^{Pl} for the DESs components and the hydrocarbons was done using the output file of the Polarizable Continuum Model (PCM) in the Material Studio software package. N_a is the Avogadro's number, V_w (15.17 cm^3/mol) and A_w (2.5 X 10^9 cm^2/mol) are the standard segment volume and area respectively. (Bharti *et al*., 2017). Thereafter the UNIQUAC volume and structural parameters for the DESs were calculated based on the molar contribution of each of the component that forms the DESs as shown in Table 4.12.

Table 4.13. UNIQUAC volume (r) and surface area (q) structural parameters of compound

	r	q
TBABPEG600	21.5625	14.6982
TBABPEG200	10.3177	6.978
TBPBPEG600	21.5625	14.6982
TBPBPEG200	10.589	72,582
TBPMSPEG600	11.2812	7.5108
TBPMSPEG200	22.526	15.231
TBABDMF	7.457	4.9591
TBABDMSO	6.7669	4.5765
TBPBDMF	7.7283	5.2393
TBPBDMSO	7.0382	4.8567
Octane	6.9894	4.9184
Toluene	4.1288	3.0705

4.4.2 Genetic Algorithm and the estimation of Binary interaction parameters

Genetic Algorithm GA is an evolutionary optimization algorithm used in non-linear optimization, which was developed by John Holland. GA is based on Charles Darwin's theory of evolution and natural selection that mimics biological evolution. GA is a population based optimization algorithm, it explores search space with a population of solutions instead of a single solution. Figure 3.6 shows the flow diagram of the algorithm used for the calculation of binary interaction parameters. Programme in GA package in Matlab software was written for the execution of these algorithm. The complete Matlab programme is in Appendix V.

The NRTL and UNIQUAC models calculated interaction parameter values and the RMSD values for all the systems are given in Table 4.13 – 4.22. The tie lines ploted using the NRTL model were almost equal to the experimental tie lines. The RMSD values were found to be between 0.0064 – 0.0008. Deviations were observed from the tie lines generated using the UNIQUAC model for the studied systems as compared to the experimental tie lines. The deviations is more noticiable in the PEG600 based DESs. The RMSD values for TBPB: PEG200 TBPMS: PEG200, TBAB: DMF, TBAB: DMSO, TBPB: DMF, TBPB: DMSO, lies between 0.0092 – 0.0061., while the PEG600 based DESs is between 0.2472 – 0.2250. The calculated volume and surface area parameters for UNIQUAC for PEG600 based DESs are large when compared with the other studied DESs, and this is likely the reason for the differences in their RMSD values.

Generally, the NRTL model gave a better fit as all the tie lines almost coincide with the experimental tie lines and hence, very low RMSD values were obtained. However, the UNQUAC model could not give a better fit when compared with the NRTL model.

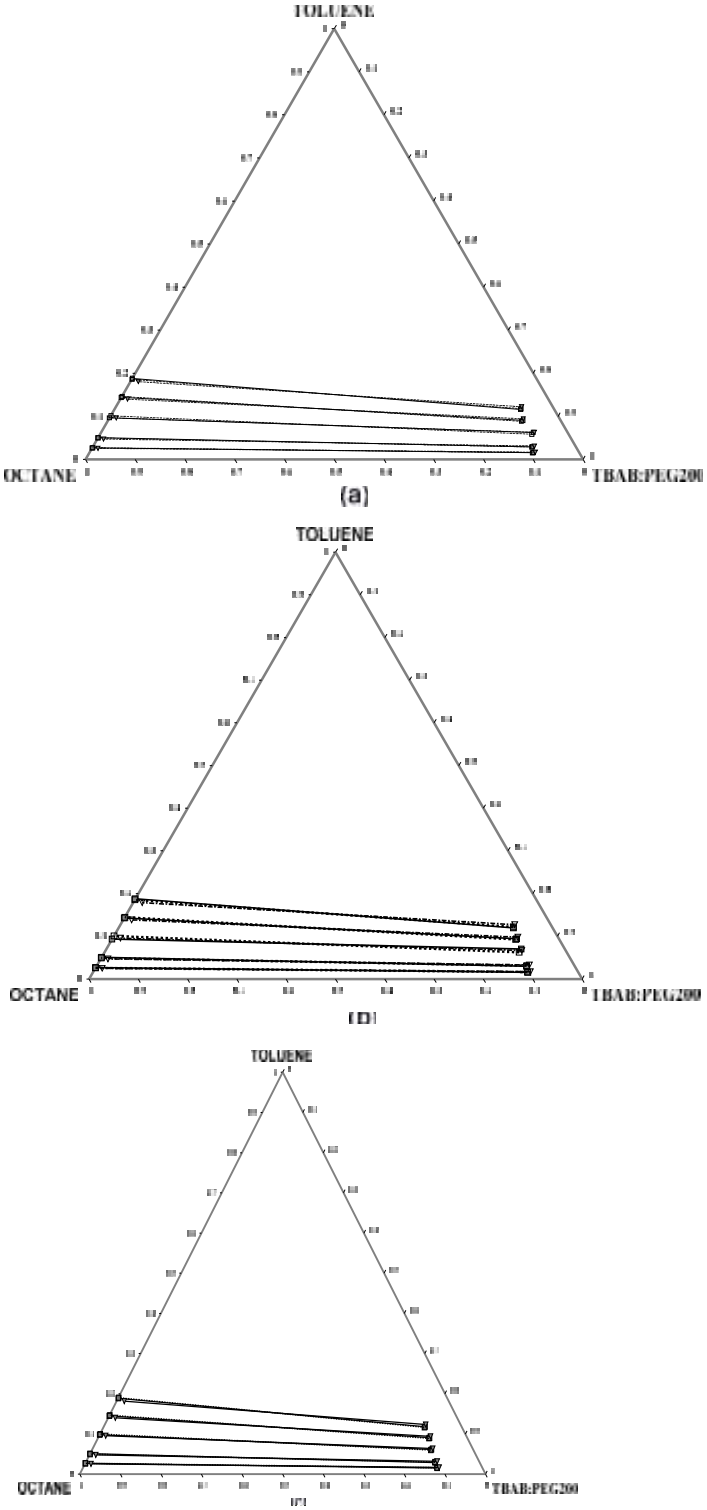

Figure 4.25. Ternary diagram for Touene(1)+Octane(2)+TBABPEG200(3) for (a) at 30 ^{O}C, (b) at 40 ^{O}C, and (c) at 50 ^{O}C. Filled square representing experimental tie-lines, Open-square representing tie-lines from NRTL calculation and filled triangle down representing tie-lines from UNIQUAC calculation.

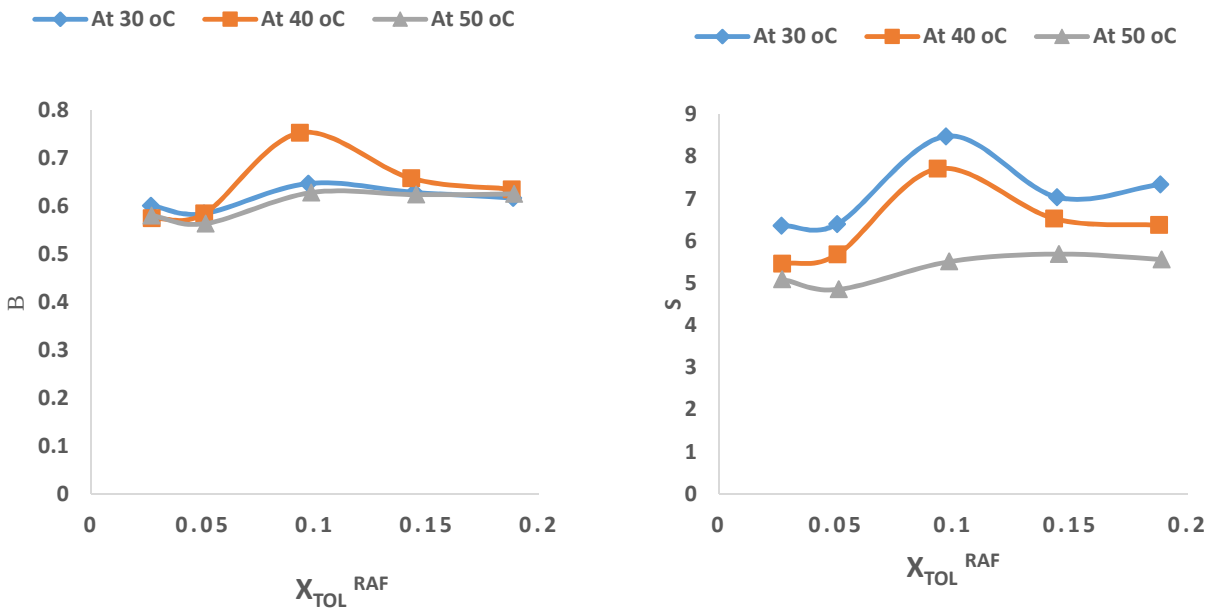

Figure 4.26. Experimental distribution coefficient (β) and selectivity (S) as a function of mole fraction of toluene in the raffinate phase (X_{tol}^{raff}) for Touene(1)+Octane(2)+TBABPEG200(3) ternary systems 30 ^{o}C , 40 ^{o}C and 50 ^{o}C.

Table 4.14. Interaction parameters for NRTL/UNIQUAC for Touene(1)+Octane(2)+TBABPEG200(3) TERNARY SYSTEM at different temperatures.

Model	Temp (^{o}C)	τ_{12}	τ_{13}	τ_{21}	τ_{23}	τ_{31}	τ_{32}	RMSD
NRTL	30	6.2226	-5.4126	0.9489	-5.3652	0.9974	9.6417	0.0030
α = 0.2	40	7.4595	-3.1760	0.8864	-2.9749	2.4616	6.4467	0.0025
	50	7.0035	-1.5875	0.7614	-1.8645	1.3024	4.8558	0.0015
UNIQUAC		A_{12}	A_{13}	A_{21}	A_{23}	A_{31}	A_{32}	
	30	0.6864	0.9889	0.7417	0.8585	0.9709	0.8753	0.0082
	40	0.6968	0.9764	0.7523	0.8981	0.9962	0.8558	0.0094
	50	0.6781	0.9793	0.7839	0.8636	0.9701	0.8529	0.0092

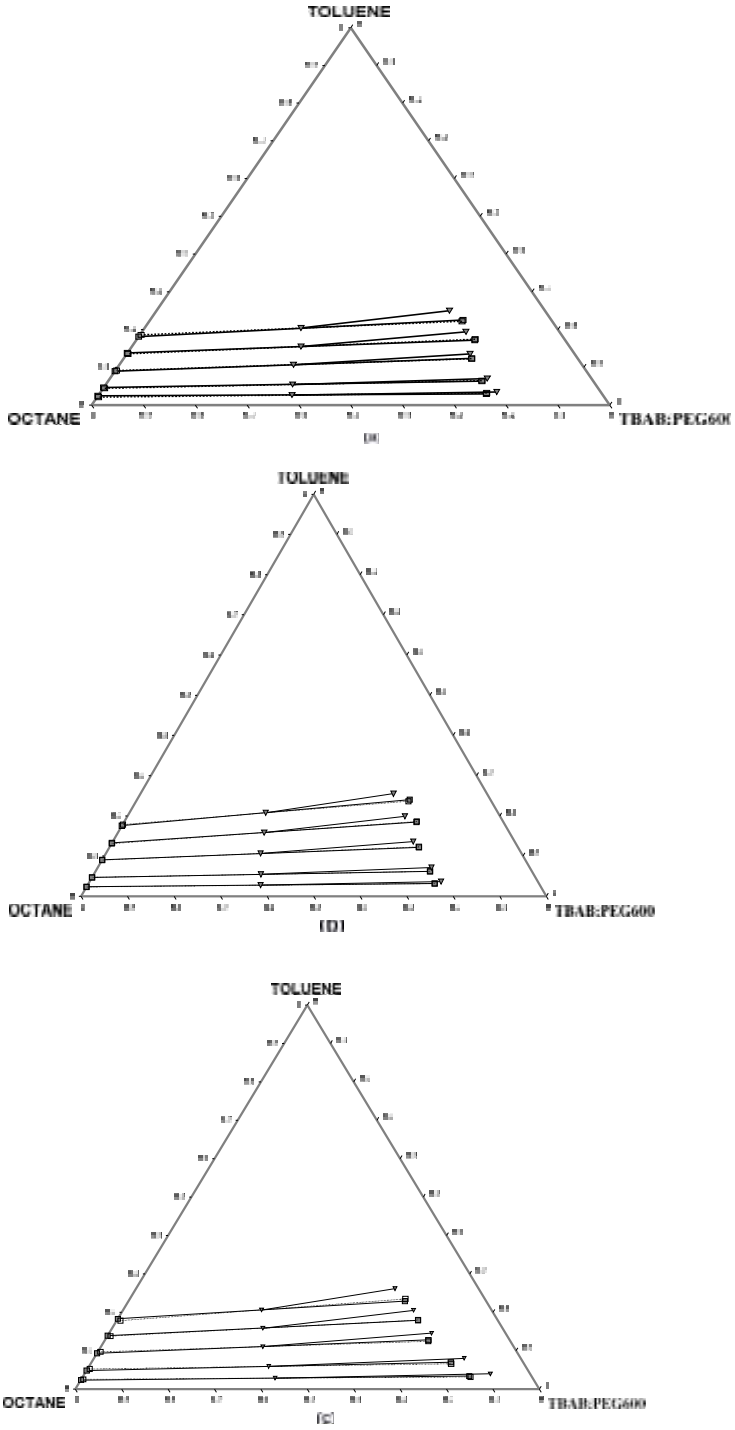

Figure 4.27. Ternary diagram for Toluene(1)+Octane(2)+TBABPEG600(3) for (a) at 30 ^{O}C, (b) at 40 ^{O}C, and (c) at 50 ^{O}C. Filled square representing experimental tie-lines, Open-square representing tie-lines from NRTL calculation and filled triangle down representing tie-lines from UNIQUAC calculation.

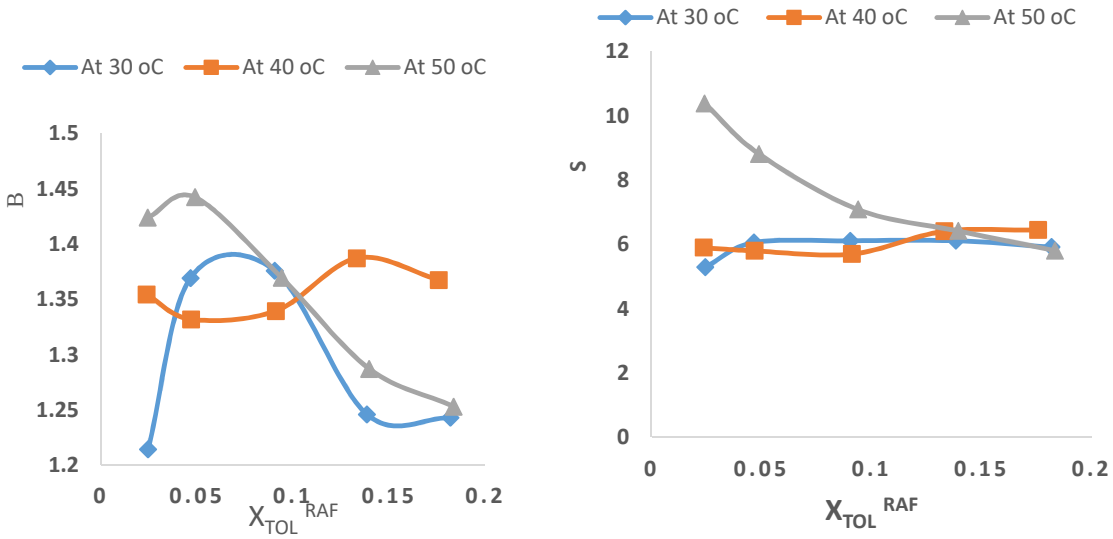

Figure 4.28. Experimental distribution coefficient (β) and selectivity (S) as a function of mole fraction of toluene in the raffinate phase (X_{tol}^{raff}) for Toluene(1)+Octane(2)+TBABPEG600(3) ternary systems 30 ºC 40 ºC and 50 ºC.

Table 4.15. Interaction parameters for NRTL/UNIQUAC for Toluene(1)+Octane(2) +TBAB: PEG600(3) TERNARY SYSTEM at different temperatures.

Model	Temp (ºC)	τ_{12}	τ_{13}	τ_{21}	τ_{23}	τ_{31}	τ_{32}	RMSD
NRTL	30	5.8315	-0.9229	-0.1707	-1.3028	3.3078	10.2589	0.0032
α = 0.2	40	8.1345	7.6012	0.0044	6.7644	2.0747	4.4045	0.0032
	50	5.1645	-2.0208	0.3469	-4.0253	-0.1535	3.4644	0.0060
UNIQUAC		A_{12}	A_{13}	A_{21}	A_{23}	A_{31}	A_{32}	
	30	0.9591	1.0021	0.9294	0.9732	0.9736	0.8908	0.2295
	40	0.9567	0.9982	0.9325	0.9513	0.9680	0.9097	0.2276
	50	0.9594	1.0227	0.9269	0.9646	0.9863	0.9424	0.2416

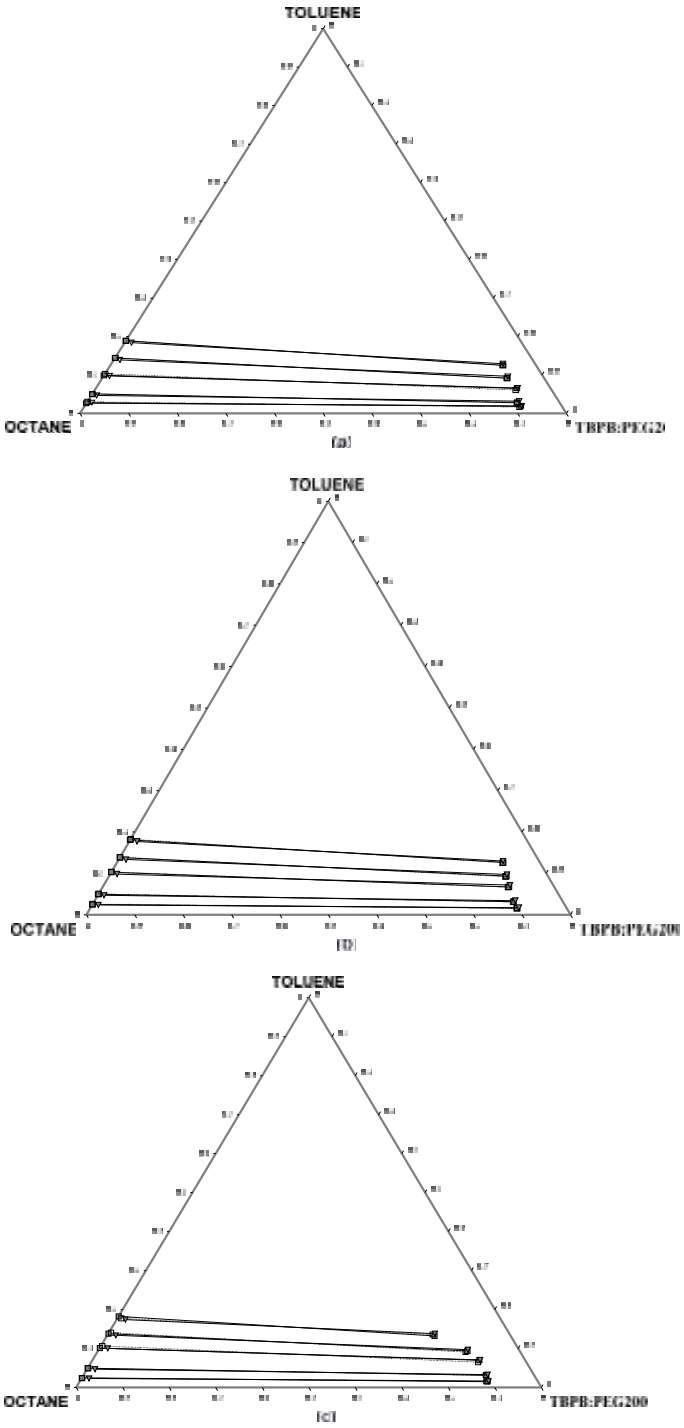

Figure 4.29. Ternary diagram for Toluene(1)+Octane(2)+TBPBPEG200(3) for (a) at 30 ^{O}C, (b) at 40 ^{O}C, and (c) at 50 ^{O}C. Filled square representing experimental tie-lines, Open-square representing tie-lines from NRTL calculation and filled triangle down representing tie-lines from UNIQUAC calculation.

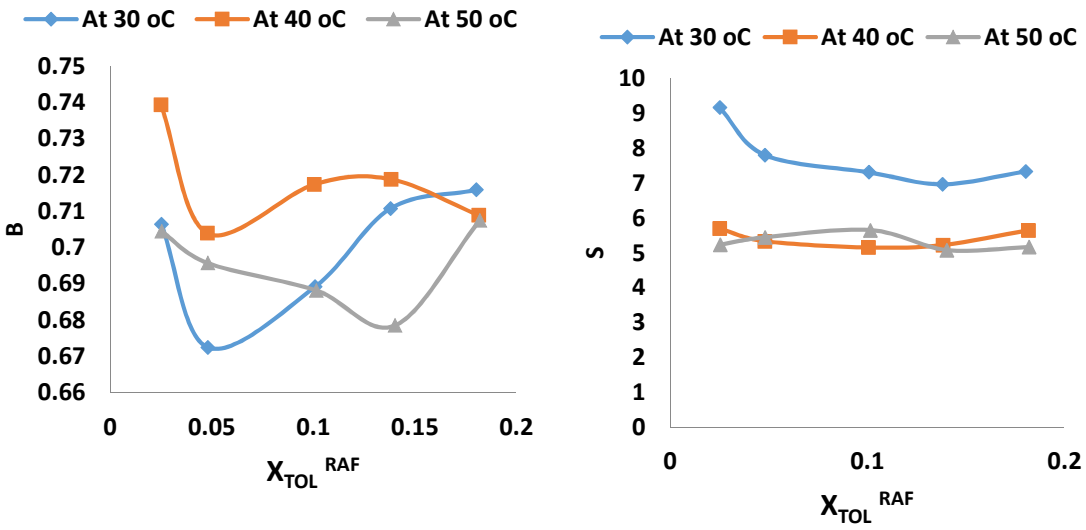

Figure 4.30. Experimental distribution coefficient (β) and selectivity (S) as a function of mole fraction of toluene in the raffinate phase (X_{tol}^{raff}) for Toluene(1)+Octane(2)+TBPBPEG200(3) ternary systems 30 °C 40 °C and 50 °C.

Table 4.16. Interaction parameters for NRTL/UNIQUAC for Toluene(1) +Octane(2) + TBPBPEG200(3) TERNARY SYSTEM at different temperatures.

Model	Temp (°C)	τ_{12}	τ_{13}	τ_{21}	τ_{23}	τ_{31}	τ_{32}	RMSD
NRTL	30	6.6352	-5.4312	1.0004	-5.8279	0.5710	8.3216	0.0026
α = 0.2	40	7.3658	-4.5298	0.8903	-5.0986	0.6628	6.8520	0.0019
	50	7.6304	-5.7627	0.9830	-3.7809	1.7031	0.0805	0.0024
UNIQUAC		A_{12}	A_{13}	A_{21}	A_{23}	A_{31}	A_{32}	
	30	0.6876	0.9977	0.7404	0.8717	0.9731	0.8732	0.0071
	40	0.6980	0.9786	0.7557	0.9033	0.9946	0.8550	0.0084
	50	0.6943	0.9638	0.7900	0.8514	0.9610	0.8593	0.0113

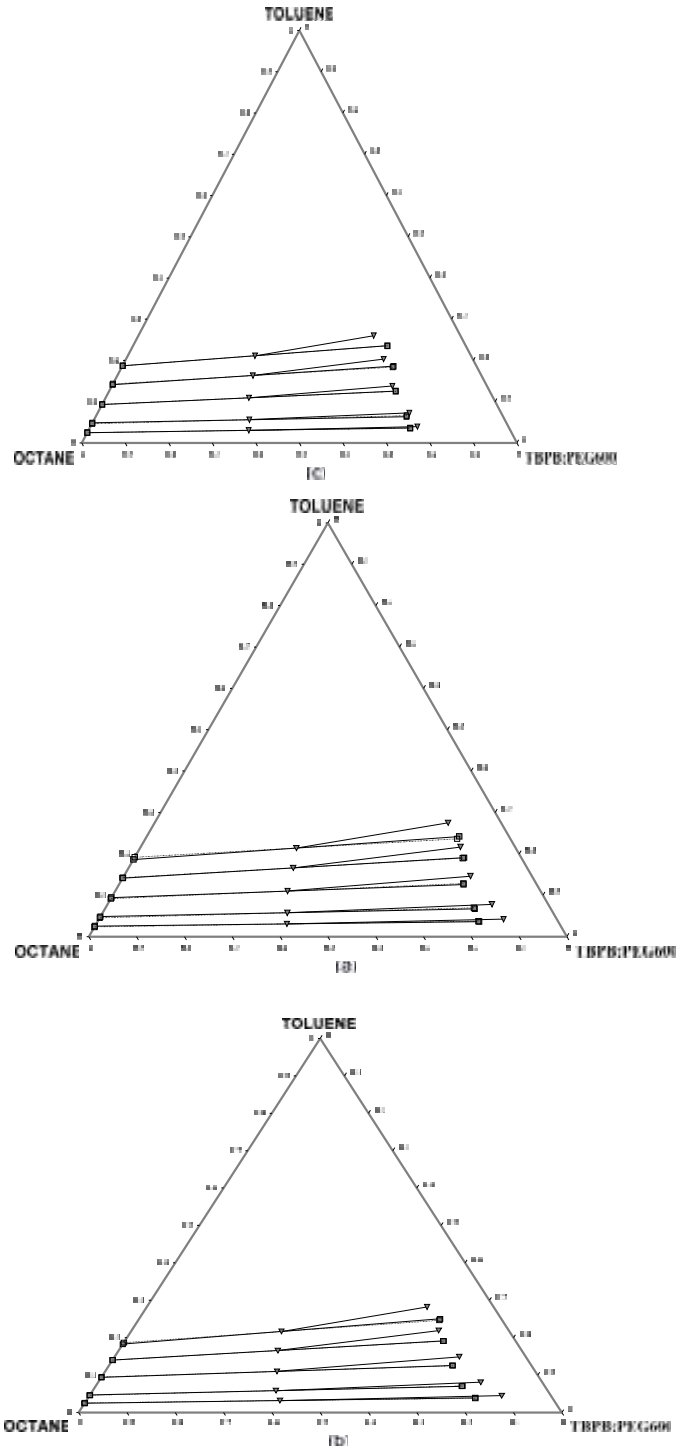

Figure 4.31. Ternary diagram for Toluene(1)+Octane(2)+TBPBPEG600(3) for (a) at 30 ^{O}C, (b) at 40 ^{O}C, and (c) at 50 ^{O}C. Filled square representing experimental tie-lines, Open-square representing tie-lines from NRTL calculation and filled triangle down representing tie-lines from UNIQUAC calculation.

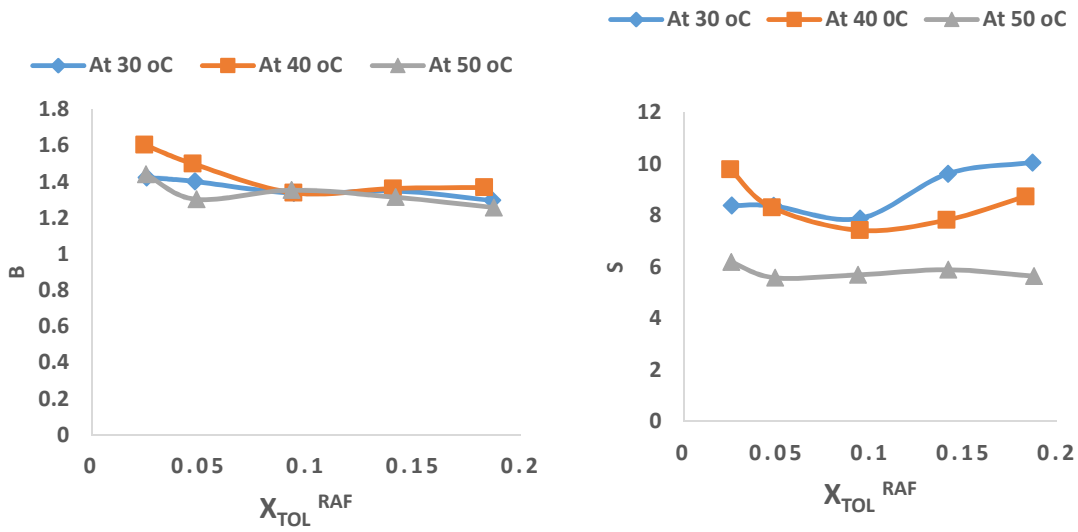

Figure 4.32. Experimental distribution coefficient (β) and selectivity (S) as a function of mole fraction of toluene in the raffinate phase (X_{tol}^{raff}) for Toluene(1)+Octane(2)+TBPBPEG600(3) ternary systems 30 ºC 40 ºC and 50 ºC.

Table 4.17. Interaction parameters for NRTL/UNIQUAC for Toluene(1) + Octane(2)+TBPBPEG600(3) TERNARY SYSTEM at different temperatures.

Model	Temp (ºC)	τ_{12}	τ_{13}	τ_{21}	τ_{23}	τ_{31}	τ_{32}	RMSD
NRTL	30	10.5249	1.0799	0.7190	0.3154	2.7040	8.4310	0.0032
α = 0.2	40	9.2665	6.7574	0.5047	6.0831	2.0519	4.2950	0.0036
	50	8.1322	-1.0956	0.0500	-3.8414	-0.5000	6.9070	0.0017
UNIQUAC		A_{12}	A_{13}	A_{21}	A_{23}	A_{31}	A_{32}	
	30	0.9632	0.9953	0.9223	0.9564	0.9870	0.9267	0.2472
	40	0.9471	1.0211	0.9387	0.9717	0.9957	0.9522	0.2427
	50	0.9541	1.0153	0.9348	0.9807	1.0072	0.9274	0.2250

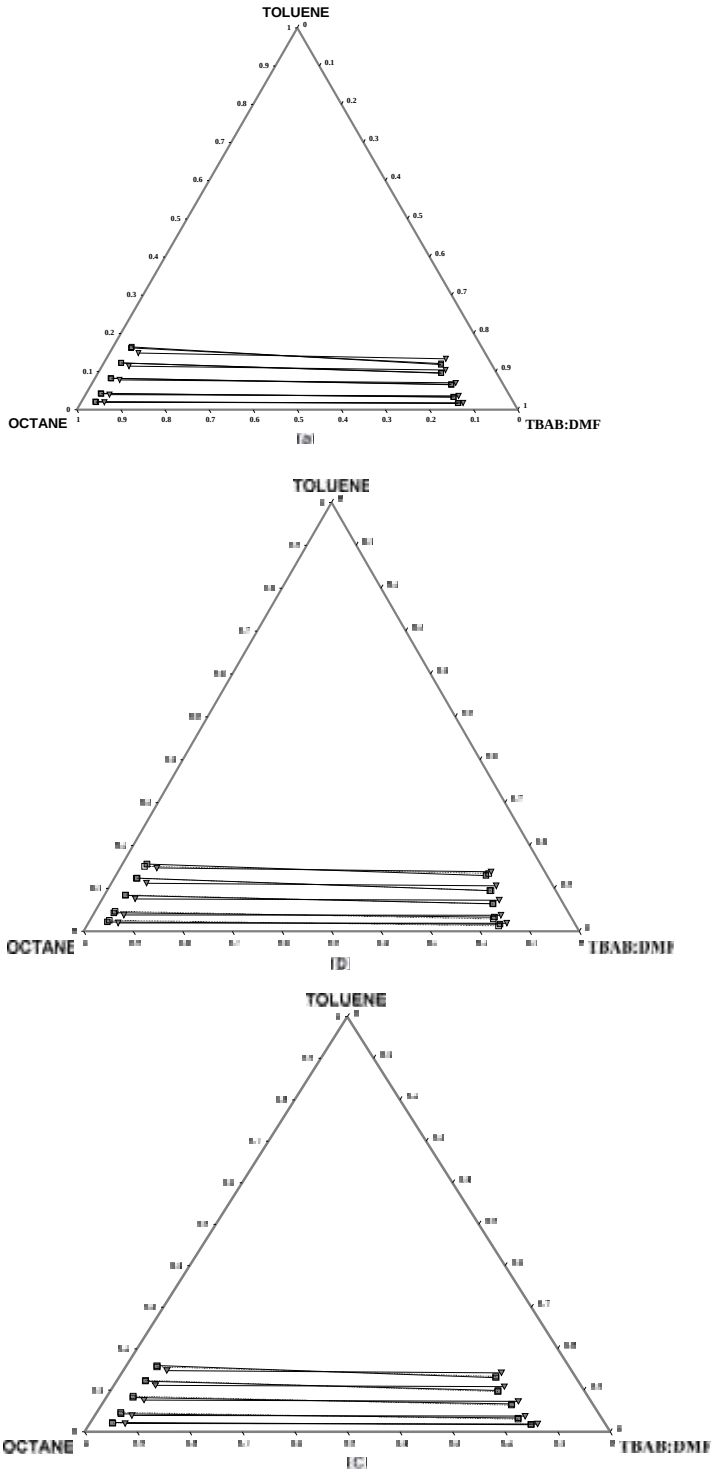

Figure 4.33. Ternary diagram for Toluene(1)+Octane(2)+TBAB:DMF(3) for (a) at 30 ^{O}C, (b) at 40 ^{O}C, and (c) at 50 ^{O}C. Filled square representing experimental tie-lines, Open-square representing tie-lines from NRTL calculation and filled triangle down representing tie-lines from UNIQUAC calculation.

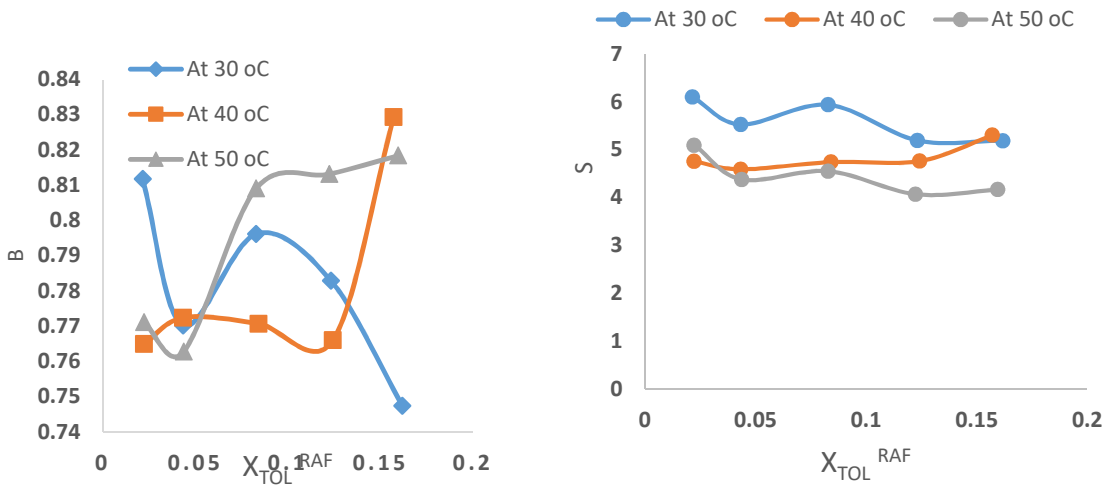

Figure 4.34. Experimental distribution coefficient (β) and selectivity (S) as a function of mole fraction of toluene in the raffinate phase (X_{tol}^{raff}) for Toluene(1)+Octane(2)+TBAB:DMF(3) ternary systems 30 °C 40 °C and 50 °C.

Table 4.18. Interaction parameters for NRTL/UNIQUAC for Toluene(1)+Octane(2) +TBAB:DMF(3) TERNARY SYSTEM at different temperatures.

Model	Temp (°C)	τ_{12}	τ_{13}	τ_{21}	τ_{23}	τ_{31}	τ_{32}	RMSD
NRTL	30	2.8949	4.1531	0.9109	4.5533	6.3019	2.6167	0.0017
α = 0.2	40	2.8207	13.9996	0.8133	15.7847	3.6379	3.9408	0.0025
	50	2.8554	9.9918	0.7674	10.0751	4.0860	1.9027	0.0020
UNIQUAC		A_{12}	A_{13}	A_{21}	A_{23}	A_{31}	A_{32}	
	30	0.6699	0.9484	0.7845	0.9367	0.8902	0.8331	0.0137
	40	0.6830	0.9200	0.7865	0.9150	0.9121	0.8644	0.0152
	50	0.6933	0.9590	0.7912	0.9414	0.8914	0.8565	0.0150

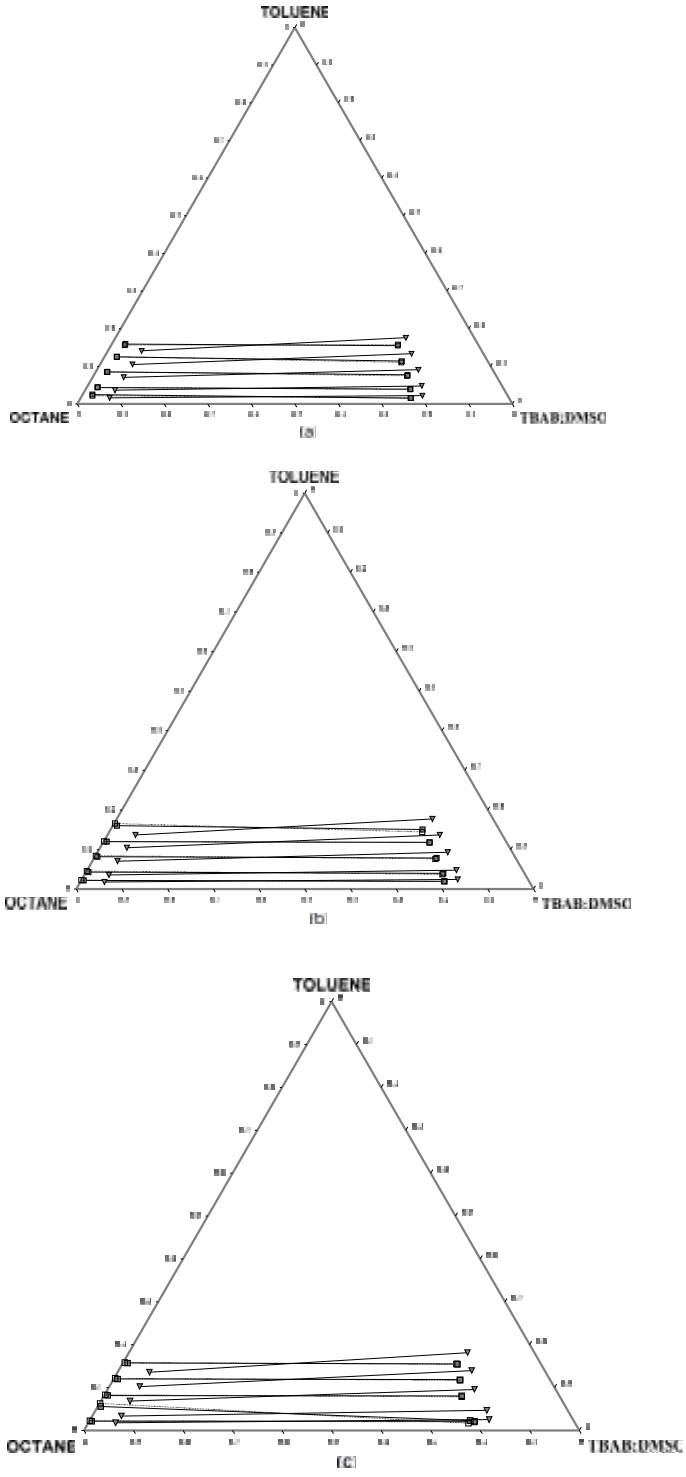

Figure 4.35. Ternary diagram for Toluene(1)+Octane(2)+TBAB:DMSO(3) for (a) at 30 ^{O}C, (b) at 40 ^{O}C, and (c) at 50 ^{O}C. Filled square representing experimental tie-lines, Open-square representing tie-lines from NRTL calculation and filled triangle down representing tie-lines from UNIQUAC calculation

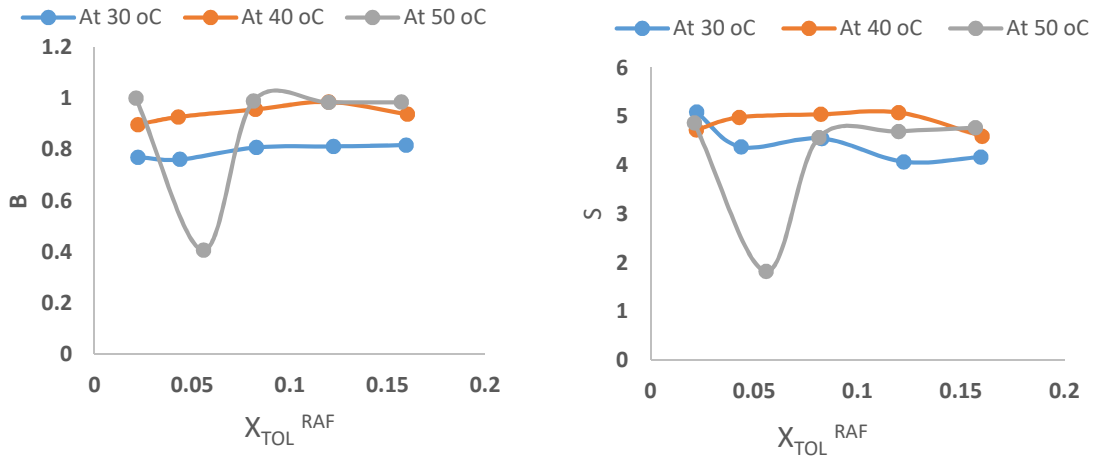

Figure 4.36 Experimental distribution coefficient (β) and selectivity (S) as a function of mole fraction of toluene in the raffinate phase (X_{tol}^{raff}) for Toluene(1)+Octane(2)+TBAB:DMSO(3) ternary systems 30 °C 40 °C and 50 °C.

Table 4.19. Interaction parameters for NRTL/UNIQUAC for Toluene(1)+Octane(2) +TBAB:DMSO(3) TERNARY SYSTEM at different temperatures.

Model	Temp (°C)	τ_{12}	τ_{13}	τ_{21}	τ_{23}	τ_{31}	τ_{32}	RMSD
NRTL	30	3.7054	7.9606	0.2157	7.9485	5.1475	3.5638	0.0018
α = 0.2	40	9.1695	11.0651	0.4852	10.7734	3.6896	2.5589	0.0037
	50	7.4986	6.5543	0.1572	6.8345	2.9284	2.6137	0.0040
UNIQUAC		A_{12}	A_{13}	A_{21}	A_{23}	A_{31}	A_{32}	
	30	0.6741	0.8661	0.7898	0.9243	0.8901	0.8594	0.0285
	40	0.6615	0.8851	0.7767	0.9043	0.8574	0.8738	0.0313
	50	0.6716	0.8808	0.7734	0.9044	0.8651	0.8907	0.0331

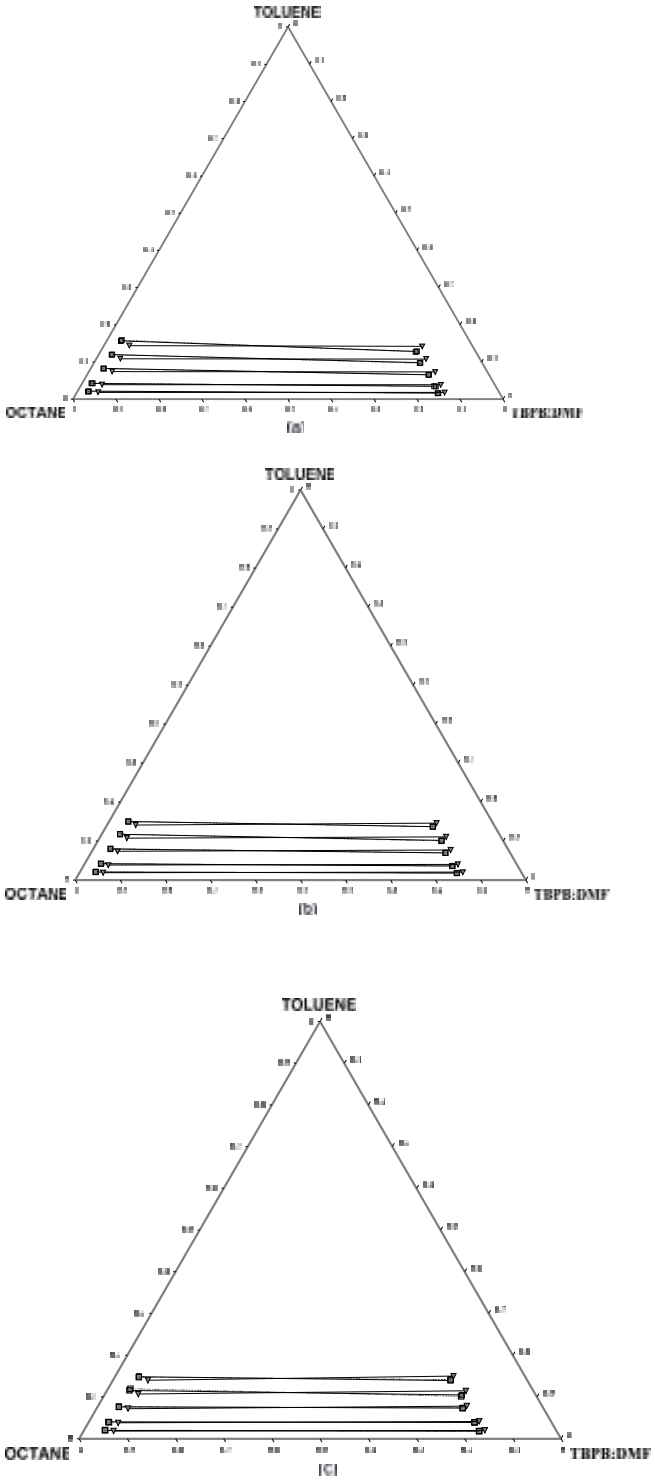

Figure 4.37. Ternary diagram for Toluene(1)+Octane(2)+TBPBDMF(3) for (a) at 30 ^{O}C, (b) at 40 ^{O}C, and (c) at 50 ^{O}C. Filled square representing experimental tie-lines, Open-square representing tie-lines from NRTL calculation and filled triangle down representing tie-lines from UNIQUAC calculation.

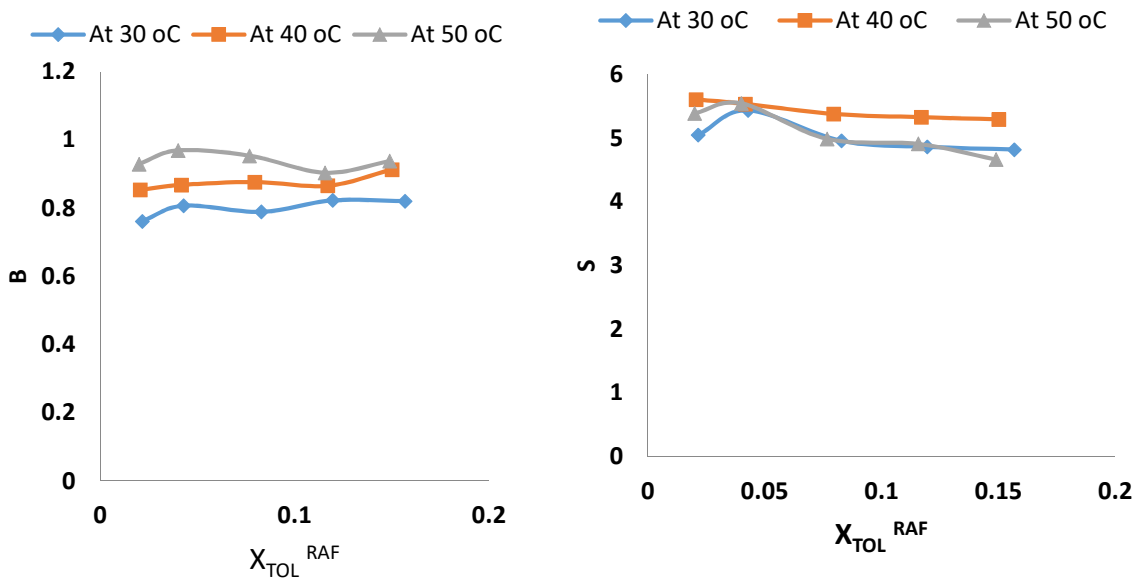

Figure 4.38. Experimental distribution coefficient (β) and selectivity (S) as a function of mole fraction of toluene in the raffinate phase (X_{tol}^{raff}) for Toluene(1)+Octane(2)+TBPBDMF(3) ternary systems 30 °C 40 °C and 50 °C.

Table 4.20. Interaction parameters for NRTL/UNIQUAC for Toluene(1) + Octane(2) +TBPBDMF(3) TERNARY SYSTEM at different temperatures.

Model	Temp (°C)	τ_{12}	τ_{13}	τ_{21}	τ_{23}	τ_{31}	τ_{32}	RMSD
NRTL	30	3.3514	-0.4030	0.7073	-1.2253	0.4605	2.7070	0.0017
α = 0.2	40	2.9711	2.9867	0.7508	3.3327	4.3567	3.0902	0.0008
	50	2.8963	8.8356	0.6849	9.1018	3.8112	2.9759	0.0017
UNIQUAC		A_{12}	A_{13}	A_{21}	A_{23}	A_{31}	A_{32}	
	30	0.6843	0.9547	0.7821	0.9258	0.9037	0.8738	0.0160
	40	0.6702	0.9477	0.8045	0.9571	0.9124	0.8736	0.0124
	50	0.6776	0.9251	0.8188	0.9375	0.8908	0.8637	0.0128

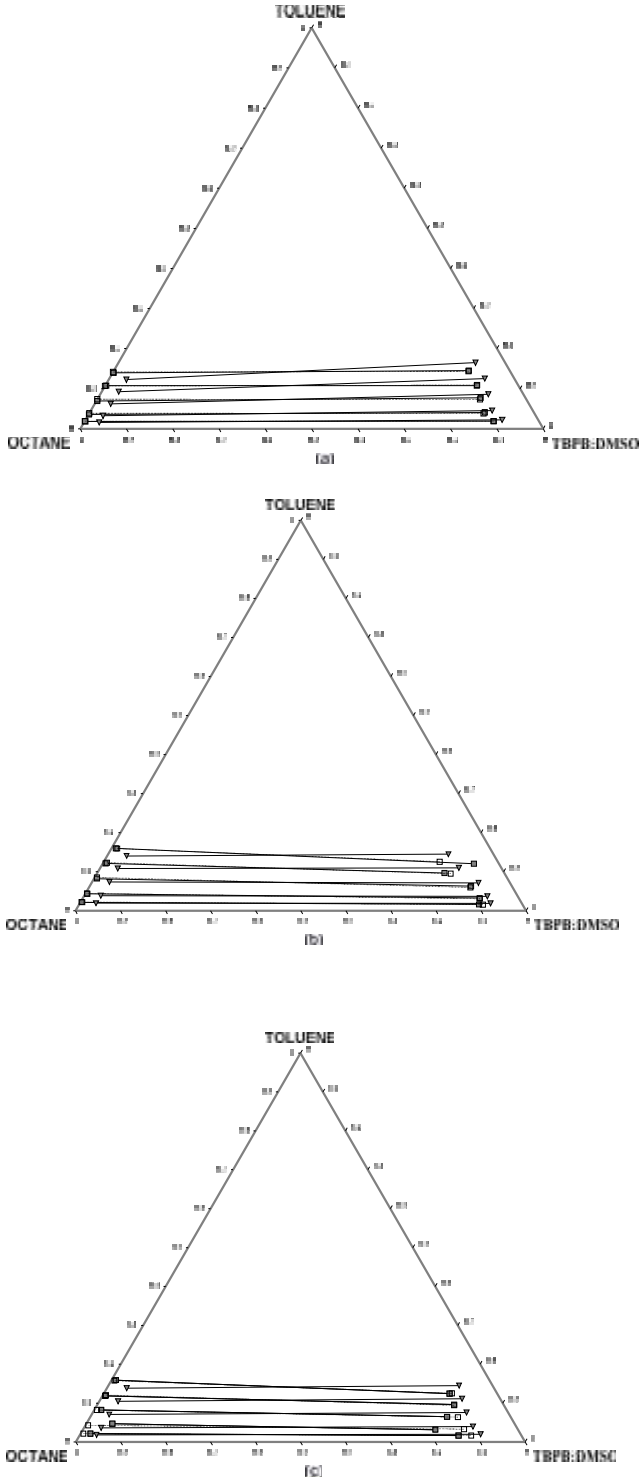

Figure 4.39. Ternary diagram for Toluene(1)+Octane(2)+TBPB:DMSO(3) for (a) at 30 ^{O}C, (b) at 40 ^{O}C, and (c) at 50 ^{O}C. Filled square representing experimental tie-lines, Open-square

representing tie-lines from NRTL calculation and filled triangle down representing tie-lines from UNIQUAC calculation

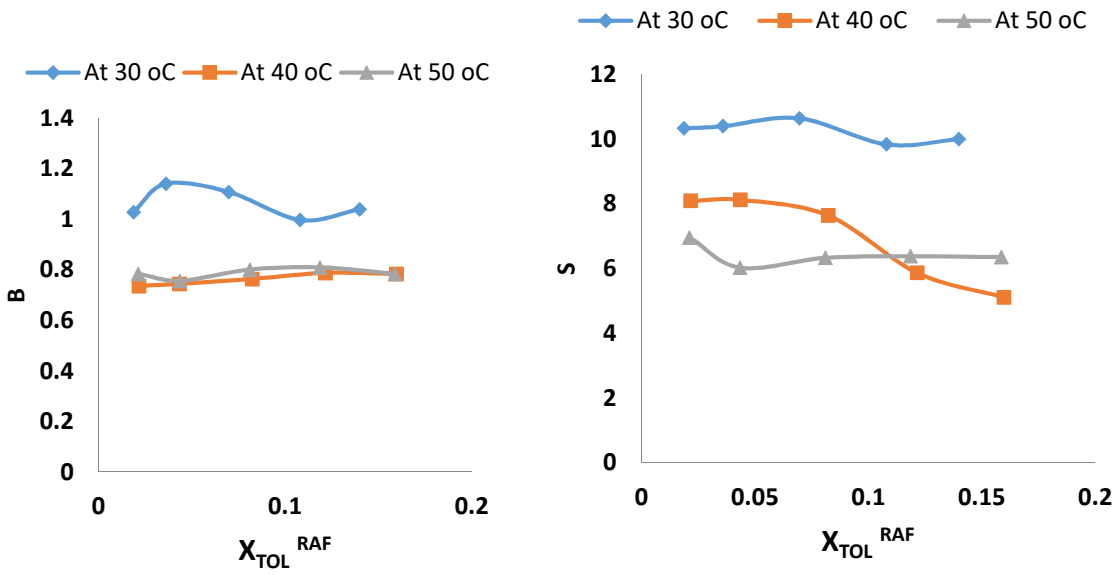

Figure 4.40. Experimental distribution coefficient (β) and selectivity (S) as a function of mole fraction of toluene in the raffinate phase (X_{tol}^{raff}) for Toluene(1)+ Octane(2)+ TBPB:DMSO(3) ternary systems 30 ºC 40 ºC and 50 ºC.

Table 4.21. Interaction parameters for NRTL/UNIQUAC for Toluene(1) + Octane(2) +TBPB:DMSO(3) TERNARY SYSTEM at different temperatures.

Model	Temp (ºC)	τ_{12}	τ_{13}	τ_{21}	τ_{23}	τ_{31}	τ_{32}	RMSD
NRTL	30	7.3510	-4.1392	0.8864	-5.5650	0.1845	7.8596	0.0021
α = 0.2	40	5.7810	-5.5256	0.9502	-4.4509	0.4858	-0.0191	0.0027
	50	4.5115	-1.1354	0.6959	-2.7060	-0.1757	6.3152	0.0021
UNIQUAC		A_{12}	A_{13}	A_{21}	A_{23}	A_{31}	A_{32}	
	30	0.6516	0.9069	0.7281	0.9357	0.8607	0.8954	0.0210
	40	0.6546	0.9243	0.7368	0.8760	0.8807	0.8745	0.0208
	50	0.6547	0.9134	0.7467	0.9173	0.8932	0.8542	0.0223

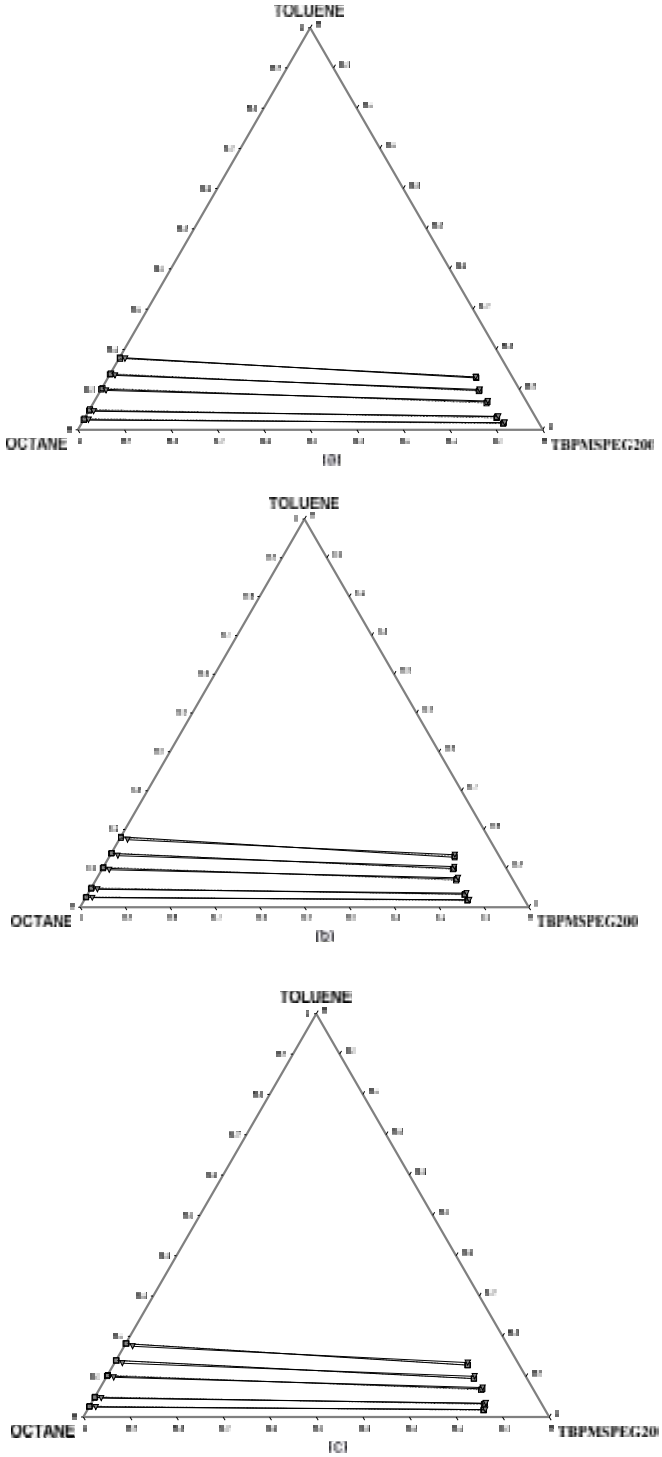

Figure 4.41. Ternary diagram for Toluene(1)+Octane(2)+TBPMS:PEG200(3) for (a) at 30 ^{O}C, (b) at 40 ^{O}C, and (c) at 50 ^{O}C. Filled square representing experimental tie-

lines, Open-square representing tie-lines from NRTL calculation and filled triangle down representing tie-lines from UNIQUAC calculation.

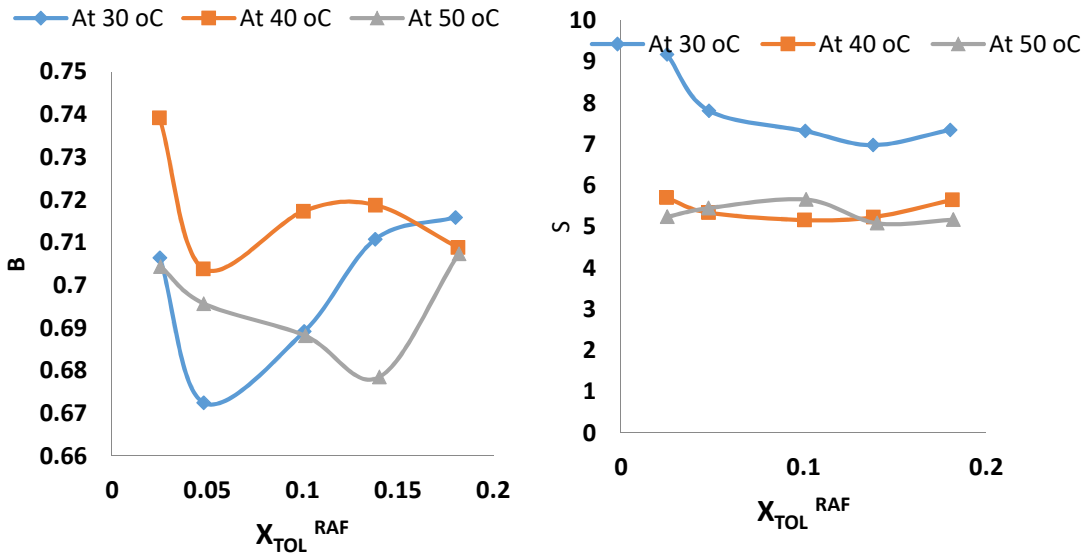

Figure 4.42. Experimental distribution coefficient (β) and selectivity (S) as a function of mole fraction of toluene in the raffinate phase (X_{tol}^{raff}) for Toluene(1)+Octane(2)+TBPMS:PEG200(3) ternary systems 30 °C 40 °C and 50 °C.

Table 4.22. Interaction parameters for NRTL/UNIQUAC for Toluene(1)+ Octane(2) +TBPMS:PEG200(3) TERNARY SYSTEM at different temperatures.

Model	Temp (°C)	τ_{12}	τ_{13}	τ_{21}	τ_{23}	τ_{31}	τ_{32}	RMSD
NRTL	30	7.1495	-5.4439	1.0739	-5.8159	0.4733	2.6762	0.0023
α = 0.2	40	7.2173	-5.4533	0.6213	-5.6813	1.3395	3.9782	0.0020
	50	7.2398	-6.8814	0.6403	-6.7451	2.0036	3.6333	0.0021
UNIQUAC		A_{12}	A_{13}	A_{21}	A_{23}	A_{31}	A_{32}	
	30	0.6947	0.9760	0.7488	0.8958	0.9382	0.8193	0.0061
	40	0.7093	0.9204	0.7839	0.8572	0.9821	0.8615	0.0092
	50	0.7010	0.9830	0.7905	0.8746	0.9912	0.8937	0.0088

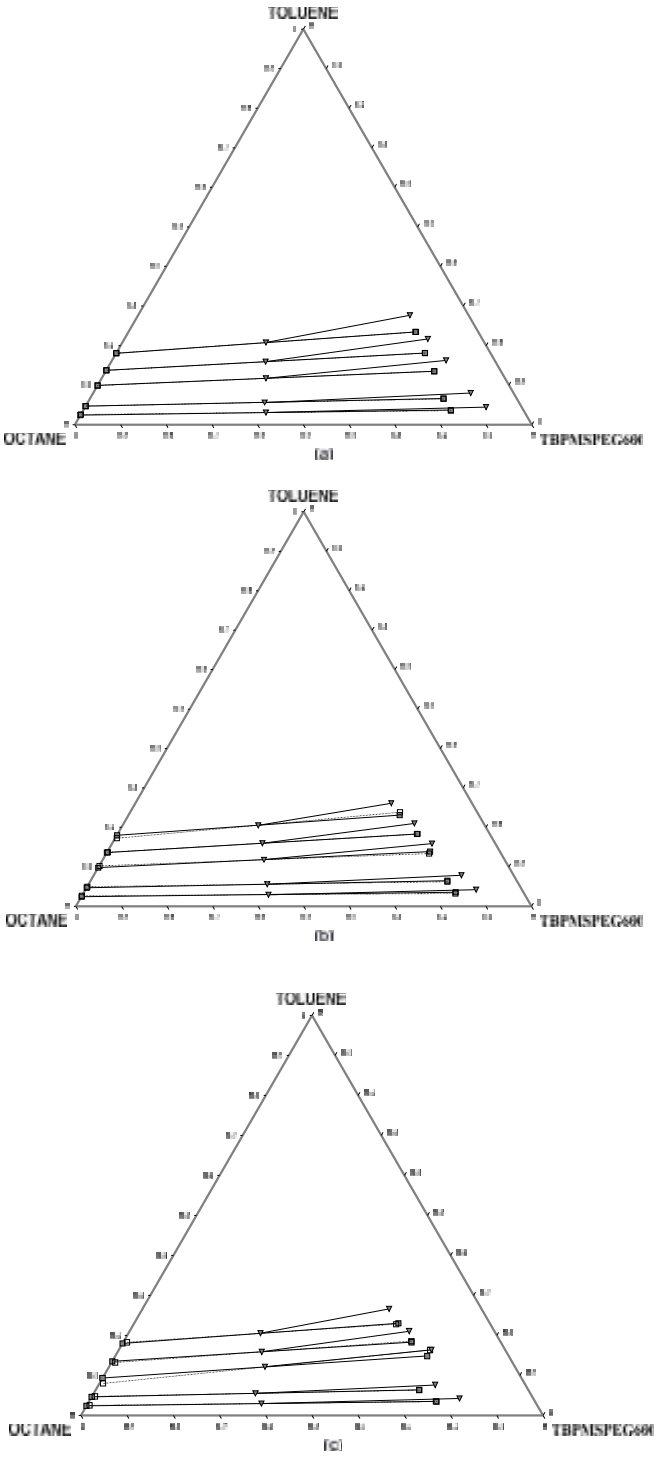

Figure 4.43. Ternary diagram for Toluene(1)+Octane(2)+TBPMSPEG600(3) for (a) at 30 ^{O}C, (b) at 40 ^{O}C, and (c) at 50 ^{O}C. Filled square representing experimental tie-lines, Open-square representing tie-lines from NRTL calculation and filled triangle down representing tie-lines from UNIQUAC calculation.

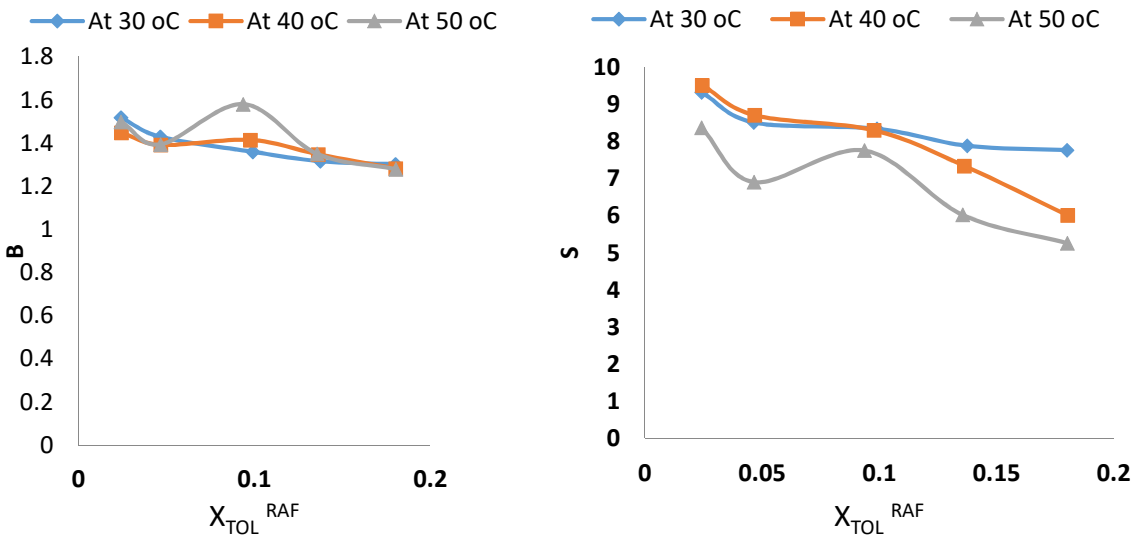

Figure 4.44. Experimental distribution coefficient (β) and selectivity (S) as a function of mole fraction of toluene in the raffinate phase (X_{tol}^{raff}) for Toluene(1)+Octane(2)+TBPMSPEG600(3) ternary systems 30 °C 40 °C and 50 °C.

Table 4.23. Interaction parameters for NRTL/UNIQUAC for Toluene(1)+Octane(2) +TBPMSPEG600(3) TERNARY SYSTEM at different temperatures.

Model	Temp (°C)	τ_{12}	τ_{13}	τ_{21}	τ_{23}	τ_{31}	τ_{32}	RMSD
NRTL	30	9.1654	4.3626	0.6047	3.6040	1.7504	3.2231	0.0011
α = 0.2	40	10.4359	-1.3671	1.0344	0.3283	3.4417	0.7718	0.0030
	50	4.9613	7.5856	-0.0148	6.8509	12.1066	3.9964	0.0064
UNIQUAC		A_{12}	A_{13}	A_{21}	A_{23}	A_{31}	A_{32}	
	30	0.9705	1.0015	0.9124	0.9808	0.9972	0.9269	0.2454
	40	0.9889	0.9862	0.8961	0.9466	0.9383	0.8833	0.2429
	50	0.9497	1.0096	0.9359	0.9681	0.9783	0.9278	0.2268

4.5 Multi stage Extractions

Multiple successive aromatics removal with the studied DESs were carried out each time with fresh DESs. Table D1 and D2, in Appendix IV, give the values for the reduction in aromatic content with increasing number of stages for the ammonium and phosphonium based DESs. Figures 4.45 and 4.46 show the reduction in aromatic content with increasing number of stages for the ammonium and phosphonium based DESs. There is gradual decrease in toluene concentration from initial concentration of 10 wt.% to less than 2 wt.% at the eight extraction stages.

Table D3 and D4 give the values for the aromatic removal efficiency for the ammonium and phosphonium based DESs. The aromatic removal efficiency is shown in Figures 4.47 to 4.48 for the ammonium and phosphonium based DESs respectively. The aromatic (toluene) removal efficiency for the ammonium based were higher in TBAB: DMF and TBAB: DMSO with 29.11 wt.% and 24.17 wt.% at the first extraction stage and 97.41 wt. % and 96.26 wt.% at the eighth extraction stages respectively. It was then followed by TBAB: PEG600 with 24.07 wt.% and 93.63 wt.% at the first and eighth extraction stage respectively. The last was TBAB: PEG200 with 19.62 wt.% and 90.35 wt.% at the first and eighth extraction stages respectively.

For the phosphonium based DESs, the aromatic (toluene) removal efficiency is higher in TBPB: DMF and TBPB: DMSO having 31.64 wt.% and 28.16 wt.% respectively at the first extraction stage and 97.98 wt.% and 96.89 wt.% respectively at the eighth extraction stage. It was then followed by TBPB: PEG600, TBPMS: PEG600 and TBPMS: PEG200 with

22.88, 24.45 and 22.74 wt.% respectively at the first extraction stage and 93.81, 93.83 and 92.73 wt.% respectively at the eighth extraction stage.

The DESs synthesized from DMF and DMSO have the best extraction performance but their major drawback is the detection of DESs in the raffinate phase during LLE experiments as compared to the other synthesized DESs. The aromatic (toluene) removal efficiency for the ammonium based DESs is in the order TBAB: DMF > TBAB: DMSO > TBAB: PEG600 > TBAB: PEG200. While for the phosphonium based DESs it was in in the order TBPB: DMF > TBPB: DMSO > TBPB: PEG600 > TBPMS: PEG600 > TBAB: PEG200 > TBPMS>PEG200. The PEG600 based DESs showed appreciable performance especially when compared to the DMF and DMSO based DESs. Their major advantage is their non-detection in the raffinate phase which is a major industrial advantage for a solvent. Based on this results DESs can be a good solvent for the removal of aromatics at low concentration using LLE processes.

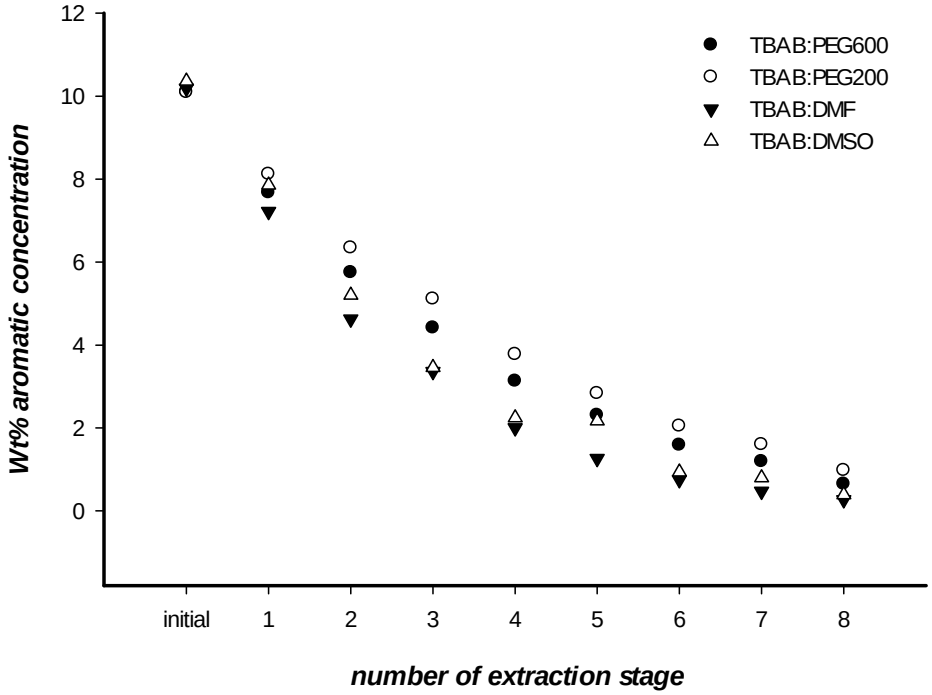

Figure 4.45. Multistage extraction for ammonium based DESs.

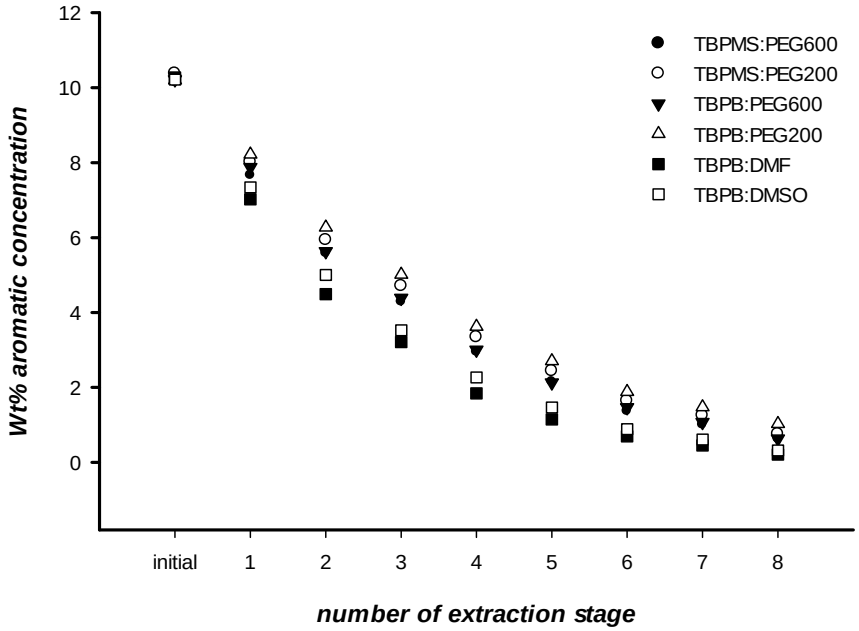

Figure 4.46 Multistage extraction for phosphonium based DESs.

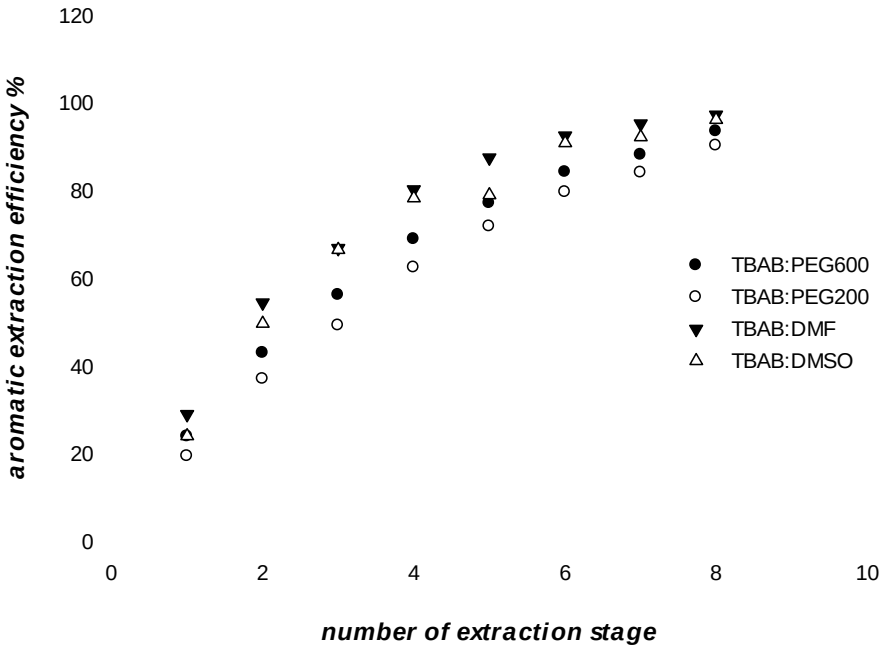

Figure 4.47 Multistage DESs extraction efficiency (%) for the ammonium based DESs.

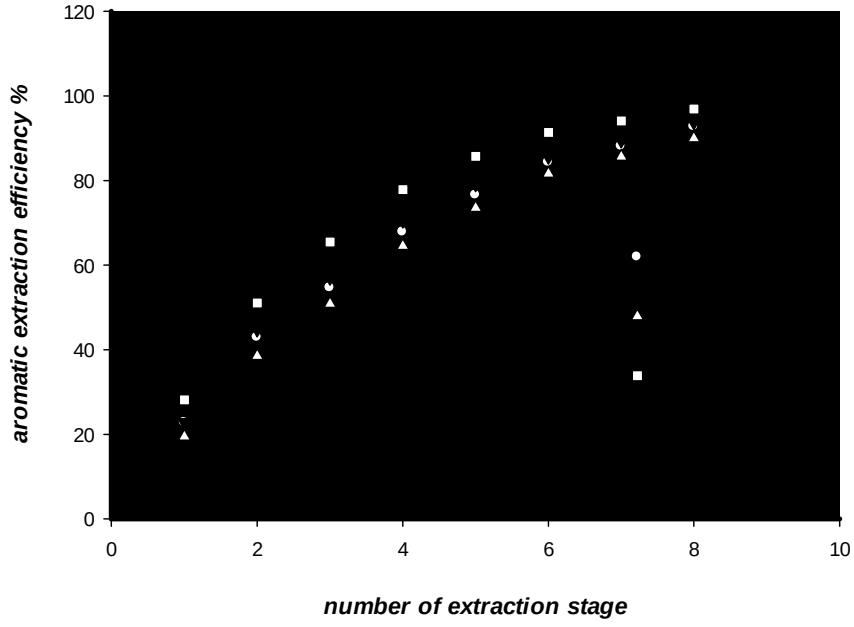

Figure 4.48 Multistage DESs extraction efficiency (%) for the phosphonium based DESs

4.5.1 Multi stage extraction with synthesized naphtha feed

Multistage extraction was carried out with synthesized naphtha feed with composition shown in Table 3.5 and based on the procedure described in Section 3.2.7.

Three DESs TBAB: PEG600, TBPB: PEG600 and TBPMS: PEG600 were selected due to their favourable performance from the multistage extraction of model fuel in Section 4.3.1. Tables D5 – D7 in Appendix IV, contain the data from the multistage extraction of synthetic naphtha for the three selected DESs. Figures 4.49, 4.50 and 4.51 shows the feed amount in wt.% in terms of benzene, toluene and xylene (BTX) reduction or removal as a function of the number of extraction stages for the three DESs.

At the 10^{th} extraction stages, the reduction of BTX concentration from the synthetic naphtha feed concentration were 0.046 wt.% for benzene, toluene with 0.267 wt.% and 0.462 wt.% for xylene using TBAB: PEG600 as solvent. For TBPB: PEG600 the BTX reduction were 0.052 wt.%, 0.255 wt.% and 0.643 wt.% for benzene, toluene and p-xylene respectively. The reduction for TBPMS: PEG600 were 0.57 wt.%, 0.264 wt.% and 0.631 wt.% for benzene, toluene and p-xylene respectively. Figures 4.52, 4.53 and 4.54 gave the profile for the BTX removal efficiency as a function of the number of extraction stages for the three selected DESs. The removal efficiency for benzene at the 10^{th} extraction stage was 98.43%, 98.15 % and 97.98% for TBAB: PEG600, TBPB: PEG600 and TBPMS: PEG600 respectively. The extraction efficiency of toluene in TBAB: PEG600, TBPB: PEG600 and TBPMS: PEG600 at the 10^{th} stage was 91.47 %, 91.85 % and 91.57 % respectively. The extraction efficiency of xylene was very poor especially when compared to those of toluene and benzene, recording 79.79%, 71.88% and 72.38% for TBAB: PEG600, TBPB: PEG600 and TBPBS:

PEG600 respectively at the 10^{th} stage. The performance of the DESs in BTX removal efficiency is in the order of TBAB: PEG600 (98%) > TBPB: PEG600 (91%) > TBPMS: PEG600 (71%)

The purity of aromatics from the sulfolane extraction process does not exceed 90% due to the extraction of non-aromatics. Therefore, there is the need for an extra stripper to increase the aromatic concentrations. Also from literature, the extraction of toluene from n-heptane mixture using IL [MBPy]BF4. show that the aromatic purity of 99% is possible (Hossain, *et al*., 2012).

Based on these findings, at low aromatic concentration LLE can be employed for the removal of aromatics using DESs. Although, the performance in the removal of xylene is very poor as compared to toluene and benzene, and this call for further investigation on order to arrive at a suitable DES combinations and also increase in the number of equilibrium extraction stages.

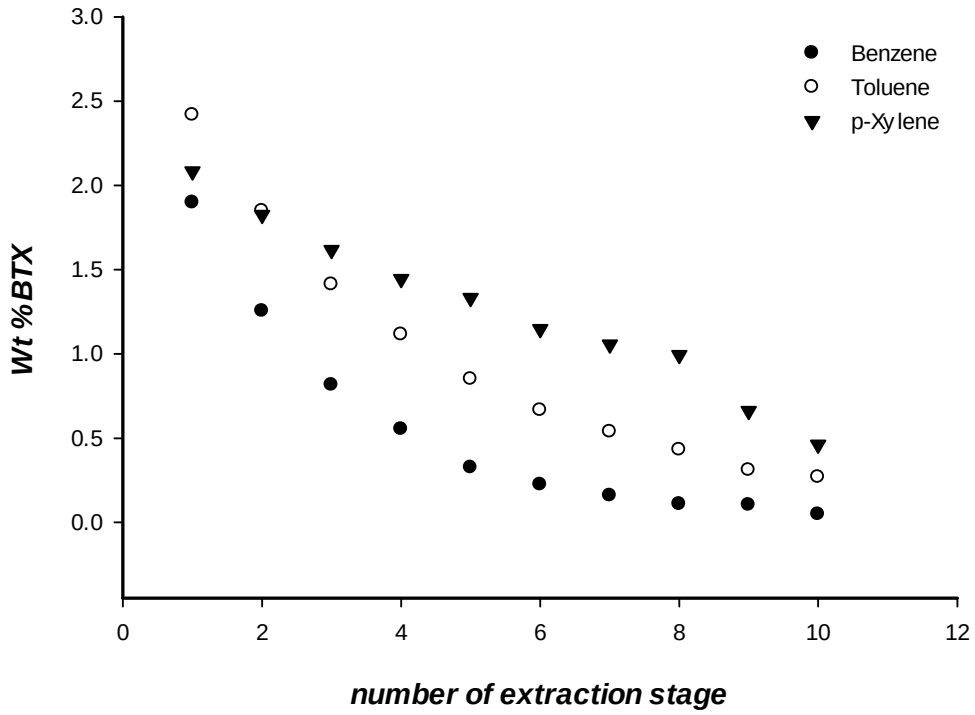

Figure 4.49 Multistage extraction for synthesized naphtha feed with TBAB: PEG600 based DESs.

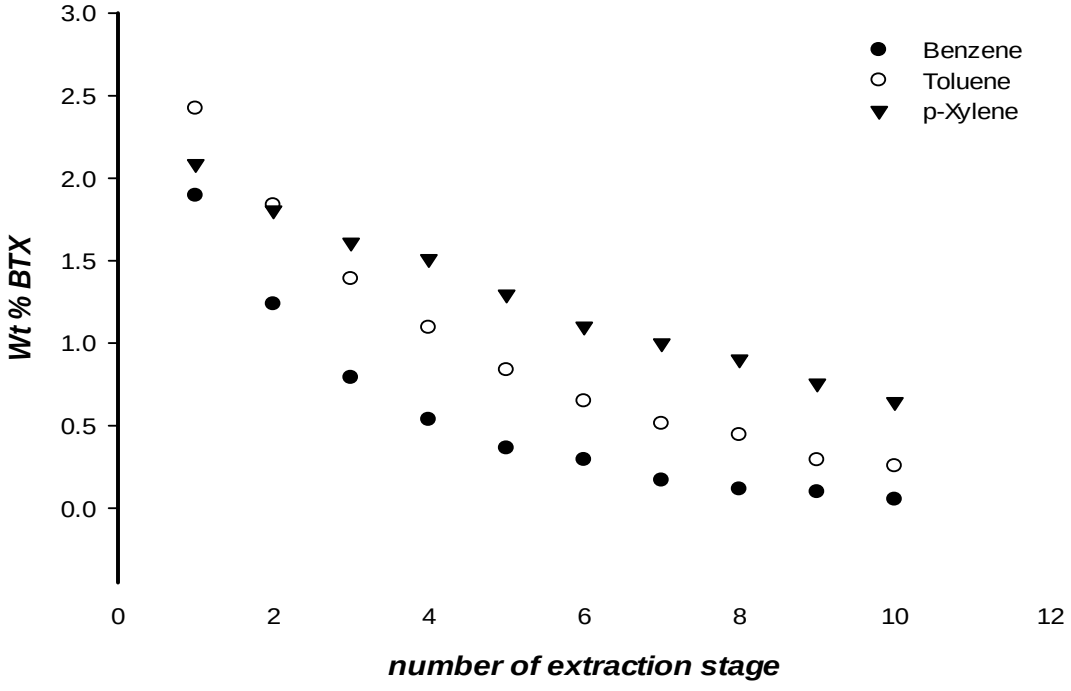

Figure 4.50: Multistage extraction for synthesized naphtha feed with TBPB: PEG600

based DESs.

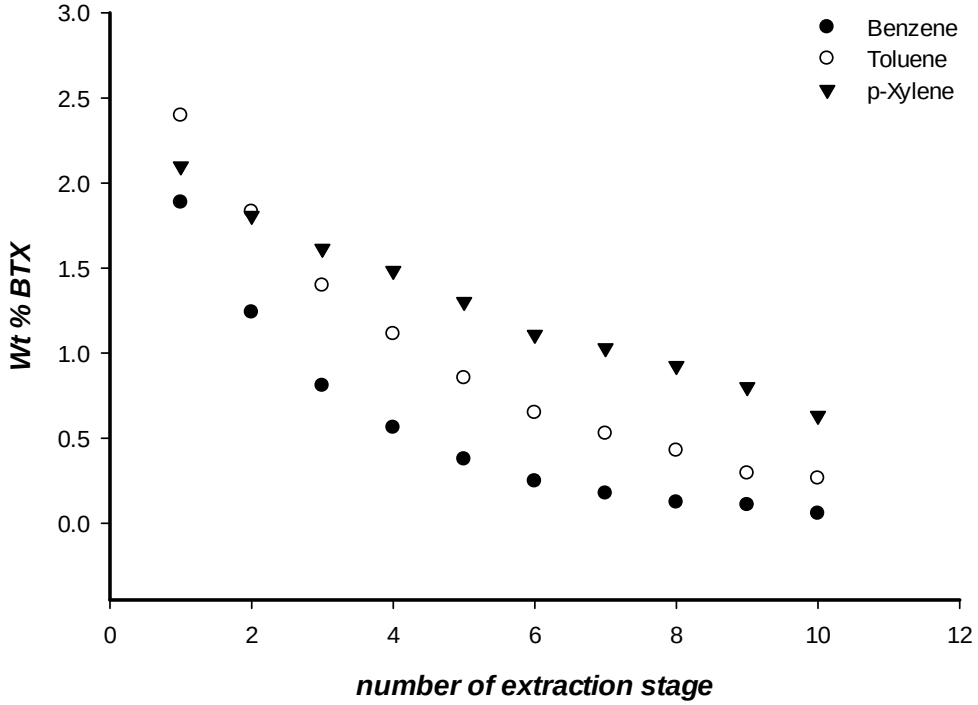

Figure 4.51: Multistage extraction for synthesized naphtha feed with TBPMS: PEG600 based DESs.

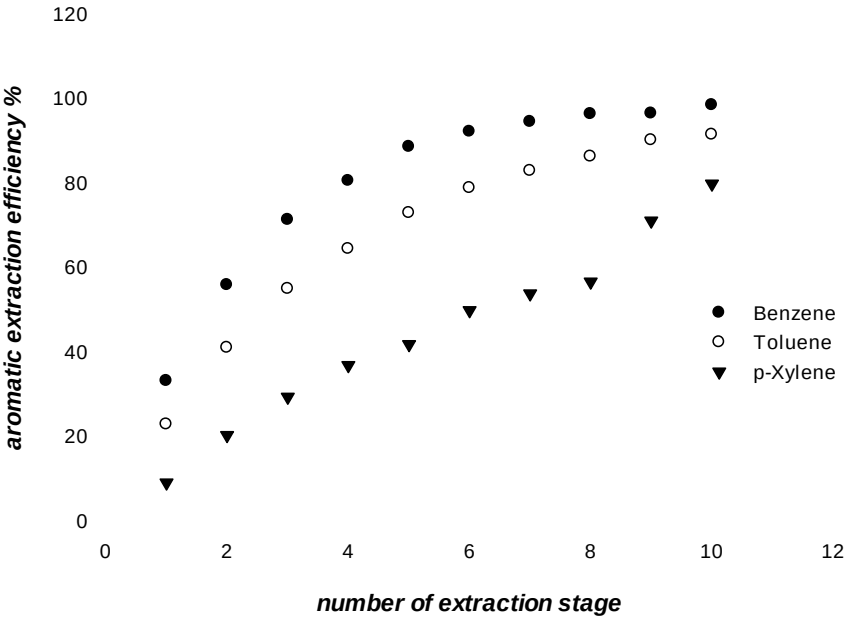

Figure 4.52: Multistage DESs equilibrium extraction efficiency (%) for synthesized naphtha feed with TBAB: PEG600 based DESs.

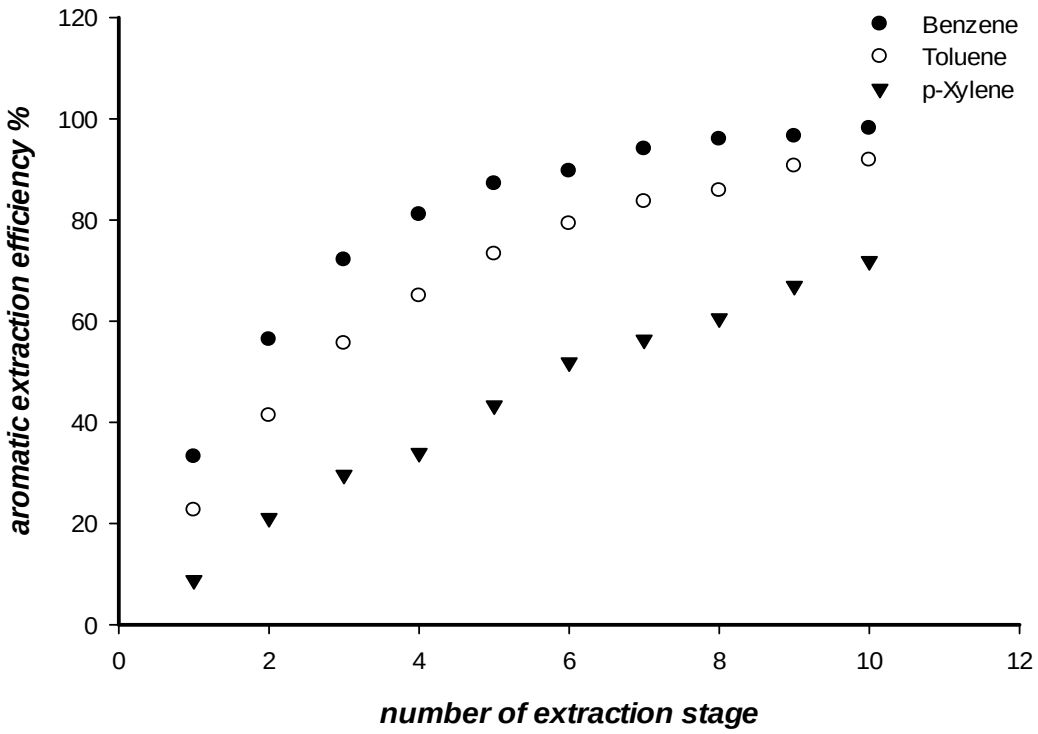

Figure 4.53: Multistage DESs equilibrium extraction efficiency (%) for synthesized naphtha feed with TBPB: PEG600 based DESs.

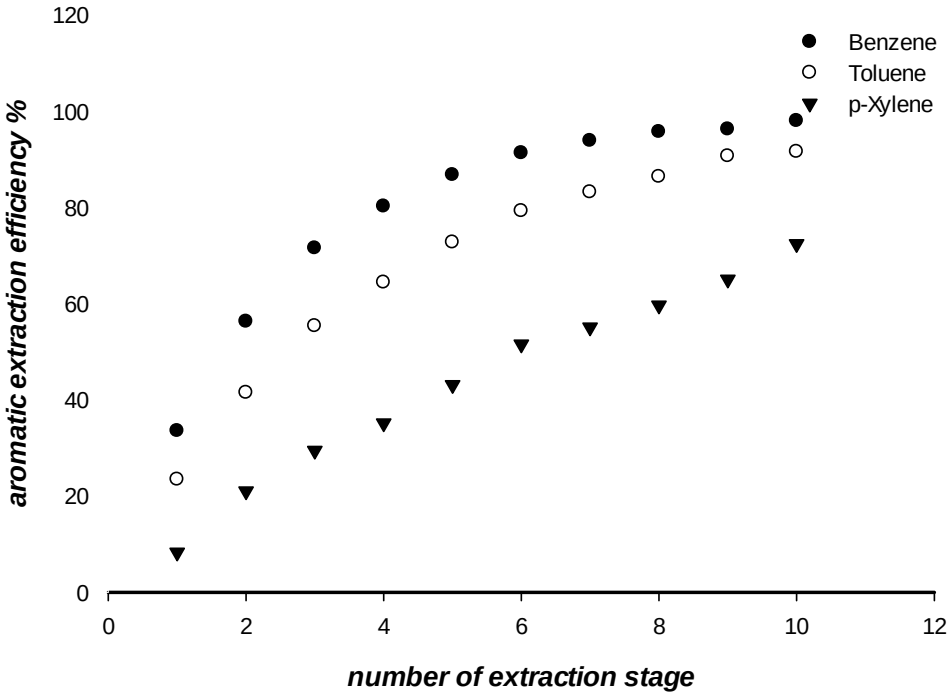

Figure 4.54: Multistage DESs equilibrium extraction efficiency (%) for synthesized naphtha feed with TBPMS: PEG600 based DESs.

4.6 Solvent Regeneration

Solvent regeneration is usually carried out in industries so as to increase the usability of the solvent with subsequent reduction in the operating cost of the extraction process. The solvent regeneration was carried out using the procedure described in Section 3.2.8.

Preliminary regeneration experiment was first carried out in laboratory electric oven. The DESs extract were left inside the oven for overnight at 70 ^{o}C. The DESs samples were then analysed with HPLC for the presence of toluene. The HPLC chromatograph shows little or no traces of trapped toluene in the extract phase this indicating that aromatics (toluene) can be removed from the DESs.

The DESs regeneration were carried out as described in Section 3.2.8. Table D11 – D14 show the results of the regeneration experiments. The ability of the regenerated DESs for extraction was also investigated and the results are shown in Figures 4.55 and 4.56. The toluene removal efficiency after three regeneration cycles showed that for TBPB: DMSO > 30%, while for TBAB: PEG600; TBPB: PEG600; TBPBS: PEG60 and TBAB: DMSO DESs the removal efficiency > 25%, then followed by TBAB: PEG200 and TBPB: PEG200 > 20%. TBAB: DMF and TBPB: DMF recorded removal efficiency of almost 30% after only one regeneration cycle. This toluene removal efficiency showed a trend that is almost similar to the original DESs from the model fuel. After the three regeneration cycles the toluene removal efficiency of the DESs remains almost constant.

FTIR analysis was performed on the regenerated DESs so as to observe for changes in the DESs structures during the regeneration process. It can provide a molecular finger prints that can be used when comparing samples. If two pure samples display the same IR spectrum, it

can be argued that they are the same compound. Figure 4.57 – 4.66 shows the FTIR spectra of the original and the regenerated DESs for both the ammonium and phosphonium based DESs Respectively.

The FTIR spectra gives similar peaks and there is no shift of peaks of the regenerated DESs when compared to spectral of the original DESs. This indicates that DESs retain their structures even after the third regeneration cycle with exception of TBAB: DMF and TBPB: DMF. Li *et al*., (2013), were able to regenerate DESs without any degradation or the loss in performance of the DESs.

Kanel, (2003), stated that to recover and reused IL, heating or evaporation of volatiles vacuum method were developed. Also the binary mixtures of IL N, N – dimethyl formamide (DMF) was separated under vacuum and there are no appreciable changes in the physical properties of the recovered IL after it was reused to at least four times (Altri, *et al*., 2010). Using rotary evaporator filled with water bath with pressure decay adjusted to the boiling point of the solvent, IL was recycled without changes in its properties (Kralisch, *et al*., 2007). IL was also regenerated using rotary evaporator operating at 75 ^{o}C under vacuum for 15 hrs, after which the performance of the regenerated IL was satisfactory and without any loss in its activity (Meindersma, 2005).

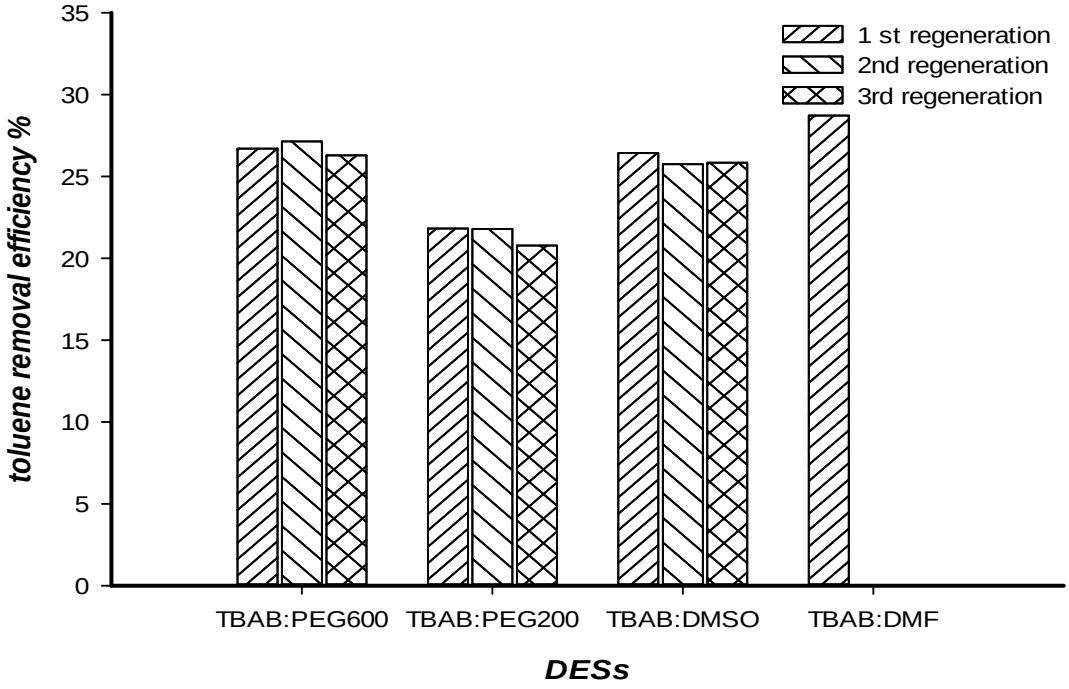

Figure 4.55: Toluene removal efficiency for different regeneration cycles with ammonium based DESs

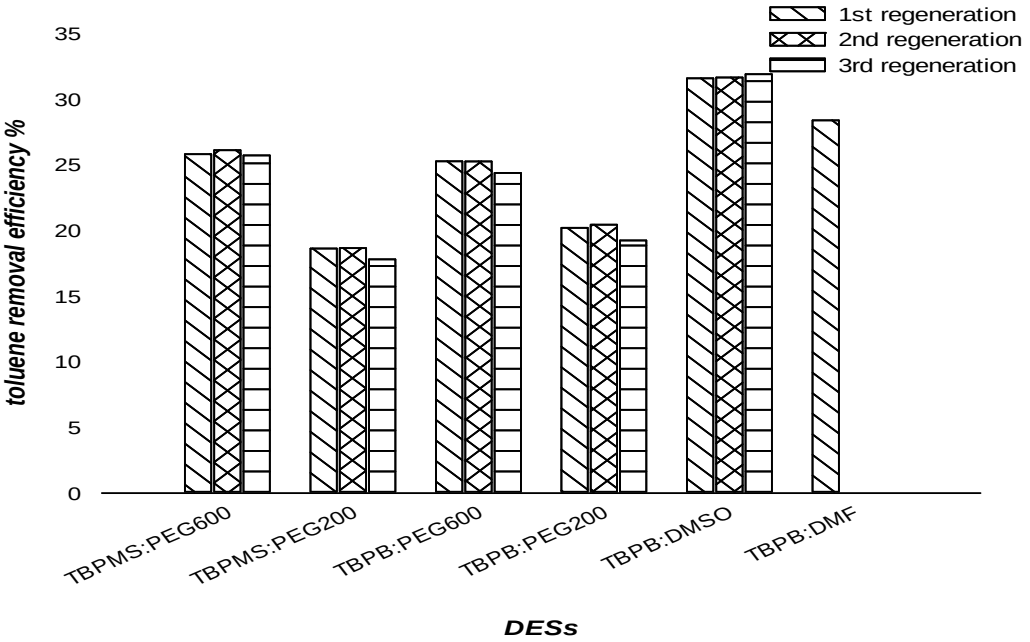

Figure 4.56: Toluene removal efficiency for different regeneration cycles with phosphonium based DESs

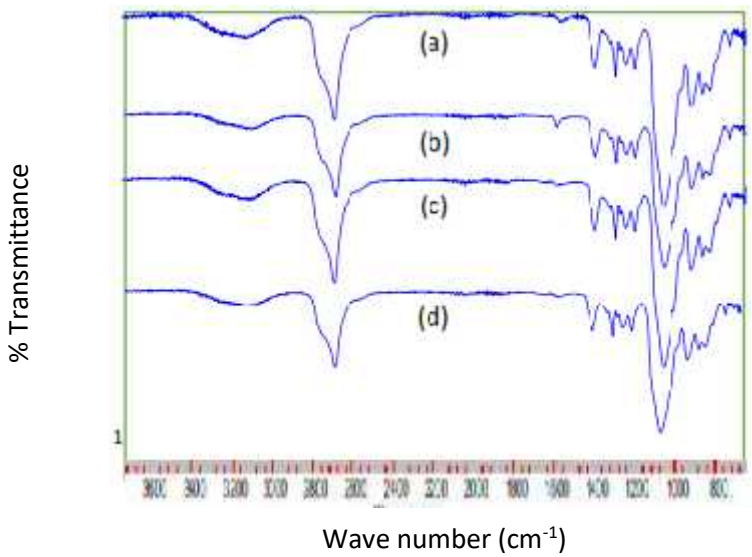

Figure 4.57: FTIR spectra of (a) TBAB: PEG600, (b) first regenerated, (c) second regenerated, (d) third regenerated.

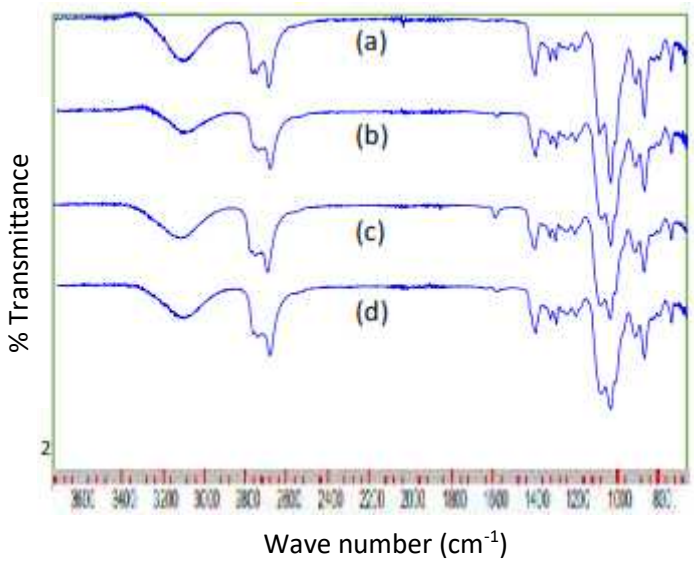

Figure 4.58 FTIR spectra of (a) TBAB: PEG200, (b) first regenerated, (c) second regenerated, (d) third regenerated.

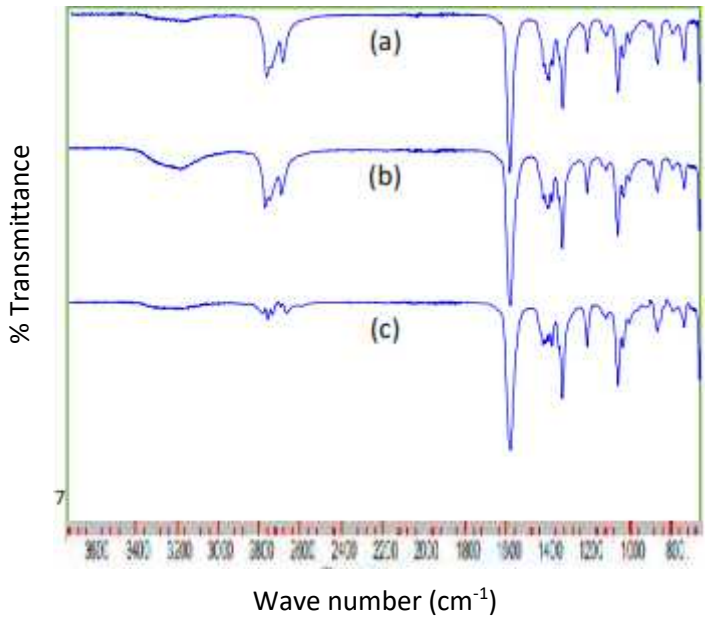

Figure 4.59 FTIR spectra of (a) TBAB: DMF, (b) first regenerated, (c) second regenerated

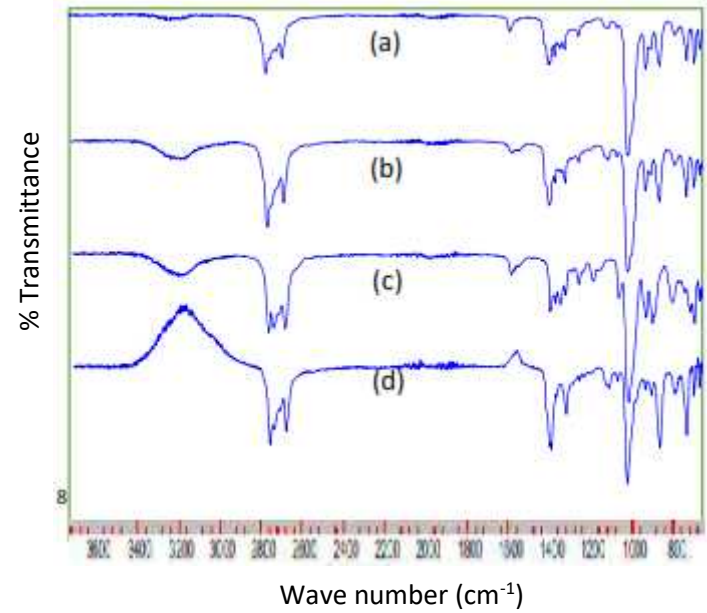

Figure 4.60 FTIR spectra of (a) TBAB: DMSO, (b) first regenerated, (c) second regenerated(d) third regenerated.

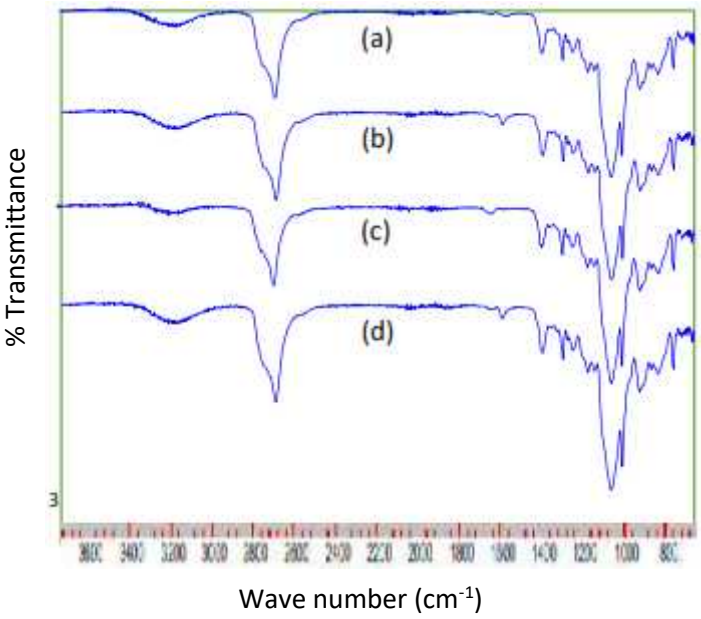

Figure 4.61 FTIR spectra of (a) TBPPMS: PEG200, (b) first regenerated, (c) second regenerated, (d) third regenerated.

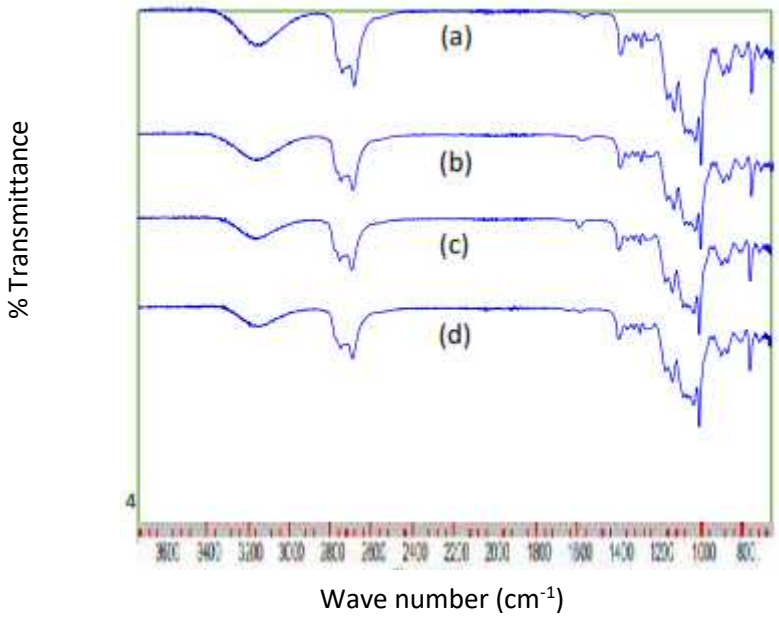

Figure 4.62 FTIR spectra of (a) TBPPMS: PEG200, (b) first regenerated, (c) second regenerated, (d) third regenerated.

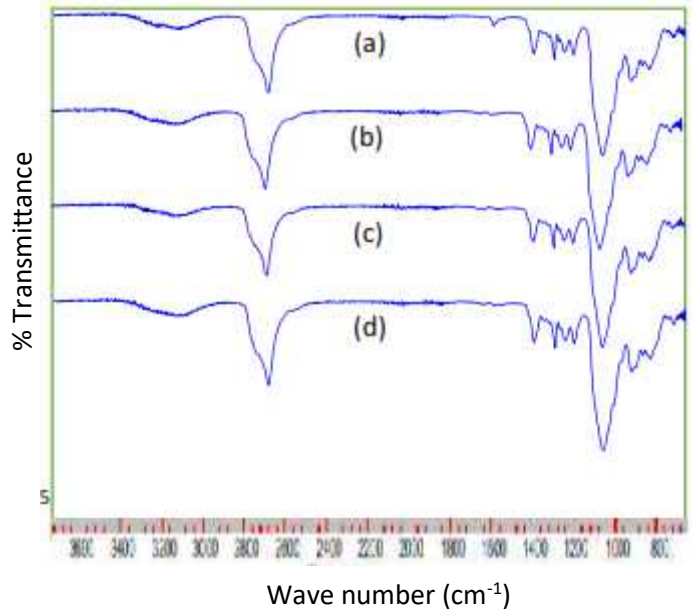

Figure 4.63 FTIR spectra of (a) TBPB: PEG600, (b) first regenerated, (c) second regenerated, (d) third regenerated.

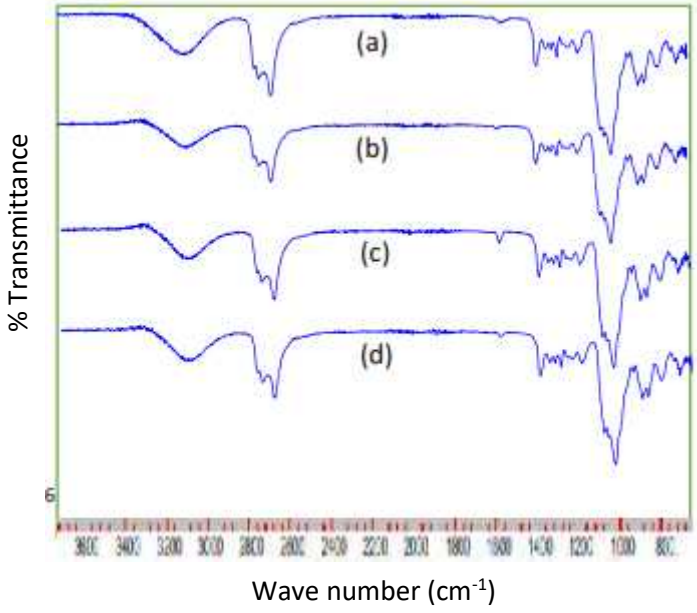

Figure 4.64 FTIR spectra of (a) TBPB: PEG200, (b) first regenerated, (c) second regenerated, (d) third regenerated.

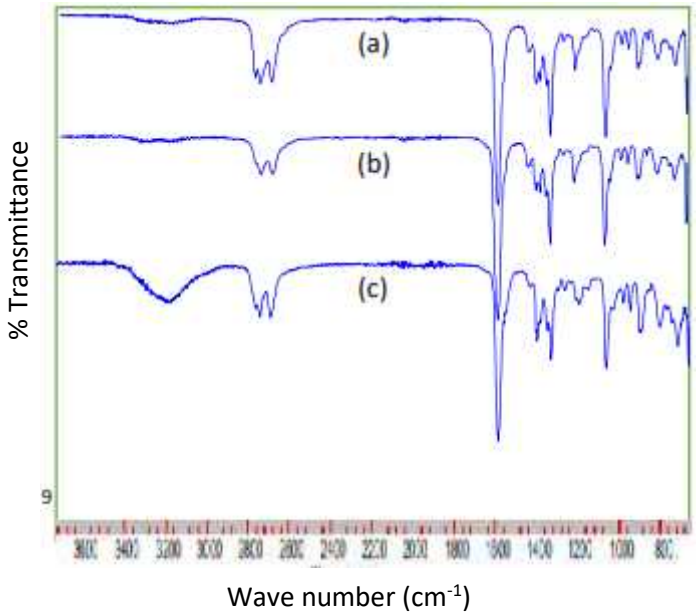

Figure 4.65 FTIR spectra of (a) TBPB: DMF, (b) first regenerated, (c) second regenerated.

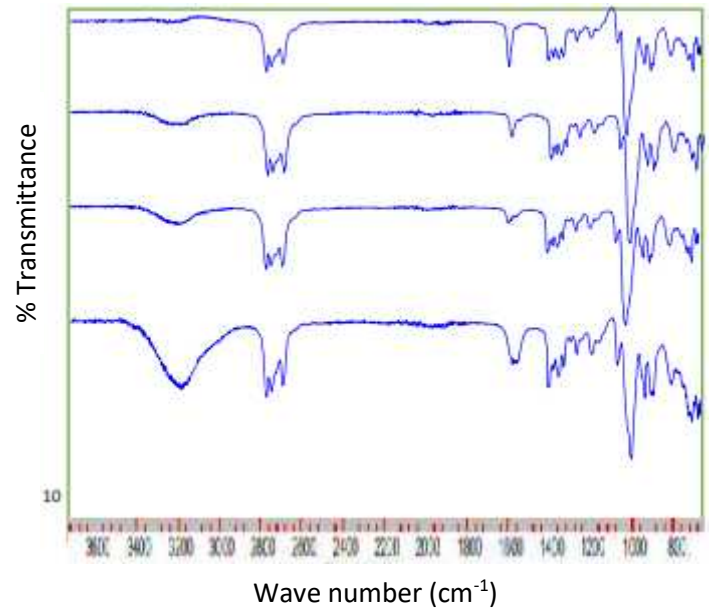

Figure 4.66 FTIR spectra of (a) TBPB: DMSO, (b) first regenerated, (c) second regenerated, (d) third regenerated.

CHAPTER FIVE

CONCLUSION AND RECOMMENDATION

5.1 CONCLUSIONS

The potential application of DESs as a low cost and environmentally friendly alternative to the conventional organic solvent in the separation of aromatic/aliphatic hydrocarbon mixtures was investigated in this thesis. Novel class of DESs were synthesised from a group of ammonium and phosphonium based DESs.

A total of two hundred and twenty-eight different types of salt: HBD combinations were tested as DESs. Ten DESs were screened and synthesised in large quanties from tetrabutyl ammonium bromide, from tetrabutyl phosphonium bromide Tetrabutyl phosphonium methane sulphonate as salts with PEG 600; PEG 200; DMSO; and DMF as HDBs at a salt: HBD molar ration of 1:2.

The dependency of density and refractive index with temperature was found to be linear and the correlation coefficient for density and refractive index gives a satisfactory fitting, with R^2 of 1 for all the studied DESs. Viscosity and conductivity were modeled using the Arrhenius-like and the VFT equations for all the DESs. A better fitting was observed for viscosity and conductivity with the VFT than the Arrhenius-like equations.

The type of HBD used was found to have a profound influence in the physical behaviour of the DESs most especially, with regards to density and viscosity which their values increase with increasing alkyl chain of the DESs. The measured properties of the DESs are similar with some of the reported literature values.

The potential of the synthesised DESs for the separation of aromatic from aliphatic hydrocarbons was carried out. Ternary diagrams for the DESs systems and the solute distribution coefficients and selectivity for the studied DESs were determined.

The degree of the consistencies of the experimental data were determined using the Othmer-Tobias and Hand correlation. The correlation factor for all the DESs is between 0.96 to 0.999 which indicates a satisfactory fitting for all studied systems and a high degree of experimental data.

The effect of temperature (ranging between 30, 40 and 50 ^{o}C) on the separation was also studied, indicating that separation is possible at low temperature. There is little temperature effect on the impact of temperature at the three different experimental temperature. These findings are very important especially when compared to the conventional organic solvents.

The solute distribution coefficient for the ternary systems of Toluene + Octane and PEG 600 based DESs is more than unity at the three different temperatures. These DESs show a positive slope indicating that toluene affinity is more towards the DESs. The solute distribution coefficient and selectivities of the remaining DESs were very close to unity. Another important property of the DESs is their non-detection in the hydrocarbon rich (raffinate) phase during the LLE experiments. With exception of DMSO and DMF based DESs.

These DESs were found to exhibit higher solute distribution coefficients at low concentration of toluene. This indicates the potential application of the DESs for the removal of low aromatic concentrations in the naphtha feed. The values of B for the studied DESs are higher or similar when compared to those reported in the literature.

Multiple successive aromatic removal with the studied DESs has been carried out each time with a fresh DESs. There is decrease in the concentration of toluene with increasing number of extraction stages for the ammonium and phosphonium based DESs. The toluene removal efficiency for all the DESs is greater than 90% at the eight equilibrium extraction stage. This show the ability of the DESs to separate the toluene from the octane to a lower concentration.

Multiple successive extraction was also carried out with synthetic naphtha feed comprising of BTX. Three DESs, TBAB: PEG600; TBPB: PEG600 and TBPMS: PEG600 were selected due to their favourable performance from the multiple extraction of the model fuel. The removal efficiency of benzene and toluene is >90% and <80% for xylene at the 10^{th} equilibrium extraction stage for the three DESs.

Solvent regeneration studies has been carried out to increase the usability of the solvents. Preliminary regeneration experiments were done on the extract from LLE experiment inside an oven and the show little or no traces of toluene in the DESs extract. The toluene removal efficiency shows a trend that is almost similar to the original DESs from the model fuel. After the three regeneration cycles the toluene removal efficiency of the DESs remains almost constant.

The FTIR spectra gives similar peaks and there is no shift of peaks of the regenerated DESs when compared to spectral of the original DESs. This indicates that DESs retain their structures even after the third regeneration cycle with exception of TBAB: DMF and TBPB: DMF

5.2 RECOMMENDATIONS

Pilot plant studies with DESs involving liquid-liquid continuous contactor need to be carried out. This study will help generate operating parameters for the pilot plant. Also in most of the studied DESs in literatures their selectivity and distribution coefficients values are not as high as that of Solfolane, and one of the superior property of DESs over sulfolane is its low volatility. This property makes the DESs as solvent not to be mixing with the raffinate phase during liquid- liquid equilibrium extractions leading to reduction in the cost of energy during regeneration. Therefore, there is a need to compare the economics of the two competing solvents.

This work focuses on the removal of aromatics from aromatic/aliphatic mixtures. It is important to carry out studies on the recovery of aromatics from the DESs which involves stripping of the aromatics from the solvent (DES) via vapour liquid extraction studies

Use of predictive models to enhance on the screening of DESs due to the labourious synthesis and screening techniques involved. This would be as a systematic approach towards the synthesis and screening of DESs for separation processes. Quantum chemical methods, COSMO-RS, COSMO-SAC models are being employed for predicting LLE involving ionic liquids and DESs.

The dependency of conductivity is both on the salt and the HBDs, in some cases, the conductivity decreases with increasing salt concentration as in TBAC:EG system (Yusof *et al.*, 2014). or conductivity increases with increasing salt concentration and through a maximum as in ChCl: EG systems. (Garc et al., 2015). Hence, it will be difficult to come up

with a clear relationship pattern in this work. Therefore, the need for systematic study on the effect of the salt and the HBD type on conductivity.

The naphtha feed is a complex mixtures of hydrocarbons and therefore studies on multi component mixtures involving aromatic and aliphatic hydrocarbons should be carried out.

CONTRIBUTION TO KNOWLEDGE

1. Novel Deep Eutectic Solvents (DESs) were synthesised
2. Sets of physical property correlations and interaction parameters for the LLE data systems which can be integrated into process simulation software.
3. A software package with GUI incorporating Genetic Algorithm (GA), Particle Swarm (PS), Simulated Annealing (PS) as global evolutionary optimization techniques for thermodynamic modelling of LLE data has been developed
4. This work was able to show that separation is possible at low aromatic concentration (2.5 – 20.0 wt%)
5. DESs structural area and volume parameters were generated and used in UNIQUAC model.

List of drafted articles

1. Separation of Toluene from Octane using New Deep Eutectic Solvent based in tetrabutyl ammonium bromide and Polyethylene Glycol
2. Physical Properties of new PEG-Based Deep Eutectic Solvents

Conferences attended

1. Aminu Mohammad, Jamil Naser, Farouq Mjalli (2017) *Aliphatic and Aromatic Separation using Deep Eutectic Solvents as Extracting Agents*. 10th International Conference on Thermal Engineering: Theory and Applications 26 – 28th February, 2017. Sultan Qaboos University, Oman
2. A.A. Muhammad, B. Y. Jibril, F. Mjalli and Naseer J.(2017) *Ionic liquid based Deep Eutectic Solvent for the Removal of Aromatic from Aliphatic hydrocarbons*.1st National conference on chemical technology (NCCT 2017). http://www.narict.gov.ng/ncct/

REFERENCES

Andrew A. P., Capper, G.,. Davies D. L., Rasheed R. K., and Tambyrajah V., (2003) *Novel solvent properties of choline chloride/urea mixtures*. The Royal Society of Chemistry 2003 CHEM. COMMUN., 2003, 70–71

Abbott, A. P., Boothby, D., Capper, G., Davies, D. L., & Rasheed, R. K. (2004*). Deep Eutectic Solvents Formed between Choline Chloride and Carboxylic Acids: Versatile Alternatives to Ionic Liquids.* Journal of the American Chemical Society, 126(29), 9142-9147.

Abbott A. P., Barron, J. C., Ryder, K. S., Wilson, D., (2007). *Eutectic-Based Ionic Liquids with metal- containing Anions and Cations.* Chem. Eur. J. 13,6495 –6501.

Abu-Eisha S.I. and Dowaidar A.M. (2008*). Liquid-Liquid Equilibrium of Ternary Systems of Cylcohexane+(Benzene+Toluene+ethylbenzene or xylene) + 4-methyl pyridinium tetrafluoroborate ionic liquids at 303.15 K*. J. Chem.Eng.Data 53; 1708-1712.

Abrams, D.S.; Prausnitz, J.M.,(1975). *Statistical thermodynamics of liquid mixtures: A new expression for the excess Gibbs energy of partly or completely miscible systems*. AIChE Journal 1975, 21, (1), 116-128.

Arce, A. Earle, M. J. Rodriguez, H. Seddon, K. R. (2007*). Separation of benzene and hexane by solvent extraction with 1 – alkyl-3-methylimidazolium bis(triflouromethyl) sulfonyl amide ionic liquids: effect of the alkyl substituent length.* J. Phy. Chem. B 2007, 111; 4732

Altri, P., Reddy. P. M. and Venkatesu, P. (2010). *Density and Ultrasonic Speed Measurement for N,N – Dimethylformamide with Ionic Liquids.* IJCA, 49A (5 - 6) pp 736 – 742.

Andreia, S. L. Gouveia, F. S. Oliveira, A. Kiki, A. K. and Isabel M. M. (2016). *Deep eutectic solvents as Azeotropic Breakers: Liquid-Liquid Extraction and COSMO-RSrediction*. ACS Sustainable Chem. Eng. DOI: 10.1021/acssuschemeng.6b01542

Bahadori , L., Chakrabarti M. H., Mjalli, F, S., AlNashef, I. M., Abdul Manan, N. S., Hashim M. A., (2013) *Physicochemical properties of ammonium-based deep eutectic solvents and their electrochemical evaluation using organometallic reference redox systems*. Electrochimica Acta 113 (2013) 205–211

Bharti, A, Kundu, D., Rabari, D., and Banerjee, T., (2017). *Phase Equilibria in Ionic Liquid Facilitated Liquid-Liquid Extractions*. Taylor and Francis Group. LLC.

Brennecke, J.F., and Maginn, E.J. Ionic Liquids: Innovative Fluids for Chemical Processing. AIChEJ. 2001, 47, 2384 – 2389

Canales R.I. and Brennecke J.F. (2013) *Comparison if Ionic Liquids to Conventional Organic Solvents for Extraction of Aromatics from Aliphatics*. ACS Publications DOI: 10.1021/acs.jeed.6b00077

Domanska, U. Pobudkowska, A. Krolikowski, M. (2007). *Separation of aromatic hydrocarbonsfrom alkanes using ammonium ionic liquid C_2NTf_2 at T = 298.15 K*. Fluid Phase Equilibra. 259 (2007) 173 – 179.

Dominguez I. Calvar N. Gomez E. and Dominguez A. (2012*). Liquid-Liquid Extraction of Aromatic Compounds from Cyclalkanes using 1-Butyl-3-methylimidazolium Methylsufate ionic liquids.* ACS Publications 2012. Doi/10.1021/je300826t

Doulabi, F. S. M. (2006). *Ternary Liquid - Liquid Equilibria for Systems of (Sulfolane + Toluene or Chloronaphthalene + Octane)*. 1431–1435.

Enyati, M. Mokhtarani, B. Sharifi, A. Anvari, S. and Mjotaba, M. (2017*). Liquid-Liquid Equilibria Data for Ethylbenzene or p-xylene with Alkane and 1-Butylpyridinium Nitrate Ionic Liquid at 298.15 K.* ACS publications. DOI: 101021/acs.jeed.6b00881.

Florindo, C., Oliveira F. S. Rebelo, L. P. N. Fernandes, A. M. and Murrucho I. M. (2014). *Insight into the synthesis and properties of deep eutectic solvents based on cholinium chloride and carboxylic acids*. ACS Sustainable Chem. Eng. 2014, 2, 2416 – 2425.

Gano Z.S. (2015) *Deep desulphurization of liquid fuels with green solvents: An Approach with Deep Eutectic Solvents.* Department of Petroleum and Chemical Engineering, College of Engineering Sultan Qaboos University Sultanate of Oman PhD thesis.

Garcia, G. Santiago A, Ullah, R., and Atilhan M (2015) *Deep Eutectic Solvents: Physicochemical Properties and Gas Separation Applications* American Chemical Society 2616 DOI: 10.1021/ef5028873 Energy Fuels 2015, 29, 2616−2644

Garcia J. Garcia S. Torrecilla J.S. and Rodriguez F. (2010*). Liquid-Liquid Equilibria for the Ternary systems {Heptane+Toluene+N-Butylpyridinium Tetraflourate borate or N-HexylpyridiniumTetraflouroborate at T = 313.15}.* J. Chem. Eng. Data 55, 2862 – 2865.

Garcia S. Lariba M. Garcia J. Torrecilla J.S. and Rodriguez F. (2011*). Liquid-Liquid Extraction of Toluene from Heptane using 1-Alkyl-3-methylimidazolium Bis(triflouromethylsulfonyl)imide ionic liquids*. J. Chem. Eng. Data 2011.

Gmehling, J. (2009) "*Present Status and Potential of Group Contribution Methods for Process Development,*" The *Journal of Chemical Thermodynamics*, Vol. *41*, No. 6, *2009*, pp. *731-747*. doi:10.1016/*j*.jct.2008.12.007.

Ghaedi, H., Ayoub, M., Sufian, S., Shariff, A. M., and Lal, B., (2017*) Densities and Refractive Indices of Potassium Carbonate Based Deep Eutectic Solvents with Dual Hydrogen Bond Donors at several temperatures* (293.15 – 343.15). DOI: 10.20a44/preprints201705.0146.0

Hansmeier, A. R. (2010). *Ionic liquids as alternative solvents for aromatics extraction* Eindhoven: Technische Universiteit Eindhoven DOI: 10.6100/IR675398

Hansmeier, A. R., Jongmans., Meindersma, G.W., de Haan, A. B., (2010) *LLE data for the ionic liquid 3-methyl-N-butyl pyridinium dicyanamidewith several aromatic and aliphatic hydrocarbons* J. Chem. Thermodynamics 42 (2010) 484–490.

Hand, D. B. (1930) "*Dineric Distribution*," J. Pys. Chem., 1930, 34(9) pp 1961-2000

Hadj-Kali, M. K., (2015) *Separation of ethylbenzene and n-octane using deep eutectic solvents* Green Process Synth 2015; 4: 117–123 DOI 10.1515/gps-2014-0088

Hadj-Kali, M. K., Sarwono, M. Hanee F. H., Irfan W.. Lahssen, E. Emad, A. Mohd A. H. and Alnashef, I. M. (2016) *Removal of thiophene from mixtures wirh n-heptane by selective extraction using deep eutectic solvents*. I & EC research. DOI: 10.1021/acs.iecr.6b01654

Hizaddin, H. F., Sarwono, M., Hashim, M. A., Alnashef, I. M., & Hadj-Kali, M. K. (2015). *Coupling the capabilities of different complexing agents into deep eutectisolvents to enhance the separation of aromatics from aliphatics.* The Journal ofChemical Thermodynamics, 84(0), 67-75.

Hayyan A. Mjalli F.S. Inas I.M. Al-Wahaibi Y.M. (2013*). Glucose based deep eutectic solvents: Physical Properties*. J. Mol. Liq. 178; 137 – 141

Hayyan A. Mjalli F.S. Al-Nashef I.M., Al-Wahaibi , T. Al-Wahaibi Y.M and Hashim M. A. (2012). *Fruit Sugar-based deep eutectic solvents and their physical properties*. Thermochemica Acta 541 (2012) 70 - 75

Hayyan A. Mjalli F.S. Hashim M. and Al-Nashef I.M. (2010). *A novel technique for separating glycerine from palm oil-based biodiesel using deep eutectic solvents*. Fuel Processing Technology 91; 116 – 120.

Hossain, A. Kim, D. H., Nguyen, D. Q,. Cheong, M., (2012). *Ionic Liquids as Benign Solvents for the Extraction of Aromatics* Bull. Korean Chem. Soc. 2012, Vol. 33, No. 10 3241 http://dx.doi.org/10.5012/bkcs.2012.33.10.3241

Kareem, M. A., Mjalli, F. S., Hashim, M. A., & AlNashef, I. M. (2012*). Liquid–liquid equilibria for the ternary system (phosphonium based deep eutectic solventbenzene–hexane) at different temperatures: A new solvent introduced*. *FluiPhase Equilibria, 314*(0), 52-59.

Kareem, M. A., Mjalli, F. S., Hashim, M. A., Hadj-Kali, M. K. O., Bagh, F. S. G., & Alnashef, I. M. (2012a). *Phase equilibria of toluene/heptane with tetrabutylphosphonium bromide based deep eutectic solvents for the potential usein the separation of aromatics from naphtha*. Fluid Phase Equilibria, 333(0), 4754.

Kareem, M. A., Mjalli, F. S., Hashim, M. A., Hadj-Kali, M. K. O., Ghareh Bagh, F. S & Alnashef, I. M. (2013). *Phase equilibria of toluene/heptane with deep eutectisolvents based on ethyltriphenylphosphonium iodide for the potential use in theseparation of aromatics from naphtha*. The Journal of Chemical Thermodynamics,65(0), 138-149.

Kareem, M. A., Mjalli, F. S., Hashim, M. A., and Al-Nashef I.M. (2010*). Phosphonium-Based Ionic Liquids Analogues and Their Physical Properties*. J. Chem. Eng. Data 2010, 55, 4632 – 4637.

Kanel, J. S. and Associates LLC (2003). Overview: *Industrial Application of Ionic Liquids for Liquid Extraction*, Chemical Industry Vision 2020 Technology Partnership Workshop New York, NY, Sept 11, 2003

Kiki A. K., Nur A. A., Fernando J. M. C., Bhajah L. (2016*) Phase behavior of ternary*

mixtures {aliphatic hydrocarbon + aromatic hydrocarbon + deep eutectic solvent }: A step forward toward "greener" extraction process. Procedia Engineering 148; 1340-1345

Kralisch, D., Reinhardt, D., and Kreisel, G. (2007). *Implementing Objectives of sustainability in to Ionic Liquid Research and Development*. Green Chem., 9,pp. 1308 - 1318

Lariba M. Navarro P. Garcia J. and Rodriguez F. (2013*). Highly Selective Extraction of Toluene from n-Heptane using [emim][SCN] Pure ionic liquids and its mixtures with several transition metal salts.* Chemical Engineering Transactions CEt. Vol; 32.

Letcher, TM and Reddy, P. (2004). *Ternary Liquid-liquid Equilibria for Mixtures of 1-Hexyl-3-methylimidazolium (Tetrafuloroborate or Hexafluorophosphate) + Ethanol + an Alkene at T = 298.2 K,* Fluid Phase Equil., 219, 107-112 (2004).

Li, C., Li, D., Zou, S., Li, Z., Yin, J., and Wang, J., (2013). *Extractive desulfurization of process fuel with ammonium-based deep eutectic solvents*. Green chemistry, 15(10) 2793-2799.

Lin, W., & Kao, N. (2002). *Liquid - Liquid Equilibria of Octane + (Benzene or Toluene or m –Xylene) + Sulfolane at 323 . 15 , 348 . 15 , and 373 . 15 K*. 1007–1011

Li, Zheng (2015). *Thermodynamic Modelling of Liquid-liquid Equilibria Using the Non ramdom Two-liquid Model and its Application. Doctoral thesis. Department of Chemical and Biomolecular Engineering.* The University of Melbourne. http://hdl.handle.net/11343/57353

Meindersma, G.W. (2005). *Extraction of aromatics from naphtha with ionic liquids*; Ph.D Thesis,University of Twente, The Netherlands,

Mirza, N. R. Nicholas N. J. Wu, Y. Smith, K. H. Kentish, S. E., and Stevens, G. W., (2016). *Viscosities and Carbon Dioxide Solubilities of Guanidine Carbonate and Malic Acid – Based Eutectic Solvent.* J. Chem. Eng. Data. ACS Publications. Doi: 10.103/acs.jced.6b00680

Mohsen-nia, M., Doulabi, F. S. M., & Manousiouthakis, V. I. (2008). *(Liquid + liquid) equilibria for ternary mixtures of (ethylene glycol + toluene + n -octane). 40*, 1269–1273. https://doi.org/10.1016/j.jct.2008.03.014

Mulyono, S., Hizaddin, H. F., Alnashef, I. M., Hashim, M. A., Fakeeha, A. H., & Hadj-Kali, M. K. (2014). *Separation of BTEX aromatics from n-octane using a (tetrabutylammonium bromide + sulfolane) deep eutectic solvent - experiments and COSMO-RS prediction.* RSC Advances, 4(34), 17597-17606.

Naseer J. Mjalli, F.S. Jibril, B. Al-Hatmi, S. and Gano, Z. (2013). *Potassium Carbonate as a salt for Deep Eutectic Solvents.* Chemical Engineering and Applications Vol. 4 No. 3. June,2013.

Oliveira, F. S., Pereiro, A. B., Rebelo, L. P. N., & Marrucho, I. M. (2013*). Deep eutectic solvents as extraction media for azeotropic mixtures. Green Chemistry, 15*(5), 1326-1330.

Othmer, D. F and Tobias, P. E. (1942) *"Toluene and acetaldehyde systems, tie line correlation partial pressures of ternary liquid systems and the prediction of tie lines.*" Ind. Eng. Chem,. Vol. 34, pp 693 – 698

Reina M.D. Gonzalez E.A. Munoz Y.M.(2013*) Study of Liquid-Liquid equilibrium of toluene+heptane with the ionic liquid 1,3-dimethylimidazolium methylsulfate at 318.15K*. AVANCES Investigacion en ingeneria Vol.9. No. 2 (2013).

Renon, H.; Prausnitz, J.M., (**1968)** *Local compositions in thermodynamic excess functions for liquid mixtures.* AIChE Journal**,** 14, (1), 135-144.

Rodriguez N. R. Reguego P. F. and Kroon M. C. (2015) *Aromatic – Aliphatic separation using deep eutectic solvents as extracting agents.* I & EC research.

Rodriguez N. R. Molina B.S. and Kroon M. C. (2016). *Aliphatic + ethanol separation via liquid-liquid extraction using Low transition temperature mixtures as extraction agents. Fluid Phase Equilibria.* 394; 71 – 82.

Richardson J.F. and Harker J.H. (2002) *Particle Technology and Separation Processes*. Coulson and Richardson's Chemical Engineering Volume 2, 5th ed.

Rodriguez H. and Brennecke J. F., (2006). *Temperature and Composition Dependence of the density and viscosity of Binary mixtures of water and IL*. J. Chem. Eng. Data, 51, 2145 – 2155..

Sander, A. Rogosic, M. Silvar, A. Zuteg, B. (2015) *Separation of Hydrocarbon by means of Liquid-Liquid extraction with Deep Eutectic Solvents.* Solvent Extraction and Ion Exchange. DOI: 10.1080/07366299.2015.1132060.

Sarwono, M.M, Hadj-Kali, M. K.O, Alnashef, I. M. (2013). *Separation of Aromatics using Benign Solvents.* International Journal of Chemical, Environmental and Biological Sciences. (IJCEBS). Volume 1, Issue 4.

Siongco, K. R., Leron R. B., Li, M. (2013) *Densities, refractive indices, and viscosities of N,N-diethylethanol ammonium chloride–glycerol or –ethylene glycol deep eutectic solvents their aqueous solutions* J. Chem. Thermodynamics 65 (2013) 65–72

Smith E. L., Abbott A. P., and Ryder K. S., (2012). *Deep Eutectic Solvents (DESs) and Their Applications* pubs.acs.org/CR dx.doi.org/10.1021/cr300162p | Chem. Rev.

Sørensen, J. M.. Arlt, W.(1980) *Liquid-Liquid Equilibrium Data Collection*, DECHEMA Chemistry Data Series, Frankfurt.

Sun, L. Morales-Collazo O. Xia H. and Brennecke J. F. (2015*). Effect of structure on Transport Properties (Viscosity, Ionic Conductivity, and Self-Diffusion Coefficient) of Aprotic Heterocyclic Anion (AHA) Room Temperature Ionic Liquids. 1 Variation of Anionic Species*. J. Phys. Chem. B. 2015, 119, 15030 – 15039 ACS Publications

Troter, D. Z. Zlatkovic, M. Z., Dokic-Stojanovic, D. R., Konstantinovic, S. S., Todorovic, Z. B. (2016). *Citric Acid-Based Deep Eutectic Solvents:Physical Properties and their Use as CoSolvent in Sulphuric Acid-Catalysed Ethanolysis of Oliec Acid.* Advanced technologies 5(1) (2016) 53 – 65.

Troter, D. Z. Todorovic, Z. B. Dusica R. D., Dordevic B. S., Todorovic, V. M. Konstantinovic S. S. and Veljkovic V. B. (2017). *The physicochemical and thermodynamic properties of the choline chloride-based deep eutectic solvents*. J. Serb. Chem. Soc. 82(9) 1039 – 1052 (2017).

Wilson, G. M. (1964). *Vapor-Liquid Equilibrium. XI. A New Expresssion for the Excess Free Energy of Mixing.* Journal of the American Chemical Society **86**:127-130, 1964.

Weissermel, K., Arpe, H. J., (2003) *Industrial Organic Chemistry*, 4th Completely Revised edition. Wiley-VCH, Weinheim, 2003. Pp 313 – 336

Yadav, A. and Pandey, S (2014) *Densities and Viscosities of (Choline Chloride + Urea) Deep Eutectic Solvent and Its Aqueous Mixtures in the Temperature Range 293.15 K to 363.15 K. J.* Chem. Eng. Data 2014, 59, 2221-2229. doi.org/10.1021/je5001796

Yusuf, R., Abdulmalek E., Sirat K., AbdulRahman A., (2014). *Tetrabutyl ammonium bromide (TBABr) – Based Eutectic Solvent (DES) and their Physical Properties.* Molecules ISSN 1420-3049. Molecule 19,8011 – 8026 doi: 10.3390/molecules 19068011

Zhang Q. Vigier, K D O Royer S. Jerome f. (2012*) Deep eutectic solvents: synthesis, properties and applications*. Chem. Soc. Rev., 41, 7108.

APPENDIXES

Appendix I: Screening results for Ammonium and Phosphonium based DESs
Table A.1 Screening results for Ammonium based DESs

S/no	DESs	Distribution coefficient	Selectivity	Aromatic removal efficiency(%)	. Cross solubility	States at room temp
1	TBAB/					
	PEG 200 (1:2)	0.6471	8.4858	17.32	NO	LQ
	PEG 400 (1:2)	0.7952	8.0576	21.63	NO	LQ
	PEG 600 (1:2)	1.3763	6.1178	24.48	NO	LQ
	DEA (1:2)	0.4012	7.8210	16.25	NO	LQ
	DMF (1:2)	0.7962	5.943	32.21	YES	LQ
	DMSO (1:2)	0.9099	4.004	31.33	YES	LQ
	MP (1:2)	--	--	--	--	--
	MMP (1:2)	--	--	--	--	--
	PYRD (1:2)	--	--	--	--	--
	FF (1:2)	--	--	--	--	--
2	TBAC/					
	EG (1:2)	--	--	--	--	--
	DMSO (1:2)	--	--	--	--	--
	PEG 200 (1:2)	--	--	--	--	--
	PEG 600 (1:2)	--	--	--	--	--
3	TPAB/					
	EG (1:2)	0.246	8.5512	10.16	NO	LQ
4	TEAB/					
	PYRD (1:2)	--	--	--	--	--
	MP(1:2)	--	--	--	--	--
	Three component DESs					
1	TBAB/					
	SF:PRD (1:2:2)	--	--	--	--	--
	SF:FF(1:6:4)	--	--	--	--	--
	SF:PYRD(1:2:2)	--	--	--	--	--
	EG:PRD(1:4:4)	--	--	--	--	--
	EG:PRD(1:4:6)	--	--	--	--	--
	EG:PRD(1:6:4)	--	--	--	--	--
2	TEAB/					
	EG:PRD(1:4:2)	--	--	--	--	--
	EG:PRD(1:4:4)	--	--	--	--	--

Table A.2 Screening results for Phosphonium based DESs

S/no	DESs	Distribution coefficient	Selectivity	Aromatic removal efficiency(%)	Cross solubility	States at room temp.
1	TBPB/					
	EG(1:2)	0.2647	9.2410	15.27	NO	LQ
	DMSO(1:2)	1.1082	10.6517	40.10	YES	LQ
	DMF(1:2)	0.7893	4.9559	31.81	YES	LQ
	PEG 200 (1:2)	0.6601	8.6212	17.98	NO	LQ
	PEG 600 (1:2)	1.3450	7.8921	21.30	NO	LQ
2	TBPMSPh/					
	DMSO(1:2)	0.8601	6.1271	31.29	YES	LQ
	DMF(1:2)	0.7721	4.3210	27.68	YES	LQ
	PEG 200 (1:2)	0.6892	7.3226	13.92	NO	LQ
	PEG 200 (1:2)	1.3168	8.3472	17.10	NO	LQ
3	Three component DESs					
	MTPPB/					
	SF:FF (1:6:4)	--	--	--	--	--
	SF:PRD (1:6:4)	--	--	--	--	--

Appendix II: Physical properties variations with temperatures

Table B.1 Experimental values density with temperature for the ammonium based DESs.

	Ammonium based salts			
T(K)	TBAB:PEG600	TBAB:PEG200	TBAB:DMF	TBAB:DMSO
303.15	1.10465	1.08867	1.02599	1.08335
313.15	1.09764	1.08177	1.01805	1.07185
323.15	1.09009	1.07488	1.00920	1.05504
333.15	1.08259	1.06805	1.00053	1.04367
343.15	1.07513	1.06123	0.99273	1.03614
353.15	1.06772	1.05446	0.98607	1.02924
363.15	1.06034	1.04770	0.98226	1.02223

Table B.2 Experimental values density with temperature for the phosphonium based DESs.

	Phosphonium based salts					
T(K)	TBPB:PEG600	TBPB:PEG200	TBPMS:PEG200	TBPMS:PEG600	TBPB:DMSO	TBPB:DMF
303.15	1.10342	1.08806	1.05961	1.08957	1.06528	1.02517
313.15	1.09578	1.08110	1.05283	1.08223	1.05820	1.01763
323.15	1.08819	1.07417	1.04604	1.07475	1.05096	1.01031
333.15	1.08067	1.06726	1.03928	1.06732	1.04359	1.00300
343.15	1.07356	1.06036	1.03244	1.05993	1.03638	0.99568
353.15	1.06555	1.05347	1.02573	1.05240	1.02917	0.98833
363.15	1.05871	1.04660	1.01850	1.04520	1.02206	0.98110

Table B.3 Experimental values viscosity with temperature for the ammonium based DESs.

	Ammonium based salts			
T(K)	TBAB:PEG600	TBAB:PEG200	TBAB:DMF	TBAB:DMSO
303.15	168	148	58	133.5
313.15	117	86	44.5	85.5
318.15	86	69	34	63.5
323.15	74.5	56.5	14.5	43
328.15	56.5	43.5	13	32.5
333.15	51	34	10	24.5
338.15	39.5	26	9	22
343.15	32	18.5	7	20
353.15	25.5	14	5	17.5

Table B.4 Experimental values viscosity with temperature for the phosphonium based DESs.

	Phosphonium based salts					
T(K)	TBPB: PEG600	TBPMS: PEG600	TBPMS: PEG200	TBPB:DMF	TBPB:DMSO	TBPB:PEG200
303.15	154.5	133	80.5	25	67	100
313.15	95	78	50.5	16	40.5	63
318.15	78.5	71	41	15	33	50
323.15	62	55.5	35	13	24	39.5
328.15	51	45	25.5	11	20	30.5
333.15	44.5	38	21	10.5	18.5	29
338.15	39	32	18.5	8.5	16	23.5
343.15	30.5	26.5	15	7	12.5	20.5
353.15	22.5	23	10	5	10	12.5

Table B.5 Percentage decrease in Experimental Viscosity Values for Ammonium based DESs

	Ammonium based			
Tep. Range	TBAB:PEG600	TBAB:PEG200	TBAB:DMF	TBAB:DMSO
303-313	30.357	41.892	23.276	35.955
313-318	26.497	19.767	23.596	25.731
318-323	13.3721	18.11594	57.35294	32.28346
323-328	24.16107	23.00885	10.34483	24.4186
328-333	9.734513	21.83908	23.07692	24.61538
333-338	22.54902	23.52941	10	10.20408
338-343	18.98734	28.84615	22.22222	9.090909
343-353	20.3125	24.32432	28.57143	12.5

Table B.6 Percentage decrease in Experimental Viscosity Values for Phosphonium based DESs

	Phosphonium based					
Tep. Range	TBPB: PEG600	TBPMS: PEG600	TBPMS: PEG200	TBPB:DMF	TBPB:DMSO	TBPB:PEG200
303-313	38.511	41.353	37.267	36.000	39.552	37.000
313-318	17.368	8.974	18.812	6.250	18.519	20.635
318-323	21.019	21.831	14.634	13.333	27.273	21.000
323-328	17.742	18.919	27.143	15.385	16.667	22.785
328-333	12.745	15.556	17.647	4.545	7.500	4.918
333-338	12.360	15.789	11.905	19.048	13.514	18.966
338-343	21.795	17.188	18.919	17.647	21.875	12.766
343-353	26.230	13.208	33.333	28.571	20.000	39.024

Table B.6 Experimental Refractive index values with temperature for the ammonium based DESs.

	Ammonium based salts			
T(K)	TBAB:PEG600	TBAB:PEG200	TBAB:DMF	TBAB:DMSO
303	1.4739	1.4763	1.4893	1.4944
313	1.4705	1.4733	1.4860	1.4908
323	1.4670	1.4702	1.4826	1.4872
333	1.4636	1.4671	1.4790	1.4835
343	1.4600	1.4640	1.4754	1.4803
353	1.4565	1.4609	1.4716	1.4771
363	1.4531	1.4578	1.4688	1.4741

Table B.7. Experimental Refractive index values with temperature for the phosphonium based DESs.

	Phosphonium based salts					
T(K)	TBPB: PEG600	TBPB: PEG200	TBPMS: PEG600	TBPMS: PEG200	TBPB :DMF	TBPB: DMSO
303	1.4757	1.4805	1.4694	1.4675	1.4855	1.4992
313	1.4722	1.4774	1.4659	1.4643	1.4821	1.4957
323	1.4688	1.4740	1.4617	1.4613	1.4789	1.4918
333	1.4655	1.4709	1.4588	1.4581	1.4753	1.4875
343	1.4621	1.4677	1.4554	1.4550	1.4719	1.4822
353	1.4588	1.4646	1.4520	1.4518	1.4686	1.4783
363	1.4553	1.4615	1.4486	1.4487	1.4653	1.4753

Table B.8 Experimental Conductivity values with temperature for the ammonium based DESs

	Ammonium based salts			
T(K)	TBAB:PEG600	TBAB:PEG200	TBAB:DMF	TBAB:DMSO
303	134	431	1562	950
313	212	800	2340	1750
323	321	1305	3270	2330
333	466	1830	4480	3480
343	680	2620	5930	4820
353	902	3450	7550	6480
363	1130	4330	9410	8450

Table B.9. Experimental Conductivity values with temperature for the phosphonium based DESs.

	Phosphonium based salts					
T(K)	TBPB: PEG600	TBPB: PEG200	TBPMS: PEG200	TBPB:DMF	TBPB:DMSO	TBPMS:PEG600
303	186.9	733	656	2230	1227	179.5
313	281	1029	1061	3200	2010	258
323	423	1428	1453	4280	3000	384
333	597	2200	2040	5690	4120	534
343	785	2860	2740	7140	5700	730
353	1016	3950	3610	8890	7500	1032
363	1730	4650	4570	10710	9280	1285

Appendix III: Average distribution coefficients

Table C1. Average distribution coefficients values at three different temperatures for the studied DESs.

	DESs	Temperatures (oC)		
		30	40	50
1	TBABPEG600	1.256	1.368	1.287
2	TBABPEG200	0.624	0.655	0.623
3	TBPBPEG600	1.327	1.368	1.294
4	TBPBPEG200	0.650	0.682	0.702
5	TBPMSPEG600	1.322	1.327	1.349
6	TBPMSPEG200	0.708	0.713	0.695
7	TBABDMF	0.766	0.798	0.813
8	TBABDMSO	0.938	0.955	0.950
9	TBPBDMF	0.815	0.891	0.930
10	TBPBDMSO	1.038	0.708	0.793

Appendix IV: Othmer – Tobias and Hand correlation graphs for the studied DESs.

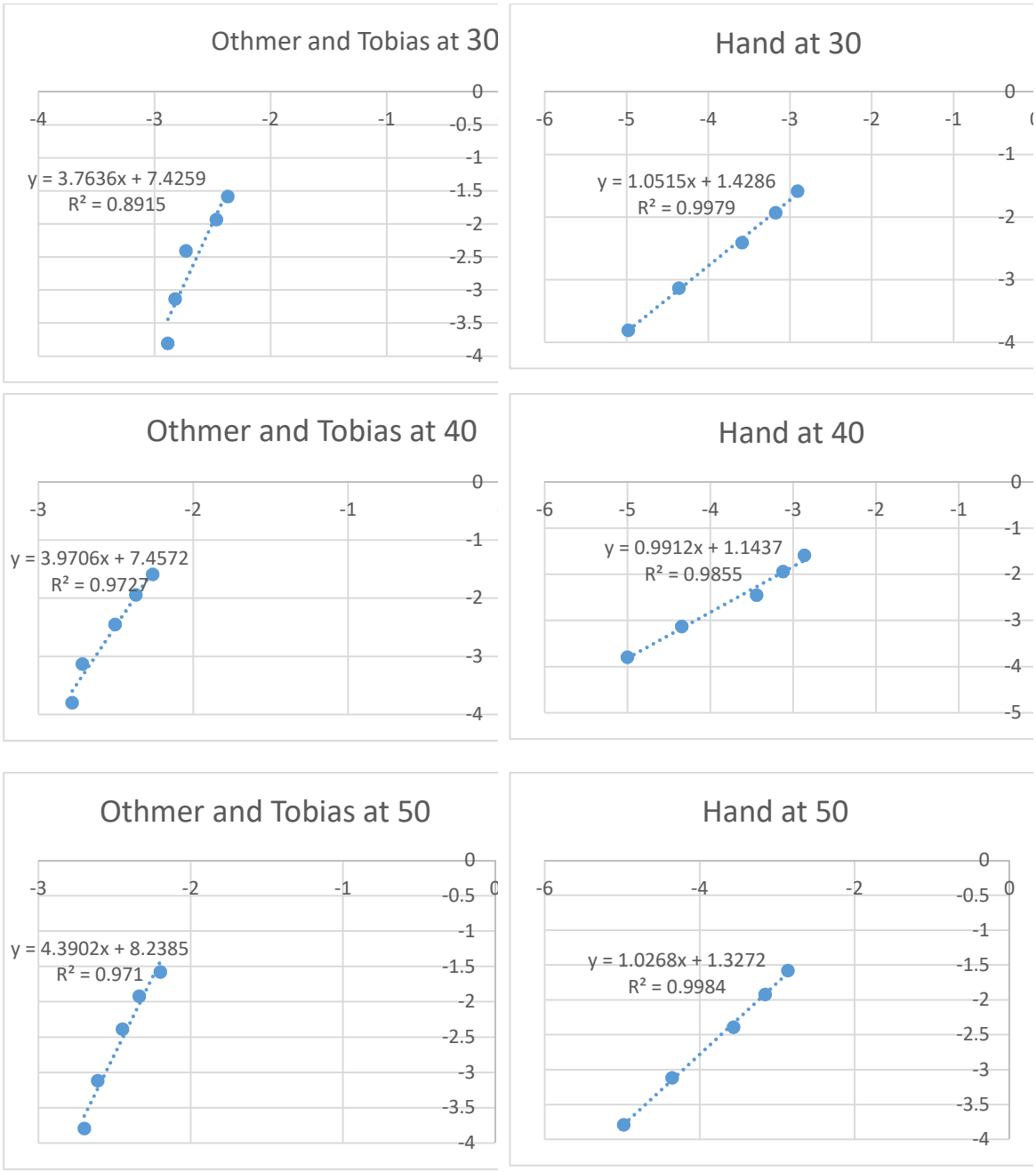

Figure C1: TBAB: PEG200 at 30, 40 and 50 ºC

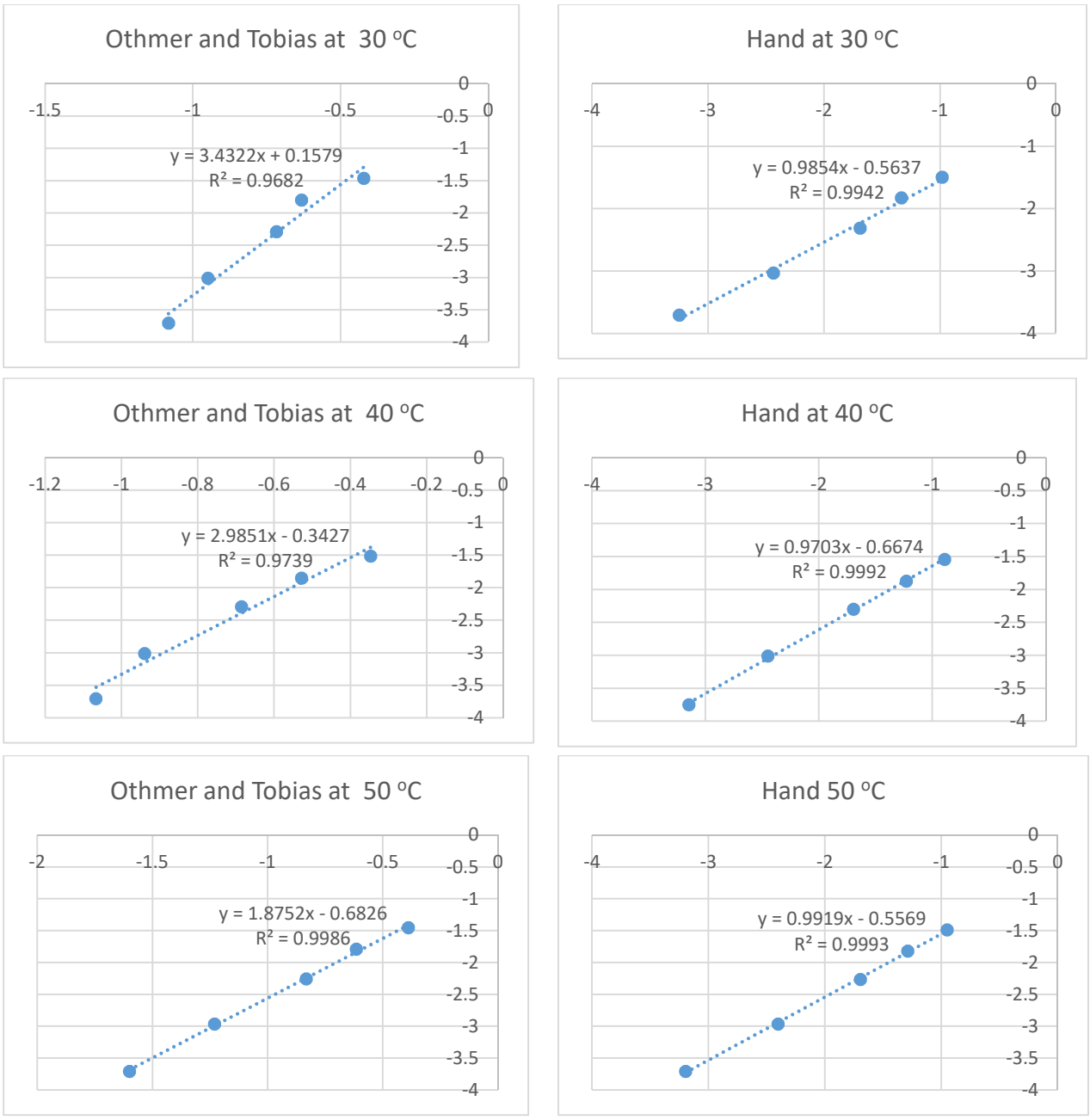

Figure C2: TBAB: PEG600 at 30, 40 and 50 °C

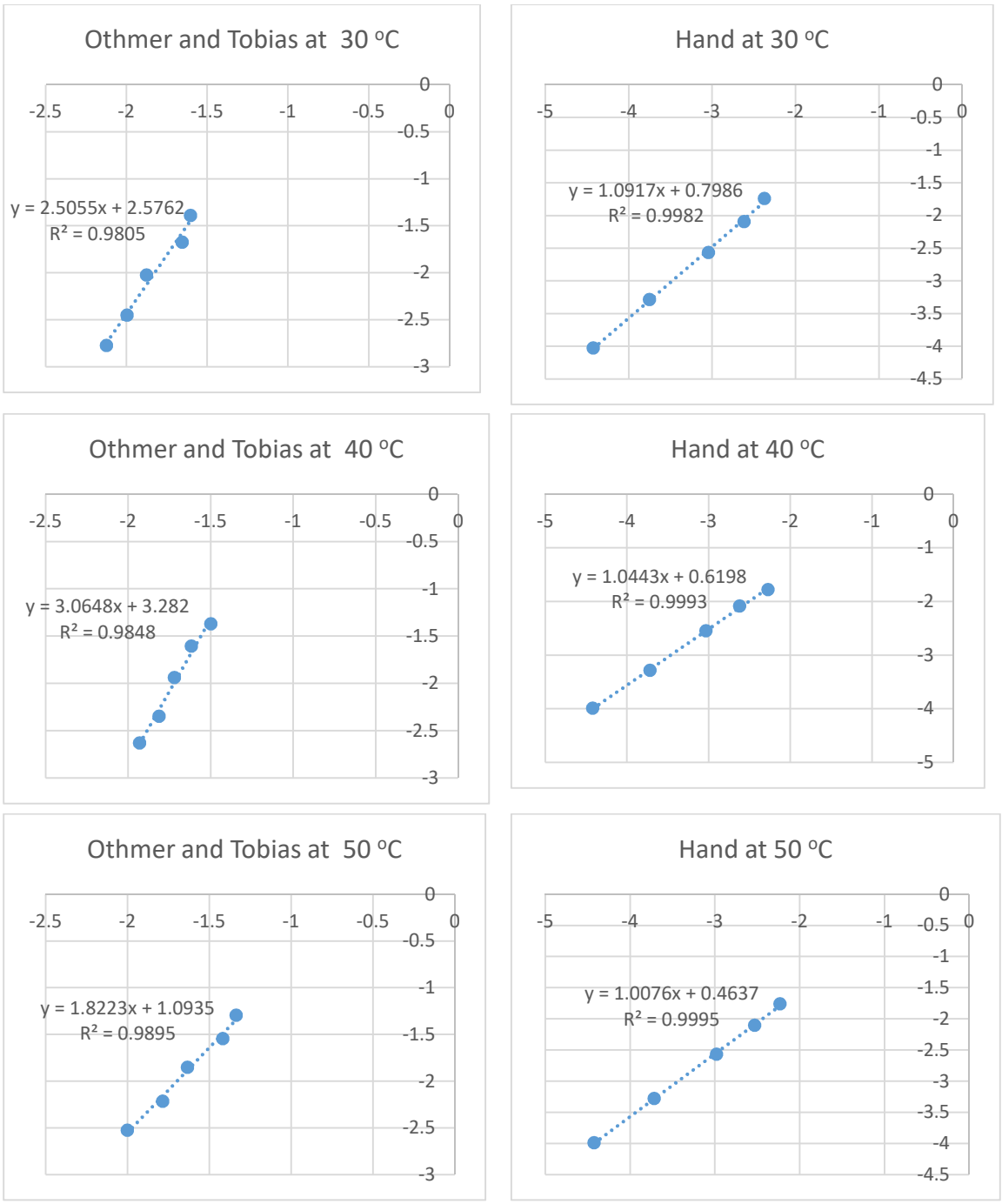

Figure C3: TBAB: DMF at 30, 40 and 50 °C

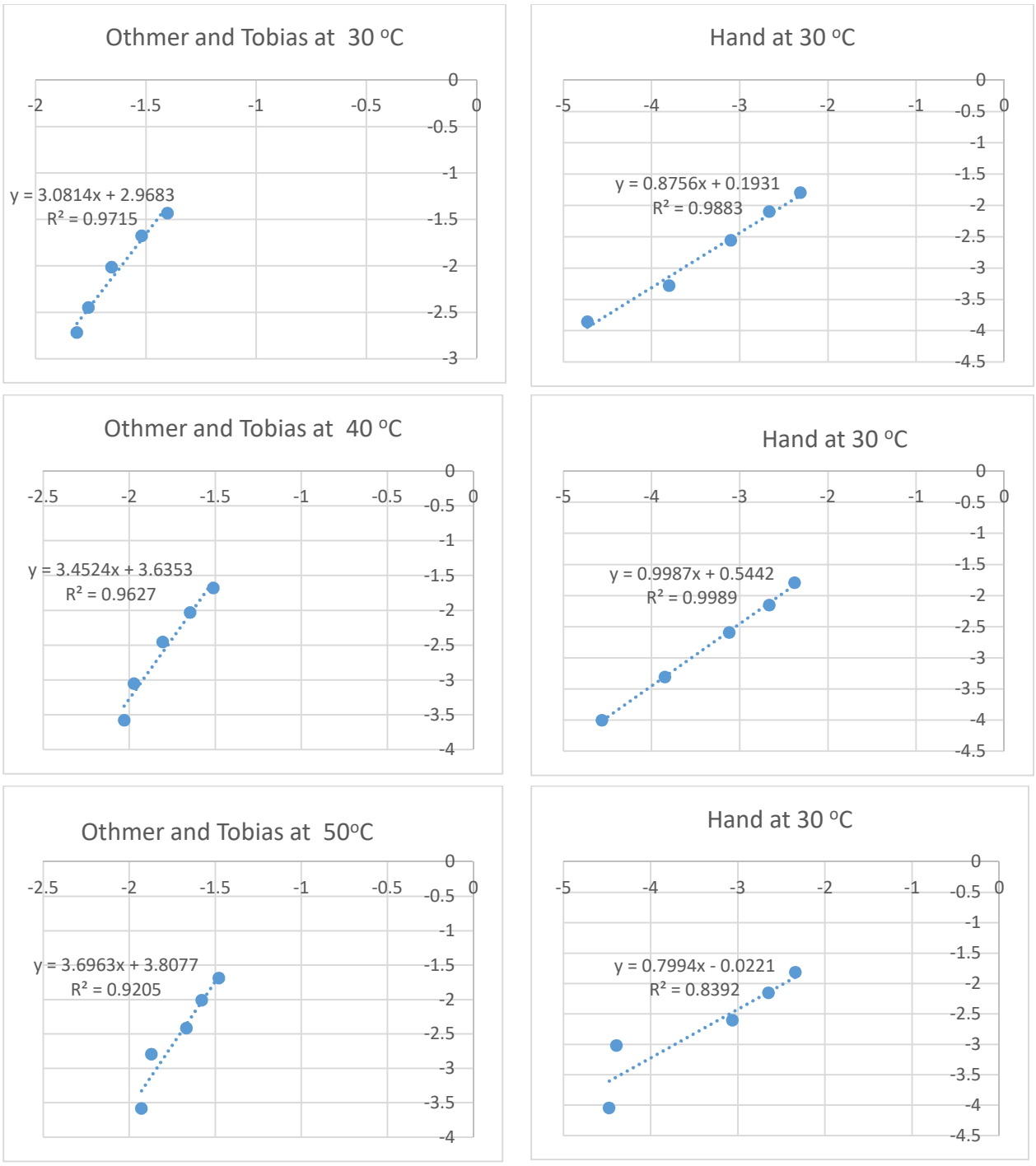

Figure C4: TBAB: DMSO at 30, 40 and 50 °C

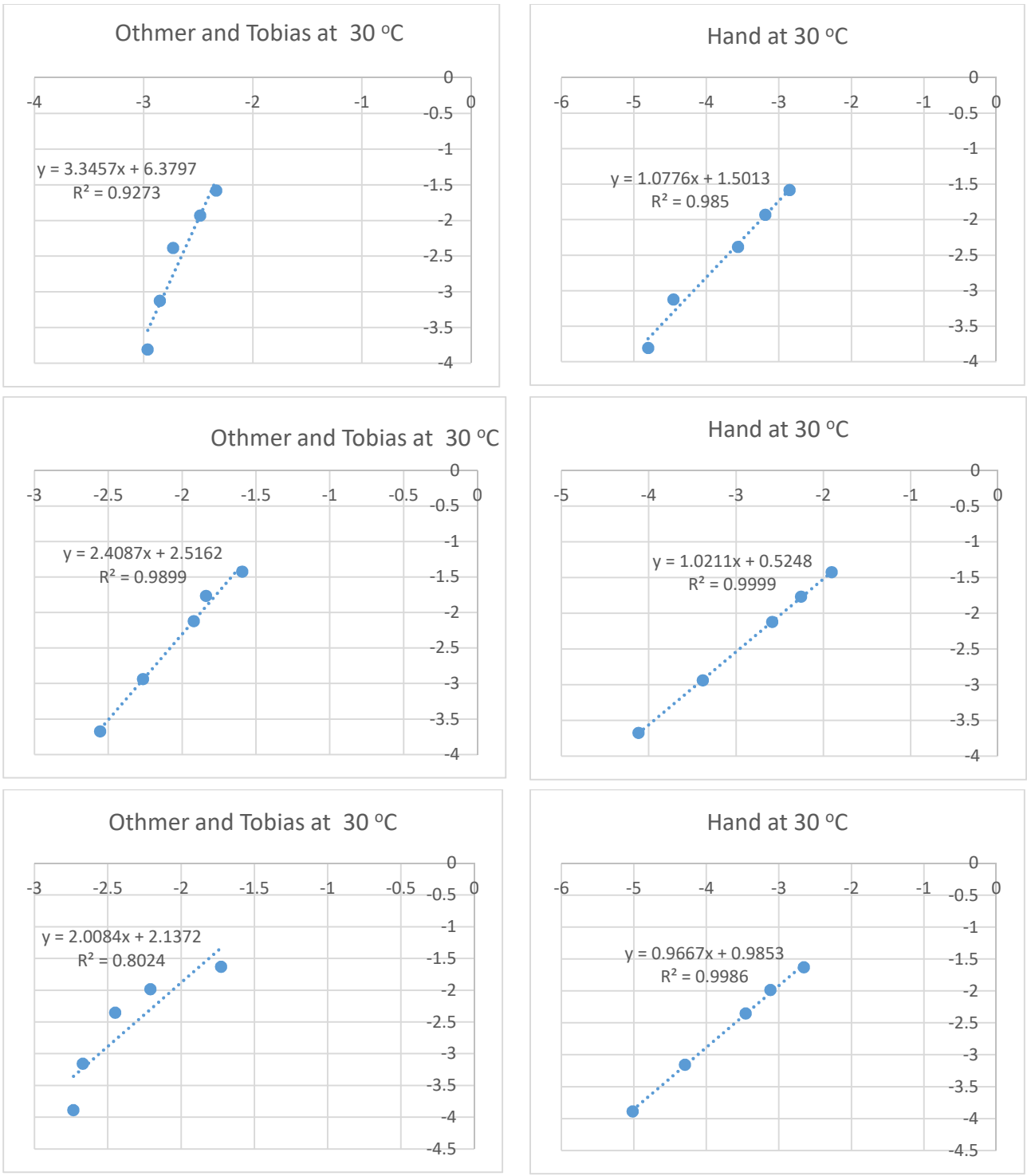

Figure C5: TBPB: PEG200 at 30, 40 and 50 °C

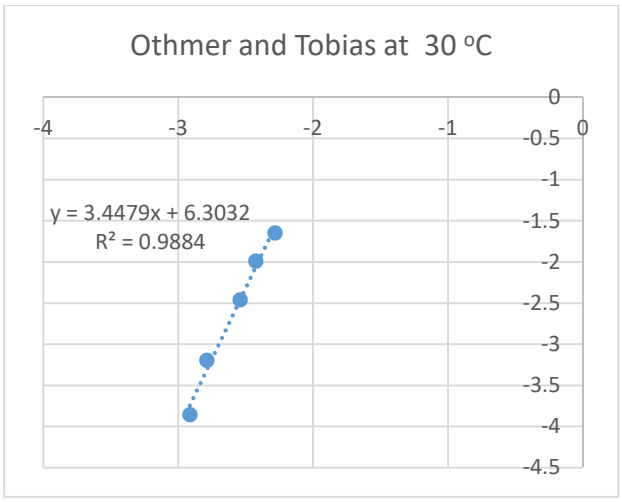

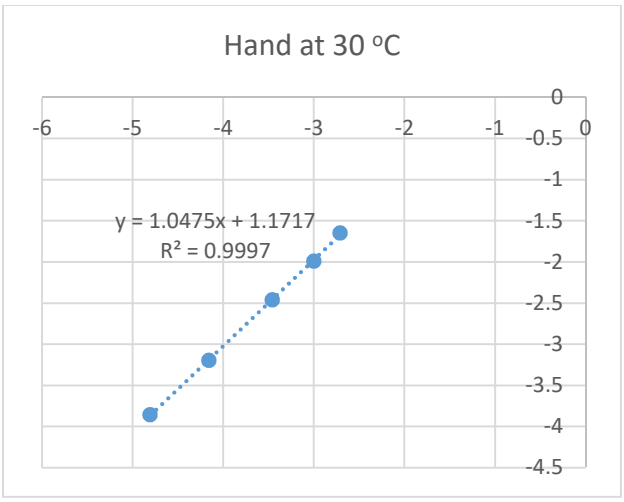

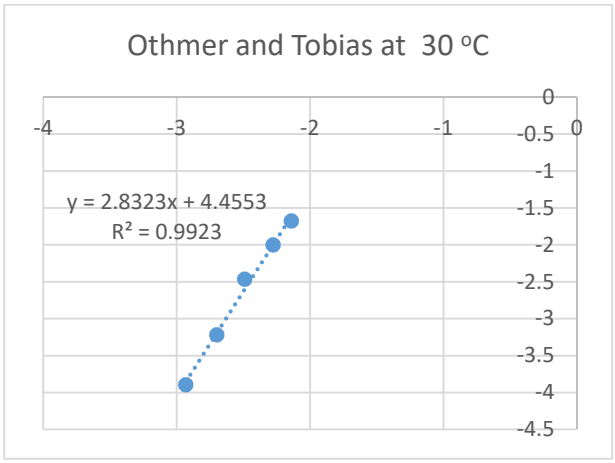

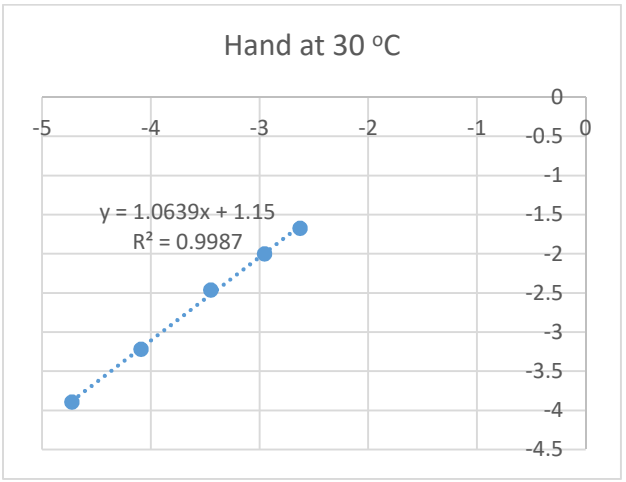

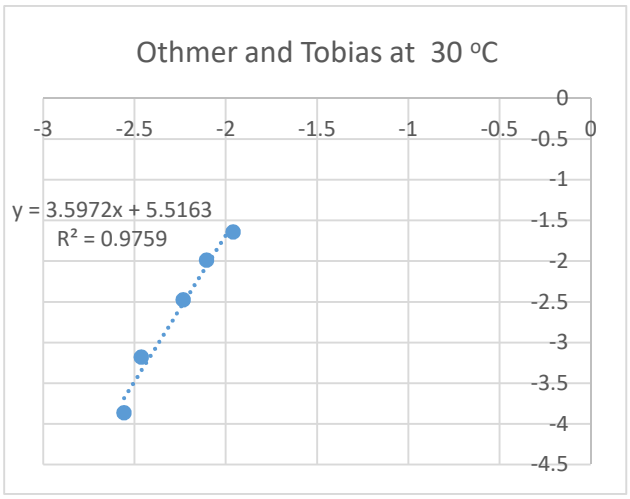

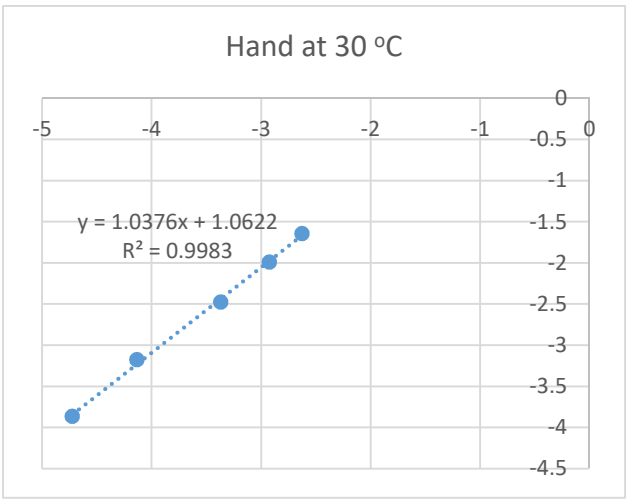

Figure C6: TBPB: PEG600 at 30, 40 and 50 °C

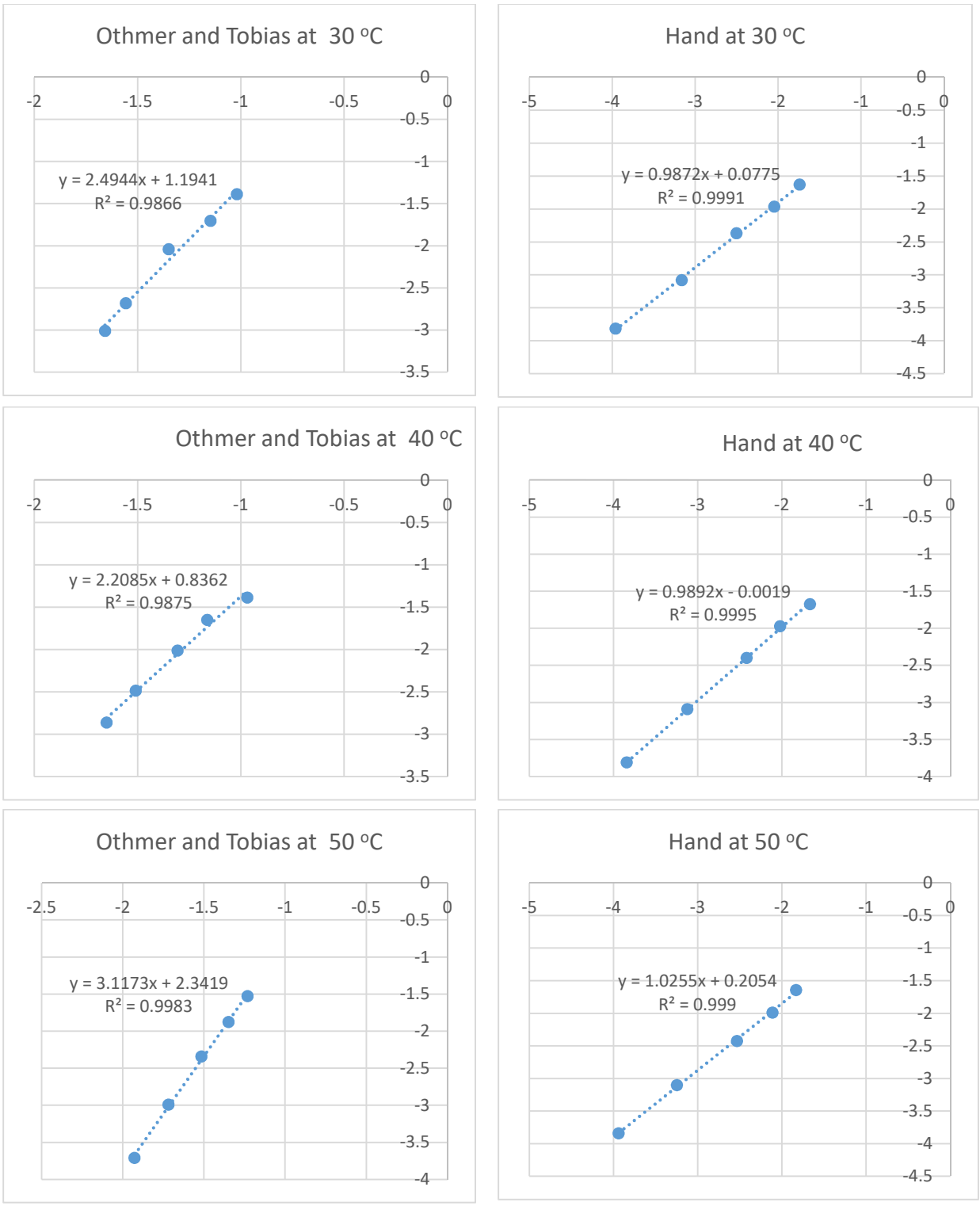

Figure C7: TBPB: DMF at 30, 40 and 50 °C

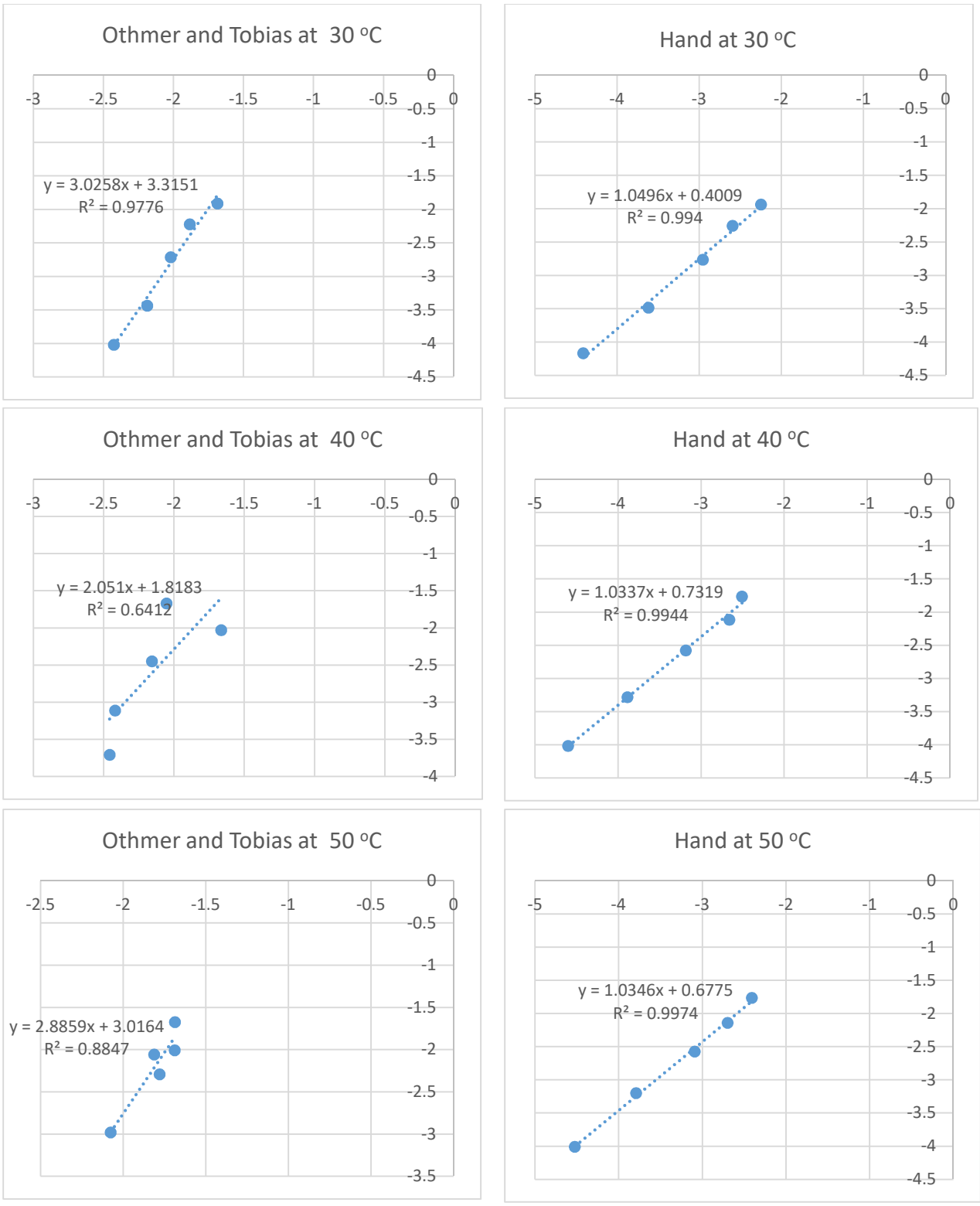

Figure C8: TBPB: DMSO at 30, 40 and 50 °C

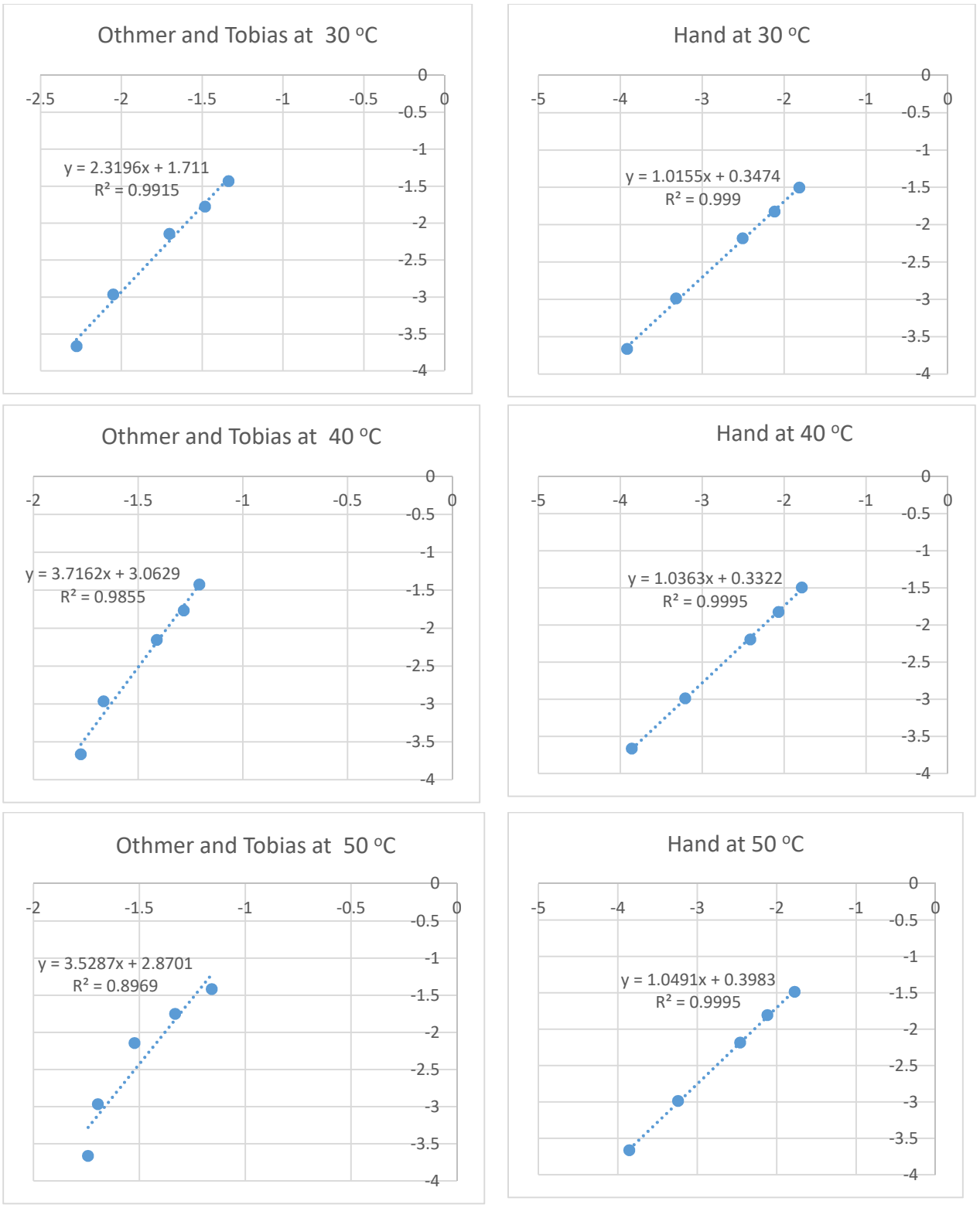

Figure C9: TBPMS: PEG200 at 30, 40 and 50 °C

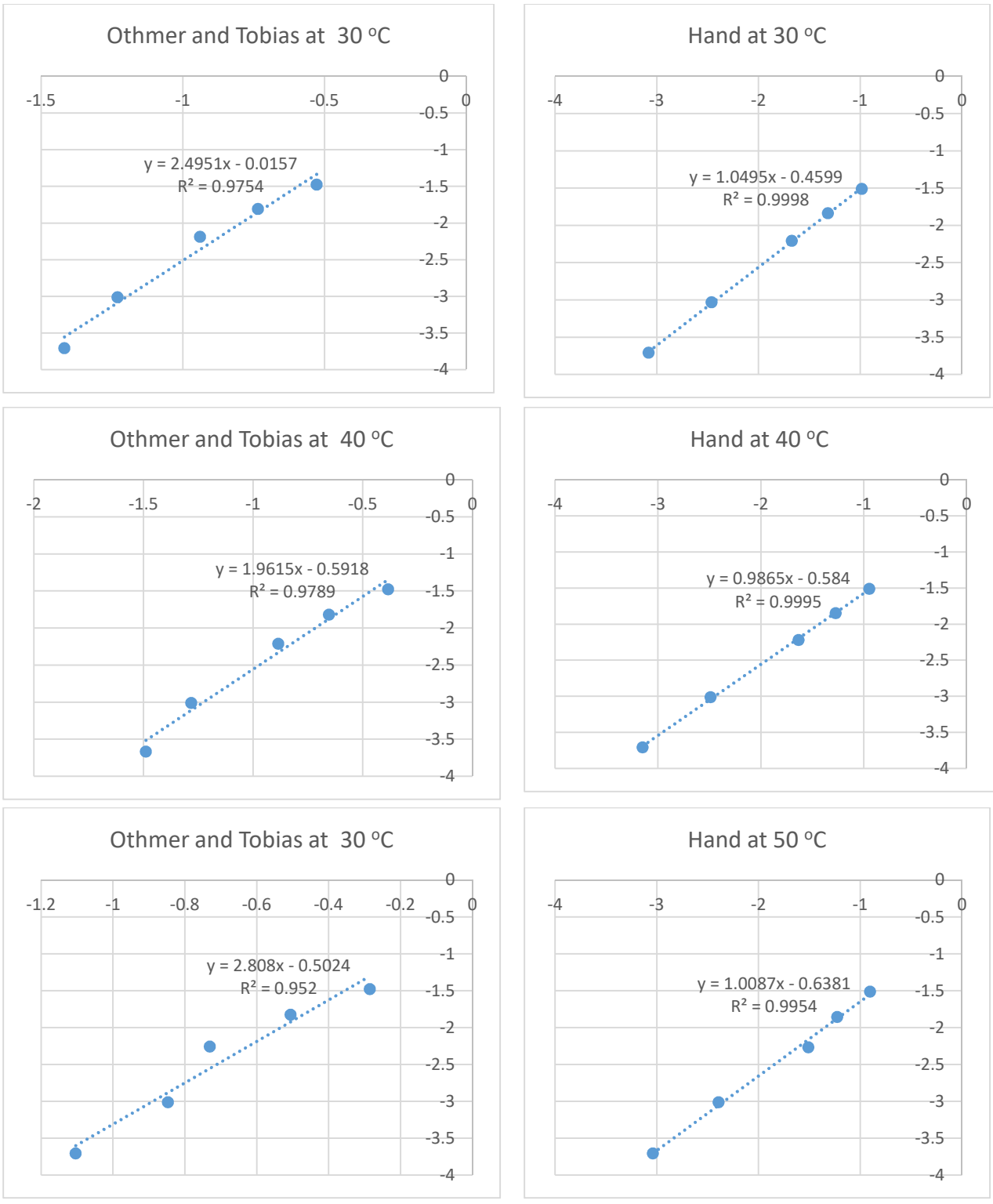

Figure C10: TBPMS: PEG600 at 30, 40 and 50 °C

Appendix V: Experimental LLE data

Table C.2.Experimental LLE data for TBAB: PEG 200 (1:2) at 30

	DES rich phase			Hydrocarbon rich phase				
% Aro	Oct	DES	Tol	Oct	DES	Tol	B_{tol}	S
			Experimental		LLE	Data	30 °C	
2.5	0.092	0.892	0.016	0.973	0.000	0.027	0.60	6.37
5	0.087	0.884	0.029	0.949	0.000	0.050	0.59	6.40
10	0.069	0.869	0.063	0.899	0.000	0.097	0.65	8.49
15	0.076	0.833	0.091	0.847	0.000	0.144	0.63	7.04
20	0.067	0.817	0.116	0.797	0.000	0.188	0.62	7.34
			NRTL	GA			30°C	
2.5	0.0860	0.8908	0.0156	0.9794	0.0008	0.0274	0.57	6.48
5	0.0831	0.8828	0.0289	0.9532	0.0008	0.0501	0.58	6.62
10	0.0753	0.8679	0.0586	0.8930	0.0008	0.1014	0.58	6.85
15	0.0743	0.8319	0.0886	0.8490	0.0007	0.1464	0.61	6.92
20	0.0680	0.8160	0.1181	0.7963	0.0007	0.1859	0.64	7.44
			UNIQUAC	GA			30 °C	
2.5	0.0757	0.8954	0.0171	0.9735	0.0122	0.0258	0.66	8.52
5	0.0739	0.8868	0.0313	0.9466	0.0127	0.0474	0.66	8.46
10	0.0686	0.8705	0.0631	0.8849	0.0137	0.0963	0.66	8.45
15	0.0711	0.8329	0.0943	0.8384	0.0146	0.1399	0.67	7.95
20	0.0676	0.8154	0.1223	0.7837	0.0157	0.1807	0.68	7.85

Table C.3.Experimental LLE data for TBAB: PEG 200 (1:2) at 40 °C

	DES rich phase			Hydrocarbon rich phase					
%Aro	Oct	DES	Tol	Oct	DES	Tol		B_{tol}	S
			Experimental		LLE	Data	40 °C		
2.5	0.103	0.882	0.015	0.973	0.000	0.027		0.58	5.46
5	0.098	0.873	0.030	0.949	0.000	0.050		0.59	5.69
10	0.088	0.842	0.070	0.903	0.000	0.093		0.75	7.72
15	0.086	0.820	0.094	0.849	0.000	0.143		0.66	6.54
20	0.079	0.801	0.119	0.798	0.000	0.188		0.64	6.38
			NRTL	GA			40°C		
2.5	0.1002	0.8812	0.0162	0.9764	0.0003	0.0258		0.63	6.12
5	0.0966	0.8722	0.0309	0.9510	0.0003	0.0491		0.63	6.20
10	0.0900	0.8411	0.0623	0.9015	0.0003	0.1007		0.62	6.20
15	0.0847	0.8191	0.0924	0.8508	0.0003	0.1446		0.64	6.42
20	0.0780	0.8001	0.1216	0.7995	0.0004	0.1854		0.66	6.72
			UNIQUAC	GA			40 °C		
2.5	0.0871	0.8866	0.0171	0.9695	0.0145	0.0247		0.69	7.71
5	0.0854	0.8769	0.0327	0.9427	0.0150	0.0470		0.70	7.68
10	0.0836	0.8444	0.0667	0.8897	0.0157	0.0956		0.70	7.43
15	0.0818	0.8207	0.0978	0.8366	0.0170	0.1384		0.71	7.23
20	0.0785	0.7999	0.1271	0.7830	0.0182	0.1788		0.71	7.09

Table C.4.Experimental LLE data for TBAB: PEG 200 (1:2) at 50

	DES rich phase			Hydrocarbon rich phase					
% Aro	Oct	DES	Tol	Oct	DES	Tol		B_{tol}	S
			Experimental		LLE	Data	50 °C		
2.5	0.111	0.873	0.016	0.973	0.000	0.027		0.58	5.09
5	0.110	0.861	0.029	0.948	0.000	0.051		0.56	4.86
10	0.102	0.836	0.062	0.898	0.000	0.098		0.63	5.51
15	0.093	0.817	0.091	0.847	0.000	0.145		0.62	5.69
20	0.090	0.792	0.118	0.797	0.000	0.189		0.63	5.57
			NRTL	GA			50°C		
2.5	0.1087	0.8722	0.0161	0.9757	0.0005	0.0269	0.60		5.37
5	0.1066	0.8601	0.0301	0.9517	0.0005	0.0499		0.60	5.39
10	0.1009	0.8350	0.0602	0.8994	0.0006	0.0998		0.60	5.38
15	0.0944	0.8159	0.0892	0.8459	0.0008	0.1468		0.61	5.44
20	0.0900	0.7907	0.1168	0.7973	0.0010	0.1902		0.61	5.44
			UNIQUAC	GA			50 °C		
2.5	0.0973	0.8774	0.0170	0.9673	0.0148	0.0258		0.66	6.55
5	0.0967	0.8647	0.0318	0.9424	0.0153	0.0479		0.66	6.47
10	0.0942	0.8381	0.0638	0.8881	0.0162	0.0955		0.67	6.30
15	0.0905	0.8176	0.0943	0.8330	0.0173	0.1406		0.67	6.17
20	0.0889	0.7909	0.1237	0.7826	0.0183	0.1820		0.68	5.98

Table C.5.Experimental LLE data for TBAB: PEG 600 (1:2) at 30

	DES rich phase			Hydrocarbon rich phase					
% Aro	Oct	DES	Tol	Oct	DES	Tol		B_{tol}	S
			Experimental		LLE	Data	30 °C		
2.5	0.224	0.747	0.029	0.976	0.000	0.024		1.21	5.30
5	0.215	0.721	0.063	0.953	0.000	0.046		1.37	6.06
10	0.204	0.672	0.124	0.908	0.000	0.090		1.38	6.12
15	0.175	0.653	0.172	0.858	0.000	0.138		1.25	6.12
20	0.170	0.604	0.226	0.812	0.000	0.182		1.24	5.93
			NRTL	GA			30°C		
2.5	0.2287	0.7466	0.0320	0.9691	0.0027	0.0210		1.52	6.46
5	0.2169	0.7206	0.0647	0.9489	0.0026	0.0444		1.46	6.38
10	0.1988	0.6717	0.1228	0.9110	0.0024	0.0913		1.35	6.16
15	0.1746	0.6527	0.1745	0.8564	0.0023	0.1357		1.29	6.31
20	0.1627	0.6038	0.2221	0.8173	0.0021	0.1860		1.19	6.00
			UNIQUAC	GA			30 °C		
2.5	0.5225	0.7645	0.0346	0.6000	0.3735	0.0265		1.31	1.50
5	0.5045	0.7283	0.0704	0.5840	0.3605	0.0545		1.29	1.50
10	0.4748	0.6628	0.1352	0.5560	0.3360	0.1070		1.26	1.48
15	0.4370	0.6255	0.1938	0.5165	0.3265	0.1550		1.25	1.48
20	0.4118	0.5656	0.2498	0.4910	0.3020	0.2040		1.22	1.46

Table C.6.Experimental LLE data for TBAB: PEG 600 (1:2) at 40 °C

	DES rich phase			Hydrocarbon rich phase					
% Aro	Oct	DES	Tol	Oct	DES	Tol		B_{tol}	S
			Experimental		LLE	Data	40 °C		
2.5	0.224	0.744	0.032	0.976	0.000	0.023		1.35	5.90
5	0.219	0.719	0.062	0.953	0.000	0.047		1.33	5.81
10	0.213	0.665	0.122	0.908	0.000	0.091		1.34	5.71
15	0.187	0.629	0.184	0.864	0.000	0.133		1.39	6.42
20	0.174	0.586	0.240	0.819	0.000	0.175		1.37	6.45
			NRTL	GA			40°C		
2.5	0.2283	0.7439	0.0318	0.9715	0.0003	0.0232		1.37	5.83
5	0.2204	0.7188	0.0620	0.9514	0.0003	0.0470		1.32	5.69
10	0.2065	0.6646	0.1229	0.9143	0.0005	0.0901		1.36	6.04
15	0.1855	0.6284	0.1860	0.8654	0.0007	0.1310		1.42	6.62
20	0.1735	0.5852	0.2366	0.8194	0.0009	0.1784		1.33	6.26
			UNIQUAC	GA			40 °C		
2.5	0.5244	0.7553	0.0365	0.6000	0.3720	0.0275		1.33	1.52
5	0.5081	0.7175	0.0714	0.5860	0.3595	0.0545		1.31	1.51
10	0.4799	0.6459	0.1360	0.5605	0.3325	0.1065		1.28	1.49
15	0.4446	0.5967	0.1987	0.5255	0.3145	0.1585		1.25	1.48
20	0.4166	0.5440	0.2551	0.4965	0.2930	0.2075		1.23	1.47

Table C.7.Experimental LLE data for TBAB: PEG 600 (1:2) at 50

	DES rich phase			Hydrocarbon rich phase					
% Aro	Oct	DES	Tol	Oct	DES	Tol		B_{tol}	S
			Experimental		LLE	Data	50 °C		
2.5	0.134	0.832	0.034	0.976	0.000	0.024		1.42	10.39
5	0.156	0.774	0.070	0.951	0.000	0.049		1.44	8.82
10	0.175	0.697	0.128	0.905	0.000	0.094		1.37	7.09
15	0.172	0.649	0.179	0.857	0.000	0.139		1.29	6.42
20	0.175	0.596	0.230	0.810	0.000	0.183		1.25	5.81
			NRTL	GA			50°C		
2.5	0.1464	0.8357	0.0321	0.9561	0.0041	0.0259		1.24	8.09
5	0.1568	0.7768	0.0663	0.9429	0.0044	0.0528		1.26	7.55
10	0.1670	0.6982	0.1248	0.9062	0.0052	0.0974		1.28	6.95
15	0.1655	0.6486	0.1801	0.8571	0.0063	0.1383		1.30	6.74
20	0.1673	0.5938	0.2351	0.8117	0.0076	0.1785		1.32	6.39
			UNIQUAC	GA			50 °C		
2.5	0.4781	0.8745	0.0401	0.5550	0.4160	0.0290		1.38	1.61
5	0.4723	0.7979	0.0805	0.5535	0.3870	0.0595		1.35	1.59
10	0.4549	0.6949	0.1458	0.5400	0.3485	0.1110		1.31	1.56
15	0.4297	0.6261	0.2054	0.5145	0.3245	0.1590		1.29	1.55
20	0.4088	0.5579	0.2619	0.4925	0.2980	0.2065		1.27	1.53

Table C.8.Experimental LLE data for TBPB: PEG 200 (1:2) at 30

	DES rich phase			Hydrocarbon rich phase					
% Aro	Oct	DES	Tol	Oct	DES	Tol		B_{tol}	S
			Experimental		LLE	Data	30 °C		
2.5	0.084	0.896	0.02	0.973	0.000	0.027		0.74	8.56
5	0.088	0.885	0.028	0.948	0.000	0.051		0.54	5.85
10	0.069	0.866	0.065	0.897	0.000	0.099		0.66	8.62
15	0.076	0.832	0.092	0.848	0.000	0.144		0.64	7.12
20	0.068	0.807	0.125	0.797	0.000	0.189		0.66	7.74
			NRTL	GA			30°C		
2.5	0.0826	0.8951	0.0168	0.9748	0.0005	0.0302		0.56	6.57
5	0.0823	0.8841	0.0291	0.9541	0.0005	0.0499		0.58	6.76
10	0.0745	0.8651	0.0610	0.8918	0.0005	0.1030		0.59	7.09
15	0.0737	0.8311	0.0917	0.8506	0.0005	0.1444		0.64	7.33
20	0.0682	0.8062	0.1255	0.7971	0.0005	0.1885		0.67	7.78
			UNIQUAC	GA			30 °C		
2.5	0.0736	0.8985	0.0189	0.9702	0.0106	0.0280		0.68	8.90
5	0.0743	0.8869	0.0320	0.9488	0.0110	0.0468		0.68	8.73
10	0.0688	0.8667	0.0659	0.8851	0.0119	0.0976		0.68	8.69
15	0.0711	0.8313	0.0964	0.8416	0.0128	0.1389		0.69	8.22
20	0.0688	0.8049	0.1290	0.7856	0.0138	0.1842		0.70	8.00

Table C.9.Experimental LLE data for TBPB: PEG 200 (1:2) at 40 ºC

	DES rich phase			Hydrocarbon rich phase					
% Aro	Oct	DES	Tol	Oct	DES	Tol		B_{tol}	S
			Experimental		LLE	Data	40 ºC		
2.5	0.102	0.882	0.016	0.975	0.000	0.025		0.64	6.07
5	0.102	0.867	0.032	0.95	0.000	0.049		0.64	5.98
10	0.094	0.839	0.067	0.893	0.000	0.103		0.65	6.23
15	0.086	0.821	0.093	0.854	0.000	0.138		0.67	6.67
20	0.076	0.798	0.127	0.806	0.000	0.181		0.7	7.44
			NRTL	GA			40ºC		
2.5	0.0997	0.8809	0.0153	0.9781	0.0003	0.0257		0.60	5.84
5	0.0982	0.8659	0.0307	0.9546	0.0003	0.0503		0.61	5.93
10	0.0918	0.8379	0.0666	0.8959	0.0003	0.1034		0.64	6.29
15	0.0866	0.8199	0.0921	0.8541	0.0004	0.1389		0.66	6.54
20	0.0800	0.7968	0.1256	0.8027	0.0004	0.1825		0.69	6.91
			UNIQUAC	GA			40 ºC		
2.5	0.0892	0.8848	0.0171	0.9718	0.0130	0.0238		0.72	7.83
5	0.0895	0.8690	0.0339	0.9470	0.0134	0.0469		0.72	7.65
10	0.0865	0.8394	0.0713	0.8861	0.0145	0.0982		0.73	7.44
15	0.0838	0.8203	0.0971	0.8425	0.0153	0.1333		0.73	7.32
20	0.0806	0.7958	0.1298	0.7886	0.0163	0.1773		0.73	7.16

Table C.10.Experimental LLE data for TBPB: PEG 200 (1:2) at 50

	DES rich phase			Hydrocarbon rich phase					
% Aro	Oct	DES	Tol	Oct	DES	Tol		B_{tol}	S
			Experimental		LLE	Data	50 ºC		
2.5	0.110	0.875	0.015	0.975	0.000	0.025		0.63	5.58
5	0.104	0.865	0.032	0.95	0.000	0.049		0.64	5.86
10	0.098	0.832	0.07	0.894	0.000	0.102		0.69	6.27
15	0.112	0.794	0.094	0.854	0.000	0.138		0.68	5.18
20	0.163	0.705	0.132	0.804	0.000	0.182		0.73	3.58
			NRTL	GA			50ºC		
2.5	0.1022	0.8768	0.0158	0.9806	0.0004	0.0242		0.65	6.26
5	0.1034	0.8664	0.0313	0.9484	0.0008	0.0496		0.63	5.79
10	0.1091	0.8316	0.0652	0.8810	0.0025	0.1067		0.61	4.93
15	0.1187	0.7915	0.0911	0.8455	0.0045	0.1408		0.65	4.61
20	0.1492	0.6986	0.1362	0.8161	0.0081	0.1776		0.77	4.19
			UNIQUAC	GA			50 ºC		
2.5	0.1063	0.8787	0.0164	0.9593	0.0159	0.0234		0.70	6.32
5	0.1041	0.8679	0.0333	0.9312	0.0164	0.0474		0.70	6.28
10	0.1018	0.8330	0.0709	0.8727	0.0174	0.1004		0.71	6.05
15	0.1079	0.7935	0.0974	0.8415	0.0180	0.1338		0.73	5.68
20	0.1350	0.7021	0.1386	0.8166	0.0184	0.1745		0.79	4.80

Table C.11. Experimental LLE data for TBPB: PEG 600 (1:2) at 30

	DES rich phase			Hydrocarbon rich phase					
% Aro	Oct	DES	Tol	Oct	DES	Tol		B_{tol}	S
			Experimental		LLE	Data	30 °C		
2.5	0.165	0.798	0.036	0.974	0.000	0.025		1.42	8.39
5	0.159	0.773	0.067	0.952	0.000	0.048		1.4	8.37
10	0.153	0.721	0.126	0.904	0.000	0.094		1.34	7.89
15	0.12	0.689	0.191	0.855	0.000	0.141		1.35	9.62
20	0.104	0.654	0.242	0.807	0.000	0.186		1.30	10.06
			NRTL	GA			30°C		
2.5	0.1712	0.7958	0.0374	0.9700	0.0000	0.0235		1.59	9.02
5	0.1614	0.7709	0.0695	0.9517	0.0000	0.0454		1.53	9.03
10	0.1459	0.7190	0.1282	0.9132	0.0000	0.0917		1.40	8.75
15	0.1209	0.6871	0.1897	0.8561	0.0000	0.1422		1.33	9.45
20	0.1064	0.6522	0.2363	0.8065	0.0000	0.1916		1.23	9.35
			UNIQUAC	GA			30 °C		
2.5	0.4878	0.8463	0.0419	0.5695	0.3990	0.0305		1.37	1.60
5	0.4716	0.8041	0.0780	0.5555	0.3865	0.0575		1.36	1.60
10	0.4434	0.7252	0.1461	0.5285	0.3605	0.1100		1.33	1.58
15	0.4030	0.6689	0.2166	0.4875	0.3445	0.1660		1.30	1.58
20	0.3730	0.6139	0.2750	0.4555	0.3270	0.2140		1.29	1.57

Table C.12.Experimental LLE data for TBPB: PEG 600 (1:2) at 40 °C

	DES rich phase			Hydrocarbon rich phase					
% Aro	Oct	DES	Tol	Oct	DES	Tol		B_{tol}	S
			Experimental		LLE	Data	40 °C		
2.5	0.160	0.801	0.039	0.975	0.000	0.025		1.61	9.8
5	0.172	0.758	0.07	0.953	0.000	0.047		1.5	8.32
10	0.163	0.711	0.126	0.904	0.000	0.094		1.34	7.43
15	0.149	0.659	0.191	0.856	0.000	0.14		1.36	7.83
20	0.127	0.623	0.25	0.811	0.000	0.183		1.37	8.74
			NRTL	GA			40°C		
2.5	0.1703	0.8015	0.0380	0.9641	0.0001	0.0260		1.59	9.02
5	0.1692	0.7585	0.0710	0.9552	0.0001	0.0460		1.53	9.03
10	0.1575	0.7114	0.1251	0.9090	0.0002	0.0949		1.40	8.75
15	0.1431	0.6592	0.1909	0.8614	0.0003	0.1402		1.33	9.45
20	0.1283	0.6230	0.2464	0.8092	0.0004	0.1867		1.23	9.35
			UNIQUAC	GA			40 °C		
2.5	0.4883	0.8529	0.0449	0.5675	0.4005	0.0320		1.37	1.60
5	0.4800	0.7918	0.0808	0.5625	0.3790	0.0585		1.36	1.60
10	0.4496	0.7131	0.1492	0.5335	0.3555	0.1100		1.33	1.58
15	0.4169	0.6355	0.2192	0.5025	0.3295	0.1655		1.30	1.58
20	0.3844	0.5799	0.2822	0.4690	0.3115	0.2165		1.29	1.57

Table C.13.Experimental LLE data for TBPB: PEG 600 (1:2) at 50

	DES rich phase			Hydrocarbon rich phase					
% Aro	Oct	DES	Tol	Oct	DES	Tol		B_{tol}	S
			Experimental		LLE	Data	50 °C		
2.5	0.227	0.737	0.036	0.975	0.000	0.025		1.44	6.19
5	0.222	0.714	0.064	0.951	0.000	0.049		1.3	5.58
10	0.215	0.659	0.126	0.905	0.000	0.093		1.35	5.69
15	0.191	0.623	0.186	0.855	0.000	0.141		1.32	5.9
20	0.18	0.585	0.236	0.806	0.000	0.187		1.26	5.65
			NRTL	GA			50°C		
2.5	0.2268	0.7365	0.0360	0.9754	0.0002	0.0250		1.44	6.19
5	0.2205	0.7135	0.0663	0.9528	0.0003	0.0467		1.42	6.13
10	0.2102	0.6585	0.1253	0.9100	0.0003	0.0937		1.34	5.79
15	0.1930	0.6224	0.1840	0.8532	0.0004	0.1430		1.29	5.69
20	0.1809	0.5843	0.2357	0.8052	0.0005	0.1873		1.26	5.60
			UNIQUAC	GA			50 °C		
2.5	0.5242	0.7514	0.0396	0.6010	0.3685	0.0305		1.30	1.49
5	0.5083	0.7166	0.0727	0.5865	0.3570	0.0565		1.29	1.48
10	0.4797	0.6449	0.1380	0.5600	0.3295	0.1095		1.26	1.47
15	0.4429	0.5920	0.2033	0.5230	0.3115	0.1635		1.24	1.47
20	0.4147	0.5408	0.2602	0.4930	0.2925	0.2115		1.23	1.46

Table C.14.Experimental LLE data for TBAB: DMF (1:2) at 30

	DES rich phase			Hydrocarbon rich phase					
% Aro	Oct	DES	Tol	Oct	DES	Tol		B_{tol}	S
			Experimental		LLE	Data	30 °C		
2.5	0.126	0.857	0.017	0.948	0.031	0.021		0.81	6.10
5	0.129	0.838	0.033	0.924	0.033	0.043		0.77	5.53
10	0.118	0.816	0.066	0.880	0.036	0.083		0.80	5.94
15	0.126	0.778	0.096	0.833	0.039	0.123		0.78	5.20
20	0.113	0.766	0.121	0.786	0.042	0.162		0.75	5.19
			NRTL	GA			30°C		
2.5	0.1247	0.8556	0.0174	0.9483	0.0334	0.0206		0.84	6.42
5	0.1256	0.8373	0.0340	0.9264	0.0347	0.0420		0.81	5.97
10	0.1187	0.8158	0.0668	0.8783	0.0372	0.0822		0.81	6.01
15	0.1221	0.7784	0.0962	0.8360	0.0395	0.1228		0.78	5.36
20	0.1147	0.7665	0.1183	0.7835	0.0424	0.1647		0.72	4.91
			UNIQUAC	GA			30 °C		
2.5	0.1065	0.8673	0.0181	0.9349	0.0527	0.0198		0.91	8.02
5	0.1090	0.8476	0.0363	0.9124	0.0545	0.0396		0.92	7.67
10	0.1049	0.8242	0.0705	0.8633	0.0580	0.0782		0.90	7.42
15	0.1110	0.7842	0.1044	0.8201	0.0612	0.1142		0.91	6.75
20	0.1040	0.7703	0.1336	0.7688	0.0654	0.1488		0.90	6.64

Table C.15. Experimental LLE data for TBAB: DMF (1:2) at 40 °C

	DES rich phase			Hydrocarbon rich phase					
% Aro	Oct	DES	Tol	Oct	DES	Tol		B_{tol}	S
			Experimental		LLE	Data	40 °C		
2.5	0.151	0.832	0.017	0.941	0.037	0.022		0.77	4.76
5	0.154	0.812	0.033	0.918	0.039	0.043		0.77	4.59
10	0.142	0.793	0.065	0.873	0.042	0.084		0.77	4.75
15	0.133	0.772	0.095	0.826	0.046	0.124		0.77	4.77
20	0.123	0.747	0.130	0.786	0.049	0.157		0.83	5.31
			NRTL	GA			40°C		
2.5	0.1490	0.8309	0.0130	0.9423	0.0388	0.0260		0.50	3.16
5	0.1499	0.8120	0.0290	0.9214	0.0396	0.0470		0.62	3.79
10	0.1403	0.7940	0.0640	0.8740	0.0417	0.0850		0.75	4.69
15	0.1329	0.7744	0.0950	0.8254	0.0443	0.1240		0.77	4.76
20	0.1235	0.7497	0.1352	0.7849	0.0469	0.1518		0.89	5.66
			UNIQUAC	GA			40 °C		
2.5	0.1266	0.8443	0.0193	0.9294	0.0599	0.0197		0.98	7.19
5	0.1294	0.8233	0.0375	0.9077	0.0619	0.0384		0.98	6.85
10	0.1238	0.8022	0.0729	0.8582	0.0659	0.0759		0.96	6.66
15	0.1197	0.7794	0.1063	0.8084	0.0705	0.1124		0.95	6.39
20	0.1167	0.7528	0.1389	0.7632	0.0737	0.1477		0.94	6.15

Table C.16. Experimental LLE data for TBAB: DMF (1:2) at 50

	DES rich phase			Hydrocarbon rich phase					
% Aro	Oct	DES	Tol	Oct	DES	Tol		B_{tol}	S
			Experimental		LLE	Data	50 °C		
2.5	0.142	0.841	0.017	0.936	0.042	0.022		0.77	5.10
5	0.158	0.808	0.033	0.910	0.047	0.044		0.76	4.38
10	0.154	0.779	0.067	0.867	0.051	0.083		0.81	4.55
15	0.164	0.737	0.099	0.821	0.055	0.122		0.81	4.07
20	0.152	0.717	0.131	0.776	0.058	0.159		0.82	4.17
			NRTL	GA			50°C		
2.5	0.1458	0.8401	0.0182	0.9324	0.0427	0.0208		0.88	5.60
5	0.1564	0.8094	0.0305	0.9119	0.0454	0.0465		0.66	3.82
10	0.1546	0.7800	0.0642	0.8666	0.0497	0.0858		0.75	4.19
15	0.1611	0.7376	0.0970	0.8241	0.0542	0.1240		0.78	4.00
20	0.1524	0.7153	0.1335	0.7758	0.0595	0.1565		0.85	4.34
			UNIQUAC	GA			50 °C		
2.5	0.1270	0.8521	0.0190	0.9144	0.0674	0.0199		0.95	6.87
5	0.1377	0.8192	0.0378	0.8951	0.0706	0.0392		0.96	6.27
10	0.1376	0.7884	0.0734	0.8503	0.0747	0.0765		0.96	5.93
15	0.1464	0.7441	0.1089	0.8078	0.0788	0.1120		0.97	5.37
20	0.1405	0.7218	0.1421	0.7588	0.0828	0.1477		0.96	5.20

Table C.17. Experimental LLE data for TBAB: DMSO (1:2) at 30

	DES rich phase			Hydrocarbon rich phase					
% Aro	Oct	DES	Tol	Oct	DES	Tol		B_{tol}	S
			Experimental		LLE	Data	30 °C		
2.5	0.225	0.759	0.016	0.953	0.022	0.022		0.77	5.10
5	0.214	0.746	0.040	0.933	0.024	0.044		0.76	4.38
10	0.202	0.721	0.077	0.888	0.026	0.083		0.81	4.55
15	0.197	0.689	0.114	0.843	0.028	0.122		0.81	4.07
20	0.186	0.659	0.155	0.804	0.030	0.159		0.82	4.17
			NRTL	GA			30°C		
2.5	0.2204	0.7578	0.0159	0.9573	0.0235	0.0221		0.72	3.12
5	0.2130	0.7455	0.0392	0.9336	0.0248	0.0448		0.88	3.84
10	0.2033	0.7208	0.0746	0.8864	0.0265	0.0854		0.87	3.81
15	0.1976	0.6890	0.1106	0.8421	0.0283	0.1254		0.88	3.76
20	0.1864	0.6586	0.1576	0.8033	0.0307	0.1564		1.01	4.34
			UNIQUAC	GA			30 °C		
2.5	0.1825	0.7823	0.0220	0.9258	0.0660	0.0165		1.33	6.76
5	0.1761	0.7675	0.0482	0.9027	0.0682	0.0368		1.31	6.71
10	0.1699	0.7384	0.0910	0.8557	0.0712	0.0709		1.28	6.46
15	0.1693	0.7015	0.1334	0.8105	0.0743	0.1052		1.27	6.07
20	0.1651	0.6671	0.1760	0.7683	0.0773	0.1412		1.25	5.80

Table C.18. Experimental LLE data for TBAB: DMSO (1:2) at 40 °C

	DES rich phase			Hydrocarbon rich phase					
% Aro	Oct	DES	Tol	Oct	DES	Tol		B_{tol}	S
				Experimental	LLE	Data	40 °C		
2.5	0.185	0.795	0.020	0.973	0.005	0.022		0.90	4.73
5	0.177	0.783	0.040	0.951	0.005	0.043		0.93	4.99
10	0.173	0.748	0.079	0.910	0.005	0.082		0.96	5.05
15	0.169	0.713	0.118	0.868	0.007	0.120		0.99	5.09
20	0.168	0.682	0.150	0.821	0.009	0.160		0.94	4.60
			NRTL	GA			40°C		
2.5	0.1851	0.7942	0.0195	0.9785	0.0002	0.0225		0.87	4.58
5	0.1802	0.7822	0.0374	0.9533	0.0002	0.0457		0.82	4.33
10	0.1742	0.7472	0.0765	0.9141	0.0005	0.0845		0.91	4.75
15	0.1677	0.7140	0.1176	0.8743	0.0009	0.1204		0.98	5.09
20	0.1656	0.6845	0.1445	0.8281	0.0017	0.1656		0.87	4.36
			UNIQUAC	GA			40 °C		
2.5	0.1417	0.8219	0.0245	0.9391	0.0526	0.0181		1.35	8.97
5	0.1378	0.8072	0.0482	0.9150	0.0537	0.0360		1.34	8.89
10	0.1388	0.7662	0.0930	0.8732	0.0556	0.0702		1.32	8.33
15	0.1396	0.7265	0.1368	0.8305	0.0582	0.1044		1.31	7.80
20	0.1408	0.6905	0.1771	0.7858	0.0614	0.1368		1.29	7.23

Table C.19. Experimental LLE data for TBAB: DMSO (1:2) at 50

	DES rich phase			Hydrocarbon rich phase					
% Aro	Oct	DES	Tol	Oct	DES	Tol		B_{tol}	S
			Experimental		LLE	Data	50 °C		
2.5	0.200	0.779	0.021	0.974	0.005	0.021		1.00	4.87
5	0.209	0.768	0.023	0.937	0.006	0.056		0.41	1.83
10	0.197	0.723	0.080	0.909	0.007	0.081		0.99	4.57
15	0.182	0.700	0.118	0.867	0.008	0.120		0.99	4.70
20	0.170	0.675	0.155	0.824	0.010	0.157		0.99	4.78
			NRTL	GA			50°C		
2.5	0.2002	0.7780	0.0195	0.9792	0.0007	0.0225	0.87		4.24
5	0.2061	0.7677	0.0165	0.9450	0.0011	0.0629		0.26	1.20
10	0.1935	0.7236	0.0782	0.9175	0.0015	0.0828		0.94	4.48
15	0.1838	0.7010	0.1168	0.8699	0.0023	0.1213		0.96	4.56
20	0.1752	0.6770	0.1542	0.8233	0.0034	0.1579		0.98	4.59
			UNIQUAC	GA			50 °C		
2.5	0.1558	0.8055	0.0251	0.9382	0.0552	0.0177		1.42	8.54
5	0.1586	0.7898	0.0468	0.9105	0.0589	0.0336		1.39	8.00
10	0.1592	0.7407	0.0954	0.8737	0.0590	0.0683		1.40	7.67
15	0.1512	0.7130	0.1395	0.8285	0.0616	0.1023		1.36	7.47
20	0.1455	0.6838	0.1812	0.7833	0.0645	0.1355		1.34	7.20

Table C.20. Experimental LLE data for TBPB: DMF (1:2) at 30

	DES rich phase			Hydrocarbon rich phase					
% Aro	Oct	DES	Tol	Oct	DES	Tol		B_{tol}	S
			Experimental		LLE	Data	30 °C		
2.5	0.144	0.840	0.016	0.953	0.026	0.021		0.76	5.05
5	0.139	0.826	0.035	0.936	0.021	0.043		0.81	5.44
10	0.141	0.794	0.065	0.885	0.030	0.083		0.79	4.96
15	0.143	0.759	0.098	0.846	0.030	0.119		0.82	4.86
20	0.136	0.735	0.129	0.800	0.033	0.157		0.82	4.82
			NRTL	GA			30°C		
2.5	0.1403	0.8410	0.0166	0.9568	0.0249	0.0204		0.81	5.55
5	0.1390	0.8227	0.0350	0.9362	0.0242	0.0430		0.81	5.48
10	0.1398	0.7947	0.0659	0.8863	0.0292	0.0821		0.80	5.09
15	0.1423	0.7580	0.0969	0.8468	0.0309	0.1201		0.81	4.80
20	0.1389	0.7335	0.1271	0.7972	0.0344	0.1589		0.80	4.59
			UNIQUAC	GA			30 °C		
2.5	0.1200	0.8550	0.0184	0.9385	0.0490	0.0186		0.99	7.74
5	0.1188	0.8359	0.0389	0.9185	0.0482	0.0391		0.99	7.69
10	0.1209	0.8056	0.0734	0.8698	0.0538	0.0746		0.98	7.08
15	0.1247	0.7670	0.1081	0.8310	0.0555	0.1089		0.99	6.62
20	0.1221	0.7410	0.1419	0.7828	0.0591	0.1440		0.99	6.32

Table C.21. Experimental LLE data for TBPB: DMF (1:2) at 40 °C

	DES rich phase			Hydrocarbon rich phase					
% Aro	Oct	DES	Tol	Oct	DES	Tol		B_{tol}	S
			Experimental		LLE	Data	40 °C		
2.5	0.144	0.839	0.018	0.946	0.034	0.021		0.85	5.61
5	0.145	0.819	0.036	0.923	0.036	0.042		0.87	5.54
10	0.144	0.787	0.070	0.882	0.038	0.080		0.88	5.38
15	0.136	0.762	0.101	0.839	0.041	0.117		0.87	5.33
20	0.138	0.725	0.137	0.800	0.043	0.150		0.91	5.30
			NRTL	GA			40°C		
2.5	0.1449	0.8374	0.0179	0.9453	0.0354	0.0211		0.85	5.53
5	0.1448	0.8183	0.0358	0.9233	0.0366	0.0422		0.85	5.41
10	0.1430	0.7866	0.0694	0.8831	0.0383	0.0806		0.86	5.32
15	0.1372	0.7622	0.1002	0.8379	0.0406	0.1178		0.85	5.19
20	0.1366	0.7253	0.1369	0.8015	0.0426	0.1501		0.91	5.35
			UNIQUAC	GA			40 °C		
2.5	0.1249	0.8499	0.0200	0.9356	0.0522	0.0190		1.05	7.89
5	0.1264	0.8291	0.0400	0.9130	0.0542	0.0381		1.05	7.58
10	0.1280	0.7947	0.0767	0.8710	0.0572	0.0734		1.04	7.11
15	0.1246	0.7678	0.1107	0.8249	0.0610	0.1074		1.03	6.82
20	0.1289	0.7287	0.1462	0.7852	0.0635	0.1410		1.04	6.32

Table C.22. Experimental LLE data for TBPB: DMF (1:2) at 50

	DES rich phase			Hydrocarbon rich phase					
% Aro	Oct	DES	Tol	Oct	DES	Tol		B_{tol}	S
			Experimental		LLE	Data	50 °C		
2.5	0.162	0.820	0.018	0.937	0.044	0.020		0.93	5.39
5	0.161	0.801	0.039	0.920	0.041	0.040		0.97	5.55
10	0.168	0.759	0.073	0.880	0.044	0.077		0.95	4.99
15	0.154	0.742	0.105	0.835	0.046	0.116		0.90	4.91
20	0.160	0.700	0.140	0.796	0.050	0.149		0.94	4.67
			NRTL	GA			50°C		
2.5	0.1625	0.8215	0.0174	0.9358	0.0432	0.0206		0.84	4.86
5	0.1612	0.8002	0.0396	0.9192	0.0424	0.0394		1.01	5.73
10	0.1646	0.7590	0.0739	0.8828	0.0446	0.0761		0.97	5.21
15	0.1560	0.7418	0.1014	0.8324	0.0468	0.1196		0.85	4.52
20	0.1572	0.7004	0.1417	0.7983	0.0502	0.1473		0.96	4.89
			UNIQUAC	GA			50 °C		
2.5	0.1451	0.8317	0.0198	0.9236	0.0622	0.0182		1.09	6.92
5	0.1465	0.8092	0.0413	0.9050	0.0619	0.0378		1.09	6.75
10	0.1532	0.7650	0.0783	0.8671	0.0652	0.0719		1.09	6.16
15	0.1453	0.7453	0.1144	0.8176	0.0691	0.1069		1.07	6.02
20	0.1519	0.7018	0.1497	0.7797	0.0727	0.1397		1.07	5.50

Table C.23. Experimental LLE data for TBPB: DMSO (1:2) at 30

	DES rich phase			Hydrocarbon rich phase					
% Aro	Oct	DES	Tol	Oct	DES	Tol		B_{tol}	S
			Experimental		LLE	Data	30 °C		
2.5	0.097	0.883	0.019	0.979	0.002	0.019		1.03	10.34
5	0.105	0.853	0.041	0.962	0.001	0.036		1.14	10.41
10	0.096	0.827	0.077	0.926	0.002	0.070		1.11	10.65
15	0.090	0.803	0.108	0.883	0.002	0.108		1.00	9.84
20	0.088	0.767	0.145	0.847	0.002	0.140		1.04	10.01
			NRTL	GA			30°C		
2.5	0.0986	0.8828	0.0190	0.9793	0.0003	0.0190		1.00	9.93
5	0.1007	0.8519	0.0384	0.9681	0.0003	0.0386		0.99	9.56
10	0.0959	0.8269	0.0732	0.9279	0.0003	0.0738		0.99	9.60
15	0.0908	0.8029	0.1092	0.8839	0.0004	0.1068		1.02	9.95
20	0.0882	0.7670	0.1434	0.8484	0.0004	0.1416		1.01	9.74
			UNIQUAC	GA			30 °C		
2.5	0.0685	0.9003	0.0223	0.9581	0.0329	0.0160		1.39	19.49
5	0.0738	0.8673	0.0454	0.9448	0.0331	0.0323		1.41	17.99
10	0.0719	0.8387	0.0859	0.9039	0.0350	0.0624		1.38	17.31
15	0.0705	0.8110	0.1253	0.8587	0.0370	0.0925		1.35	16.50
20	0.0721	0.7713	0.1648	0.8213	0.0384	0.1225		1.35	15.32

Table C.24. Experimental LLE data for TBPB: DMSO (1:2) at 40 °C

	DES rich phase			Hydrocarbon rich phase					
% Aro	Oct	DES	Tol	Oct	DES	Tol		B_{tol}	S
			Experimental		LLE	Data	40 °C		
2.5	0.089	0.895	0.016	0.974	0.004	0.022		0.74	8.09
5	0.087	0.880	0.032	0.951	0.005	0.043		0.75	8.13
10	0.091	0.846	0.063	0.908	0.006	0.082		0.76	7.65
15	0.116	0.788	0.096	0.864	0.006	0.122		0.79	5.87
20	0.125	0.749	0.125	0.817	0.010	0.160		0.78	5.11
			NRTL	GA			40°C		
2.5	0.0873	0.8962	0.0156	0.9764	0.0022	0.0224		0.70	7.79
5	0.0893	0.8813	0.0306	0.9493	0.0031	0.0444		0.69	7.33
10	0.0962	0.8461	0.0597	0.9034	0.0053	0.0853		0.70	6.57
15	0.1120	0.7851	0.0948	0.8685	0.0083	0.1232		0.77	5.97
20	0.1209	0.7453	0.1256	0.8216	0.0131	0.1594		0.79	5.35
			UNIQUAC	GA			40 °C		
2.5	0.0683	0.9117	0.0187	0.9462	0.0357	0.0193		0.97	13.42
5	0.0682	0.8955	0.0367	0.9226	0.0369	0.0382		0.96	13.00
10	0.0718	0.8585	0.0714	0.8824	0.0387	0.0735		0.97	11.94
15	0.0865	0.7956	0.1101	0.8513	0.0401	0.1080		1.02	10.03
20	0.0931	0.7551	0.1447	0.8094	0.0432	0.1405		1.03	8.95

Table C.25. Experimental LLE data for TBPB: DMF (1:2) at 50

	DES rich phase			Hydrocarbon rich phase					
% Aro	Oct	DES	Tol	Oct	DES	Tol		B_{tol}	S
			Experimental		LLE	Data	50 °C		
2.5	0.110	0.873	0.017	0.976	0.003	0.021		0.78	6.96
5	0.120	0.848	0.033	0.952	0.004	0.043		0.76	6.03
10	0.115	0.820	0.065	0.912	0.003	0.081		0.80	6.33
15	0.110	0.794	0.096	0.867	0.006	0.119		0.81	6.38
20	0.101	0.774	0.124	0.821	0.006	0.159		0.78	6.36
			NRTL	GA			50°C		
2.5	0.1108	0.8716	0.0164	0.9736	0.0059	0.0216		0.76	6.67
5	0.1142	0.8474	0.0331	0.9563	0.0061	0.0429		0.77	6.46
10	0.1117	0.8183	0.0639	0.9139	0.0061	0.0821		0.78	6.37
15	0.1083	0.7946	0.0943	0.8674	0.0068	0.1207		0.78	6.26
20	0.1024	0.7743	0.1252	0.8183	0.0071	0.1577		0.79	6.34
			UNIQUAC	GA			50 °C		
2.5	0.0813	0.8909	0.0197	0.9520	0.0368	0.0184		1.07	12.54
5	0.0872	0.8641	0.0396	0.9336	0.0379	0.0366		1.08	11.58
10	0.0869	0.8317	0.0759	0.8915	0.0392	0.0705		1.08	11.04
15	0.0861	0.8041	0.1111	0.8450	0.0420	0.1044		1.06	10.44
20	0.0827	0.7803	0.1451	0.7962	0.0442	0.1383		1.05	10.10

Table C.26. Experimental LLE data for TBPMS: PEG200 (1:2) at 30

	DES rich phase			Hydrocarbon rich phase					
% Aro	Oct	DES	Tol	Oct	DES	Tol		B_{tol}	S
			Experimental		LLE	Data	30 °C		
2.5	0.075	0.907	0.018	0.975	0.000	0.025		0.71	9.18
5	0.082	0.886	0.032	0.951	0.000	0.048		0.67	7.82
10	0.084	0.846	0.069	0.895	0.000	0.101		0.69	7.32
15	0.087	0.815	0.098	0.855	0.000	0.138		0.71	6.98
20	0.079	0.792	0.129	0.807	0.000	0.180		0.72	7.35
			NRTL	GA			30°C		
2.5	0.0794	0.9072	0.0152	0.9700	0.0004	0.0278		0.55	6.68
5	0.0815	0.8861	0.0293	0.9509	0.0005	0.0506		0.58	6.76
10	0.0819	0.8457	0.0664	0.8966	0.0009	0.1036		0.64	7.02
15	0.0827	0.8143	0.0963	0.8588	0.0013	0.1397		0.69	7.16
20	0.0787	0.7907	0.1317	0.8068	0.0019	0.1772		0.74	7.62
			UNIQUAC	GA			30 °C		
2.5	0.0747	0.9091	0.0179	0.9630	0.0103	0.0250		0.72	9.23
5	0.0769	0.8875	0.0335	0.9441	0.0106	0.0464		0.72	8.86
10	0.0778	0.8462	0.0716	0.8900	0.0114	0.0981		0.73	8.35
15	0.0795	0.8142	0.1001	0.8519	0.0119	0.1354		0.74	7.92
20	0.0768	0.7900	0.1312	0.7992	0.0127	0.1772		0.74	7.70

Table C.27. Experimental LLE data for TBPMS: PEG200 (1:2) at 40 °C

	DES rich phase			Hydrocarbon rich phase					
% Aro	Oct	DES	Tol	Oct	DES	Tol		B_{tol}	S
			Experimental		LLE	Data	40 °C		
2.5	0.126	0.855	0.018	0.975	0.000	0.025		0.74	5.71
5	0.125	0.841	0.034	0.951	0.000	0.048		0.70	5.35
10	0.124	0.804	0.072	0.896	0.000	0.100		0.72	5.17
15	0.117	0.783	0.099	0.854	0.000	0.138		0.72	5.24
20	0.101	0.770	0.129	0.806	0.000	0.181		0.71	5.66
			NRTL	GA			40°C		
2.5	0.1266	0.8547	0.0165	0.9743	0.0004	0.0265		0.62	4.79
5	0.1245	0.8406	0.0319	0.9513	0.0005	0.0501		0.64	4.87
10	0.1203	0.8034	0.0690	0.8996	0.0007	0.1030		0.67	5.01
15	0.1144	0.7822	0.0975	0.8565	0.0009	0.1395		0.70	5.23
20	0.1043	0.7689	0.1313	0.8026	0.0012	0.1787		0.73	5.65
			UNIQUAC	GA			40 °C		
2.5	0.1153	0.8580	0.0188	0.9674	0.0150	0.0241		0.78	6.55
5	0.1150	0.8432	0.0359	0.9433	0.0155	0.0459		0.78	6.42
10	0.1149	0.8043	0.0756	0.8885	0.0165	0.0960		0.79	6.09
15	0.1117	0.7820	0.1041	0.8436	0.0174	0.1323		0.79	5.94
20	0.1044	0.7674	0.1353	0.7880	0.0186	0.1739		0.78	5.87

Table C.28. Experimental LLE data for TBPMS: PEG200 (1:2) at 50

	DES rich phase			Hydrocarbon rich phase					
% Aro	Oct	DES	Tol	Oct	DES	Tol		B_{tol}	S
			Experimental		LLE	Data	50 °C		
2.5	0.131	0.851	0.018	0.975	0.000	0.025		0.70	5.24
5	0.121	0.845	0.033	0.951	0.000	0.048		0.70	5.45
10	0.109	0.821	0.070	0.895	0.000	0.101		0.69	5.66
15	0.114	0.791	0.095	0.852	0.000	0.140		0.68	5.09
20	0.110	0.761	0.129	0.805	0.000	0.182		0.71	5.17
			NRTL	GA			50°C		
2.5	0.1271	0.8508	0.0164	0.9787	0.0004	0.0266		0.62	4.75
5	0.1219	0.8447	0.0311	0.9499	0.0005	0.0499		0.62	4.86
10	0.1138	0.8205	0.0672	0.8900	0.0008	0.1037		0.65	5.07
15	0.1120	0.7902	0.0951	0.8538	0.0010	0.1399		0.68	5.18
20	0.1071	0.7599	0.1288	0.8077	0.0014	0.1822		0.71	5.33
			UNIQUAC	GA			50 °C		
2.5	0.1176	0.8535	0.0183	0.9713	0.0144	0.0246		0.74	6.14
5	0.1130	0.8468	0.0343	0.9423	0.0150	0.0464		0.74	6.16
10	0.1080	0.8210	0.0726	0.8805	0.0162	0.0979		0.74	6.05
15	0.1097	0.7895	0.1010	0.8415	0.0170	0.1333		0.76	5.81
20	0.1085	0.7579	0.1347	0.7927	0.0180	0.1755		0.77	5.61

Table C.29. Experimental LLE data for TBPMS: PEG600 (1:2) at 30

	DES rich phase			Hydrocarbon rich phase					
% Aro	Oct	DES	Tol	Oct	DES	Tol		B_{tol}	S
			Experimental		LLE	Data	30 °C		
2.5	0.159	0.805	0.037	0.976	0.000	0.024		1.52	9.33
5	0.160	0.774	0.066	0.953	0.000	0.046		1.43	8.52
10	0.147	0.719	0.135	0.899	0.000	0.099		1.36	8.35
15	0.143	0.676	0.181	0.859	0.000	0.137		1.32	7.89
20	0.136	0.629	0.235	0.814	0.000	0.180		1.30	7.77
			NRTL	GA			30°C		
2.5	0.1616	0.8049	0.0354	0.9734	0.0001	0.0256		1.38	8.33
5	0.1587	0.7739	0.0650	0.9543	0.0001	0.0470		1.38	8.32
10	0.1466	0.7187	0.1352	0.8994	0.0003	0.0988		1.37	8.40
15	0.1412	0.6755	0.1808	0.8608	0.0005	0.1372		1.32	8.03
20	0.1347	0.6282	0.2342	0.8153	0.0008	0.1808		1.30	7.84
			UNIQUAC	GA			30 °C		
2.5	0.4874	0.8774	0.0441	0.5675	0.4025	0.0305		1.45	1.68
5	0.4740	0.8262	0.0798	0.5565	0.3870	0.0560		1.43	1.67
10	0.4379	0.7313	0.1625	0.5230	0.3595	0.1170		1.39	1.66
15	0.4147	0.6639	0.2166	0.5010	0.3380	0.1590		1.36	1.65
20	0.3885	0.5948	0.2766	0.4750	0.3145	0.2075		1.33	1.63

Table C.30. Experimental LLE data for TBPMS: PEG600 (1:2) at 40 °C

	DES rich phase			Hydrocarbon rich phase					
% Aro	Oct	DES	Tol	Oct	DES	Tol		B_{tol}	S
			Experimental		LLE	Data	40 °C		
2.5	0.149	0.816	0.035	0.975	0.000	0.024		1.45	9.51
5	0.152	0.783	0.065	0.953	0.000	0.047		1.39	8.71
10	0.153	0.708	0.138	0.901	0.000	0.098		1.42	8.31
15	0.158	0.658	0.184	0.860	0.000	0.136		1.35	7.34
20	0.174	0.595	0.231	0.814	0.000	0.180		1.28	6.01
			NRTL	GA			40°C		
2.5	0.1468	0.8168	0.0325	0.9764	0.0000	0.0265		1.23	8.16
5	0.1503	0.7837	0.0623	0.9539	0.0001	0.0497		1.25	7.96
10	0.1563	0.7080	0.1337	0.8970	0.0007	0.1024		1.31	7.49
15	0.1609	0.6570	0.1833	0.8564	0.0017	0.1368		1.34	7.13
20	0.1714	0.5920	0.2386	0.8160	0.0036	0.1725		1.38	6.59
			UNIQUAC	GA			40 °C		
2.5	0.4845	0.8576	0.0421	0.5620	0.4080	0.0295		1.43	1.66
5	0.4719	0.8069	0.0784	0.5525	0.3915	0.0560		1.40	1.64
10	0.4415	0.7022	0.1586	0.5270	0.3540	0.1180		1.34	1.60
15	0.4236	0.6376	0.2100	0.5090	0.3290	0.1600		1.31	1.58
20	0.4087	0.5612	0.2614	0.4940	0.2975	0.2055		1.27	1.54

Table C.31.Experimental LLE data for TBPMS: PEG600 (1:2) at 50

	DES rich phase			Hydrocarbon rich phase					
% Aro	Oct	DES	Tol	Oct	DES	Tol		B_{tol}	S
			Experimental		LLE	Data	50 °C		
2.5	0.214	0.751	0.036	0.976	0.000	0.024		1.48	6.73
5	0.236	0.700	0.064	0.953	0.000	0.047		1.37	5.55
10	0.176	0.675	0.149	0.905	0.000	0.094		1.59	8.15
15	0.193	0.624	0.183	0.861	0.000	0.135		1.35	6.03
20	0.198	0.571	0.231	0.814	0.000	0.180		1.28	5.27
			NRTL	GA			50°C		
2.5	0.2153	0.7521	0.0347	0.9674	0.0061	0.0254		1.37	6.14
5	0.2239	0.7004	0.0634	0.9581	0.0063	0.0478		1.33	5.68
10	0.1813	0.6739	0.1637	0.8929	0.0075	0.0801		2.04	10.07
15	0.1903	0.6221	0.1860	0.8573	0.0078	0.1325		1.40	6.32
20	0.1915	0.5681	0.2284	0.8145	0.0083	0.1830		1.25	5.31
			UNIQUAC	GA			50 °C		
2.5	0.5199	0.7980	0.0423	0.5950	0.3755	0.0300		1.41	1.61
5	0.5149	0.7286	0.0765	0.5945	0.3500	0.0555		1.38	1.59
10	0.4581	0.6764	0.1642	0.5405	0.3375	0.1215		1.35	1.59
15	0.4443	0.6048	0.2109	0.5270	0.3120	0.1590		1.33	1.57
20	0.4230	0.5339	0.2662	0.5060	0.2855	0.2055		1.30	1.55

Appendix VI: Multistage extraction

Table D1: multistage extraction for ammonium based DESs. Showing the reduction in toluene concentration with the corresponding number of equilibrium extraction stages.

No.of ext. stages	TBAB:PEG600	TBAB:PEG200	TBAB:DMF	TBAB:DMSO
initial	10.10427	10.08608	10.18732	10.36348
1	7.67219	8.11718	7.22148	7.85857
2	5.74816	6.33929	4.62605	5.20064
3	4.41223	5.10867	3.36166	3.45705
4	3.13013	3.77354	1.9989	2.23914
5	2.30118	2.83042	1.26178	2.1648
6	1.58318	2.04373	0.75108	0.93436
7	1.18466	1.59351	0.47041	0.79432
8	0.64357	0.97324	0.26434	0.3874

Table D2: multistage extraction for phosphonium based DESs. Showing the reduction in toluene concentration with the corresponding number of equilibrium extraction stages.

No.of ext. stages	TBPMS:PEG600	TBPMS:PEG200	TBPB:PEG600	TBPB:PEG200	TBPB:DMF	TBPB:DMSO
0	10.14227	10.37951	10.21751	10.19723	10.2732	10.21658
1	7.66282	8.01912	7.87929	8.2163	7.02272	7.33971
2	5.58126	5.93407	5.63667	6.27289	4.49152	5.00092
3	4.28836	4.71066	4.39289	5.01488	3.2135	3.52738
4	2.95461	3.34687	3.00742	3.62313	1.83912	2.26353
5	2.14957	2.44112	2.12937	2.70343	1.14507	1.4624
6	1.36694	1.63671	1.46726	1.8814	0.69501	0.8829
7	1.00012	1.24581	1.07295	1.47104	0.45001	0.6048
8	0.62543	0.75421	0.6326	1.0231	0.2075	0.31752

Table D3. Multistage DESs extraction efficiency (%) for the ammonium based DESs with the corresponding number of equilibrium extraction stages

No.of ext. stages	TBAB:PEG600	TBAB:PEG200	TBAB:DMF	TBAB:DMSO
1	24.06982	19.52096	29.11305	24.17055
2	43.11158	37.14813	54.59012	49.81763
3	56.33302	49.3493	67.00153	66.642
4	69.02171	62.58665	80.37855	78.39394
5	77.22567	71.93736	87.61421	79.11126
6	84.33157	79.73712	92.62731	90.98411
7	88.27565	84.2009	95.3824	92.33539
8	93.63071	90.35066	97.40521	96.26187

Table D4. Multistage DESs extraction efficiency (%) for the phosphonium based DESs with the corresponding number of equilibrium extraction stages

No.of ext. stages	TBPMS:PEG600	TBPMS:PEG200	TBPB:PEG600	TBPB:PEG200	TBPB:DMF	TBPB:DMSO
1	24.4467	22.74086	22.88444	19.42616	31.64038	28.15884
2	44.97031	42.829	44.83323	38.48437	56.27925	51.05094
3	57.71795	54.61578	57.00626	50.82115	68.71958	65.47396
4	70.86836	67.75503	70.56602	64.46947	82.09789	77.84454
5	78.80583	76.48136	79.1596	73.48858	88.85381	85.68601
6	86.52235	84.23134	85.63975	81.54989	93.23473	91.35816
7	90.13909	87.99741	89.49891	85.57412	95.61957	94.08021
8	93.83343	92.73366	93.80867	89.96688	97.98018	96.89211

Table D5: multistage extraction for synthesized naphtha feed with TBAB: PEG600 based DESs.

No.of ext. stages	Benzene	Toluene	p-Xylene
1	1.89793	2.41756	2.08335
2	1.25354	1.84857	1.82616
3	0.815208	1.41117	1.61801
4	0.552459	1.11436	1.44568
5	0.324068	0.848848	1.33247
6	0.221956	0.664024	1.14833
7	0.1568	0.53685	1.0567
8	0.10456	0.429937	0.99358
9	0.10064	0.30853	0.662263
10	0.044517	0.267245	0.462393

Table D6: multistage extraction for synthesized naphtha feed with TBPB: PEG600 based DESs.

No.of ext. stages	Benzene	Toluene	p-Xylene
1	1.89455	2.4226	2.08677
2	1.23715	1.83732	1.80572
3	0.790413	1.38943	1.61062
4	0.536019	1.09511	1.51142
5	0.363184	0.836534	1.29657
6	0.292754	0.648505	1.10155
7	0.168189	0.511647	0.99901
8	0.114228	0.444031	0.901968
9	0.09754	0.291462	0.755788
10	0.052541	0.255118	0.643296

Table D7: multistage extraction for synthesized naphtha feed with TBPMS: PEG600 based DESs.

No.of ext. stages	Benzene	Toluene	p-Xylene
1	1.88643	2.39732	2.09837
2	1.24109	1.83265	1.80749
3	0.808655	1.39863	1.6148
4	0.561395	1.11409	1.48461
5	0.376617	0.853859	1.30249
6	0.247555	0.649794	1.10895
7	0.175091	0.527788	1.02858
8	0.122821	0.427717	0.924233
9	0.10743	0.29369	0.800457
10	0.057362	0.263943	0.63191

Table D8. Multistage DESs equilibrium extraction efficiency (%) for synthesized naphtha feed with TBAB: PEG600 based DESs.

No.of ext.	Extraction efficiency(%)		
stages	Benzene	Toluene	p-Xylene
1	33.09704	22.79447	8.942503
2	55.8121	40.96534	20.18357
3	71.26352	54.93385	29.28123
4	80.52555	64.41257	36.8133
5	88.57644	72.89177	41.7614
6	92.17595	78.79419	49.80965
7	94.47272	82.85553	53.81455
8	96.31421	86.26983	56.57335
9	96.45239	90.147	71.05431
10	98.43076	91.46545	79.79007

Table D9. Multistage DESs equilibrium extraction efficiency (%) for synthesized naphtha feed with TBPB: PEG600 based DESs.

No.of ext. stages	Extraction efficiency(%)		
	Benzene	Toluene	p-Xylene
1	33.21618	22.63351	8.793024
2	56.38986	41.32461	21.07695
3	72.13755	55.62812	29.60423
4	81.10507	65.02732	33.93999
5	87.19759	73.28503	43.33049
6	89.68028	79.28979	51.85428
7	94.07126	83.66039	56.33602
8	95.97341	85.81973	60.57746
9	96.56167	90.69207	66.96659
10	98.14789	91.85273	71.8833

Table D10. Multistage DESs equilibrium extraction efficiency (%) for synthesized naphtha feed with TBPMS: PEG600 based DESs.

No.of ext. stages	Extraction efficiency(%).		
	Benzene	Toluene	p-Xylene
1	33.50242	23.44084	8.28602
2	56.25097	41.47375	20.99958
3	71.49452	55.33431	29.42153
4	80.21055	64.42119	35.11178
5	86.72407	72.73175	43.07175
6	91.27356	79.24863	51.53085
7	93.82796	83.14493	55.0436
8	95.6705	86.34072	59.60432
9	96.21304	90.62092	65.01423
10	97.97795	91.5709	72.38095

Table D11. Extractive performance in terms of toluene concentration for the regenerated ammonium based DESs

DES	%toluene comp	initial	1st	2nd	3rd
TBAB:PEG600	10.34802	7.50432	7.58508	7.539177	7.62738
TBAB:PEG200	10.34802	7.94067	8.089615	8.09282	8.19709
TBAB:DMSO	10.34802	6.91446	7.61233	7.68339	7.67363
TBAB:DMF	10.34802	6.83885	7.37583	nd	nd

Table D12 Extractive performance in terms of toluene removal efficiency for the regenerated ammonium based DESs

DES	1st	2nd	3rd
TBAB:PEG600	26.70018	27.14377	26.29141
TBAB:PEG200	21.82451	21.79354	20.78591
TBAB:DMSO	26.43684	25.75014	25.84446
TBAB:DMF	28.72231	nd	nd

Table D13. Extractive performance in terms of toluene concentration for the regenerated phosphonium based DESs

DES	%toluene comp	initial	1st	2nd	3rd
TBPMS:PEG600	10.34802	7.5438	7.68081	7.650192	7.69141
TBPMS:PEG200	10.34802	8.40432	8.42381	8.42043	8.50889
TBPB:PEG600	10.34802	7.72964	7.73678	7.73804	7.82843
TBPB:PEG200	10.34802	7.96024	8.26103	8.23556	8.3598
TBPB:DMSO	10.34802	7.01197	7.08461	7.07842	7.05242
TBPB:DMF	10.34802	6.846	7.41516	nd	nd

Table D14. Extractive performance in terms of toluene removal efficiency for the regenerated phosphonium based DESs

DES	1st	2nd	3rd
TBPMS:PEG600	25.77508	26.07096	25.67264
TBPMS:PEG200	18.59496	18.62762	17.77277
TBPB:PEG600	25.2342	25.22202	24.34852
TBPB:PEG200	20.16801	20.41415	19.21353
TBPB:DMSO	31.53656	31.59638	31.84764
TBPB:DMF	28.34223	nd	nd

Appendix V : MatLab Codes

ThermoModelling.m file

```
function varargout = ThermoModelling(varargin)
% THERMOMODELLING M-file for ThermoModelling.fig
%      THERMOMODELLING, by itself, creates a new THERMOMODELLING or raises
the existing
%      singleton*.
%
%      H = THERMOMODELLING returns the handle to a new THERMOMODELLING or
the handle to
%      the existing singleton*.
%
%     THERMOMODELLING('CALLBACK',hObject,eventData,handles,...) calls the
local
%      function named CALLBACK in THERMOMODELLING.M with the given input
arguments.
%
%               THERMOMODELLING('Property','Value',...)  creates  a  new
THERMOMODELLING or raises the
%      existing singleton*.  Starting from the left, property value pairs
are
%      applied to the GUI before ThermoModelling_OpeningFcn gets called.
An
%          unrecognized  property  name  or  invalid  value  makes  property
application
%        stop.  All inputs are passed to ThermoModelling_OpeningFcn via
varargin.
%
%       *See GUI Options on GUIDE's Tools menu.  Choose "GUI allows only
one
%      instance to run (singleton)".
%
% See also: GUIDE, GUIDATA, GUIHANDLES
% Edit the above text to modify the response to help ThermoModelling
% Last Modified by GUIDE v2.5 17-Dec-2018 21:58:51
% Begin initialization code - DO NOT EDIT

gui_Singleton = 1;
gui_State = struct('gui_Name',       mfilename, ...
                   'gui_Singleton',  gui_Singleton, ...
                   'gui_OpeningFcn', @ThermoModelling_OpeningFcn, ...
                   'gui_OutputFcn',  @ThermoModelling_OutputFcn, ...
                   'gui_LayoutFcn',  [] , ...
                   'gui_Callback',   []);
if nargin && ischar(varargin{1})
    gui_State.gui_Callback = str2func(varargin{1});
end

if nargout
    [varargout{1:nargout}] = gui_mainfcn(gui_State, varargin{:});
```

```
else
    gui_mainfcn(gui_State, varargin{:});
end
% End initialization code - DO NOT EDIT

% --- Executes just before ThermoModelling is made visible.
function ThermoModelling_OpeningFcn(hObject, eventdata, handles, varargin)
% This function has no output args, see OutputFcn.
% hObject    handle to figure
% eventdata  reserved - to be defined in a future version of MATLAB
% handles    structure with handles and user data (see GUIDATA)
% varargin   command line arguments to ThermoModelling (see VARARGIN)

% Choose default command line output for ThermoModelling
handles.output = hObject;

% Update handles structure
guidata(hObject, handles);

% UIWAIT makes ThermoModelling wait for user response (see UIRESUME)
% uiwait(handles.figure1);

 % --- Outputs from this function are returned to the command line.
function   varargout   =   ThermoModelling_OutputFcn(hObject,   eventdata,
handles)
% varargout  cell array for returning output args (see VARARGOUT);
% hObject    handle to figure
% eventdata  reserved - to be defined in a future version of MATLAB
% handles    structure with handles and user data (see GUIDATA)

% Get default command line output from handles structure
varargout{1} = handles.output;

 % --- Executes on button press in pushbutton1.
function pushbutton1_Callback(hObject, eventdata, handles)
% hObject    handle to pushbutton1 (see GCBO)
% eventdata  reserved - to be defined in a future version of MATLAB
% handles    structure with handles and user data (see GUIDATA)
Main

par1=sprintf('%.3f', par1);
par2=sprintf(txtFormat, par2);
par3=sprintf(txtFormat, par3);
r2=sprintf('%.3f', r2);
sse=sprintf('%.3f', SSE);
rmse=sprintf('%.3f', RMSE);
rmsd=sprintf('%.3f', RMSD);
par1_ex=sprintf('%s', par1_ex);
par2_ex=sprintf('%s', par2_ex);
par3_ex=sprintf('%s', par3_ex);
model_ex = sprintf('%s', model_ex);

set(handles.par1, 'String', par1);
```

```
set(handles.par2, 'String', par2);
set(handles.par3, 'String', par3);
set(handles.R2, 'String', r2);
set(handles.sse, 'String', sse);
set(handles.rmse, 'String', rmse);
set(handles.rmsd, 'String', rmsd);
set(handles.par1_ex, 'String', par1_ex);
set(handles.par2_ex, 'String', par2_ex);
set(handles.par3_ex, 'String', par3_ex);
set(handles.R2_ex, 'String',['R^2'] );
set(handles.sse_ex, 'String', 'SSE');
set(handles.rmse_ex, 'String', 'RMSE');
set(handles.rmsd_ex, 'String', 'RMSD');
set(handles.model_eqn, 'String', model_ex);


% --- Executes on selection change in dataMenu.
function dataMenu_Callback(hObject, eventdata, handles)
% hObject    handle to dataMenu (see GCBO)
% eventdata  reserved - to be defined in a future version of MATLAB
% handles    structure with handles and user data (see GUIDATA)

% Hints: contents = get(hObject,'String') returns dataMenu contents as
cell array
%       contents{get(hObject,'Value')} returns selected item from dataMenu
% --- Executes during object creation, after setting all properties.
function dataMenu_CreateFcn(hObject, eventdata, handles)
% hObject    handle to dataMenu (see GCBO)
% eventdata  reserved - to be defined in a future version of MATLAB
% handles    empty - handles not created until after all CreateFcns called

% Hint: popupmenu controls usually have a white background on Windows.
%       See ISPC and COMPUTER.
if         ispc         &&         isequal(get(hObject,'BackgroundColor'),
get(0,'defaultUicontrolBackgroundColor'))
    set(hObject,'BackgroundColor','white');
end


 % --- Executes on selection change in modelMenu.
function modelMenu_Callback(hObject, eventdata, handles)
% hObject    handle to modelMenu (see GCBO)
% eventdata  reserved - to be defined in a future version of MATLAB
% handles    structure with handles and user data (see GUIDATA)

% Hints: contents = get(hObject,'String') returns modelMenu contents as
cell array
%      contents{get(hObject,'Value')} returns selected item from modelMenu

% --- Executes during object creation, after setting all properties.
function modelMenu_CreateFcn(hObject, eventdata, handles)
% hObject    handle to modelMenu (see GCBO)
% eventdata  reserved - to be defined in a future version of MATLAB
% handles    empty - handles not created until after all CreateFcns called
```

```
% Hint: popupmenu controls usually have a white background on Windows.
%       See ISPC and COMPUTER.
if         ispc         &&         isequal(get(hObject,'BackgroundColor'),
get(0,'defaultUicontrolBackgroundColor'))
    set(hObject,'BackgroundColor','white');
end

function table_Callback(hObject, eventdata, handles)
% hObject    handle to table (see GCBO)
% eventdata  reserved - to be defined in a future version of MATLAB
% handles    structure with handles and user data (see GUIDATA)

% Hints: get(hObject,'String') returns contents of table as text
%        str2double(get(hObject,'String')) returns contents of table as a
double



% --- Executes during object creation, after setting all properties.
function table_CreateFcn(hObject, eventdata, handles)
% hObject    handle to table (see GCBO)
% eventdata  reserved - to be defined in a future version of MATLAB
% handles    empty - handles not created until after all CreateFcns called

% Hint: edit controls usually have a white background on Windows.
%       See ISPC and COMPUTER.
if         ispc         &&         isequal(get(hObject,'BackgroundColor'),
get(0,'defaultUicontrolBackgroundColor'))
    set(hObject,'BackgroundColor','white');
end

function n_Callback(hObject, eventdata, handles)
% hObject    handle to n (see GCBO)
% eventdata  reserved - to be defined in a future version of MATLAB
% handles    structure with handles and user data (see GUIDATA)

% Hints: get(hObject,'String') returns contents of n as text
%          str2double(get(hObject,'String')) returns contents of n as a
double

% --- Executes during object creation, after setting all properties.
function n_CreateFcn(hObject, eventdata, handles)
% hObject    handle to n (see GCBO)
% eventdata  reserved - to be defined in a future version of MATLAB
% handles    empty - handles not created until after all CreateFcns called

% Hint: edit controls usually have a white background on Windows.
%       See ISPC and COMPUTER.
if         ispc         &&         isequal(get(hObject,'BackgroundColor'),
get(0,'defaultUicontrolBackgroundColor'))
    set(hObject,'BackgroundColor','white');
end
```

```
function k_Callback(hObject, eventdata, handles)
% hObject    handle to k (see GCBO)
% eventdata  reserved - to be defined in a future version of MATLAB
% handles    structure with handles and user data (see GUIDATA)

% Hints: get(hObject,'String') returns contents of k as text
%          str2double(get(hObject,'String')) returns contents of k as a
double


% --- Executes during object creation, after setting all properties.
function k_CreateFcn(hObject, eventdata, handles)
% hObject    handle to k (see GCBO)
% eventdata  reserved - to be defined in a future version of MATLAB
% handles    empty - handles not created until after all CreateFcns called

% Hint: edit controls usually have a white background on Windows.
%       See ISPC and COMPUTER.
if         ispc         &&         isequal(get(hObject,'BackgroundColor'),
get(0,'defaultUicontrolBackgroundColor'))
    set(hObject,'BackgroundColor','white');
end

function R2_Callback(hObject, eventdata, handles)
% hObject    handle to R2 (see GCBO)
% eventdata  reserved - to be defined in a future version of MATLAB
% handles    structure with handles and user data (see GUIDATA)

% Hints: get(hObject,'String') returns contents of R2 as text
%          str2double(get(hObject,'String')) returns contents of R2 as a
double


% --- Executes during object creation, after setting all properties.
function R2_CreateFcn(hObject, eventdata, handles)
% hObject    handle to R2 (see GCBO)
% eventdata  reserved - to be defined in a future version of MATLAB
% handles    empty - handles not created until after all CreateFcns called

% Hint: edit controls usually have a white background on Windows.
%       See ISPC and COMPUTER.
if         ispc         &&         isequal(get(hObject,'BackgroundColor'),
get(0,'defaultUicontrolBackgroundColor'))
    set(hObject,'BackgroundColor','white');
end


function tau_y_Callback(hObject, eventdata, handles)
```

```
% hObject    handle to tau_y (see GCBO)
% eventdata  reserved - to be defined in a future version of MATLAB
% handles    structure with handles and user data (see GUIDATA)

% Hints: get(hObject,'String') returns contents of tau_y as text
%        str2double(get(hObject,'String')) returns contents of tau_y as a
double


% --- Executes during object creation, after setting all properties.
function tau_y_CreateFcn(hObject, eventdata, handles)
% hObject    handle to tau_y (see GCBO)
% eventdata  reserved - to be defined in a future version of MATLAB
% handles    empty - handles not created until after all CreateFcns called

% Hint: edit controls usually have a white background on Windows.
%       See ISPC and COMPUTER.
if         ispc         &&         isequal(get(hObject,'BackgroundColor'),
get(0,'defaultUicontrolBackgroundColor'))
    set(hObject,'BackgroundColor','white');
end


% --- Executes on selection change in optimMenu.
function optimMenu_Callback(hObject, eventdata, handles)
% hObject    handle to optimMenu (see GCBO)
% eventdata  reserved - to be defined in a future version of MATLAB
% handles    structure with handles and user data (see GUIDATA)

% Hints: contents = get(hObject,'String') returns optimMenu contents as
cell array
%      contents{get(hObject,'Value')} returns selected item from optimMenu


% --- Executes during object creation, after setting all properties.
function optimMenu_CreateFcn(hObject, eventdata, handles)
% hObject    handle to optimMenu (see GCBO)
% eventdata  reserved - to be defined in a future version of MATLAB
% handles    empty - handles not created until after all CreateFcns called

% Hint: popupmenu controls usually have a white background on Windows.
%       See ISPC and COMPUTER.
if         ispc         &&         isequal(get(hObject,'BackgroundColor'),
get(0,'defaultUicontrolBackgroundColor'))
    set(hObject,'BackgroundColor','white');
end

function par2_Callback(hObject, eventdata, handles)
% hObject    handle to par2 (see GCBO)
% eventdata  reserved - to be defined in a future version of MATLAB
% handles    structure with handles and user data (see GUIDATA)

% Hints: get(hObject,'String') returns contents of par2 as text
```

```
%        str2double(get(hObject,'String')) returns contents of par2 as a
double

% --- Executes during object creation, after setting all properties.
function par2_CreateFcn(hObject, eventdata, handles)
% hObject    handle to par2 (see GCBO)
% eventdata  reserved - to be defined in a future version of MATLAB
% handles    empty - handles not created until after all CreateFcns called

% Hint: edit controls usually have a white background on Windows.
%       See ISPC and COMPUTER.
if         ispc         &&         isequal(get(hObject,'BackgroundColor'),
get(0,'defaultUicontrolBackgroundColor'))
    set(hObject,'BackgroundColor','white');
end



function par3_Callback(hObject, eventdata, handles)
% hObject    handle to par3 (see GCBO)
% eventdata  reserved - to be defined in a future version of MATLAB
% handles    structure with handles and user data (see GUIDATA)

% Hints: get(hObject,'String') returns contents of par3 as text
%        str2double(get(hObject,'String')) returns contents of par3 as a
double

% --- Executes during object creation, after setting all properties.
function par3_CreateFcn(hObject, eventdata, handles)
% hObject    handle to par3 (see GCBO)
% eventdata  reserved - to be defined in a future version of MATLAB
% handles    empty - handles not created until after all CreateFcns called

% Hint: edit controls usually have a white background on Windows.
%       See ISPC and COMPUTER.
if         ispc         &&         isequal(get(hObject,'BackgroundColor'),
get(0,'defaultUicontrolBackgroundColor'))
    set(hObject,'BackgroundColor','white');
end

function edit20_Callback(hObject, eventdata, handles)
% hObject    handle to R2 (see GCBO)
% eventdata  reserved - to be defined in a future version of MATLAB
% handles    structure with handles and user data (see GUIDATA)

% Hints: get(hObject,'String') returns contents of R2 as text
%          str2double(get(hObject,'String')) returns contents of R2 as a
double

% --- Executes during object creation, after setting all properties.
function edit20_CreateFcn(hObject, eventdata, handles)
% hObject    handle to R2 (see GCBO)
% eventdata  reserved - to be defined in a future version of MATLAB
% handles    empty - handles not created until after all CreateFcns called
```

```
% Hint: edit controls usually have a white background on Windows.
%       See ISPC and COMPUTER.
if         ispc         &&         isequal(get(hObject,'BackgroundColor'),
get(0,'defaultUicontrolBackgroundColor'))
    set(hObject,'BackgroundColor','white');
end

 function par1_Callback(hObject, eventdata, handles)
% hObject    handle to par1 (see GCBO)
% eventdata  reserved - to be defined in a future version of MATLAB
% handles    structure with handles and user data (see GUIDATA)

% Hints: get(hObject,'String') returns contents of par1 as text
%        str2double(get(hObject,'String')) returns contents of par1 as a
double

% --- Executes during object creation, after setting all properties.
function par1_CreateFcn(hObject, eventdata, handles)
% hObject    handle to par1 (see GCBO)
% eventdata  reserved - to be defined in a future version of MATLAB
% handles    empty - handles not created until after all CreateFcns called

% Hint: edit controls usually have a white background on Windows.
%       See ISPC and COMPUTER.
if         ispc         &&         isequal(get(hObject,'BackgroundColor'),
get(0,'defaultUicontrolBackgroundColor'))
    set(hObject,'BackgroundColor','white');
end

 function model_eqn_Callback(hObject, eventdata, handles)
% hObject    handle to model_eqn (see GCBO)
% eventdata  reserved - to be defined in a future version of MATLAB
% handles    structure with handles and user data (see GUIDATA)

% Hints: get(hObject,'String') returns contents of model_eqn as text
%        str2double(get(hObject,'String')) returns contents of model_eqn
as a double

% --- Executes during object creation, after setting all properties.
function model_eqn_CreateFcn(hObject, eventdata, handles)
% hObject    handle to model_eqn (see GCBO)
% eventdata  reserved - to be defined in a future version of MATLAB
% handles    empty - handles not created until after all CreateFcns called

% Hint: edit controls usually have a white background on Windows.
%       See ISPC and COMPUTER.
if         ispc         &&         isequal(get(hObject,'BackgroundColor'),
get(0,'defaultUicontrolBackgroundColor'))
    set(hObject,'BackgroundColor','white');
end

function Dev_Callback(hObject, eventdata, handles)
```

```
% hObject    handle to Dev (see GCBO)
% eventdata  reserved - to be defined in a future version of MATLAB
% handles    structure with handles and user data (see GUIDATA)

% Hints: get(hObject,'String') returns contents of Dev as text
%         str2double(get(hObject,'String')) returns contents of Dev as a
double
% --- Executes during object creation, after setting all properties.
function Dev_CreateFcn(hObject, eventdata, handles)
% hObject    handle to Dev (see GCBO)
% eventdata  reserved - to be defined in a future version of MATLAB
% handles    empty - handles not created until after all CreateFcns called

% Hint: edit controls usually have a white background on Windows.
%       See ISPC and COMPUTER.
if         ispc         &&         isequal(get(hObject,'BackgroundColor'),
get(0,'defaultUicontrolBackgroundColor'))
    set(hObject,'BackgroundColor','white');
end

 function par1_ex_Callback(hObject, eventdata, handles)
% hObject    handle to par1_ex (see GCBO)
% eventdata  reserved - to be defined in a future version of MATLAB
% handles    structure with handles and user data (see GUIDATA)

% Hints: get(hObject,'String') returns contents of par1_ex as text
%        str2double(get(hObject,'String')) returns contents of par1_ex as
a double



% --- Executes during object creation, after setting all properties.
function par1_ex_CreateFcn(hObject, eventdata, handles)
% hObject    handle to par1_ex (see GCBO)
% eventdata  reserved - to be defined in a future version of MATLAB
% handles    empty - handles not created until after all CreateFcns called

% Hint: edit controls usually have a white background on Windows.
%       See ISPC and COMPUTER.
if         ispc         &&         isequal(get(hObject,'BackgroundColor'),
get(0,'defaultUicontrolBackgroundColor'))
    set(hObject,'BackgroundColor','white');
end

function par2_ex_Callback(hObject, eventdata, handles)
% hObject    handle to par2_ex (see GCBO)
% eventdata  reserved - to be defined in a future version of MATLAB
% handles    structure with handles and user data (see GUIDATA)

% Hints: get(hObject,'String') returns contents of par2_ex as text
%        str2double(get(hObject,'String')) returns contents of par2_ex as
a double

 % --- Executes during object creation, after setting all properties.
```

```
function par2_ex_CreateFcn(hObject, eventdata, handles)
% hObject    handle to par2_ex (see GCBO)
% eventdata  reserved - to be defined in a future version of MATLAB
% handles    empty - handles not created until after all CreateFcns called

% Hint: edit controls usually have a white background on Windows.
%       See ISPC and COMPUTER.
if         ispc         &&         isequal(get(hObject,'BackgroundColor'),
get(0,'defaultUicontrolBackgroundColor'))
    set(hObject,'BackgroundColor','white');
end

function par3_ex_Callback(hObject, eventdata, handles)
% hObject    handle to par3_ex (see GCBO)
% eventdata  reserved - to be defined in a future version of MATLAB
% handles    structure with handles and user data (see GUIDATA)

% Hints: get(hObject,'String') returns contents of par3_ex as text
%        str2double(get(hObject,'String')) returns contents of par3_ex as
a double



% --- Executes during object creation, after setting all properties.
function par3_ex_CreateFcn(hObject, eventdata, handles)
% hObject    handle to par3_ex (see GCBO)
% eventdata  reserved - to be defined in a future version of MATLAB
% handles    empty - handles not created until after all CreateFcns called

% Hint: edit controls usually have a white background on Windows.
%       See ISPC and COMPUTER.
if         ispc         &&         isequal(get(hObject,'BackgroundColor'),
get(0,'defaultUicontrolBackgroundColor'))
    set(hObject,'BackgroundColor','white');
end

 function R2_ex_Callback(hObject, eventdata, handles)
% hObject    handle to R2_ex (see GCBO)
% eventdata  reserved - to be defined in a future version of MATLAB
% handles    structure with handles and user data (see GUIDATA)

% Hints: get(hObject,'String') returns contents of R2_ex as text
%        str2double(get(hObject,'String')) returns contents of R2_ex as a
double
% --- Executes during object creation, after setting all properties.
function R2_ex_CreateFcn(hObject, eventdata, handles)
% hObject    handle to R2_ex (see GCBO)
% eventdata  reserved - to be defined in a future version of MATLAB
% handles    empty - handles not created until after all CreateFcns called

% Hint: edit controls usually have a white background on Windows.
%       See ISPC and COMPUTER.
if         ispc         &&         isequal(get(hObject,'BackgroundColor'),
get(0,'defaultUicontrolBackgroundColor'))
```

```
    set(hObject,'BackgroundColor','white');
end

function Dev_ex_Callback(hObject, eventdata, handles)
% hObject    handle to Dev_ex (see GCBO)
% eventdata  reserved - to be defined in a future version of MATLAB
% handles    structure with handles and user data (see GUIDATA)

% Hints: get(hObject,'String') returns contents of Dev_ex as text
%        str2double(get(hObject,'String')) returns contents of Dev_ex as
a double

% --- Executes during object creation, after setting all properties.
function Dev_ex_CreateFcn(hObject, eventdata, handles)
% hObject    handle to Dev_ex (see GCBO)
% eventdata  reserved - to be defined in a future version of MATLAB
% handles    empty - handles not created until after all CreateFcns called

% Hint: edit controls usually have a white background on Windows.
%       See ISPC and COMPUTER.
if         ispc         &&         isequal(get(hObject,'BackgroundColor'),
get(0,'defaultUicontrolBackgroundColor'))
    set(hObject,'BackgroundColor','white');
end

function sse_Callback(hObject, eventdata, handles)
% hObject    handle to sse (see GCBO)
% eventdata  reserved - to be defined in a future version of MATLAB
% handles    structure with handles and user data (see GUIDATA)

% Hints: get(hObject,'String') returns contents of sse as text
%        str2double(get(hObject,'String')) returns contents of sse as a
double



% --- Executes during object creation, after setting all properties.
function sse_CreateFcn(hObject, eventdata, handles)
% hObject    handle to sse (see GCBO)
% eventdata  reserved - to be defined in a future version of MATLAB
% handles    empty - handles not created until after all CreateFcns called

% Hint: edit controls usually have a white background on Windows.
%       See ISPC and COMPUTER.
if         ispc         &&         isequal(get(hObject,'BackgroundColor'),
get(0,'defaultUicontrolBackgroundColor'))
    set(hObject,'BackgroundColor','white');
end

 function sse_ex_Callback(hObject, eventdata, handles)
% hObject    handle to sse_ex (see GCBO)
% eventdata  reserved - to be defined in a future version of MATLAB
% handles    structure with handles and user data (see GUIDATA)
```

```
% Hints: get(hObject,'String') returns contents of sse_ex as text
%        str2double(get(hObject,'String')) returns contents of sse_ex as
a double


 % --- Executes during object creation, after setting all properties.
function sse_ex_CreateFcn(hObject, eventdata, handles)
% hObject    handle to sse_ex (see GCBO)
% eventdata  reserved - to be defined in a future version of MATLAB
% handles    empty - handles not created until after all CreateFcns called

% Hint: edit controls usually have a white background on Windows.
%       See ISPC and COMPUTER.
if         ispc         &&         isequal(get(hObject,'BackgroundColor'),
get(0,'defaultUicontrolBackgroundColor'))
    set(hObject,'BackgroundColor','white');
end


 function rmse_Callback(hObject, eventdata, handles)
% hObject    handle to rmse (see GCBO)
% eventdata  reserved - to be defined in a future version of MATLAB
% handles    structure with handles and user data (see GUIDATA)

% Hints: get(hObject,'String') returns contents of rmse as text
%        str2double(get(hObject,'String')) returns contents of rmse as a
double


 % --- Executes during object creation, after setting all properties.
function rmse_CreateFcn(hObject, eventdata, handles)
% hObject    handle to rmse (see GCBO)
% eventdata  reserved - to be defined in a future version of MATLAB
% handles    empty - handles not created until after all CreateFcns called

% Hint: edit controls usually have a white background on Windows.
%       See ISPC and COMPUTER.
if         ispc         &&         isequal(get(hObject,'BackgroundColor'),
get(0,'defaultUicontrolBackgroundColor'))
    set(hObject,'BackgroundColor','white');
end



function rmse_ex_Callback(hObject, eventdata, handles)
% hObject    handle to rmse_ex (see GCBO)
% eventdata  reserved - to be defined in a future version of MATLAB
% handles    structure with handles and user data (see GUIDATA)

% Hints: get(hObject,'String') returns contents of rmse_ex as text
%        str2double(get(hObject,'String')) returns contents of rmse_ex as
a double


 % --- Executes during object creation, after setting all properties.
function rmse_ex_CreateFcn(hObject, eventdata, handles)
% hObject    handle to rmse_ex (see GCBO)
% eventdata  reserved - to be defined in a future version of MATLAB
```

```
% handles    empty - handles not created until after all CreateFcns called

% Hint: edit controls usually have a white background on Windows.
%       See ISPC and COMPUTER.
if         ispc         &&         isequal(get(hObject,'BackgroundColor'),
get(0,'defaultUicontrolBackgroundColor'))
    set(hObject,'BackgroundColor','white');
end

 function rmsd_Callback(hObject, eventdata, handles)
% hObject    handle to rmsd (see GCBO)
% eventdata  reserved - to be defined in a future version of MATLAB
% handles    structure with handles and user data (see GUIDATA)

% Hints: get(hObject,'String') returns contents of rmsd as text
%        str2double(get(hObject,'String')) returns contents of rmsd as a
double

 % --- Executes during object creation, after setting all properties.
function rmsd_CreateFcn(hObject, eventdata, handles)
% hObject    handle to rmsd (see GCBO)
% eventdata  reserved - to be defined in a future version of MATLAB
% handles    empty - handles not created until after all CreateFcns called

% Hint: edit controls usually have a white background on Windows.
%       See ISPC and COMPUTER.
if         ispc         &&         isequal(get(hObject,'BackgroundColor'),
get(0,'defaultUicontrolBackgroundColor'))
    set(hObject,'BackgroundColor','white');
end



function rmsd_ex_Callback(hObject, eventdata, handles)
% hObject    handle to rmsd_ex (see GCBO)
% eventdata  reserved - to be defined in a future version of MATLAB
% handles    structure with handles and user data (see GUIDATA)

% Hints: get(hObject,'String') returns contents of rmsd_ex as text
%        str2double(get(hObject,'String')) returns contents of rmsd_ex as
a double

 % --- Executes during object creation, after setting all properties.
function rmsd_ex_CreateFcn(hObject, eventdata, handles)
% hObject    handle to rmsd_ex (see GCBO)
% eventdata  reserved - to be defined in a future version of MATLAB
% handles    empty - handles not created until after all CreateFcns called

% Hint: edit controls usually have a white background on Windows.
%       See ISPC and COMPUTER.
if         ispc         &&         isequal(get(hObject,'BackgroundColor'),
get(0,'defaultUicontrolBackgroundColor'))
    set(hObject,'BackgroundColor','white');
end
```

MAIN FILE.m

```
% clear all
% clc

tic

% Read data from data file
DataFile3

rng default % for reproducibility

Data3_val = get(handles.optimMenu,'Value');
Data3_str = get(handles.optimMenu, 'String');

switch Data3_str{Data3_val};

    case 'Genetic Algorithm'
        % GENETIC ALGORITHM
        OptimMethod = 'GENETIC ALGORITHM';
        MaxGen = 20*NVARS;
        popSize = 100;
        options   =   optimoptions(@ga,'Display','iter','MaxGenerations',
MaxGen,'MutationFcn',@mutationadaptfeasible,...
            'PopulationSize',
popSize,'PlotFcn',{@gaplotbestf,@gaplotbestindiv,@gaplotexpectation,@gapl
otstopping});
        A = []; b =[];  Aeq = []; beq =[];
        NONLCON = [];
        [par,fval,    exitflag,    output,    population,    scores]    =
ga(@(par)ObjectiveFunctionFile(par,      xI,      xII,      z,      model,
extraPar),NVARS,A,b,Aeq,beq,lb,ub,NONLCON,options)

    case 'Particle Swarm'
        % PARTICLE SWARM
        OptimMethod = 'PARTICLE SWARM';
        MaxSwarmSize = 10*NVARS;
        options  =  optimoptions(@particleswarm,'SwarmSize',MaxSwarmSize,
'Display', 'iter');
        [par,fval,             exitflag,             output]             =
particleswarm(@(par)ObjectiveFunctionFile(par,   xI,   xII,   z,   model,
extraPar),NVARS, lb, ub, options)

    case 'Simulated Annealing'
        % SIMULATED ANNEALING
        OptimMethod ='SIMULATED ANNEALING';
        x0 = par0; %5.*ones(1,NVARS);
        options = optimoptions(@simulannealbnd,'Display', 'iter');
        [par,fval,             exitflag,             output]             =
simulannealbnd(@(par)ObjectiveFunctionFile(par,   xI,   xII,   z,   model,
extraPar),x0,lb,ub,options)
```

```
    case 'PatternSearch'
        % PATTERNSEARCH
        OptimMethod ='PATTERNSEARCH';
        options        =        optimoptions(@patternsearch);%,'Display',
'iter','Algorithm','levenberg-marquardt');
        options.Display = 'iter';
        A = []; b =[];  Aeq = []; beq =[];
        [par,fval,exitflag,      output]      =      patternsearch(@(par)
ObjectiveFunctionFile(par,        xI,        xII,        z,        model,
extraPar),par0,A,b,Aeq,beq,lb,ub,options);

    case 'Lsqnonlin'
        % LSQNONLIN
        OptimMethod = 'LSQNONLIN';
        options          =          optimoptions(@lsqnonlin);%,'Display',
'iter','Algorithm','levenberg-marquardt');
        options.Display = 'iter';
        [par,resnorm,    residual,    exitflag,    output,    lambda]    =
lsqnonlin(@(par)   ObjectiveFunctionFile(par,   xI,   xII,   z,   model,
extraPar),par0,lb,ub,options);
        fval = ObjectiveFunctionFile(par, z, xI, xII, model, extraPar);

    case 'Fmincon'
        % FMINCON
        OptimMethod ='FMINCON';
        options           =           optimoptions(@fmincon);%,'Display',
'iter','Algorithm','levenberg-marquardt');
        options.Display = 'iter';
        A = []; b =[];  Aeq = []; beq =[];
        [par,fval,exitflag,output,lambda]        =        fmincon(@(par)
ObjectiveFunctionFile(par,        xI,        xII,        z,        model,
extraPar),par0,A,b,Aeq,beq,lb,ub);

    case 'Fminunc'
        % FMINUNC
        OptimMethod = 'FMINUNC';
        options           =           optimoptions(@fminunc);%,'Display',
'iter','Algorithm','levenberg-marquardt');
        options.Display = 'iter';
        [par,fval,exitflag,output,lambda]        =        fminunc(@(par)
ObjectiveFunctionFile(par, xI, xII, z, model, extraPar),par0,options);

    case 'Fminsearch'
        % FMINSEARCH
        OptimMethod = 'FMINSEARCH';
        options           =           optimset(@fminsearch);%,'Display',
'iter','Algorithm','levenberg-marquardt');
        options.Display = 'iter';
        [par,fval,exitflag,output]          =          fminsearch(@(par)
ObjectiveFunctionFile(par, xI, xII, z, model, extraPar),par0,options);
end

% RESULTS
```

```
[xI_calc xII_calc param] = Flash_Calculation(par, z, xI, xII, model,
extraPar);
CalcData =[xI_calc xII_calc];

Exp = [xI(:,1);xI(:,2);xI(:,3);xII(:,1);xII(:,2);xII(:,3)];
Calc                                                                =
[xI_calc(:,1);xI_calc(:,2);xI_calc(:,3);xII_calc(:,1);xII_calc(:,2);xII_c
alc(:,3)];

% Calculating RMSD
[m c] = size(xI);

RMSD = sqrt(fval/2/m/c)

[res, r2, r2adj, SSE, RMSE] = stat_data(par,Exp,Calc);

%Create Plot
axes(handles.axes1)
plot (Exp,Calc,'o',[0:1], [0:1])
xlabel('Experimental values'); ylabel('Predicted values');
axis([0 1 0 1]);
set(handles.axes1,'XMinorTick','on')
grid off

switch nComp
    case 3
        txtFormat = '%.3f %.3f %.3f \n';
        txtFormat2 = '%.3f %.3f %.3f %.3f %.3f %.3f \n';
    case 4
        txtFormat  = '%.3f %.3f %.3f %.3f \n';
        txtFormat2  = '%.3f %.3f %.3f %.3f %.3f %.3f %.3f %.3f \n';
end

switch Data2_str{Data2_val};
    case 'NRTL'
        G = exp(-alpha*param);
        par1 = alpha;    par1_ex = 'Alpha';
        par2 = param;      par2_ex = 'Tau';
        par3 = G;                  par3_ex = 'G';
        model_ex = TextFilename(caseNo, model, OptimMethod);
    case 'UNIQUAC'
        par1 = [];                par1_ex = '';
        par2 = exp(-param/T);     par2_ex = 'Tau';
        par3 = param;    par3_ex = 'Aij';
        model_ex = TextFilename(caseNo, model, OptimMethod);
end

elapsedTime_sec = toc;
elapsedTime_min = elapsedTime_sec/60;
elapsedTime_hrs = elapsedTime_sec/3600;

% Transfer data to Excel
```

```
 DataTransfer_ExcelFile

% Transfer data to text file
DataTransfer_TextFile

 Flash_Calculation.m

function [xI_calc xII_calc param] = Flash_Calculation(par, z, xI, xII,
model, extraPar)

[r n] = size(xI);
count = 0;
param = zeros(n);
for i = 1:n
    for j = 1:n
        if i~= j
            count = count + 1;
            param(i,j) = par(count);
        end
    end
end

switch model
    case 'NRTL'
        tau = param;
        alpha = extraPar.alpha;
        gammaI = NRTLModel(xI, alpha, tau);
        gammaII = NRTLModel(xII, alpha, tau);

    case 'UNIQUAC'
        Aji = param;
        r =extraPar.r;
        q =extraPar.q;
        T =extraPar.T;
        gammaI = UNIQUACModel(xI,Aji,r,q, T);
        gammaII = UNIQUACModel(xII,Aji,r,q, T);
end


K = gammaI./gammaII;

phi = 0.05;
% options = optimoptions('fsolve','Display','iter');
phi = fsolve(@(phi)NonlinearEqn(phi, z, K), phi);%,options);
xI_calc = z./(1 + phi.*(K-1));
xII_calc = K.*xI_calc;

    function  f = NonlinearEqn(phi, z, K)
        f = sum(sum(z.*(1-K./(1+ phi.*(K-1)))));
    end
end
```

ObjectiveFunctionFile.m

```
function y = ObjectiveFunctionFile(par, xI, xII, z, model, extraPar)

[xI_calc xII_calc] = Flash_Calculation(par, z, xI, xII, model, extraPar);
y =sum(sum((xI - xI_calc).^2 + (xII - xII_calc).^2));

end
```

NRTLModel.m

```
function gamma = NRTLModel(X, alpha, tau)
% Computer Code for calculating Activity Coefficients
%  (NRTL model)

[N comp]= size(X);

G = exp(-alpha.*tau);

for i = 1:N

    x = X(i,:);
    E = ones(size(x'));
    Y = G'*x';
    Z = (tau.*G)'*x'./Y;
    lngamma = Z + G.*(tau-E*Z')*(x'./Y);
    gamma(i,:) = (exp(lngamma))';

    end
end
```

UNIQUACModel.m

```
function gamma = UNIQUACModel(X,Aji,r,q, T)
% Computer Code for calculating Activity Coefficients (UNIQUAC model)

tau = exp(-Aji/T);

z=10;
[N comp]= size(X);

for i = 1:N
    x = X(i,:);
    identMat=ones(size(x));
    l = (z/2)*(r-q)+1-r;
    theta=(x.*q)/(x*q');
    phi=(x.*r)/(x*r');
    E=theta*tau;
    E_o=identMat'*E;
    theta_o=identMat'*theta;
    lngamma_c=log(phi./x)+(z/2)*q.*log(theta./phi)+l-(phi./x).*(x*l');
    lngamma_r=q.*(1-log(E)-sum(((tau.*theta_o)./E_o)'));
```

```
    gamma(i,:)=exp(lngamma_c+lngamma_r);
end
end
```

Data Transfer_TextFile.m

```
%%%%%%%%%%%%%%%%%%%%%%%%%%%%%%%%%%%%%%%%%%%%%%%%%%
% TRANSFER RESULTS TO EXCEL                       %
%%%%%%%%%%%%%%%%%%%%%%%%%%%%%%%%%%%%%%%%%%%%%%%%%%
% Textfilename =input('Enter Name of Text File (e.g ''Results.txt >>' );
Textfilename = TextFilename(caseNo, model, OptimMethod);
fid = fopen(Textfilename,'w');
if fid == 0
    warndlg('Text file is not available','!! WARNING !!');
else
    fprintf(fid,'%s \n','');
    fprintf(fid,'%s \n','');
    fprintf(fid,'%s \n','                         DEPARTMENT OF CHEMICAL
ENGINEERING');
    fprintf(fid,'%s \n','                        AHMADU BELLO UNIVERSITY,
ZARIA');
    fprintf(fid,'%s \n','');
    fprintf(fid,'%s \n','');
    fprintf(fid,'                                                    Date:
%s \n',date);
    fprintf(fid,'                                            Elapsed Time
(seconds):  %6.2f \n',elapsedTime_sec);
    fprintf(fid,'                                            Elapsed Time
(minutes):  %6.2f \n',elapsedTime_min);
    fprintf(fid,'                                            Elapsed Time
(hours):    %6.2f \n',elapsedTime_hrs);
    fprintf(fid,'%s \n','');
    fprintf(fid,'%s \n','');
    fprintf(fid,'Source of Data:      %s \n',RefMat);
    fprintf(fid,'System:              %s \n',systemName);
    fprintf(fid,'No. of Components:   %d \n',nComp);
    fprintf(fid,'Model:               %s \n',OptimMethod);
    fprintf(fid,'Optimisation Method: %s \n',model);
    fprintf(fid,'%s \n','');
    fprintf(fid,'%s \n','OPTIMISATION RESULTS');
    fprintf(fid,'%s \n','');
    fprintf(fid,'RMSD:                %10.5f \n',RMSD);
    fprintf(fid,'%s \n','');
    fprintf(fid,'%s \n','Model Parameters');
    fprintf(fid,'%s \n','');

    switch model
        case 'NRTL'
            fprintf(fid,'Alpha:                 %10.4f \n',alpha);
            fprintf(fid,'%s \n','');
            fprintf(fid,'%s \n','Tau  ');
            switch nComp
                case 3
```

```
                    fprintf(fid,'%10.4f %10.4f %10.4f \n',param);
                    fprintf(fid,'%s \n','');
                    fprintf(fid,'%s \n','G  ');
                    fprintf(fid,'%10.4f    %10.4f    %10.4f    \n',exp(-
alpha*param));
                case 4
                    fprintf(fid,'%10.4f %10.4f %10.4f %10.4f \n',param);
                    fprintf(fid,'%s \n','');
                    fprintf(fid,'%s \n','   G  ');
                    fprintf(fid,'%10.4f  %10.4f  %10.4f  %10.4f  \n',exp(-
alpha*param));
            end

        case 'UNIQUAC'
            switch nComp
                case 3
                    fprintf(fid,'%s \n','   Tau  ');
                    fprintf(fid,'%10.4f %10.4f %10.4f \n',exp(-param/T));
                    fprintf(fid,'%s \n','  ');
                    fprintf(fid,'%s \n','   Aij  ');
                    fprintf(fid,'%10.4f %10.4f %10.4f \n',param);
                case 4
                    fprintf(fid,'%s \n','   Tau  ');
                    fprintf(fid,'%10.4f  %10.4f  %10.4f  %10.4f  \n',exp(-
param/T));
                    fprintf(fid,'%s \n','  ');
                    fprintf(fid,'%s \n','   Aij  ');
                    fprintf(fid,'%10.4f %10.4f %10.4f %10.4f \n',param);
            end
    end
    switch nComp
        case 3
            fprintf(fid,'%s \n', ' ');
            fprintf(fid,'%s \n', 'Experimental Data');
            fprintf(fid,'%s \n', '-------------------------------------
-------------------------');
            fprintf(fid,'%s  \n',  '                              Phase  I
Phase II          ');
            fprintf(fid,'%s \n', '------------------------------      --
-------------------------');
            fprintf(fid,'%s \n', '       x1         x2         x3       x1
x2        x3');
              fprintf(fid,'%s \n', '-------------------------------------
-------------------------');
            fprintf(fid,'%10.4f  %10.4f  %10.4f  %10.4f  %10.4f  %10.4f
\n',ExpData);
            fprintf(fid,'%s \n', '-------------------------------------
-------------------------');

            fprintf(fid,'%s \n', ' ');
            fprintf(fid,'%s \n', 'Calculated Data');
            fprintf(fid,'%s \n', '-------------------------------------
-------------------------');
            fprintf(fid,'%s  \n',  '                              Phase  I
Phase II          ');
```

```
            fprintf(fid,'%s \n', '------------------------------      --
--------------------------');
            fprintf(fid,'%s \n', '       x1         x2         x3        x1
x2        x3');
            fprintf(fid,'%s \n', '-------------------------------------
--------------------------');
            fprintf(fid,'%10.4f   %10.4f   %10.4f   %10.4f   %10.4f   %10.4f
\n',CalcData);
            fprintf(fid,'%s \n', '-------------------------------------
--------------------------');

        case 4
            fprintf(fid,'%s \n', ' ');
            fprintf(fid,'%s \n', 'Experimental Data')
            fprintf(fid,'%s \n', '-------------------------------------
-----------------------------------------------');
            fprintf(fid,'%s  \n',  '                                  Phase  I
Phase II          ');
            fprintf(fid,'%s \n', '-------------------------------------
----      ------------------------------------');
            fprintf(fid,'%s \n', '       x1         x2         x3         x4
x1         x2         x3         x4');
            fprintf(fid,'%s \n', '-------------------------------------
-----------------------------------------------');
            fprintf(fid,'%10.4f %10.4f %10.4f %10.4f %10.4f %10.4f %10.4f
%10.4f \n',ExpData);
            fprintf(fid,'%s \n', ' ');
            fprintf(fid,'%s \n', 'Calculated Data');
            fprintf(fid,'%s \n', '-------------------------------------
-----------------------------------------------');
            fprintf(fid,'%s  \n',  '                                  Phase  I
Phase II          ');
            fprintf(fid,'%s \n', '-------------------------------------
----      ------------------------------------');
            fprintf(fid,'%s \n', '       x1         x2         x3         x4
x1         x2         x3         x4');
            fprintf(fid,'%s \n', '-------------------------------------
-----------------------------------------------');
            fprintf(fid,'%10.4f %10.4f %10.4f %10.4f %10.4f %10.4f %10.4f
%10.4f \n',CalcData);
            fprintf(fid,'%10.4f %10.4f %10.4f %10.4f %10.4f %10.4f %10.4f
%10.4f \n',ExpData);

    end
end

fclose(fid);
```

Data Transfer ExcelFile.m

```
%%%%%%%%%%%%%%%%%%%%%%%%%%%%%%%%%%%%%%%%%%%%%%%%%%%%%%%%%%%%%%%%%%%%%%%
% TRANSFER RESULTS TO EXCEL                                             %
%%%%%%%%%%%%%%%%%%%%%%%%%%%%%%%%%%%%%%%%%%%%%%%%%%%%%%%%%%%%%%%%%%%%%%%
```

```
str1=sprintf('%d',nComp+11);
str2=sprintf('%d',nComp+4);
str3=sprintf('%d',nComp+9);
str4=sprintf('%d',m+18);
str5=sprintf('%d',2*nComp + 1);
str6=sprintf('%d',2*nComp + 11);

filename ='ResultsFile.xlsx';
channel = ddeinit('excel','ResultsFile.xlsx'); % Initiated the dynamic
data transfer

if channel == 0
    warndlg('Excel File "ResultsFile.xlsx" is closed','!! WARNING !!')
else
    rc = ddepoke(channel, 'r4c4:r4c4', RefMat);
    rc = ddepoke(channel, 'r5c4:r5c4', systemName);
    rc = ddepoke(channel, 'r6c4:r6c4', nComp);
    rc = ddepoke(channel, 'r7c4:r7c4', model);
    rc = ddepoke(channel, 'r8c4:r8c4', OptimMethod);
    rc = ddepoke(channel, 'r15c2:r15c3', RMSD);
    rc = ddepoke(channel, ['r19c2:r' str4 'c' str5], ExpData);
    rc = ddepoke(channel, ['r19c12:r' str4 'c' str6], CalcData);
    rc = ddepoke(channel, 'r4c20:r4c20', date);
    rc = ddepoke(channel, 'r5c20:r5c20', elapsedTime_sec);
    rc = ddepoke(channel, 'r6c20:r6c20', elapsedTime_min);
    rc = ddepoke(channel, 'r7c20:r7c20', elapsedTime_hrs);

    switch model
        case 'NRTL'
            rc = ddepoke(channel, 'r12c2:r12c3', alpha);
            rc = ddepoke(channel, ['r12c5:r' str1 'c' str2], param);
            rc = ddepoke(channel, ['r12c10:r' str1 'c' str3], exp(-
alpha.*param));
            rc = ddepoke(channel, 'r11c10:r11c10', 'G');
        case 'UNIQUAC'
            rc = ddepoke(channel, 'r12c2:r12c3', ' ');
            rc = ddepoke(channel, ['r12c5:r' str1 'c' str2], exp(-
param/T));
            rc = ddepoke(channel, ['r12c10:r' str1 'c' str3], param);
            rc = ddepoke(channel, 'r11c10:r11c10', 'Aij');
    end

end
```

DataFile3.m

```
% Data1_val = get(handles.dataMenu,'Value');
% Data1_str = get(handles.dataMenu, 'String');
% switch Data1_str{Data1_val};

Data1_str = get(handles.dataMenu, 'String');
```

```
switch Data1_str;
case '1'
        RefMat = 'Tetrabutyl ammonium bromide with PEG200 (1:2) as DES';
        systemName = 'Octane - DES - Toluene @ 30 0C';
        nComp = 3;
        caseNo = 'Data1';

        data =[1    0.092   0.892   0.016   0.973   eps 0.027   0.60    6.37
            2   0.087   0.884   0.029   0.949   eps 0.050   0.59    6.40
            3   0.069   0.869   0.063   0.899   eps 0.097   0.65    8.49
            4   0.076   0.833   0.091   0.847   eps 0.144   0.63    7.04
            5   0.067   0.817   0.116   0.797   eps 0.188   0.62    7.34];

        T = 298.15; % K
        alpha = 0.2;
        % r = [5.8463   6.487162789 3.9228];
        % q = [5.008    5.389730232 2.968];

        r = [6.9894 10.3177 4.1288];
        q = [4.9184 6.9780  3.0705];
    case '2'
       RefMat = 'Tetrabutyl ammonium bromide with PEG200 (1:2) as DES';
        systemName = 'Octane - DES - Toluene @ 40 0C';
        nComp = 3;
        caseNo = 'Data2';

        data =[1    0.103   0.882   0.015   0.973   eps 0.027   0.58    5.46
            2   0.098   0.873   0.030   0.949   eps 0.050   0.59    5.69
            3   0.088   0.842   0.070   0.903   eps 0.093   0.75    7.72
            4   0.086   0.820   0.094   0.849   eps 0.143   0.66    6.54
            5   0.079   0.801   0.119   0.798   eps 0.188   0.64    6.38];
        T = 298.15; % K
        alpha = 0.2;
        % r = [5.8463   6.487162789 3.9228];
        % q = [5.008    5.389730232 2.968];

        r = [6.9894 10.3177 4.1288];
        q = [4.9184 6.9780  3.0705];

    case '3'
        RefMat = 'Tetrabutyl ammonium bromide with PEG200 (1:2) as DES';
        systemName = 'Octane - DES - Toluene @ 50 0C';
        nComp = 3;
        caseNo = 'Data3';

        data =[1    0.111   0.873   0.016   0.973   eps 0.027   0.58    5.09
            2   0.110   0.861   0.029   0.948   eps 0.051   0.56    4.86
            3   0.102   0.836   0.062   0.898   eps 0.098   0.63    5.51
            4   0.093   0.817   0.091   0.847   eps 0.145   0.62    5.69
            5   0.090   0.792   0.118   0.797   eps 0.189   0.63    5.57];
        T = 298.15; % K
        alpha = 0.2;
        % r = [5.8463   6.487162789 3.9228];
        % q = [5.008    5.389730232 2.968];
```

```
    r = [6.9894 10.3177 4.1288];
    q = [4.9184 6.9780  3.0705];


case '4'
    RefMat = 'Tetrabutyl ammonium bromide with PEG600 (1:2) as DES';
    systemName = 'Octane - DES - Toluene @ 30 0C';
    nComp = 3;
    caseNo = 'Data4';

    data =[1    0.224   0.747   0.029   0.976   eps 0.024   1.21    5.30
        2   0.215   0.721   0.063   0.953   eps 0.046   1.37    6.06
        3   0.204   0.672   0.124   0.908   eps 0.090   1.38    6.12
        4   0.175   0.653   0.172   0.858   eps 0.138   1.25    6.12
        5   0.170   0.604   0.226   0.812   eps 0.182   1.24    5.93];

    T = 298.15; % K

    alpha = 0.2;
    % r = [5.8463   13.2541321  3.9228];
    % q = [5.008    10.80330568 2.968];

    r = [6.9028 20.6124 4.0942];
    q = [4.8989 14.0320 3.0476];

case '5'
   RefMat = 'Tetrabutyl ammonium bromide with PEG600 (1:2) as DES';
    systemName = 'Octane - DES - Toluene @ 40 0C';
    nComp = 3;
    caseNo = 'Data5';

    data =[1    0.224   0.744   0.032   0.976   eps 0.023   1.35    5.90
        2   0.219   0.719   0.062   0.953   eps 0.047   1.33    5.81
        3   0.213   0.665   0.122   0.908   eps 0.091   1.34    5.71
        4   0.187   0.629   0.184   0.864   eps 0.133   1.39    6.42
        5   0.174   0.586   0.240   0.819   eps 0.175   1.37    6.45];

    T = 298.15; % K
    alpha = 0.2;
    % r = [5.8463   13.2541321  3.9228];
    % q = [5.008    10.80330568 2.968];

    r = [6.9028 20.6124 4.0942];
    q = [4.8989 14.0320 3.0476];

case '6'
    RefMat = 'Tetrabutyl ammonium bromide with PEG600 (1:2) as DES';
    systemName = 'Octane - DES - Toluene @ 50 0C';
    nComp = 3;
    caseNo = 'Data6';
```

```
        data =[1     0.134    0.832    0.034    0.976    eps 0.024    1.42
10.39
            2   0.156   0.774   0.070   0.951   eps 0.049   1.44    8.82
            3   0.175   0.697   0.128   0.905   eps 0.094   1.37    7.09
            4   0.172   0.649   0.179   0.857   eps 0.139   1.29    6.42
            5   0.175   0.596   0.230   0.810   eps 0.183   1.25    5.81];

        T = 298.15; % K
        alpha = 0.2;
        % r = [5.8463   13.2541321  3.9228];
        % q = [5.008    10.80330568 2.968];

        r = [6.9028 20.6124 4.0942];
        q = [4.8989 14.0320 3.0476];


    case '7'
        RefMat = 'Tetrabutyl phosphonium bromide with PEG200 (1:2) as DES';
        systemName = 'Octane - DES - Toluene @ 30 0C';
        nComp = 3;
        caseNo = 'Data7';

        data =[1    0.084   0.896   0.02    0.973   eps 0.027   0.74    8.56
            2   0.088   0.885   0.028   0.948   eps 0.051   0.54    5.85
            3   0.069   0.866   0.065   0.897   eps 0.099   0.66    8.62
            4   0.076   0.832   0.092   0.848   eps 0.144   0.64    7.12
            5   0.068   0.807   0.125   0.797   eps 0.189   0.66    7.74];

        T = 298.15; % K
        alpha = 0.2;
        % r = [5.8463   6.627599762 3.9228];
        % q = [5.008    5.50207981  2.968];

        r = [6.9894 10.5890 4.1288];
        q = [4.9184 7.2582  3.0705];

    case '8'
       RefMat = 'Tetrabutyl phosphonium bromide with PEG200 (1:2) as DES';
        systemName = 'Octane - DES - Toluene @ 40 0C';
        nComp = 3;
        caseNo = 'Data8';

        data =[1    0.102   0.882   0.016   0.975   eps 0.025   0.64    6.07
            2   0.102   0.867   0.032   0.95    eps 0.049   0.64    5.98
            3   0.094   0.839   0.067   0.893   eps 0.103   0.65    6.23
            4   0.086   0.821   0.093   0.854   eps 0.138   0.67    6.67
            5   0.076   0.798   0.127   0.806   eps 0.181   0.7 7.44];
        T = 298.15; % K
        alpha = 0.2;
        % r = [5.8463   6.627599762 3.9228];
        % q = [5.008    5.50207981  2.968];

        r = [6.9894 10.5890 4.1288];
```

```
    q = [4.9184 7.2582  3.0705];

case '9'
    RefMat = 'Tetrabutyl phosphonium bromide with PEG200 (1:2) as DES';
    systemName = 'Octane - DES - Toluene @ 50 0C';
    nComp = 3;
    caseNo = 'Data9';

    data =[1    0.110   0.875   0.015   0.975   eps 0.025   0.63    5.58
        2   0.104   0.865   0.032   0.95    eps 0.049   0.64    5.86
        3   0.098   0.832   0.07    0.894   eps 0.102   0.69    6.27
        4   0.112   0.794   0.094   0.854   eps 0.138   0.68    5.18
        5   0.163   0.705   0.132   0.804   eps 0.182   0.73    3.58];

    T = 298.15; % K
    alpha = 0.2;
    % r = [5.8463   6.627599762 3.9228];
    % q = [5.008    5.50207981  2.968];

    r = [6.9894 10.5890 4.1288];
    q = [4.9184 7.2582  3.0705];


case '10'
    RefMat = 'Tetrabutyl phosphonium bromide with PEG600 (1:2) as DES';
    systemName = 'Octane - DES - Toluene @ 30 0C';
    nComp = 3;
    caseNo = 'Data10';

    data =[1    0.165   0.798   0.036   0.974   eps 0.025   1.42    8.39
        2   0.159   0.773   0.067   0.952   eps 0.048   1.4 8.37
        3   0.153   0.721   0.126   0.904   eps 0.094   1.34    7.89
        4   0.12    0.689   0.191   0.855   eps 0.141   1.35    9.62
        5   0.104   0.654   0.242   0.807   eps 0.186   1.30    10.06];

    T = 298.15; % K
    alpha = 0.2;
    % r = [5.8463   13.40151719 3.9228];
    % q = [5.008    10.92121375 2.968];

    r = [6.9894 21.5625 4.1288];
    q = [4.9184 14.6982 3.0705];

case '11'
   RefMat = 'Tetrabutyl phosphonium bromide with PEG600 (1:2) as DES';
    systemName = 'Octane - DES - Toluene @ 40 0C';
    nComp = 3;
    caseNo = 'Data11';

    data =[1    0.160   0.801   0.039   0.975   eps 0.025   1.61    9.8
        2   0.172   0.758   0.07    0.953   eps 0.047   1.5 8.32
        3   0.163   0.711   0.126   0.904   eps 0.094   1.34    7.43
        4   0.149   0.659   0.191   0.856   eps 0.14    1.36    7.83
```

```
            5   0.127   0.623   0.25    0.811   eps 0.183   1.37    8.74];

        T = 298.15; % K
        alpha = 0.2;
        % r = [5.8463   13.40151719 3.9228];
        % q = [5.008    10.92121375 2.968];

        r = [6.9894 21.5625 4.1288];
        q = [4.9184 14.6982 3.0705];

    case '12'
        RefMat = 'Tetrabutyl phosphonium bromide with PEG600 (1:2) as DES';
        systemName = 'Octane - DES - Toluene @ 50 0C';
        nComp = 3;
        caseNo = 'Data12';

        data =[1    0.227   0.737   0.036   0.975   eps 0.025   1.44    6.19
            2   0.222   0.714   0.064   0.951   eps 0.049   1.3 5.58
            3   0.215   0.659   0.126   0.905   eps 0.093   1.35    5.69
            4   0.191   0.623   0.186   0.855   eps 0.141   1.32    5.9
            5   0.18    0.585   0.236   0.806   eps 0.187   1.26    5.65];

        T = 298.15; % K
        alpha = 0.2;
        % r = [5.8463   13.40151719 3.9228];
        % q = [5.008    10.92121375 2.968];

        r = [6.9894 21.5625 4.1288];
        q = [4.9184 14.6982 3.0705];


   case '13'
        RefMat = 'Tetrabutyl ammonium bromide with DMF (1:2) as DES';
        systemName = 'Octane - DES - Toluene @ 30 0C';
        nComp = 3;
        caseNo = 'Data13';

        data =[1    0.126   0.857   0.017   0.948   0.031   0.021   0.81
6.10
            2   0.129   0.838   0.033   0.924   0.033   0.043   0.77    5.53
            3   0.118   0.816   0.066   0.880   0.036   0.083   0.80    5.94
            4   0.126   0.778   0.096   0.833   0.039   0.123   0.78    5.20
            5    0.113    0.766    0.121    0.786    0.042    0.162    0.75
5.19];

        T = 298.15; % K
        alpha = 0.2;
        % r = [5.8463   4.504212446 3.9228];
        % q = [5.008    3.803369956 2.968];

        r = [6.9894 7.4570  4.1288];
        q = [4.9184 4.9591  3.0705];
    case '14'
```

```
        RefMat = 'Tetrabutyl ammonium bromide with DMF (1:2) as DES';
         systemName = 'Octane - DES - Toluene @ 40 0C';
         nComp = 3;
         caseNo = 'Data14';

         data =[1    0.151   0.832   0.017   0.941   0.037   0.022   0.77
4.76
             2   0.154   0.812   0.033   0.918   0.039   0.043   0.77    4.59
             3   0.142   0.793   0.065   0.873   0.042   0.084   0.77    4.75
             4   0.133   0.772   0.095   0.826   0.046   0.124   0.77    4.77
             5    0.123    0.747    0.130    0.786    0.049    0.157    0.83
5.31];

         T = 298.15; % K
         alpha = 0.2;
         % r = [5.8463   4.504212446 3.9228];
         % q = [5.008    3.803369956 2.968];

         r = [6.9894 7.4570  4.1288];
         q = [4.9184 4.9591  3.0705];

    case '15'
         RefMat = 'Tetrabutyl ammonium bromide with DMF (1:2) as DES';
         systemName = 'Octane - DES - Toluene @ 50 0C';
         nComp = 3;
         caseNo = 'Data15';

         data =[1    0.142   0.841   0.017   0.936   0.042   0.022   0.77
5.10
             2   0.158   0.808   0.033   0.910   0.047   0.044   0.76    4.38
             3   0.154   0.779   0.067   0.867   0.051   0.083   0.81    4.55
             4   0.164   0.737   0.099   0.821   0.055   0.122   0.81    4.07
             5    0.152    0.717    0.131    0.776    0.058    0.159    0.82
4.17];

         T = 298.15; % K
         alpha = 0.2;
         % r = [5.8463   4.504212446 3.9228];
         % q = [5.008    3.803369956 2.968];

         r = [6.9894 7.4570  4.1288];
         q = [4.9184 4.9591  3.0705];


    case '16'
         RefMat = 'Tetrabutyl ammonium bromide with DMSO(1:2) as DES';
         systemName = 'Octane - DES - Toluene @ 30 0C';
         nComp = 3;
         caseNo = 'Data16';

         data =[1    0.225   0.759   0.016   0.953   0.022   0.022   0.77
5.10
             2   0.214   0.746   0.040   0.933   0.024   0.044   0.76    4.38
```

```
            3   0.202   0.721   0.077   0.888   0.026   0.083   0.81    4.55
            4   0.197   0.689   0.114   0.843   0.028   0.122   0.81    4.07
            5    0.186    0.659    0.155    0.804    0.030    0.159    0.82
4.17];

        T = 298.15; % K
        alpha = 0.2;
        % r = [5.8463   4.275725432 3.9228];
        % q = [5.008    3.620580345 2.968];

        r = [6.9894 6.7669  4.1288];
        q = [4.9184 4.5765  3.0705];
    case '17'
       RefMat = 'Tetrabutyl ammonium bromide with DMSO(1:2) as DES';
        systemName = 'Octane - DES - Toluene @ 40 0C';
        nComp = 3;
        caseNo = 'Data17';

        data =[1    0.185   0.795   0.020   0.973   0.005   0.022   0.90
4.73
            2   0.177   0.783   0.040   0.951   0.005   0.043   0.93    4.99
            3   0.173   0.748   0.079   0.910   0.005   0.082   0.96    5.05
            4   0.169   0.713   0.118   0.868   0.007   0.120   0.99    5.09
            5    0.168    0.682    0.150    0.821    0.009    0.160    0.94
4.60];

        T = 298.15; % K
        alpha = 0.2;
        % r = [5.8463   4.275725432 3.9228];
        % q = [5.008    3.620580345 2.968];

        r = [6.9894 6.7669  4.1288];
        q = [4.9184 4.5765  3.0705];

    case '18'
        RefMat = 'Tetrabutyl ammonium bromide with DMSO(1:2) as DES';
        systemName = 'Octane - DES - Toluene @ 50 0C';
        nComp = 3;
        caseNo = 'Data18';

        data =[1    0.200   0.779   0.021   0.974   0.005   0.021   1.00
4.87
            2   0.209   0.768   0.023   0.937   0.006   0.056   0.41    1.83
            3   0.197   0.723   0.080   0.909   0.007   0.081   0.99    4.57
            4   0.182   0.700   0.118   0.867   0.008   0.120   0.99    4.70
            5    0.170    0.675    0.155    0.824    0.010    0.157    0.99
4.78];

        T = 298.15; % K
        alpha = 0.2;
        % r = [5.8463   4.275725432 3.9228];
        % q = [5.008    3.620580345 2.968];
```

```
        r = [6.9894 6.7669  4.1288];
        q = [4.9184 4.5765  3.0705];

         case '19'
        RefMat = 'Tetrabutyl phosphonium bromide with DMF (1:2) as DES';
        systemName = 'Octane - DES - Toluene @ 30 0C';
        nComp = 3;
        caseNo = 'Data19';

        data =[1    0.144   0.840   0.016   0.953   0.026   0.021   0.76
5.05
            2   0.139   0.826   0.035   0.936   0.021   0.043   0.81    5.44
            3   0.141   0.794   0.065   0.885   0.030   0.083   0.79    4.96
            4   0.143   0.759   0.098   0.846   0.030   0.119   0.82    4.86
            5    0.136    0.735    0.129    0.800    0.033    0.157    0.82
4.82];

        T = 298.15; % K
        alpha = 0.2;
        % r = [5.8463   4.561775131 3.9228];
        % q = [5.008    3.849420105 2.968];

        r = [6.9894 7.7283  4.1288];
        q = [4.9184 5.2393  3.0705];

    case '20'
       RefMat = 'Tetrabutyl phosphonium bromide with DMF (1:2) as DES';
        systemName = 'Octane - DES - Toluene @ 40 0C';
        nComp = 3;
        caseNo = 'Data20';

        data =[1    0.144   0.839   0.018   0.946   0.034   0.021   0.85
5.61
            2   0.145   0.819   0.036   0.923   0.036   0.042   0.87    5.54
            3   0.144   0.787   0.070   0.882   0.038   0.080   0.88    5.38
            4   0.136   0.762   0.101   0.839   0.041   0.117   0.87    5.33
            5    0.138    0.725    0.137    0.800    0.043    0.150    0.91
5.30];

        T = 298.15; % K
        alpha = 0.2;
        % r = [5.8463   4.561775131 3.9228];
        % q = [5.008    3.849420105 2.968];

        r = [6.9894 7.7283  4.1288];
        q = [4.9184 5.2393  3.0705];

    case '21'
        RefMat = 'Tetrabutyl phosphonium bromide with DMF (1:2) as DES';
        systemName = 'Octane - DES - Toluene @ 50 0C';
        nComp = 3;
        caseNo = 'Data21';
```

```
        data =[1    0.162   0.820   0.018   0.937   0.044   0.020   0.93
5.39
            2   0.161   0.801   0.039   0.920   0.041   0.040   0.97    5.55
            3   0.168   0.759   0.073   0.880   0.044   0.077   0.95    4.99
            4   0.154   0.742   0.105   0.835   0.046   0.116   0.90    4.91
            5    0.160    0.700    0.140    0.796    0.050    0.149    0.94
4.67];

        T = 298.15; % K
        alpha = 0.2;
        % r = [5.8463   4.561775131 3.9228];
        % q = [5.008    3.849420105 2.968];

        r = [6.9894 7.7283  4.1288];
        q = [4.9184 5.2393  3.0705];

    case '22'
        RefMat = 'Tetrabutyl phosphonium bromide with DMSO(1:2) as DES';
        systemName = 'Octane - DES - Toluene @ 30 0C';
        nComp = 3;
        caseNo = 'Data22';

        data =[1    0.097   0.883   0.019   0.979   0.002   0.019   1.03
10.34
            2    0.105    0.853    0.041    0.962    0.001    0.036    1.14
10.41
            3    0.096    0.827    0.077    0.926    0.002    0.070    1.11
10.65
            4   0.090   0.803   0.108   0.883   0.002   0.108   1.00    9.84
            5    0.088    0.767    0.145    0.847    0.002    0.140    1.04
10.01];

        T = 298.15; % K
        alpha = 0.2;
        %  r = [5.8463  4.496751734 3.9228];
        % q = [5.008    3.797401388 2.968];

        r = [6.9894 7.0382  4.1288];
        q = [4.9184 4.8567  3.0705];
    case '23'
       RefMat = 'Tetrabutyl phosphonium bromide with DMSO(1:2) as DES';
        systemName = 'Octane - DES - Toluene @ 40 0C';
        nComp = 3;
        caseNo = 'Data23';

        data =[1    0.089   0.895   0.016   0.974   0.004   0.022   0.74
8.09
            2   0.087   0.880   0.032   0.951   0.005   0.043   0.75    8.13
            3   0.091   0.846   0.063   0.908   0.006   0.082   0.76    7.65
            4   0.116   0.788   0.096   0.864   0.006   0.122   0.79    5.87
            5    0.125    0.749    0.125    0.817    0.010    0.160    0.78
5.11];
```

```
        T = 298.15; % K
        alpha = 0.2;
        % r = [5.8463   4.496751734 3.9228];
        % q = [5.008    3.797401388 2.968];

        r = [6.9894 7.0382  4.1288];
        q = [4.9184 4.8567  3.0705];

    case '24'
        RefMat = 'Tetrabutyl phosphonium bromide with DMSO(1:2) as DES';
        systemName = 'Octane - DES - Toluene @ 50 0C';
        nComp = 3;
        caseNo = 'Data24';

        data =[1    0.110   0.873   0.017   0.976   0.003   0.021   0.78
6.96
            2   0.120   0.848   0.033   0.952   0.004   0.043   0.76    6.03
            3   0.115   0.820   0.065   0.912   0.003   0.081   0.80    6.33
            4   0.110   0.794   0.096   0.867   0.006   0.119   0.81    6.38
            5    0.101    0.774    0.124    0.821    0.006    0.159    0.78
6.36];

        T = 298.15; % K
        alpha = 0.2;
        %   r = [5.8463 4.496751734 3.9228];
        %  q = [5.008   3.797401388 2.968];

        r = [6.9894 7.0382  4.1288];
        q = [4.9184 4.8567  3.0705];

         case '25'
        RefMat = 'TetrabutylphosphoniumMethanesulfonate with PEG200 (1:2)
as DES';
        systemName = 'Octane - DES - Toluene @ 30 0C';
        nComp = 3;
        caseNo = 'Data25';

        data =[1    0.075   0.907   0.018   0.975   eps 0.025   0.71    9.18
            2   0.082   0.886   0.032   0.951   eps 0.048   0.67    7.82
            3   0.084   0.846   0.069   0.895   eps 0.101   0.69    7.32
            4   0.087   0.815   0.098   0.855   eps 0.138   0.71    6.98
            5   0.079   0.792   0.129   0.807   eps 0.180   0.72    7.35];

        T = 298.15; % K
        alpha = 0.2;
        %  r = [5.8463  6.961155408 3.9228];
        % q = [5.008    5.768924326 2.968];

        r = [6.9028 21.5700 4.0942];
        q = [4.8989 14.4864 3.0476];

    case '26'
```

```
       RefMat = 'TetrabutylphosphoniumMethanesulfonate with PEG200 (1:2)
as DES';
        systemName = 'Octane - DES - Toluene @ 40 0C';
        nComp = 3;
        caseNo = 'Data26';

        data =[1    0.126   0.855   0.018   0.975   eps 0.025   0.74    5.71
            2   0.125   0.841   0.034   0.951   eps 0.048   0.70    5.35
            3   0.124   0.804   0.072   0.896   eps 0.100   0.72    5.17
            4   0.117   0.783   0.099   0.854   eps 0.138   0.72    5.24
            5   0.101   0.770   0.129   0.806   eps 0.181   0.71    5.66];

        T = 298.15; % K
        alpha = 0.2;
        %  r = [5.8463  6.961155408 3.9228];
        %  q = [5.008   5.768924326 2.968];

        r = [6.9894 11.2812 4.1288];
        q = [4.9184 7.5108  3.0705];

    case '27'
        RefMat = 'TetrabutylphosphoniumMethanesulfonate with PEG200 (1:2)
as DES';
        systemName = 'Octane - DES - Toluene @ 50 0C';
        nComp = 3;
        caseNo = 'Data27';

        data =[1    0.131   0.851   0.018   0.975   eps 0.025   0.70    5.24
            2   0.121   0.845   0.033   0.951   eps 0.048   0.70    5.45
            3   0.109   0.821   0.070   0.895   eps 0.101   0.69    5.66
            4   0.114   0.791   0.095   0.852   eps 0.140   0.68    5.09
            5   0.110   0.761   0.129   0.805   eps 0.182   0.71    5.17];

        T = 298.15; % K
        alpha = 0.2;
        % r = [5.8463   6.961155408 3.9228];
        % q = [5.008    5.768924326 2.968];

        r = [6.9894 11.2812 4.1288];
        q = [4.9184 7.5108  3.0705];


    case '28'
        RefMat = 'TetrabutylphosphoniumMethanesulfonate with PEG600 (1:2)
as DES';
        systemName = 'Octane - DES - Toluene @ 30 0C';
        nComp = 3;
        caseNo = 'Data28';

        data =[1    0.159   0.805   0.037   0.976   eps 0.024   1.52    9.33
            2   0.160   0.774   0.066   0.953   eps 0.046   1.43    8.52
            3   0.147   0.719   0.135   0.899   eps 0.099   1.36    8.35
            4   0.143   0.676   0.181   0.859   eps 0.137   1.32    7.89
```

```
            5   0.136   0.629   0.235   0.814   eps 0.180   1.30    7.77];
        T = 298.15; % K
        alpha = 0.2;
        % r = [6.9894   22.5260 4.1288];
        % q = [4.9184   15.2310 3.0705];

        r = [6.9894 22.5260 4.1288];
        q = [4.9184 15.2310 3.0705];

    case '29'
       RefMat = 'TetrabutylphosphoniumMethanesulfonate with PEG600 (1:2)
as DES';
        systemName = 'Octane - DES - Toluene @ 40 0C';
        nComp = 3;
        caseNo = 'Data29';

        data =[1    0.149   0.816   0.035   0.975   eps 0.024   1.45    9.51
            2   0.152   0.783   0.065   0.953   eps 0.047   1.39    8.71
            3   0.153   0.708   0.138   0.901   eps 0.098   1.42    8.31
            4   0.158   0.658   0.184   0.860   eps 0.136   1.35    7.34
            5   0.174   0.595   0.231   0.814   eps 0.180   1.28    6.01];
        T = 298.15; % K
        alpha = 0.2;
        % r = [5.8463   13.72333262 3.9228];
        % q = [5.008    11.1786661  2.968];

        r = [6.9894 22.5260 4.1288];
        q = [4.9184 15.2310 3.0705];

    case '30'
        RefMat = 'TetrabutylphosphoniumMethanesulfonate with PEG600 (1:2)
as DES';
        systemName = 'Octane - DES - Toluene @ 50 0C';
        nComp = 3;
        caseNo = 'Data30';

        data =[1    0.214   0.751   0.036   0.976   eps 0.024   1.48    6.73
            2   0.236   0.700   0.064   0.953   eps 0.047   1.37    5.55
            3   0.176   0.675   0.149   0.905   eps 0.094   1.59    8.15
            4   0.193   0.624   0.183   0.861   eps 0.135   1.35    6.03
            5   0.198   0.571   0.231   0.814   eps 0.180   1.28    5.27];
        T = 298.15; % K
        alpha = 0.2;
        % r = [5.8463   13.72333262 3.9228];
        % q = [5.008    11.1786661  2.968];

        r = [6.9894 22.5260 4.1288];
        q = [4.9184 15.2310 3.0705];


end
xI = data(:,2:nComp+1);
xII = data(:,nComp+2:2*nComp+1);
```

```
ExpData = [xI xII];
z = (xI+xII)./2;
NVARS = nComp*(nComp -1);
lb = [-inf]*ones(1,NVARS);
ub = [inf]*ones(1,NVARS);
% lb = [-76 70 400 100 80 80];
% ub = [-70 80 450 120 90 90];
par0 = 10*ones(1,NVARS);

Data2_val = get(handles.modelMenu,'Value');
Data2_str = get(handles.modelMenu, 'String')
switch Data2_str{Data2_val};
    case 'NRTL'
        model = 'NRTL'
        extraPar = struct('T', T, 'alpha', alpha);
    case 'UNIQUAC'
        model = 'UNIQUAC'
        extraPar = struct('T', T, 'r', r, 'q', q);
end
```

regdata.m

```
function [std,varresid,r2,cor,vcv,varinf]=regdata(param,yfit,ydata,jac)

%[std,varresid,r2,cor,vcv,varinf]=regdata(param,yfit,ydata,jac)
% Calculate and Plot regression statistics from lsqcurvefit.m
% OUT
% std -standard error of each parameter
% varresid- Variance of residuals
% r2    - R^2 Correlation coefficient
% cor   - Correlation matrix for Parameters
% vcv   - Variance Covariance Matrix for Parameters
% varinf- Variance inflation factors >10 implies Multicollinearity in x's
% IN
% param -Least squares parameter values
% yfit   -Response fit using param to get yfit from lsqcurvefit use
yfit=residual+ydata
%                                   where residual is the error matrix from
lsqcurvefit
% ydata -Response data
% jac   -Jacobian value at Least squares parameter values

% Arthur Jutan Univ of Western Ontario Dept of Chemical Engineering
% ajutan@julian.uwo.ca
% Revised 11-20-98,5-19-99
yfit
ydata
e=yfit(:)-ydata(:); %error vectorize the Y matrix for multiple ouputs
ss=e'*e % best sum of squares
m=length(yfit);n=length(param);
if (m~=n),varresid=ss./(m-n);else, var=NaN;end % variance of Residuals
```

```
% CALC VARIANCE COV MATRIX AND CORRELATION MATRIX OF PARAMETERS
%convert jac to full matrix for ver 5.3
    jac=full(jac);%aj 99
    xtx=jac'*jac;
      xtxinv=inv(xtx);

      %calc correlation matrix cor and variance inflation varinf
    varinf = diag(xtxinv);
    cor = xtxinv./sqrt(varinf*varinf');




      disp(' Least Squares Estimates of Parameters')
      disp(param')
      disp(' correlation matrix for parameters ')
      disp(cor)
      vcv=xtxinv.*varresid; % mult by var of residuals~=pure error
      disp('Variance inflation Factors >10 ==> Multicollinearity in x"s')
      disp(varinf')

%Formulae   for   vcv=(x'.vo.x)^-1   *sigma^2   where   meas   error   Var,
v=[vo]*sigma^2
      std=sqrt(diag(vcv)) % calc std error for each param
      disp(' 95%Confidence Interval for each parameter ')
      lowerlimit=param'-std;
      upperlimit=param'+std;
      disp(' Lower Limit CI ')
      disp(lowerlimit)
      disp(' Upper Limit CI ')
      disp(upperlimit)
%Calculate R^2 (Ref Draper & Smith p.46)
      r=corrcoef(ydata(:),yfit(:));
      r2=r(1,2).^2;
      disp('Variance of Residuals  ' )
      disp(  varresid )
      disp( 'Correlation Coefficient R^2')
      disp(r2)
```

stat_data.m

```
function [res, r2, r2adj, SSE, RMSE] = stat_data(param,yfit,ydata)
%
% [res, r2, r2adj, sse, rmse] = stat_data(param,yfit,ydata)
% Calculate and Plot goodnesss of fit statistics from regression results
%
% OUT
% res - residuals from fitted model
% r2  - R^2 Correlation coefficient
% r2  - Adjusted R^2 Correlation coefficient
```

```
% SSE - Sum of Squares Due to Error
% RMSE - Root Mean Squared Error
%
% IN
% param -Least squares parameter values
% yfit   -Response fit using param to get yfit from lsqcurvefit use
yfit=residual+ydata
%                                  where residual is the error matrix from
lsqcurvefit
% ydata -Response data

% Saidu M. Waziri of Department of Chemical Engineering, ABU Zaria, Nigeria
% Revised 02-01-2013

%Determine No of Variables and Parameters
n=length(yfit);m=length(param);

%Residuals
res=ydata-yfit;

%SUM OF SQUARED ERROR
SSE = sum((ydata-yfit).^2);

%Calculate R^2
ybar = mean(ydata);
SST = sum((ydata-ybar).^2);
r2=1-SSE/SST;

%Calculate Adjusted R^2
r2adj=1- SSE*(n-1)/SST/(n-m);

%RMSE
RMSE = sqrt(SSE/(n-m));

% % Plot the residuals vs data
% t=1:n;
% tt=zeros(1,n);

% subplot(2,1,1)
% plot(t,ydata,'o',t,yfit,'r-')
% legend('ydata','ymodel')
% title(' ydata and ymodel versus observation number')
% xlabel(' observation number');
% ylabel(' ydata o and ymodel-')
% grid;
%
% subplot(2,1,2)
% plot(t,res,'o-', t, tt)
% title(' Residuals Plot')
% xlabel(' observation number');
% ylabel(' Residual ')
% grid;
```

TextFilename.m

```
function name = TextFilename(caseNo, model, OptimMethod)

name = strcat(caseNo,'_',model,'_',OptimMethod,'.txt');
```

GUI output

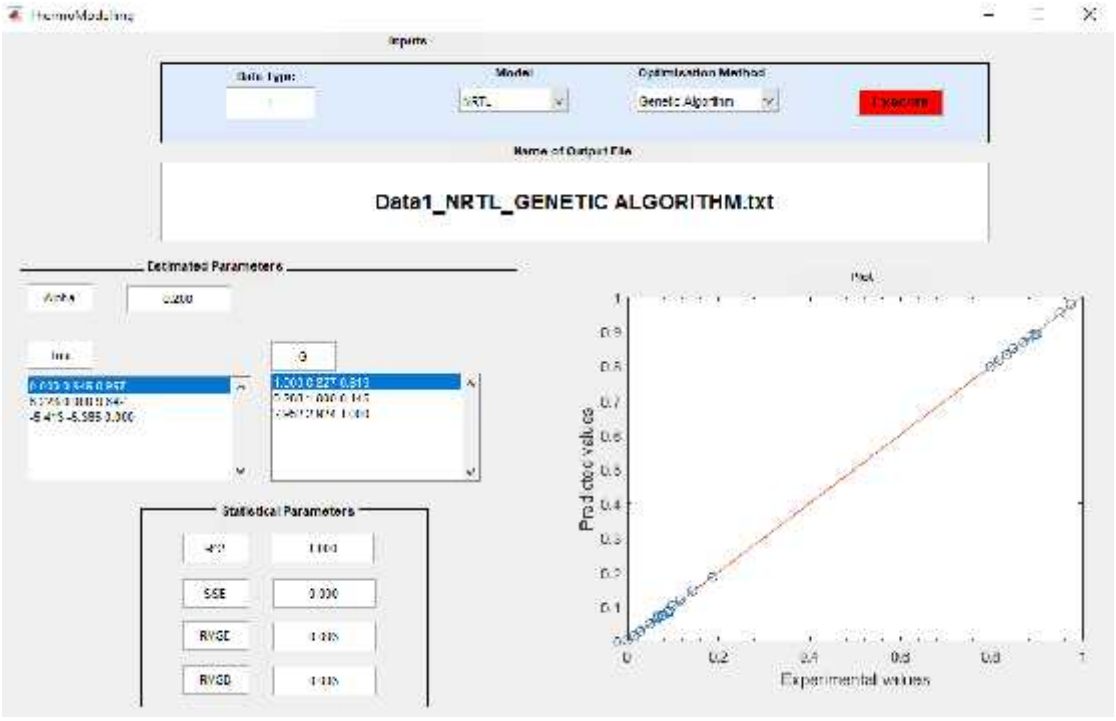

ResultFile.xlsx (sheet 1 and sheet 2)

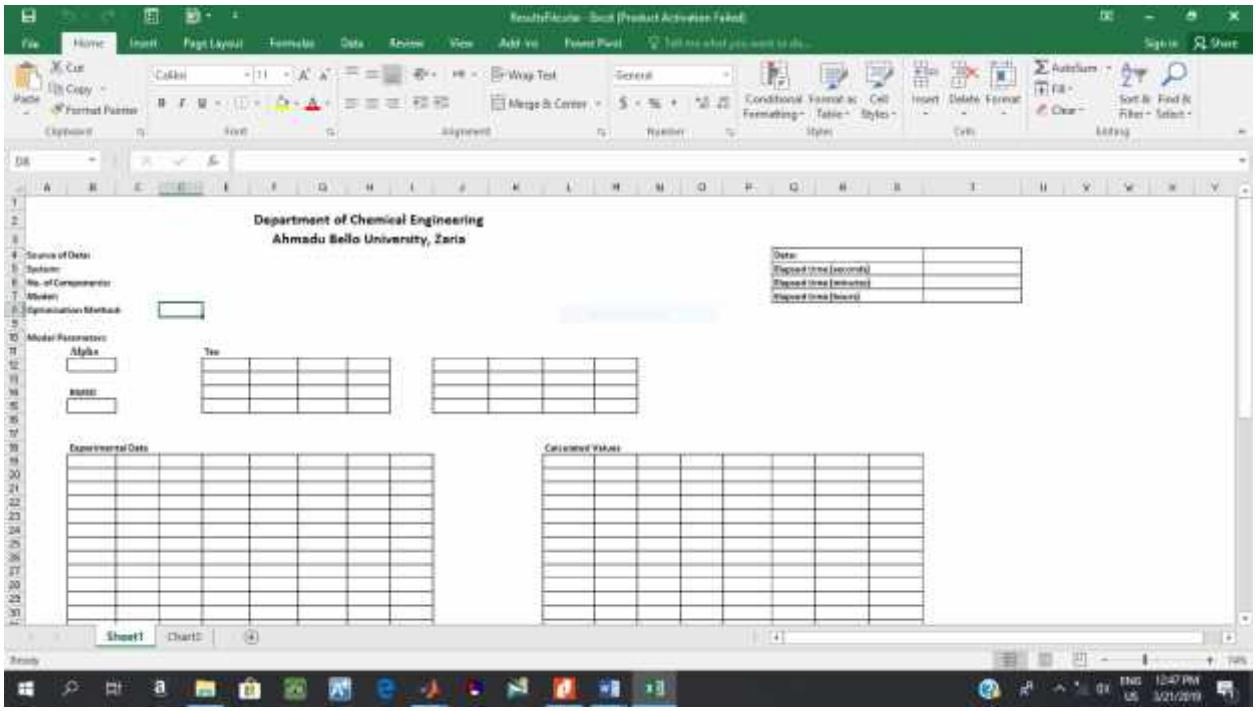
Department of Chemical Engineering
Ahmadu Bello University, Zaria
Source of Data:
System:
No. of Components:
Model:
Optimization Method:
Model Parameters:
Alpha
Beta
Experimental Data
Calculated Values
Sheet1
Chart2

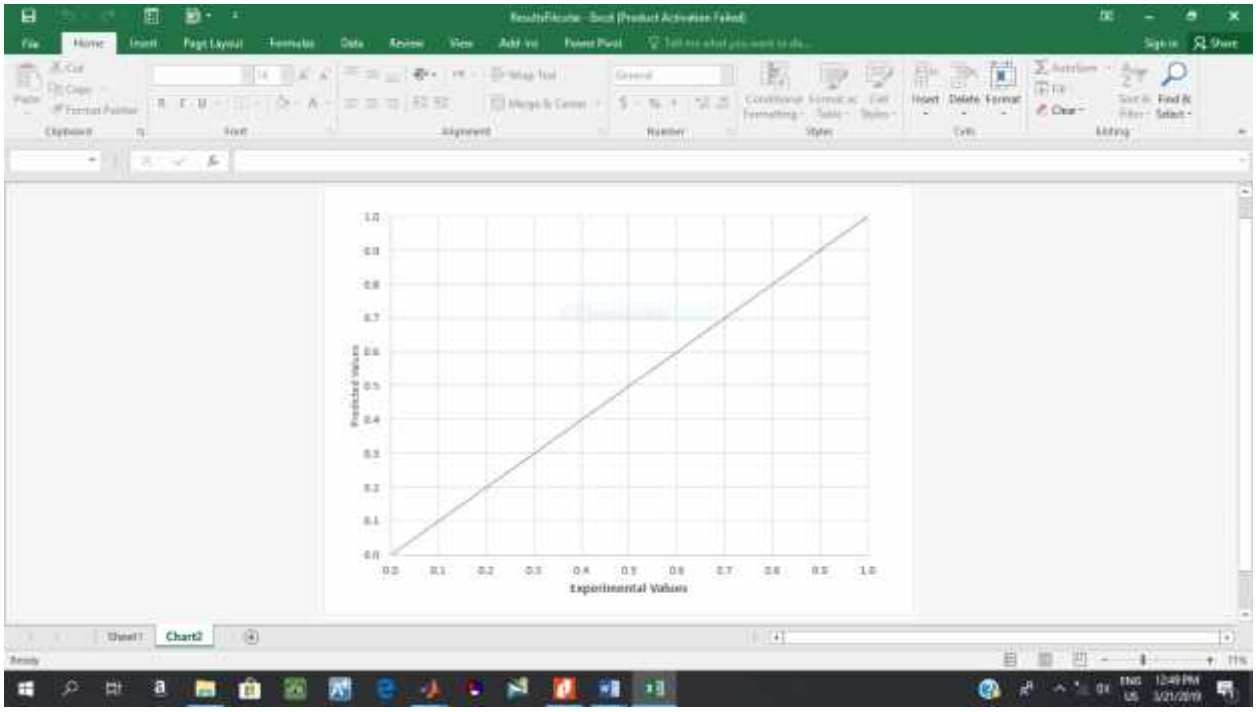
Predicted Values
Experimental Values
Chart1
Chart2